

UNIVERZITA KARLOVA V PRAZE
FARMACEUTICKÁ FAKULTA V HRADCI KRÁLOVÉ
Katedra biochemických věd

**Studium antiproliferačních účinků nových
chelátorů železa**

Disertační práce

Mgr. Eliška Potůčková

Vedoucí disertační práce: Doc. PharmDr. Tomáš Šimůnek, Ph.D.
Konzultant: Prof. Des R. Richardson
PharmDr. Lucie Vostatková, Ph.D.

Hradec Králové, 2014

Poděkování

Největší dík patří mému školiteli Doc. PharmDr. Tomáši Šimůnkovi, Ph.D. za jeho trpělivé a pohodové vedení, udělování cenných rad a přátelský přístup během celého doktorského studia. Za umožnění tříměsíční stáže na jeho pracovišti a cenné konzultace děkuji Prof. Desovi R. Richardsonovi z Univerzity v Sydney (Austrálie). Děkuji také všem kolegům z katedry biochemických věd, katedry anorganické a organické chemie a katedry farmaceutické chemie a kontroly léčiv Farmaceutické fakulty UK v Hradci Králové a Ústavu farmakologie Lékařské fakulty UK v Hradci Králové, bez kterých by předložená práce ani nemohla vzniknout. Nemalý dík patří také zahraničním spolupracovníkům z Univerzity v Sydney (Austrálie) a ze Slezské Univerzity v Katovicích (Polsko).

Za finanční podporu děkuji grantovým agenturám (GAUK 299511, GAČR 13-15008S, UNCE 204019/304019/2012, PRVOUK P40 a SVV 260 065).

V neposlední řadě pak patří velké poděkování mé rodině a přátelům za celkovou podporu během studia.

Prohlášení

Prohlašuji, že tato práce je mým původním autorským dílem, které jsem vypracovala samostatně pod vedením svého školitele. Veškerá literatura a další zdroje, z nichž jsem při zpracování čerpala, jsou uvedeny v seznamu použité literatury a v práci řádně citovány. Práce nebyla využita k získání jiného nebo stejného titulu.

Eliška Potůčková

Abstrakt

Univerzita Karlova v Praze

Farmaceutická fakulta v Hradci Králové

Katedra biochemických věd

Kandidát:

Mgr. Eliška Potůčková

Školitel:

Doc. PharmDr. Tomáš Šimůnek, Ph.D.

Název disertační práce:

Studium antiproliferačních účinků nových chelátorů železa

Chelátory železa představují zajímavou skupinu potenciálních protinádorových léčiv, ale také léčiv schopných chránit citlivé tkáně před oxidačním stresem. Tato práce se zabývá především designem a syntézou nových chelátorů železa odvozených od struktury salicylaldehyd isonikotinoyl hydrazonu (SIH) a úvodním studiem jejich farmakologických a toxikologických vlastností. Antiproliferační účinky těchto látek byly studovány na buněčné linii lidského prsního adenokarcinomu a linii lidské promyelocytární leukémie a jejich možná nespecifická toxicita na buněčné linii, odvozené od neonatální potkaní srdeční tkáně. Během této studie byly popsány některé nové vztahy závislosti chemické struktury a účinku, které budou využity k dalšímu výzkumu. V druhé části této práce byla prověřována možnost souběžného podání chelátorů železa a léčiv používaných v terapii rakoviny prsu. Zde byly identifikovány antracyklinové antibiotikum doxorubicin a zejména pak antagonist estrogenních receptorů tamoxifen jako léčiva potenciálně vhodná pro kombinovanou léčbu s použitím chelátorů železa. Dále byla sledována biologická aktivita thiosemikarbazonových chelátorů, kde byla opět popsána závislost struktur chelátorů a jejich biologických vlastností. U jednoho z nejnadějnějších thiosemikarbazonových chelátorů identifikovaných za posledních několik let byla charakterizována jeho biologická aktivita, a chelatační a antiproliferační aktivity jeho nedávno identifikovaných metabolitů první fáze biotransformace. Bylo zjištěno, že metabolity jsou o několik řádů méně antiproliferačně aktivní než mateřská látka a netoxické. Dále byla studována schopnost chelátorů železa chránit srdeční buňky před oxidačním poškozením a před antracyklinovou toxicitou. Náš výzkum umožnil popsat závislosti a

souvislosti důležité pro další vývoj selektivních antiproliferačních chelátorů železa a také některé nové poznatky, týkající se protektivního působení chelátorů železa na srdeční tkáň.

Abstract

Charles University in Prague

Faculty of Pharmacy in Hradec Králové

Department of Biochemical Sciences

Candidate:

Mgr. Eliška Potůčková

Supervisor:

Doc. PharmDr. Tomáš Šimůnek, Ph.D.

Title of Doctoral Thesis:

Study of antiproliferative effects of novel iron chelators

Recent studies demonstrate that iron chelators possess marked potential as anticancer agents and also as substances protecting sensitive tissues against oxidative stress. This thesis is dealing mainly with design and synthesis of new antiproliferative iron chelators based on the structure of salicylaldehyde isonicotinoyl hydrazone (SIH) and with a characterization of their pharmacological and toxicological properties. Antiproliferative effects of these substances were studied on human breast adenocarcinoma cell line and human leukemic cell line and the non-specific toxicity on neonatal rat cardiac tissue-derived cells. During these studies some novel structure-activity relationships have been found. Furthermore, the suitability of simultaneous administration of iron chelators with antineoplastic agents used in breast cancer treatment was studied. In this project the anthracycline antibiotic, doxorubicin, and, in particular, the estrogen receptor antagonist, tamoxifen, were identified as the most suitable agents for potential treatment combined with iron chelation therapy. The characterization of biological activities and structure-activity relationships of thiosemicarbazone chelators was also studied. One of the most potent thiosemicarbazone chelators identified in last years was characterized in terms of its biological activities. The chelation and antiproliferative activities of its recently identified phase I metabolites were also characterized and compared to the parent substance. The metabolic products were a few orders of magnitude less antiproliferatively active than its parent substance and non-toxic. Finally, we studied the ability of iron chelators to protect cardiac cells against oxidative stress-induced injury and anthracycline toxicity. Collectively, our results are important for further

development of this novel group of potential anticancer agents and substances able to protect cardiac tissue.

Obsah

1	Úvod	10
2	Teoretická část	11
2.1	Metabolismus železa	11
2.1.1	<i>Vlastnosti železa v organismu</i>	11
2.1.2	<i>Příjem a výdej železa</i>	11
2.1.3	<i>Vstřebávání železa z potravy</i>	12
2.1.4	<i>Transport železa do buněk</i>	13
2.1.5	<i>Distribuce železa v buňce</i>	13
2.1.6	<i>Transport železa z buněk</i>	14
2.1.7	<i>Regulační mechanismy</i>	15
2.2	Rakovina prsu.....	17
2.2.1	<i>Incidence a mortalita</i>	17
2.2.2	<i>Diagnostika</i>	17
2.2.3	<i>Rozdělení</i>	18
2.2.4	<i>Léčba</i>	19
2.2.5	<i>Význam železa u rakoviny prsu</i>	24
2.3	Chelátory železa	24
2.3.1	<i>Použití chelátorů železa</i>	25
2.3.2	<i>Rozdělení chelátorů železa</i>	26
3	Cíle práce	33
4	Komentáře k pracím	34
4.1	Popis závislostí chemické struktury a biologických účinků nových analogů SIH I.....	34
4.2	Popis závislostí chemické struktury a biologických účinků nových analogů SIH II.....	36

4.3	<i>In vitro</i> studie současného působení chelátorů železa a klinicky používaných chemoterapeutik na buněčné linie rakoviny prsu	37
4.4	Popis závislosti chemické struktury a biologických účinků nových thiosemikarbazonů	39
4.5	Studie biologických účinků chelátoru Bp4eT a jeho metabolitů	41
4.6	Porovnání klinicky používaných a experimentálních chelátorů železa jako ochrany před oxidačním stresem	42
4.7	Katalytické inhibitory topoizomerázy II rozdílně modulují toxicitu antracyklinů k srdečním a rakovinným buňkám	43
5	Souhrnná diskuse.....	46
6	Závěry.....	50
7	Podíl předkladatelky na publikacích zahrnutých v disertační práci.....	51
8	Seznam zkratk.....	54
9	Seznam použité literatury	55
10	Přehled publikační činnosti	77
11	Prezentace na konferencích	79
12	Přílohy	81

1 Úvod

Nádorová onemocnění jsou velmi rozšířená a často smrtelná onemocnění, která postihují osoby každého věku a pohlaví. Nejčastěji se však vyskytují u osob staršího věku, kterého se lidé častěji dožívají v rozvinutých zemích. Díky vysoké úrovni medicíny v rozvinutých zemích a díky screeningovým programům u některých typů rakoviny se zvýšila šance včasné diagnostiky rakovinných onemocnění a tím se i rozšířil prostor pro jejich léčbu. Současná léčba klasickými chemoterapeutiky však není vždy účinná nebo ji kvůli zdravotnímu stavu pacienta není možné použít. V průběhu léčby může navíc docházet ke vzniku rezistence rakovinných buněk k podávanému chemoterapeutiku, což je indikací pro změnu léčby. Z těchto důvodů je žádoucí vyvíjet nová léčiva působící na jiné buněčné struktury a procesy, než působí léčiva stávající.

Nadějným přístupem k léčbě rakoviny, který je prozatím ve fázi experimentů ale i prvních klinických studií, je použití chelátorů železa. Tyto látky jsou schopny vázat nitrobuněčné železo a vynášet ho z buňky ven, čímž způsobí jeho nedostatek pro důležité buněčné procesy, jako je syntéza DNA nebo buněčné dýchání. Rakovinná buňka, které je železo odebráno, nemůže pokračovat v nekontrolovaném dělení a umírá apoptózou (Kalinowski *et al.* 2005, Richardson *et al.* 2009). U některých chelátorů železa byl dokonce zaznamenán vyšší antiproliferační účinek na rakovinné buňky rezistentní k běžné chemoterapii než na buňky k této léčbě citlivé (Whitnall *et al.* 2006).

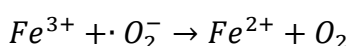
Tato práce je součástí širšího výzkumu vztahu chemické struktury nových aroyldihydraxonových chelátorů železa a jejich biologické aktivity. Nejvíce je pak zaměřena na antiproliferační aktivitu zmíněných látek a mechanismus jejich protinádorového působení. Vzhledem k nedostatečným znalostem o efektu společného podávání chelátorů železa a běžně klinicky používaných chemoterapeutik, je jedna část práce věnována sledování antiproliferačního působení kombinací chelátorů železa s chemoterapeutiky, používanými v terapii rakoviny prsu. V rámci zahraniční spolupráce s Univerzitou v Sydney (Austrálie) a se Slezskou Univerzitou v Katovicích (Polsko) je sem zahrnut i popis biologických aktivit nových chelátorů ze skupiny thiosemikarbazonů. Další částí této práce je sledování biologické aktivity nově identifikovaných metabolitů, první fáze biotransformace, nadějně látky ze skupiny thiosemikarbazonů. V posledních částech práce je studován potenciál chelátorů železa předcházet poškození srdečních buněk oxidačním stresem a antracykliny.

2 Teoretická část

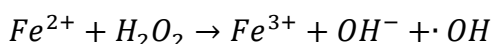
2.1 Metabolismus železa

2.1.1 Vlastnosti železa v organismu

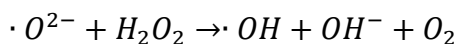
Železo je přechodný prvek nepostradatelný pro život. V biologickém prostředí se nachází ve dvou formách, železnaté a železité. Ve vodném prostředí železnaté ionty přecházejí samovolně na železité, které se hydratují za vzniku $\text{Fe}(\text{OH})_3$. Rozpustnost železitých iontů je poměrně nízká. Při pH 7,0 se pohybuje v řádu 10^{-17} mol/l. Rozpustnost železnatých iontů se při stejných podmínkách pohybuje v řádu 10^{-1} mol/l (Aisen *et al.* 1980, Arredondo *et al.* 2005). Nepostradatelnost železa spočívá právě ve schopnosti přechodu železnatého iontu na železitý a naopak, což ho předurčuje být součástí oxidačních a redukčních enzymů v organismu (Dawson *et al.* 1987, Solomon *et al.* 2000). Pokud je však železo volné může spontánně katalyzovat takzvanou Fentonovu reakci, kdy železnaté ionty reagují s peroxidem vodíku nebo s lipidy obsahujícími peroxiskupinu za vzniku železitého iontu, hydroxidového aniontu a vysoce reaktivních hydroxidových, popřípadě lipidových, radikálů. Tyto radikály mohou poškozovat lipidy, proteiny i nukleové kyseliny (Gutteridge 1986, Kehrer 2000, Hentze *et al.* 2004). Z tohoto důvodu se v organismu vyvinuly různé transportní a skladovací proteiny, aby bylo volné železo co nejvíce eliminováno (Hentze *et al.* 2010, Oliveira *et al.* 2014).



Redukce železa



Fentonova reakce



Haber-Weissova reakce

Obrázek 2.1 Reakce katalyzované železem (Fe), při kterých vznikají volné radikály. (Kehrer 2000)

2.1.2 Příjem a výdej železa

Tělo dospělého člověka obsahuje přibližně 3 až 5 g železa, což odpovídá zhruba 45–55 mg železa na 1 kg hmotnosti. Přibližně 70 % tohoto železa je součástí molekul transportujících kyslík, hemoglobinu v červených krvinkách a myoglobinu ve svalech (Fairweather-Tait *et al.* 2013, Oliveira *et al.* 2014). Železo potřebné k syntéze

hemoglobinu je velmi efektivně recyklováno při zániku starých erytrocytů, pohlcením těchto erytrocytů buňkami retikulo-endoteliálního systému, které uvolní železo obsažené v hemoglobinu do dalšího oběhu.

Denní ztráty železa jsou velmi malé, a proto ani jeho denní příjem není velký. Zdravý jedinec vyloučí jen cca 1-2 mg železa denně deskvamací buněk střevní sliznice, kůže, buněk močových cest a potem. Mladé ženy ztrácejí více železa během menstruačního krvácení (Hentze *et al.* 2010, Fairweather-Tait *et al.* 2013).

2.1.3 Vstřebávání železa z potravy

Železo je z potravy vstřebáváno zejména v duodenu a horní části jejunu. Do těla prochází přes apikální část enterocytů jako hemové a nehemové (Hentze *et al.* 2010, Oliveira *et al.* 2014). Hemové železo je přenášeno prostřednictvím přenašeče hemu (heme carrier protein 1; HCP1), ale pravděpodobně i jinými mechanismy (Shayeghi *et al.* 2005, Nakai *et al.* 2007). V enterocyty je železo z hemu uvolněno enzymem hemoxygenázou do takzvaného rezervoáru volného železa (labile iron pool; LIP) (Ferris *et al.* 1999). Je to jakási zásobárna volného, rychle použitelného železa, které je nespecificky vázáno na nízkomolekulární látky, jako jsou fosfáty, nukleotidy, aminokyseliny a podobně (Kakhlon *et al.* 2002), nebo je vázáno na transportní proteiny, chaperony (Leidgens *et al.* 2013). Nehemové železo je do enterocytu přenášeno transportérem divalentních iontů (divalent metal transporter 1; DMT1) (Mims *et al.* 2005). Před samotným transportem však železo musí být redukováno na železnaté ionty, což zajišťuje enzym duodenální cytochrom B (duodenal cytochrome B; DCYTB) (McKie *et al.* 2001). Z nedávných výzkumů vyplývá, že DCYTB není pro redukcii železa esenciální a proto se předpokládá přítomnost i jiných ferroreduktáz vázaných na apikální membránu enterocytů (McKie 2008). Železo přenesené do enterocytu se opět stává součástí LIP. Z enterocytů je pak na bazolaterální straně železo uvolňováno do mezibuněčného prostoru pomocí ferroportinu 1 (Donovan *et al.* 2000). Zde je železo oxidováno hephaestinem anebo ceruloplasminem na železité ionty (Vulpe *et al.* 1999), které se okamžitě navazují na transportní protein transferrin (Tf), který zajišťuje distribuci železa v těle.

2.1.4 Transport železa do buněk

V tělních tekutinách je železo transportováno vázané na Tf. Tento glykoprotein je schopen vázat dva železití ionty, přičemž je tato vazba závislá na fyziologickém pH a přítomnosti bikarbonátu (Princiotta *et al.* 1975, Richardson *et al.* 1997). Lidský plazmatický Tf je optimálně saturován cca z 30 % (Hentze *et al.* 2010). Buňky přijímají železo z krve receptorem zprostředkovanou endocytózou, kdy se dvě molekuly Tf váží na transferrinový receptor (TfR) 1 nebo 2 a celý tento komplex podléhá endocytóze. V endozomu dochází ke snížení pH protonovou pumpou závislou na ATP, což snižuje afinitu Tf k železu (Dautry-Varsat *et al.* 1983). Uvolněné železití ionty jsou pak redukovány na rozpustné železnaté pomocí enzymu z rodiny metaloreduktáz, STEAP3 (six-transmembrane epithelial antigen of the prostate 3), (Ohgami *et al.* 2005) a uvolněny do cytoplazmy pomocí přenašeče DMT1. Endozom s Tf a TfR poté putuje zpět k povrchu buňky, kde je Tf uvolněn a TfR je k dispozici pro navázání dalšího komplexu Tf-železo (Dautry-Varsat *et al.* 1983). Kromě endocytózy zprostředkované receptorem existuje i na receptoru nezávislý příjem železa do buňky, ten ovšem ještě nebyl dostatečně objasněn. Má se za to, že by se na něm mohl podílet DMT1 (Shindo *et al.* 2006) a přenašeč zinku Zip14 (Liuzzi *et al.* 2006).

2.1.5 Distribuce železa v buňce

Železo, které se dostane do LIP, je využíváno k syntéze enzymů v cytoplazmě nebo v mitochondriích nebo je skladováno pro pozdější použití ve skladovacím proteinu ferritinu. Ferritin je protein složený z lehkých (L) a těžkých (H) podjednotek, jejichž poměr se liší tkáň od tkáně. Ferritin má schopnost oxidovat železnaté ionty z LIP na ionty železité, které v tomto redoxním stavu ukládá. Při uvolnění železitých iontů z ferritinu se pak opět redukuje na železnaté (Torti *et al.* 2002).

V nitrobuněčné distribuci a metabolismu železa je ještě mnoho neznámého. Část železa je využita hned v cytoplazmě, například jako součást enzymu ribonukleotid reduktázy (Nordlund *et al.* 1990), ale většina metabolismu železa probíhá v mitochondriích, protože mitochondrie jsou centrem pro syntézu hemu a Fe-S klastrů (Dunn *et al.* 2007, Richardson *et al.* 2010). Do transportu železa z cytoplazmy do mitochondrií je pravděpodobně zapojeno více dosud ne plně identifikovaných transportérů (Richardson *et al.* 2010). Přes vnitřní mitochondriální membránu je železo transportováno přenašeči mitoferrinem 1 a 2 (Paradkar *et al.* 2009). Po inkorporaci

železa do porfyrinové struktury enzymem ferrochelatázou je vzniklý hem exportován z mitochondrií pravděpodobně prostřednictvím proteinu vážícího hem (hem-binding protein; HBP) (Taketani *et al.* 1998). Důležitou roli v mitochondriích hraje chaperon frataxin, který pravděpodobně přenáší železo k syntéze Fe-S klastrů (Dunn *et al.* 2007, Richardson *et al.* 2010). Kompletní Fe-S klastry jsou pravděpodobně transportovány z mitochondrií pomocí efluxního proteinu závislého na ATP, ABCB7 (Bekri *et al.* 2000). Přebytečné železo je v mitochondriích ukládáno do mitochondriálního ferritinu, aby se zamezilo jeho schopnosti katalyzovat vznik reaktivních forem kyslíku (ROS) (Richardson *et al.* 2010).

2.1.5.1 Erytrocyty

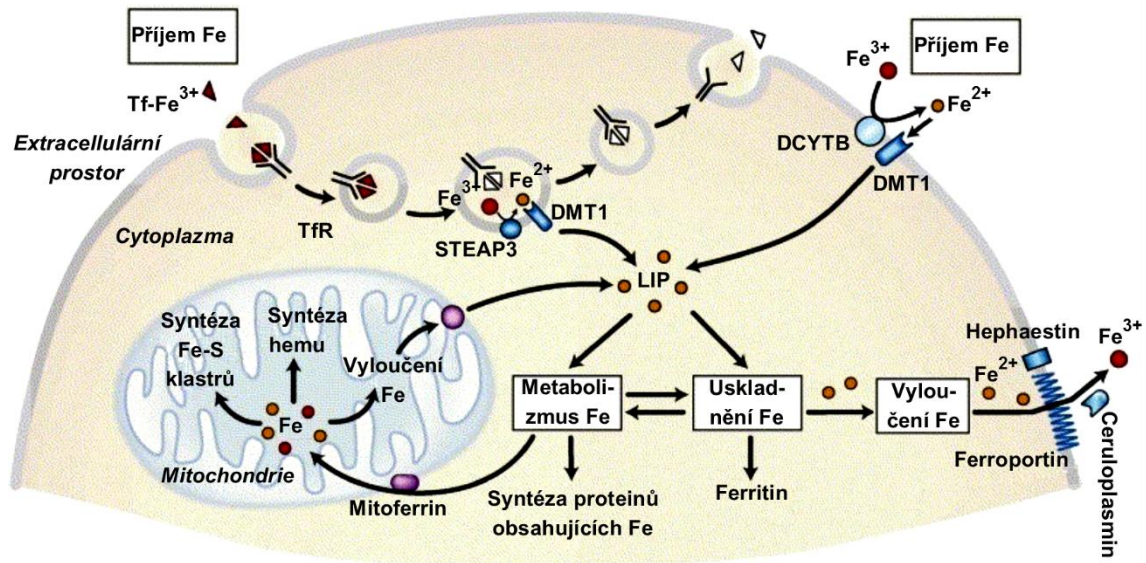
Erytrocyty jsou buňky s nejvyšším obsahem železa v těle. Metabolismus železa v jejich progenitorových buňkách je soustředěn hlavně na syntézu hemu. Mnoho výše uvedených poznatků o metabolismu železa v buňce bylo objeveno právě u erytroblastů (Richardson *et al.* 1997, Hentze *et al.* 2010).

2.1.5.2 Makrofágy

Makrofágy jsou soustředěné na recyklaci železa obsaženého v erytrocytech. Pinocytózou pohlcují senescentní erytrocyty a zajišťují jejich rozložení na znovu použitelné stavební jednotky. Železo z hemu je zde uvolněno enzymem hemoxygenázou a transportováno ven z buňky, kde se váže na plazmatický Tf (Richardson *et al.* 1997, Dunn *et al.* 2007).

2.1.6 Transport železa z buněk

Volné železo je z buněk vylučováno ferroportinem 1 (Donovan *et al.* 2000). Pro přenos hemového železa má buňka k dispozici efluxní transportér FLVCR (Feline leukaemic virus receptor) a protein závislý na ATP, ABCG2. Jedná se ale spíše o stresové uvolnění hemu v případě přetížení buňky hemovým železem (Latunde-Dada *et al.* 2006).



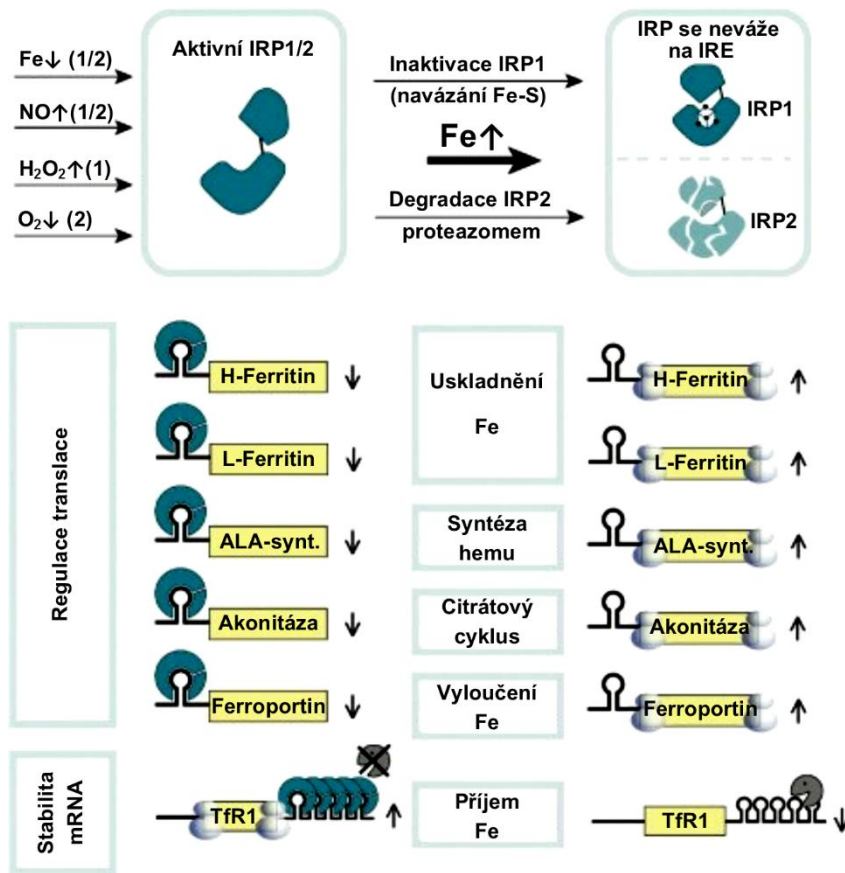
Obrázek 2.2 Distribuce železa (Fe) v buňce. Podrobný popis je obsažen v textu. Převzato a upraveno (Wallander *et al.* 2006).

2.1.7 Regulační mechanismy

2.1.7.1 Buněčné

Na úrovni buňky je metabolismus železa regulován proteiny regulujícími železo (iron regulatory protein, IRP), které se váží na odpovídající vazná místa na mRNA (iron responsive element; IRE) pro klíčové proteiny metabolismu železa. mRNA pro těžký (H) i pro lehký (L) řetězec skladovacího proteinu ferritinu, mRNA prvního enzymu syntézy hemu, 5-aminolevulátsyntázy (ALA-synt.), mRNA pro IRP1 popřípadě akonitázu (viz. níže) a mRNA ferroportinu 1 mají po jednom IRE na 5' nepřekládaném konci a navázáním IRP dojde k zablokování translace daného proteinu, zabráněním nasednutí malé podjednotky ribozomu. mRNA pro TfR 1 má na svém 3' nepřekládaném konci více IRE a navázání IRP na tyto místa chrání tuto mRNA před degradací a tím zvyšuje její translaci (Guo *et al.* 1995, Hentze *et al.* 2004). IRP existují ve dvou formách, které jsou odlišně regulovány. IRP1 se váže na IRE pouze při nízké hladině nitrobuněčného železa. Pokud je železa v buňce dostatek, váže se na IRP1 Fe-S klastr, čímž IRP1 ztrácí schopnost vázat se na IRE a funguje dále jako enzym akonitáza v citrátovém cyklu. Vazba Fe-S klastru je plně reverzibilní (Beinert *et al.* 1996). IRP2 je v případě správné nebo vyšší hladiny železa degradován ubiquitin – proteazomovým systémem (Guo *et al.* 1995). IRP také reagují zvýšenou vazností na IRE v přítomnosti

ROS, oxidu dusnatého nebo hypoxie (Pantopoulos *et al.* 1995, Iwai *et al.* 1998, Hentze *et al.* 2004).



Obrázek 2.3 Regulace metabolismu železa (Fe) v rámci buňky. Podrobný popis je v textu. Převzato a upraveno (Hentze *et al.* 2004).

2.1.7.2 *Systemové*

Regulaci hladiny železa v těle obstarává hormon syntetizovaný v hepatocytech, hepcidin. Je to protizánětlivě působící látka, která je v plazmě navázána na α_2 -makroglobulin (Peslova *et al.* 2009). Hecpidin se váže na ferroportin a způsobuje jeho internalizaci a degradaci v lysosomech (Nemeth *et al.* 2004, Yeh *et al.* 2004). Tímto procesem se sníží příjem železa ze střeva a zároveň i efflux železa z makrofágů. Exprese hepcidinu v hepatocytech je regulována hladinou železa v krvi, zásobami železa v játrech, erythropoetickou aktivitou, hypoxií a zánětlivými stavy (Fleming 2008, Hentze *et al.* 2010). Vysoká saturace Tf železem aktivuje transkripci hepcidinu a tím sníží vstřebávání železa do krve. Stejný efekt, zvýšení exprese hepcidinu, má i přítomnost zánětlivých cytokinů, interleukinů 1 a 6. Snížení hladiny železa v krvi je

v tomto případě obranná reakce proti patogenům, které potřebují železo pro svůj metabolismus. Na druhé straně růstový faktor uvolňovaný dozrávajícími červenými krvinkami, GDF15 (growth and differentiation factor 15), snižuje transkripci hepcidinu a zvyšuje hladinu železa v krvi. Snížení exprese hepcidinu je způsobeno i hypoxií přes signalizační dráhu faktoru indukovaného hypoxií (hypoxia inducible factor; HIF) (Fleming 2008, Hentze *et al.* 2010).

2.2 Rakovina prsu

Rakovina je zejména v rozvinutém světě jednou z hlavních příčin dlouhodobé pracovní neschopnosti i smrti. Rakovina se může rozvinout v jakékoli části těla a v jakémkoli orgánovém systému (Jemal *et al.* 2011, Siegel *et al.* 2013). Vzhledem k zaměření experimentální části této práce a rozsahu tématu nádorových onemocnění, zde bude zmíněna pouze rakovina prsu.

2.2.1 Incidence a mortalita

Rakovina prsu tvoří, dle mezinárodních statistik z roku 2008, asi 23 % ze všech nově diagnostikovaných nádorových onemocnění a 14 % úmrtí mezi všemi úmrtími na nádorová onemocnění (Jemal *et al.* 2011). Postihuje především ženy, u nichž patří mezi nejčastější typ nádorových onemocnění. Nejdůležitějšími rizikovými faktory jsou zvyšující se věk mateřství nebo jeho úplná absence, absence kojení, obezita a hormonální substituční terapie u starších žen (Jemal *et al.* 2011, DeSantis *et al.* 2014). Svou roli mohou sehrát i rodinné predispozice obzvláště mutace v tumor supresorových genech BRCA1 nebo BRCA2 (King *et al.* 2003). Díky mamografickému screeningu se v rozvinutých zemích relativně zvýšila včasná diagnóza této choroby a tím i možnost její úspěšné léčby (Jemal *et al.* 2011, DeSantis *et al.* 2014).

2.2.2 Diagnostika

Rakovinu prsu může někdy žena sama nahmatat jako bouličku v prsu nebo může registrovat změny vzhledu bradavky nebo kůže prsu. Podle některých poznatků ovšem nemá pravidelné prohmatávání prsu v diagnostice přílišný význam (Kosters *et al.* 2003). Dalším, spolehlivějším, způsobem diagnostiky je ultrazvukové nebo mamografické radiologické vyšetření. V České republice se plošný mamografický screening provádí u

žen od 45 let každé dva roky (ČR 2009). Při pozitivním mamografickém nálezů obvykle následuje biopsie s histologickým vyšetřením a vyšetření biochemických markerů (Petruzelka *et al.* 2002).

2.2.3 Rozdělení

Vzhledem k tomu, že každý pacient má svůj jedinečný typ rakoviny, bylo třeba vymyslet systém pro rychlou orientaci lékařů. Aspektů, podle kterých lze rakovinu prsu dělit na různá stádia, je více, proto se zde omezíme na dva nejpoužívanější, které se ovšem většinou kombinují.

2.2.3.1 Velikost a invazivnost nádoru

Velikost a invazivnost nádoru hodnotí systém „TNM“ (Tumor, Node, Metastasis). Písmeno „T“ označuje přítomnost rakovinných buněk v oblasti primárního nádoru a číslo za tímto písmenem označuje velikost nádoru. Písmeno „N“ značí rakovinné buňky přítomné v nejbližších mízních uzlinách, kam byly doneseny lymfou, a číslo za tímto písmenem označuje počet ovlivněných uzlin. Písmeno „M“ značí, že rakovinné buňky jsou ve vzdálených lymfatických uzlinách (Singletary *et al.* 2006). Modelové hodnocení nádoru menšího než 2 cm, bez infiltrace mízních uzlin pak může vypadat takto: T1, N0, M0.

2.2.3.2 Genotyp

Dělení podle databáze TCGA (The Cancer Genome Atlas) vychází z genotypizace pěti set vzorků různých rakovin prsu. Rakovina prsu zde byla rozdělena na čtyři základní subtypy: luminální A, luminální B, bazální a obohacený o receptor lidského epidermálního růstového faktoru 2 (human epidermal growth factor receptor 2; HER2) (Ma *et al.* 2013). Luminální typy jsou nejvíce heterogenní skupinou, co se genové exprese týče. Exprimují estrogenový receptor, transkripční faktory GATA3, FOXA1, XBP1, regulátor apoptózy Bcl-2 a protoonkogen MYB. Tento genový profil je charakteristický pro epiteliální buňky mlékovodů. Luminální typ B se od luminálního typu A liší nižší expresí luminálních genů, zvýšenou expresí genů podporujících proliferaci a horší prognózou. Bazální typ exprimuje geny pro keratiny 5, 6 a 17 a hojně i geny podporující buněčné dělení. Bazální typ často neexprimuje estrogenové,

progesteronové ani HER2 receptory a tím se řadí mezi takzvaně „trojitě-negativní“ rakoviny prsu. Typ obohacený o HER2 receptor je specifikován zejména zvýšenou expresí tohoto receptoru a růstového faktoru GRB7 (Sorlie *et al.* 2003, Cancer Genome Atlas 2012, Ma *et al.* 2013).

2.2.4 Léčba

2.2.4.1 Chirurgie

Chirurgický zásah je v případě rakoviny prsu zpravidla prvním krokem. Může být odstraněn jen lokalizovaný nádor (tumorektomie), čtvrtina prsu (quadranektomie) nebo v případě rozsáhlejšího nádoru celý prs (mastektomie). Podle výsledků biopsie jsou odstraněny i postižené mízní uzliny v podpaží (Veronesi *et al.* 2002).

2.2.4.2 Radioterapie

Radioterapie často navazuje na chirurgické odnětí nádoru. Může být vnější nebo vnitřní. Vnitřní radioterapie (brachyterapie) je prováděna během operace, kdy je otevřená operační rána ještě před zašitím ozářena z bezprostřední blízkosti. Tento přístup by měl zahubit případné neodstraněné rakovinné buňky na okraji operačního pole a zabránit jejich šíření (Belletti *et al.* 2008, Vaidya *et al.* 2011). Dále po operaci nebo i u žen před operací je ozařován celý prs. Ozařování zvnějšku musí být prováděno velmi opatrně, aby nedošlo k nadměrnému ozáření okolních orgánů jako je srdce, plíce, popřípadě druhý prs (Clarke *et al.* 2005, Vaidya *et al.* 2010).

2.2.4.3 Farmakoterapie

2.2.4.3.1 Blokáda působení estrogenu

Tamoxifen je široce používaný kompetitivní inhibitor estrogenových receptorů, který je používán samozřejmě jen u nádorů exprimujících estrogenové receptory. Jde hlavně o adjuvantní terapii před nebo po chirurgickém odstranění nádoru, která zabraňuje estrogení stimulaci růstu rakovinných buněk (Fisher *et al.* 1998, Brunton *et al.* 2011).

Obdobné použití mají i inhibitory enzymu aromatázy (anastrozol, letrozol, emestan), které blokují přeměnu androgenů na estrogeny. Zatímco anastrozol a letrozol

jsou takzvané nesteroidní inhibitory aromatázy a váží se na aromatázu kompetitivně, exemestan je steroidní inhibitor aromatázy, který je nekompetitivní, a jeho navázání vede k degradaci enzymu (Smith *et al.* 2003, Brunton *et al.* 2011).

2.2.4.3.2 Progestiny a androgeny

Syntetické analogy progesteronu a androgenů mohou být použity u metastazující rakoviny prsu, která exprimuje progesteronové a estrogenové receptory. Je to až druhořadá možnost terapie vhodná pro kachektické pacienty (Brunton *et al.* 2011).

2.2.4.3.3 Monoklonální protilátky a cílené malé molekuly

Cílená terapie je poměrně nový přístup k léčbě rakoviny. V terapii rakoviny prsu je hlavně zaměřená na HER2 receptor. Humanizovaná monoklonální protilátka transtuzumab se váže na HER2, zabraňuje jeho dimerizaci a tím aktivaci tyrozinkináz. Tímto mechanismem se blokuje dráha vedoucí k buněčnému dělení a k angiogenezi. V terapii se může kombinovat s klasickým chemoterapeutikem/stabilizátorem mikrotubulů paclitaxelem. Zavedení transtuzumabu do léčby vedlo k velkému zlepšení prognózy pacientek s nádory, které exprimují více HER2, protože tyto nádory příliš nereagovaly na klasickou chemoterapii (Vogel *et al.* 2002).

Lapatinib je malá molekula, která se váže na jiné místo HER2 než transtuzumab, ale váže se také na HER1, proto je možné lapatinib použít i při rezistenci k transtuzumabu nebo tyto dvě látky kombinovat (Blackwell *et al.* 2010). Lapatinib je také možné kombinovat s prekurzorem pyrimidinového analogu/antimetabolitu 5-fluorouracilu, capecitabinem (Geyer *et al.* 2006).

Bevacizumab je humanizovaná protilátka proti vaskulárnímu endoteliálnímu růstovému faktoru A (vascular endothelial growth factor A; VEGF-A). Blokací tohoto proteinu inhibuje angiogenezi. Používá se při léčbě metastazující rakoviny prsu v kombinaci s paclitaxelem (Miller *et al.* 2007).

2.2.4.3.4 Klasická chemoterapie

Pokud jsou rakovinné buňky trojitě-negativní na výskyt receptorů, je indikována klasická chemoterapie. Tato chemoterapie se může ale používat i u nádorů exprimujících estrogenové, progesteronové nebo HER2 receptory a kombinovat

s antiestrogeny i protilátkami a to hlavně v případech, kdy se předpokládá horší odpověď nádoru k monoterapii a pokud je pozitivní nález v mízních uzlinách (Goldhirsch *et al.* 2009). Přehled farmakoterapie uvádí tabulka 2.1. Látky označované za klasickou chemoterapii jsou zde uvedeny v částech I.-III. Pro léčbu rakoviny se tyto látky kombinují a podávají se v cyklech. Jednou takovou kombinací může být čtrnáctidenní cyklus denního podávání alkylační látky cyklofosfamidu a analogu kyseliny listové/antimetabolitu methotrexátu doplněný 1. a 8. den o dávku 5-fluorouracilu, který se opakuje každé čtyři týdny. Další cyklus je například čtrnáctidenní cyklus denního podávání cyklofosfamidu doplněný 1. a 8. den o dávku antracyklinového antibiotika/blokátoru enzymu topoizomerázy II α doxorubicinu (nebo epirubicinu) a 5-fluorouracilu, také s opakováním každé čtyři týdny. Dále je možná i kombinace cyklofosfamidu s doxorubicinem (nebo epirubicinem) 28 dní, následovaná paclitaxelem (nebo docetaxelem). Chemoterapie se vždy volí individuálně podle histologie a rozsahu neoplastického onemocnění (Goldhirsch *et al.* 2001, Moller *et al.* 2008).

Tabulka 2.1 Přehled farmakoterapie používané při léčbě neoplastických onemocnění. Převzato a upraveno z Goodman & Gilman's The Pharmacological Basis of Therapeutics – 12. vydání (Brunton *et al.* 2011).

Třída látek	Typ látek	Zástupci
I. Alkylační látky	Dusíkaté yperity	mechlorethamin
		cyklofosfamid, ifosfamid
		melphalan
		chlorambucil
	Deriváty methylhydrazinu	prokarbazin (<i>N</i> -methylhydrazin)
	Alkylsulfonáty	busulfan
	Deriváty nitrosomočoviny	karmustin
		streptozocin
		bendamustin
	Triazeny	dakarbazin, temozolomid
Koordinační komplexy platiny	cisplatina, karboplatina, oxaliplatina	

Třída látek	Typ látek	Zástupci
II. Antimetabolity	Analogy kyseliny listové	methotrexát
		pemetrexed
	Pyrimidinové analogy	5-fluorouracil, capecitabin
		cytarabin
		gemcitabin
		5-aza-cytidin, deoxy-5-aza-cytidin
	Purinové analogy	6-merkaptopurin
		6-thioguanin
		pentostatin
		fludarabin
		clofarabin
		nelarabin

Třída látek	Typ látek	Zástupci
III. Přírodní produkty	Vinca alkaloidy	vinblastin
		vinorelbin
		vinkristin
	Taxany	paclitaxel, docetaxel
	Podofylotoxiny	etoposid
		teniposid
	Camptoteciny	topotecan, irinotecan
	Antibiotika	dactinomycin (actinomycin D)
		daunorubicin
		doxorubicin
	Echinocandiny	trabectedin
	Antracendiony	mitoxantron
		bleomycin
mitomycin C		
Enzymy	L-asparagináza	

Třída látek	Typ látek	Zástupci
IV. Hormony a jejich antagonisté	Supresor adrenokortikálních hormonů	mitotan
	Hormony kůry nadledvin	prednison a jeho analogy
	Progestiny	hydroxyprogesteron kapronát, medroxyprogesteron acetát, megestrol acetát
	Estrogeny	diethylstilbestrol, ethynilestradiol
	Antiestrogeny	tamoxifen, toremifen
	Inhibitory aromatázy	anastrozol, letrozol, exemestan
	Androgeny	testosteron propionát, fluoxymesteron
	Antiandrogen	flutamid, casodex
	Analog gonadotropního hormonu	leuprolid

Třída látek	Typ látek	Zástupci
V. Různé	Substituovaná močovina	hydroxyurea
	Diferenciační látky	tretinoin, oxid arzenitý
		inhibitor histon-deacetylázy (vorinostat)
	Inhibitory tyrozinkinázy	imatinib
		dasatinib, nilotinib
		gefitinib, erlotinib
		sorafenib
		sunitinib
		lapatinib
	Inhibitor proteazomu	bortezomib
	Cytokiny	interferon α , interleukin 2
	Imunomodulátory	thalidomid
lenalidomid		
Inhibitory mTOR	temsirolimus, everolimus	

2.2.5 Význam železa u rakoviny prsu

Železo je rizikovým faktorem pro vznik rakoviny kvůli jeho schopnosti katalyzovat reakce, při kterých vznikají ROS (viz kapitola 2.1.1). Z několika studií vyplývá, že lidé se zvýšeným obsahem železa v normální prsní tkáni mohou mít vyšší šanci k onemocnění rakovinou, obzvláště pak ti, kteří přijímají železo v hemové podobě (Cui *et al.* 2007, Kallianpur *et al.* 2008). Z tohoto důvodu může být i vyšší predispozice k rakovině prsu u žen po menopauze, kterým se již nesnižuje hladina železa menstruačním krvácením (Hong *et al.* 2007, Huang 2008).

Hladina železa je ovšem důležitá i během onemocnění rakovinou prsu. Rakovinné buňky jsou typické svým rychlým růstem a dělením, a proto potřebují více nutričních a stopových prvků (Ionescu *et al.* 2006). Železo je důležité pro katalýzu mnoha buněčných reakcí i pro enzym ribonukleotid reduktázu, která je bezprostředně spjatá se syntézou DNA. Rakovinné buňky tedy potřebují vyšší přísun železa než normální somatické buňky. Rakovinné buňky proto také exprimují na svém povrchu více TfR pro příjem železa (Shindelman *et al.* 1981) a naopak méně efluxního proteinu ferroportinu (Pinnix *et al.* 2010). Navíc mají rakovinné buňky schopnost vytvářet hormon hepcidin, běžně syntetizovaný v játrech, který podporuje internalizaci ferroportinu (Pinnix *et al.* 2010). Některé buňky rakoviny prsu dokonce na základě estrogení stimulace syntetizují protein podobný Tf, aby zvýšily přísun železa z okolí (Vandewalle *et al.* 1989, Vyhlidal *et al.* 2002). Železo je v buňkách nejen ihned používáno, ale buňka si tvoří zásoby ve skladovacím proteinu ferritinu (Elliott *et al.* 1993). U žen s rakovinou prsu byl zaznamenán i zvýšený sérový ferritin, který byl špatným prognostickým faktorem (Jacobs *et al.* 1976).

2.3 Chelátory železa

Za chelátor železa lze označit, každou látku, která je schopna nespecificky vázat přechodné prvky. V této kapitole bude probírána skupina látek, která je schopná vázat železo relativně specificky, což je klíčem její biologické aktivity.

2.3.1 Použití chelátorů železa

2.3.1.1 Nemoci s přetížením železem

První indikací chelátorů železa byla onemocnění s přetížením železem, kde zvýšené ukládání železa způsobuje nadměrný oxidační stres, hlavně v srdci, játrech a pankreatu, zvýšené riziko vzniku rakoviny a snížení imunity (Jomova *et al.* 2011, Oliveira *et al.* 2014). Mezi tato onemocnění patří porucha vstřebávání železa hereditární hemochromatóza, kdy je příjem železa patologicky zvýšen (Fleming *et al.* 2002). Dále neurologické postižení Friedreichova ataxie, kdy je kumulace železa způsobena sníženou expresí mitochondriálního proteinu frataxinu (Richardson 2003). Druhotně může vznikat přetížení železem při opakovaných krevních transfúzích podávaných pacientům s thalasemií nebo s myelodysplastickým syndromem (Olivieri *et al.* 1997, Greenberg 2006). Podáním chelátoru železa lze docílit normalizace hladiny železa v těle a tím prodloužení života. U těchto onemocnění se používají chelátory desferrioxamin, desferasirox a deferipron (Kwiatkowski 2011).

2.3.1.2 Léčba nádorových onemocnění

Chelátory železa jsou v současné době široce zkoumanou skupinou pro léčbu rakoviny (Buss *et al.* 2003, Richardson *et al.* 2009). Použitím chelátorů železa u rakovinných buněk je zasaženo hned několik signálních drah. Přímo je zasažena už dříve zmiňovaná ribonukleotid reduktáza, kde chelátor odstraní tyrozilový radikál z R2 podjednotky a zamezí tak přeměně ribonukleotidů na deoxyribonukleotidy, katalyzované tímto enzymem (Nyholm *et al.* 1993). Touto blokací se může aktivovat tumor supresorový protein p53, který dále blokuje buněčné dělení (Tanaka *et al.* 2000). Nedostatek železa nepřímo ovlivňuje průběh buněčného cyklu změnou exprese proteinů nutných k progresi buněčného cyklu. Chelátory železa způsobují snížení aktivity cyklin dependentních kináz (CDK) 2 a 4 a cyklinů A, D a E a naopak zvyšují transkripci inhibitoru CDK, proteinu p21. Tyto zásahy do průběhu buněčného cyklu vedou k zástavě buňky mezi fázemi G₁ a S (Le *et al.* 2002, Yu *et al.* 2007). Chelatace železa také vyvolává zvýšenou expresi HIF, který může způsobit nechtěné zvýšení vaskularizace tumoru, ale pokud je v buňce kumulován vede k zastavení buněčného dělení a apoptóze. HIF působí zvýšenou expresí supresoru metastazování NDRG1 a pro-apoptotického faktoru BNIP3 (Pahl *et al.* 2005, Kovacevic *et al.* 2011b).

2.3.2 *Rozdělení chelátorů železa*

Chelátory železa jsou velmi heterogenní skupinou látek. Dělí se podle různých kritérií. Zde budeme používat dělení na přírodní látky a jejich analogy a na syntetické látky. Důležitou charakteristikou je lipofilita chelátorů, která je klíčová pro průchod přes buněčnou membránu a determinující, jestli bude látka orálně aktivní nebo ji bude třeba podávat injekčně. Obecně platí, že více lipofilní látky mají většinou silnější antiproliferační účinky (Kalinowski *et al.* 2005, Pahl *et al.* 2005). Další obecnou charakteristikou chelátorů je počet vazných míst v molekule chelátoru, tzv. denticita. Atom železa má šest koordinačních vazeb, které by pro plnou chelataci měly být vázány na molekulu chelátoru. Chelátory, které mají šest vazných míst, nazýváme hexadentální, chelátory s třemi vaznými místy (jeden atom železa je plně chelátován dvěma molekulami chelátoru) jsou tridentální a chelátory s dvěma vaznými místy (jeden atom železa je plně chelátován třemi molekulami chelátoru) jsou bidentální (Liu *et al.* 2002).

2.3.2.1 Přírodní látky a jejich analogy

2.3.2.1.1 Siderofory

Siderofory jsou látky produkované mikroorganismy (bakteriemi, nižšími houbami a řasami), které chelatují železo z okolí a usnadňují jeho příjem do buňky (Neilands 1995).

2.3.2.1.1.1 *Desferrioxamin*

Desferrioxamin je siderofor poprvé identifikovaný v 60. letech 20. století. Tento hexadentální chelátor železitých iontů byl izolován z aktinobakterie *Streptomyces pilosus* a po klinických studiích byl roku 1968 schválen americkou agentorou FDA (Food and Drug Administration) jako léčivo pro terapii nemocí s přetížením železem. Od té doby stále zůstává v praktickém použití (Buss *et al.* 2003, Sharpe *et al.* 2011). V různých studiích prokázal desferrioxamin antiproliferační potenciál (Dezza *et al.* 1989, Donfrancesco *et al.* 1990, Hann *et al.* 1992) a zároveň byl také jádrem pro výzkum molekulárních mechanismů deprivace železa (viz. kapitola 2.3.1.2). Tato látka má však nevýhodu v krátkém biologickém poločasu (cca 10 min) a v nízké lipofilitě,

kvůli které nelze podat perorálně a do buněk prochází jen pomalu pinocytózou. Pro podání desferrioxaminu je proto potřeba použít dlouhé a opakované subkutánní infuze, které nejsou pro pacienty pohodlné ani příjemné (Kwiatkowski 2011). Proto probíhá výzkum lipofilních chelátorů železa, které je možné podávat perorálně.

2.3.2.1.1.2 *Desferrithiocin*

Desferrithiocin je tridentální siderofor, který je možné podávat perorálně. Je produkovaný bakterií *Streptomyces antibioticus* (Buss *et al.* 2003, Sharpe *et al.* 2011) a kromě silné afinity k železitým iontům může vázat i ionty zinku a mědi (Anderegg *et al.* 1990). Vykazoval protinádorové účinky především na hepatocelulární karcinom (Kicic *et al.* 2002), ale při delším podávání hlodavcům a opicím působil snižování tělesné hmotnosti a nefrotoxicitu (Bergeron *et al.* 1993). Chemickými modifikacemi byl pozměněn na stejně protinádorově účinné látky s nižší toxicitou (Bergeron *et al.* 2012).

2.3.2.1.1.3 *Desferri-exocheliny*

Desferri-exocheliny jsou skupinou látek produkovanou bakterií *Mycobacterium tuberculosis*. Tyto látky jsou hexadentální a jsou schopné vyvazovat železo i z Tf a z ferritinu (Gobin *et al.* 1996). Byla u nich zaznamenána schopnost selektivně navozovat apoptózu u linií prsního karcinomu, přičemž nebyly toxické k normální prsní tkáni (Pahl *et al.* 2001).

2.3.2.1.2 Chelátory rostlinného původu

2.3.2.1.2.1 *Curcumin*

Curcumin je polyfenolická látka izolovaná z Kurkumy (*Curcuma longa*) používané hojně v Indii a Číně jako koření (Hatcher *et al.* 2008). Ve vodném prostředí a fyziologickém pH váže hlavně železité ionty a vytváří s nimi komplexy $[\text{Fe}^{3+}(\text{H}_2\text{curcumin})(\text{OH})_2]$ (Bernabe-Pineda *et al.* 2004). Tato látka má komplexní protizánětlivé i protinádorové účinky. Curcumin ovlivňuje signalizační dráhu transcripčního faktoru NF- κ B, který dále inhibuje prozánětlivý enzym cyklooxygenázu 2 (COX2), snižuje expresi cyklinu D1, anti-apoptických proteinů Bcl-2 and Bcl-X_L a pro-angiogenního proteinu VEGF-A (Hatcher *et al.* 2008, Kunnumakkara *et al.* 2009). V současné době probíhají klinické studie curcuminu jako chemoterapeutika a

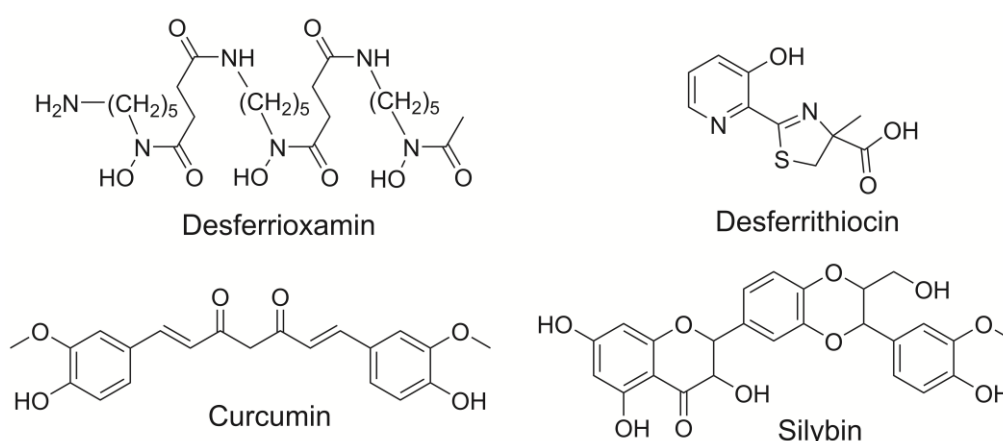
chemopreventiva při různých nádorových onemocnění, např. kolorektálního karcinomu, rakoviny pankreatu nebo myelomu. V již proběhlých studiích byla prokázána jeho nízká toxicita (Hatcher *et al.* 2008).

2.3.2.1.2.2 Silybin

Silybin je látka z plodu Ostropestřece mariánského (*Silbum marianum*). Je to látka s hepatoprotektivními účinky, která je špatně rozpustná ve vodě (Jacobs *et al.* 2002). Bylo prokázáno, že tvoří komplexy s železitými ionty (Borsari *et al.* 2001). Silybin snižuje expresi prozánětlivých cytokinů (Tyagi *et al.* 2009) a byly u něj prokázány protirakovinné účinky *in vitro* i *in vivo* (Gharagozloo *et al.* 2008, Li *et al.* 2008, Singh *et al.* 2008, Cui *et al.* 2009).

2.3.2.1.2.3 Polyfenoly ze zeleného čaje

Výtažek ze zeleného čaje obsahuje katechiny s antioxidačními účinky, které byly zkoumány jako prevence neurodegenerativních onemocnění (Mandel *et al.* 2006), ale také jako možná prevence rozvoje rakovinných onemocnění a prostředek ke snížení invazivity nádorů (Zaveri 2006, Thangapazham *et al.* 2007). Z některých studií vyplývá, že tyto látky jsou schopné chelátovat železo (Guo *et al.* 1996, Ryan *et al.* 2007). Není ovšem zcela objasněné, jaký efekt by mělo podávání vysokých dávek katechinů na organismus (Sharpe *et al.* 2011).



Obrázek 2.4 Chemické vzorce vybraných chelátorů ze skupiny přírodních látek.

2.3.2.2 Syntetické chelátory

2.3.2.2.1 Deferipron

Deferipron (L1) je bidentální lipofilní chelátor železa. Byla to první látka s možností perorálního podání pro pacienty s nemocemi s přetížením železem, která se dostala do klinického testování v 80. letech 20. století (Kwiatkowski 2011). Byl prokázán jeho efekt na snížení depozice železa v srdeční tkáni a zlepšení srdečních funkcí (Anderson *et al.* 2002, Piga *et al.* 2003). V průběhu jeho testování byly ale pozorovány nežádoucí účinky v podobě agranulocytózy a neutropenie (Cohen *et al.* 2003) a v jedné studii i zvýšení výskytu jaterní fibrózy (Olivieri *et al.* 1998). Po zvážení přínosu a rizika pro pacienty bylo v roce 1999 uděleno povolení pro léčbu v Evropě a v některých asijských zemích. Americká FDA však deferipron nikdy nepovolila (Kalinowski *et al.* 2005, Sharpe *et al.* 2011). Jako výhodné se ukázalo kombinovat deferipron s desferrioxaminem, kdy se může snížit dávka obou chelátorů, a tím se sníží i výskyt nežádoucích účinků (Berdoukas *et al.* 2009). Deferipron v některých studiích prokázal i antiproliferační účinky (Chenoufi *et al.* 1998, Simonart *et al.* 2002).

2.3.2.2.2 Deferasirox

Deferasirox (ICL670A) je tridentální, lipofilní, perorálně účinný chelátor železa. Byl vyvinut firmou Novartis a v roce 2005 schválen FDA a později i Evropskou unií pro léčbu nemocí s přetížením železem (Kwiatkowski 2011, Sharpe *et al.* 2011). Deferasirox má vysokou afinitu k železitým iontům, ale může vázat i hliník (Heinz *et al.* 1999). Bylo prokázáno, že deferasirox snižuje zásoby železa v játrech a v sérovém ferritinu (Cappellini *et al.* 2006) a stabilizuje zásoby železa v srdeční tkáni (Pennell *et al.* 2010, Wood *et al.* 2010). V současné době je zkoumána vysoká antiproliferační účinnost této látky, která by se v budoucnu mohla používat i v terapii rakovinných onemocnění (Ohyashiki *et al.* 2009, Ford *et al.* 2013, Lui *et al.* 2013).

2.3.2.2.3 Tachpyridin

Tachpyridin je hexadentální chelátor, který může vázat železnaté, vápenaté, manganaté, hořečnaté, měďnaté a zinečnaté ionty (Torti *et al.* 1998). Za jeho protinádorovou účinnost na různých nádorech (Torti *et al.* 1998, Abeysinghe *et al.* 2001) jsou ovšem zodpovědné komplexy se železem. Tachpyridin může totiž vázat i

železité ionty, které redukuje na železnaté, za vzniku ROS (Haber-Weissova reakce) (Samuni *et al.* 2002).

2.3.2.2.4 Dexrazoxan

Dexrazoxan (ICRF-187) je katalytický inhibitor topoizomerázy II vyvinutý k léčbě rakovinných onemocnění (Fattman *et al.* 1996). Je to cyklický analog kyseliny ethylendiamintetraoctové (EDTA), která je chelátorem širokého spektra kovů a se železem tvoří redox-aktivní komplexy (Huang *et al.* 1982). Dexrazoxan se po vstupu do buněk aktivuje na otevřený analog ADR-925, který váže železo s vysokou afinitou (Weiss *et al.* 1999). Jako velmi výhodné se ukázalo kombinovat dexrazoxan s antracyklinovými antibiotiky, kdy dexrazoxan snižuje jejich kardiotoxicitu. Dlouho se mělo za to, že dexrazoxan přeměněný na ADR-925 vyvazuje železo z redox-aktivních komplexů antracyklinových antibiotik a předchází tak oxidačnímu stresu v srdeční tkáni (Swain *et al.* 1997, Popelova *et al.* 2009). Novější hypotézou je ochrana srdečních buněk katalytickou inhibicí topoizomerázy II β dexrazoxanem, což blokuje vznik dvouřetězcových zlomů DNA způsobených antracyklinovými antibiotiky. Cíl antracyklinových antibiotik v rakovinných buňkách je totiž topoizomeráza II α (Vejpgangsa *et al.* 2014).

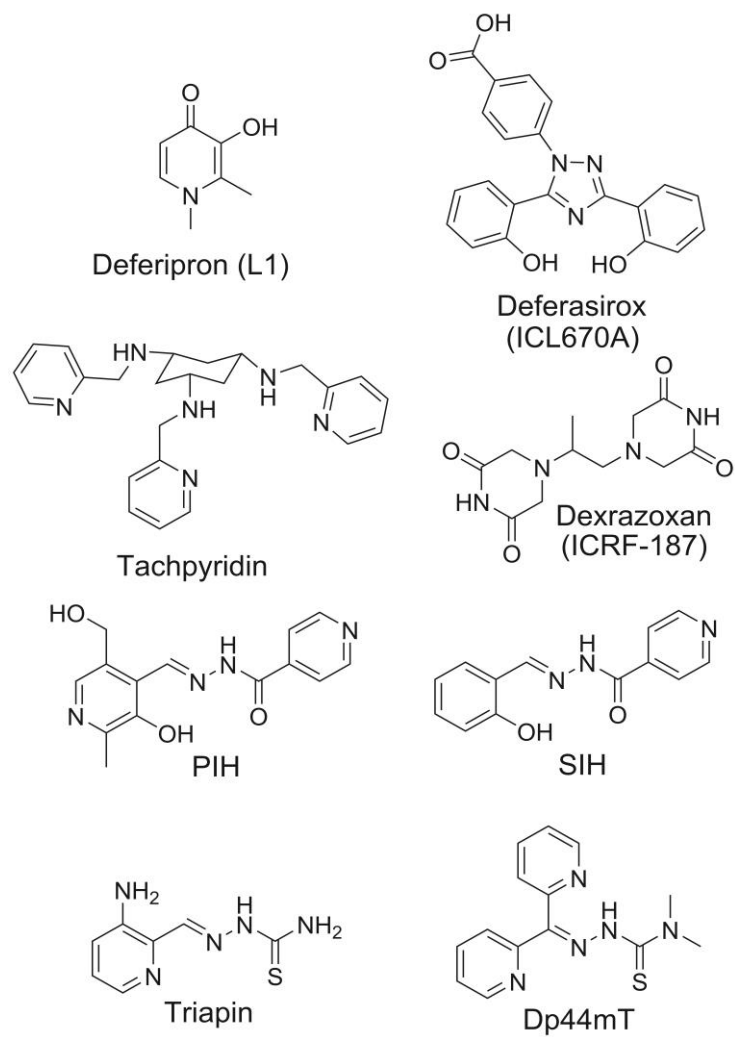
2.3.2.2.5 Aroylhydrazony

Tyto tridentální, lipofilní chelátory železitých iontů jsou odvozené od pyridoxal isonikotinoyl hydrazonu (PIH), který byl v roce 1954 připraven a později odhalena jeho schopnost chelatovat železo v laboratoři profesora Poňky (Ponka *et al.* 1979). PIH byl studován jako nadějná, perorálně dostupná látka pro léčbu nemocí s přetížením železem, ale nebyl uveden do klinické praxe. Od látky PIH bylo odvozeno mnoho derivátů a i několik sérií látek (Baker *et al.* 1992, Richardson *et al.* 1995). Jako silný chelátor železa s antioxidačními účinky se projevil SIH. Tato látka prokázala kardioprotektivní, radioprotektivní ale i antiproliferační účinky (Horackova *et al.* 2000, Simunek *et al.* 2008, Berndt *et al.* 2010). Přičemž její krátkodobý i dlouhodobý toxicitní profil byl velmi příznivý (Klimtova *et al.* 2003). Antiproliferačními účinky látek odvozených od SIH se detailněji zabývají další části této práce. Jinou sérií jsou látky odvozené od 2-hydroxy-1-naftylaldehyd isonikotinoyl hydrazonu (NIH), které jsou lipofilnější než

předchozí série a mají vysokou antiproliferační aktivitu (Richardson *et al.* 1995, Richardson *et al.* 1997).

2.3.2.2.6 Thiosemikarbazony

Od aroylhydrazonových chelátorů železa se postupným vývojem došlo k thiosemikarbazonům. Thiosemikarbazony jsou tridentální, lipofilní chelátory železa a mědi, s kterými mohou tvořit komplexy katalyzující vznik ROS. Některé látky tedy působí antiproliferativně jak deplecí železa, tak i produkcí ROS (Sartorelli *et al.* 1976, Noulisri *et al.* 2009). Některé látky z této skupiny prokazují velmi vysokou antiproliferativní účinnost a zároveň nízkou toxicitu k nenádorovým buňkám (Richardson *et al.* 2006, Kalinowski *et al.* 2007). Chelátor železa triapin byl dokonce přijat do klinického testování, během něhož se ale projevil nežádoucí účinky v podobě hypoxie, methemoglobinemie, neutropenie a leukopenie (Murren *et al.* 2003, Knox *et al.* 2007, Ma *et al.* 2008). V současné době bylo připraveno již velké množství thiosemikarbazonů, z nichž ty nejnadějnější jsou dále zkoumány. Z nejuspěšnějších můžeme jmenovat například di-2-pyridylketon-4,4-dimethyl-3-thiosemikarbazon (Dp44mT) (Noulisri *et al.* 2009, Rao *et al.* 2009), di-2-pyridylketon-4-cyklohexyl-4-methyl-3-thiosemikarbazon (DpC) (Kovacevic *et al.* 2011a), 2-benzoylpyridin-4,4-dimethyl-3-thiosemikarbazon (Bp44mT) (Yu *et al.* 2012) a 2-benzoylpyridin-4-ethyl-3-thiosemikarbazon (Bp4eT) (Stariat *et al.* 2012). Touto skupinou látek jsme se také zabývali v části této práce.



Obrázek 2.5 Chemické vzorce vybraných syntetických chelátorů.

3 Cíle práce

- Studium antiproliferačního působení nových analogů odvozených od chelátoru železa SIH. Sledování jejich chelatační aktivity, toxicity k nenádorovým buňkám a dalších vlastností.
- *In vitro* hodnocení společného podávání chelátorů železa a klinicky používaných chemoterapeutik pro léčbu rakoviny prsu. Kvantitativní vyjádření synergických, aditivních nebo antagonistických účinků.
- Studium biologických vlastností nových chelátorů železa ze skupiny thiosemikarbazonů.
- Studium biologických vlastností nadějného thiosemikarbazonového chelátoru, Bp4eT a antiproliferačního a toxického působení jeho metabolitů po první fázi biotransformace.
- Charakterizace kardioprotektivních a redoxních vlastností klinicky používaných a experimentálních chelátorů železa.
- Studium protektivního účinku katalytického inhibitoru topoizomerázy II a prochelátoru železa dexrazoxanu proti antracyklinové kardiotoxicitě a vliv společného podávání antracyklinů a katalytických inhibitorů topoizomerázy II na proliferaci nádorových buněk.

4 Komentáře k pracím

Tato disertační práce je předkládána jako komentovaný soubor prací. Čtyři práce byly otištěny v impaktovaných časopisech, jedna práce je v současné době v recenzním řízení v odborném časopise a dvě práce jsou ve formě připravovaných rukopisů. Všechny publikace (rukopisy) jsou původní experimentální práce zaměřené na charakterizaci antiproliferačních účinků nových chelátorů železa nebo na jejich schopnost předcházet kardiotoxickým inzultům.

Tato disertační práce byla vypracována jako součást dlouhodobého výzkumu realizovaného na pracovištích Farmaceutické a Lékařské fakulty Univerzity Karlovy v Hradci Králové v rámci Centra pro výzkum toxických a protektivních účinků léčiv na kardiovaskulární systém, které je jedním z univerzitních výzkumných center Univerzity Karlovy v Praze (UNCE 204019/304019/2012).

4.1 Popis závislostí chemické struktury a biologických účinků nových analogů SIH I

Macková E, Hrušková K, Bendová P, Vávrová A, Jansová H, Hašková P, Kovaříková P, Vávrová K, Šimůnek T. Methyl and ethyl ketone analogs of salicylaldehyde isonicotinoyl hydrazone: novel iron chelators with selective antiproliferative action. *Chem Biol Interact.* 2012; **197**(2-3): 69-79. IF₂₀₁₂ = 2,967

Chelátor železa SIH je z farmakologicko/toxikologického hlediska v mnoha směrech velmi zajímavá látka (Simunek *et al.* 2005, Berndt *et al.* 2010). Mimo jiné má i antiproliferační účinky (Laskey *et al.* 1988). Jeho zásadní nevýhodou je však náchylnost k hydrolytickému štěpení hydrazonové vazby. Pro zvýšení stability byla na katedře anorganické a organické chemie FaF UK připravena série devíti analogů SIH, u kterých byla prokázána signifikantně vyšší stabilita v králičí plazmě (Hruskova *et al.* 2011). Cílem naší práce pak bylo prověřit míru a specifitu antiproliferačních účinků této série látek.

Antiproliferační účinky methyl- a ethyl-analogů SIH s různými substituenty na aromatickém cyklu v ketonické části molekuly byly studovány na buněčné linii lidského prsního adenokarcinomu MCF-7 a na buněčné linii lidské promyelocytární leukémie HL-60. Toxicita k nenádorovým buňkám byla pak sledována na buněčné linii H9c2 odvozené od neonatální potkaní srdeční tkáně. Sedm z devíti nových analogů SIH

prokázalo vyšší selektivitu k nádorovým buňkám, tedy vysoký antiproliferační účinek a nízkou toxicitu k nenádorovým buňkám. Dvě látky s druhou hydroxy skupinou v poloze 4 nebo 6 na aromatickém jádře byly ale naopak toxicitější k srdečním buňkám. Tato modifikace se tedy ukázala jako nevhodná pro terapeutické využití. Látky s methoxy skupinou v poloze 4 nebo s chlorem v poloze 5 na aromatickém jádře dosáhly dobré antiproliferační účinnosti, ale jejich specifita se oproti původnímu chelátoru SIH příliš nezvýšila. Na druhou stranu selektivita látky s hydroxy skupinou v poloze 4 a acetylovou skupinou v poloze 5 na aromatickém kruhu nebo látky s šestičlenným cyklem kondenzovaným k aromatickému jádru byla poměrně vysoká, nicméně jejich antiproliferační účinnost se projevovала až ve vyšších koncentracích.

Jako látky s nejvyšším protinádorovým potenciálem, tedy specifickou antiproliferační účinností, se projevíly analogy SIH s methylem nebo s ethylem v sousedství hydrazonové vazby a methylanalog s nitroskupinou v poloze 5 na aromatickém kruhu, tedy látky (*E*)-*N'*-(1-(2-hydroxyfenyl)ethyliden)isonikotinohydrazid (HAPI), (*E*)-*N'*-(1-(2-hydroxyfenyl)propyliden)isonikotinohydrazid (HPPI) a (*E*)-*N'*-(1-(2-hydroxy-5-nitrofenyl)ethyliden)isonikotinohydrazid (NHAPI). U těchto látek jsme dále studovali jejich vliv na progresi buněčného cyklu a schopnost navodit apoptózu a výsledky jsme porovnávali s původním chelátorem SIH. Všechny testované látky, SIH, HAPI, HPPI a NHAPI, ukázaly schopnost navozovat buněčnou smrt cestou apoptózy. Nové látky byly však aktivnější při nižších koncentracích než původní SIH a díky jejich vyšší stabilitě byly po 72 hodinové inkubaci i výrazně účinnější než SIH. U všech testovaných látek byla zaznamenána dávkově závislá schopnost navozovat zástavu mezi G₁ a S fázemi buněčného cyklu. Při měření aktivit kaspáz při vyšších koncentracích nových chelátorů se projevil pokles jejich aktivity oproti vzestupu aktivity kaspáz při nižších koncentracích, což napovídá, že zatímco nižší koncentrace studovaných chelátorů navozují apoptózu, vyšší koncentrace mohou buňku směřovat k nekrotické smrti.

U všech nových analogů SIH jsme dále sledovali vliv železa na jejich antiproliferační působení kultivací MCF-7 buněk se směsí chelátorů s železitou solí v poměru 2:1, kdy by měly vznikat plně chelátované železité komplexy. Všechny chelátory s výjimkou NHAPI prokázaly nižší účinek, pokud byly podány se železem, než když byly podány samotné. Chelátor NHAPI ale naopak při inkubaci se železem prokázal zvýšení antiproliferační aktivity v porovnání se samotným NHAPI. Kvůli tomuto výsledku jsme provedli test oxidace askorbátu u všech železitých komplexů

testovaných analogů SIH. Komplex NHAPI se železem ovšem oxidaci askorbátu nezvyšoval. Naopak chelátor HAPI a několik dalších ukázalo antioxidační působení.

Tato práce identifikovala důležité vztahy struktury a účinku ketonických analogů SIH, které byly využity k vývoji dalších, ještě účinnějších antiproliferačně aktivních látek (Mackova *et al.* 2012).

4.2 Popis závislostí chemické struktury a biologických účinků nových analogů SIH II

Potůčková E, Hrušková K, Špirková IA, Pravidíková K, Kolbabová L, Hergeselová T, Hašková P, Jansová H, Macháček M, Jirkovská A, Richardson V, Lane DJR, Kalinowski DS, Richardson DR, Vávrová K, Šimůnek T. Structure-activity relationships of novel salicylaldehyde isonicotinoyl hydrazone (SIH) analogs: iron chelation, anti-oxidant and cytotoxic properties.

Tato práce přímo navazuje na předchozí publikaci (Mackova *et al.* 2012). Na základě našich výsledků bylo kolegy na katedře anorganické a organické chemie FaF UK připraveno dalších jedenáct analogů látek SIH, HAPI a HPPI. Byla provedena redukce hydrazonové vazby, bromace aromatického kruhu v ketonické části v poloze 5, záměna 2-hydroxyfenylového fragmentu za pyridin-2-ylový a obměny v délce a větvení alkylového řetězce v sousedství hydrazonové vazby.

Nejprve jsme prověřili schopnost nových látek chelátovat železo a to jak v roztoku (pomocí fluorescenčního chelátoru calceinu), tak v buňkách prsního adenokarcinomu MCF-7 (pomocí esterifikovaného calceinu, který je schopen procházet přes buněčné membrány). Výsledky ukázaly, že látky s redukovanou hydrazonovou vazbou a látky s větvením na α -uhlíku alkylového řetězce v sousedství hydrazonové vazby ztratily nebo měly už jen velmi malou schopnost vázat železo. Ostatní látky měly míru chelatace železa podobnou chelátoru SIH, který byl použit jako referenční látka. Dále jsme testovali schopnost látek mobilizovat radioaktivní železo ^{59}Fe z buněk nebo zabránit jeho příjmu do buněk z Tf značeného ^{59}Fe . Výsledky těchto metod zcela korelovaly s chelatačními experimenty v roztoku a v buňkách. Komplexy chelátorů se železem byly podrobeny testu oxidace askorbátu v roztoku, kde původní chelátor SIH ukázal antioxidační účinky, chelátor (*E*)-*N'*-[1-(pyridin-2-yl)ethyliden]isonikotinohydrazid (2API) s pyridin-2-ylovým uskupením namísto 2-

hydroxyfenylového se projevil prooxidačně, ale ostatní chelátory nebyly schopné ani podpořit ani zabránit oxidaci askorbátu.

Sledovali jsme také schopnost těchto látek ochránit buňky H9c2, odvozené od potkaní srdeční tkáň, před oxidačním stresem způsobeným 200 μ M peroxidem vodíku. Protekci poskytovaly v různých koncentracích všechny nové látky kromě výše zmíněných analogů s redukovanou hydrazonovou vazbou a s větvením na α -uhlíku alkylového řetězce v sousedství hydrazonové vazby, které pozbyly schopnost chelatovat železo. Nejlépe protektivně účinnou látkou byl chelátor (*E*)-*N'*-(7-hydroxy-2,3-dihydro-1*H*-inden-1-yliden)isonikotinohydrazid (7HII) s alkylovým řetězcem zacykleným do pětičlenného cyklu kondenzovaného s aromatickým jádrem. Dále jsme porovnávali antiproliferační účinky nových látek na nádorovou buněčnou linii MCF-7 a nenádorovou linii H9c2. Látky s redukovanou hydrazonovou vazbou a s větvením na α -uhlíku alkylového řetězce v sousedství hydrazonové vazby byly málo antiproliferačně účinné. Látky bromované a látky 2API a 7HII byly silně antiproliferačně účinné, ale jejich specifita k nádorovým buňkám nebyla příliš zřetelná. Jako nejperspektivnější látky se specifickým antiproliferačním účinkem se projeví analogy SIH s propylem a izobutytem v sousedství hydrazonové vazby. Tyto látky dosáhly vyšší antiproliferační účinnosti a zároveň vyšší specifity než mateřská látka SIH.

Tato studie prokázala nezbytnost hydrazonové vazby pro chelatační i ostatní účinky aroylhydrazonů. Zároveň ukázala perspektivní směr zvýšení antiproliferačních účinků prodlužováním a větvením, v jiné než α -poloze, alkylového řetězce v sousedství hydrazonové vazby. Větvení alkylového řetězce v α -poloze způsobovalo sterické bránění chelatačního místa molekuly.

4.3 *In vitro* studie současného působení chelátorů železa a klinicky používaných chemoterapeutik na buněčné linie rakoviny prsu

Potůčková E, Jansová H, Macháček M, Vávrová A, Hašková P, Tichotová T, Richardson V, Kalinowski DS, Richardson DR, Šimůnek T. Quantitative analysis of the anti-proliferative activity of combinations of selected iron-chelating agents and clinically used anti-neoplastic drugs. *PLoS One*. 2014; **9**(2): e88754. IF₂₀₁₂ = 3,730

Jak bylo již uvedeno v teoretické části, v léčbě rakoviny prsu se velmi často používají kombinace více různých cytostatik (Goldhirsch *et al.* 2001, Moller *et al.*

2008). Proto je důležité u nových potenciálních chemoterapeutik, jako jsou i chelátory železa, prověřit možnost současného podávání s již klinicky používanými léčivy. Podle literatury doposud nebyla provedena žádná systematická studie zabývající se kombinací chelátorů železa a klinicky používaných chemoterapeutik. V této publikaci jsme se tedy zabývali kombinováním čtyř chelátorů železa s různými vlastnostmi (hydrofilní a antioxidační siderofor desferrioxamin, lipofilní a antioxidační aroylhydrazon SIH, analog chelátoru SIH NHAPI a lipofilní a prooxidační thiosemikarbazon Dp44mT (Kalinowski *et al.* 2005, Mackova *et al.* 2012)) a šesti chemoterapeutik používaných při léčbě rakoviny prsu s různým mechanismem účinku (stabilizátor mikrotubulů paclitaxel, pyrimidinový analog/antimetabolit 5-fluorouracil, antracyklinové antibiotikum/blokátor enzymu topoizomerázy II α doxorubicin, inhibitor metabolismu kyseliny listové methotrexát, aktivní metabolit alkylační látky cyklofosfamidu 4-hydroperxycyklofosfamid a antagonist estrogenního receptoru tamoxifen (Brunton *et al.* 2011)). Pokusy jsme prováděli na buněčné linii MCF-7 (exprimující estrogenní receptory), kdy byly buňky inkubované s testovanými látkami po dobu 72 hodin. Studie byla navržena podle metody Chou-Talalay, která je schopna kvantitativně vyjádřit míru synergického, aditivního nebo antagonistického efektu kombinace látek (Chou *et al.* 1984).

Chelátor desferrioxamin, který se klinicky používá k léčbě nemocí s přetížením železem, působil ve vyšších koncentracích antagonisticky se všemi testovanými klinicky používanými léčivy. Tato charakterizace je nepříznivá, protože většina antineoplastické léčby je právě ve vyšších dávkách podávána. SIH prokázal synergický účinek s 4-hydroperxycyklofosfamidem v nízkých a středních dávkách, s methotrexátem ve velmi vysokých dávkách a nejsilnější synergický účinek s tamoxifenem v celém dávkovém rozmezí. Chelátory NHAPI a Dp44mT působily aditivně nebo synergicky se všemi testovanými protinádorovými léčivy, a to ve většině dávkových rozmezí. Jako nejvhodnější chelátory pro kombinace se proto ukázaly NHAPI a Dp44mT. Tyto chelátory měly nejlepší účinnost v kombinaci s doxorubicinem (aditivní nebo mírně antagonistický či synergický efekt) a zejména pak s tamoxifenem (silný synergismus).

V rámci studie byly prověřovány i kombinace látek s komplexy chelátorů se železem a v případě Dp44mT i s mědí v dávkách odpovídajících koncentraci IC₅₀ (koncentrace látky inhibující buněčnou proliferaci na 50 % kontroly). V případě chelátoru SIH použití komplexu se železem signifikantně změnilo antagonistickou

kombinaci s doxorubicinem na synergickou, ale na druhou stranu také změnilo synergismus s tamoxifenem na antagonismus. Chelátor NHAPI v podobě komplexu se železem změnil synergické působení s 5-fluorouracilem, doxorubicinem a metotrexátem na antagonistické. Synergie s tamoxifenem se ale projevila i s komplexem NHAPI-železo. Kovové komplexy Dp44mT působily synergicky (popřípadě aditivně) se všemi testovanými látkami.

Nejlepší identifikované synergické kombinace chelátorů NHAPI a Dp44mT s tamoxifenem byly potvrzeny i na další buněčné linii prsního karcinomu exprimující estrogenový receptor T47D, přičemž na buněčné linii neexprimující estrogenové receptory MDA-MB-231 působily kombinace dle očekávání antagonisticky.

Kombinace chelátoru NHAPI a jeho komplexu se železem byla dále studována na buněčné linii MCF-7. Synergický efekt kombinací byl potvrzen měřením elektrické impedance, které umožňuje sledovat růst buněk v čase, sledováním progresu buněčného cyklu a měřením změn potenciálu vnitřní mitochondriální membrány. Zde byla pozorována schopnost chelátoru NHAPI zastavovat buňky v S-fázi buněčného cyklu. Kombinace NHAPI s tamoxifenem pak způsobovala jasné zablokování buněk mezi G₁ a S fázemi buněčného cyklu a výraznou depolarizaci vnitřní mitochondriální membrány.

Výsledky této studie poukázaly na některé synergické kombinace, obzvláště ty s tamoxifenem, a také zdůraznily hypotézu, že existuje určité spojení metabolismu železa s estrogení signalizací v buňkách rakoviny prsu (Potuckova *et al.* 2014).

4.4 Popis závislostí chemické struktury a biologických účinků nových thiosemikarbazonů

Serda M, Kalinowski DS, Rasko N, Potůčková E, Mrozek-Wilczkiewicz A, Musiol R, Małecki JG, Sajewicz M, Ratuszna A, Muchowicz A, Gołąb J, Šimůnek T, Richardson DR, Polanski J. Exploring the anti-cancer activity of novel thiosemicarbazones generated through the combination of retro-fragments.

Tato studie vznikla na základě spolupráce tří pracovišť: Slezské Univerzity v Katovicích v Polsku, Univerzity v Sydney v Austrálii a naší laboratoře. Na základě některých vysoce antiproliferačně aktivních thiosemikarbazonových chelátorů železa jako jsou Dp44mT a DpC (Kovacevic *et al.* 2011a) a předchozího studia chinolinových thiosemikarbazonů (Serda *et al.* 2012) bylo vytipováno šest zajímavých ketonických

částí a šest potenciálně účinných thiosemikarbazidových částí molekul, kde byl dusík N4 součástí piperazinu nebo morfolinu, nebo byl substituován methylem a cyklohexylem, které byly kombinovány dohromady. Tímto přístupem bylo na Slezské Univerzitě v Polsku připraveno 35 nových látek ze skupiny thiosemikarbazonů.

U všech připravených látek byla studována antiproliferační účinnost na buněčných liniích lidského kolorektálního karcinomu HCT116 (jak exprimujících, tak neexprimujících protein p53 důležitý pro kontrolu poškození genomu), na lidských lymfoblastomových buňkách Raji, linii lidského cervikálního karcinomu HeLa a lidského neuroblastomu SK-N-MC. Nespecifická toxicita pak byla sledována na lidských fibroblastech NHDF. Výsledky proliferačních pokusů na obou subklonech buněčné linie HCT116 ukázaly, že antiproliferační působení chelátorů železa je nezávislé na tom, jestli buňka syntetizuje či nesyntetizuje protein p53. Také spojení lipofility těchto nových sérií látek s jejich antiproliferačním účinkem nebylo jednoznačné. Nejsilnější antiproliferační účinky na nádorových buňkách měla série látek odvozených od di-2-pyridylketonu (série 1). Látky odvozené od chinolin-2-karbaldehydu (série 2) a 8-hydroxychinolin-2-karbaldehydu (série 3) byly středně antiproliferačně aktivní a látky odvozené od 7-hydroxychinolin-8-karbaldehydu (série 4), chinoxalin-2-karbaldehydu (série 5) a salicylaldehydu (série 6) projevíly jen slabé antiproliferační účinky. Jako látky s nejvyšším antiproliferačním působením byly identifikovány chelátory s označením 1b, 1d, 2b, 2f a 3c. Při porovnání antiproliferačního působení látek na linii HCT116 a toxického působení na fibroblastovou linii NHDF, určujícím specifické působení látek na rakovinné buňky, byly identifikovány látky 1d a 3c jako nejnadějnější pro další výzkum.

Dále byla testována schopnost všech látek mobilizovat radioaktivní izotop železa ^{59}Fe z buněk nebo zabraňovat jeho příjmu do buněk z železem ^{59}Fe značeného Tf. Série 1, 3, 4 a 6 prokázaly v těchto studiích vysokou aktivitu, přičemž látky ze sérií 2 a 5 byly aktivní méně. Výsledky mobilizačních pokusů s železem ^{59}Fe však plně nekorelovaly s výsledky antiproliferačního působení nových látek. Proto byl zařazen i test schopnosti železitých komplexů těchto látek usnadňovat nebo zabraňovat oxidaci askorbátu. Po výsledku testu oxidace askorbátu bylo patrné, že nejvíce antiproliferačně aktivní jsou látky, které měly v kombinaci se železem schopnost katalyzovat vznik ROS, což byly zejména látky ze série 1 a 2. Látky ze sérií 3, 4, 5 a 6 působily spíše antioxidačně.

Výsledky této studie ukázaly, že nejvíce antiproliferačně účinné látky se skupiny thiosemikarbazonů mají po chelataci železa schopnost katalyzovat vznik ROS. Jako

látky s nejvyšším potenciálem se projevíly chelátory s označením 1d a 3c, které budou předmětem dalších studií.

4.5 Studie biologických účinků chelátoru Bp4eT a jeho metabolitů

Potůčková E, Roh J, Macháček M, Stariat J, Šesták V, Jansová H, Hašková P, Jirkovská A, Vávrová K, Kovaříková P, Richardson DR, Šimůnek T. *In vitro* characterization of pharmacological properties of the anticancer iron chelator Bp4eT and its phase I metabolites.

Bp4eT je jedním z velmi nadějných antiproliferačně působících chelátorů železa ze skupiny thiosemikarbazonů. Tento chelátor byl již dříve charakterizován (Kalinowski *et al.* 2007, Merlot *et al.* 2010, Yu *et al.* 2012), ale identifikace metabolitů první fáze biotransformace Bp4eT proběhla teprve nedávno na katedře farmaceutické chemie a kontroly léčiv naší fakulty. Bylo zjištěno, že tato látka je metabolizována na amidrazonový metabolit N^3 -ethyl- N^1 -[fenyl(pyridin-2-yl)methylen]formamidrazon (Bp4eA) a na semikarbazonový metabolit 2-benzoylpyridin-4-ethyl-3-semikarbazon (Bp4eS) (Stariat *et al.* 2012). Vzhledem k tomu, že metabolismus léčiva je důležitou součástí preklinických studií, rozhodli jsme se prověřit biologickou aktivitu metabolitů Bp4eT v porovnání s mateřskou látkou.

Nejprve jsme provedli studii chelatační aktivity Bp4eT a jeho metabolitů v buňkách prsního adenokarcinomu MCF-7 pomocí esterifikovaného fluorescenčního chelátoru calceinu. Podle výsledků této studie oba metabolity téměř ztratily schopnost chelátovat železo. Tento výsledek byl nepřímě potvrzen i nízkou schopností těchto látek mobilizovat železo ^{59}Fe z buněk nebo zabraňovat jeho příjmu do buněk z železem ^{59}Fe značeného Tf.

Dále jsme sledovali antiproliferační účinky Bp4eT a jeho metabolitů na buněčných liniích MCF-7 (prsní karcinom), HL-60 (leukémie), HCT116 (kolorektální karcinom) a A549 (plicní karcinom) a jejich toxicitu k nenádorovým liniím H9c2 (kardiomyoblasty) a 3T3 (fibroblasty). Zjistili jsme, že mateřská látka Bp4eT je vysoce antiproliferačně aktivní k třem použitým rakovinným buněčným liniím, ale na linii A549 působí antiproliferačně až v koncentracích srovnatelných s jeho nespecifickou toxicitou k nenádorovým liniím. Oba metabolity Bp4eT měly silně sníženou

antiproliferační aktivitu i toxicitu v porovnání s mateřskou látkou Bp4eT, a to i více než tisícinásobně.

Studovali jsme také vliv těchto látek na progresi buněčného cyklu a na aktivaci apoptotické buněčné smrti. Ukázalo se, že v koncentraci, kdy Bp4eT navozoval zablokování MCF-7 buněk mezi G₁ a S fázemi a navozoval apoptózu aktivací kaskády kaspáz, se jeho metabolity nelišily od neovlivněné kontroly.

Tato studie ukázala, že chelátor Bp4eT se metabolizuje na antiproliferačně neúčinné a zároveň netoxické látky.

4.6 Porovnání klinicky používaných a experimentálních chelátorů železa jako ochrany před oxidačním stresem

Bendová P, Macková E, Hašková P, Vávrová A, Jirkovský E, Štěrba M, Popelová O, Kalinowski DS, Kovaříková P, Vávrová K, Richardson DR, Šimůnek T. Comparison of clinically used and experimental iron chelators for protection against oxidative stress-induced cellular injury. *Chem Res Toxicol.* 2010; **23**(6):1105-14.

IF₂₀₁₀ = 4,148

Mnoho klinicky používaných cytostatik může způsobovat v organismu produkci ROS, která vystavuje citlivé tkáně, jako jsou neurony či srdeční buňky, oxidačnímu stresu a může způsobit jejich poškození (Chen *et al.* 2007). Výhodou některých chelátorů železa jako potenciálních cytostatik je jejich vlastnost zabraňovat produkci ROS vyvázáním volného železa a zabráněním katalýzy Fentonovy a Haber-Weissovy reakce (Kalinowski *et al.* 2005, Simunek *et al.* 2005). Proto jsme v této práci sledovali protektivní účinky klinicky používaných a experimentálních chelátorů železa na srdeční buňky a také redoxní vlastnosti zmíněných látek.

Jako model oxidačního stresu na buněčné linii H9c2 jsme použili 24 hodinovou inkubaci s 200 μM koncentrací tercbutylhydroperoxidu, navozující silné morfologické změny a buněčnou smrt. Buňky jsme se snažili chránit před oxidačním stresem současnou inkubací s různými koncentracemi klinicky používaných chelátorů EDTA, desferrioxaminu, deferipronu a deferasiroxu a s experimentálními chelátory PIH, SIH a Dp44mT. Všechny studované chelátory kromě EDTA poskytovaly jistou protekci proti oxidačnímu stresu, i když efektivní koncentrace se velmi lišily. Nejnižší koncentrace pro protekci byla potřebná u chelátoru Dp44mT, ovšem těsně nad ní už se projevovala

vlastní toxicita této látky. Tento efekt byl patrný i u chelátoru deferasiroxu. Nezbytnost chelatace železa pro protektivní účinek jsme potvrdili přidáním železa k efektivní dávce chelátoru, kdy protekce všech chelátorů vymizela.

Dále jsme určovali vlastní toxicitu chelátorů a jejich komplexů se železem po 24 a 72 hodinové inkubaci. Kvůli nízké rozpustnosti některých látek bylo možné sledovat zřetelný pokles viability až po 72 hodinách. Toxické koncentrace po této delší inkubaci se téměř u všech chelátorů překrývaly s koncentracemi pro protekci buněk, jen chelátor SIH ukázal svou nízkou toxicitu, kdy koncentrace toxického působení převyšovala koncentraci potřebnou pro protekci před oxidačním stresem. Dále byly všechny látky kromě EDTA v komplexu se železem méně toxické než bez železa, což potvrzuje deprivaci železa jako mechanismus toxického působení. V případě EDTA byl komplex se železem toxičtější, což ukazuje na potenciaci redoxního cyklení železa.

Při studiu schopnosti vázat železo z LIP se projevila neschopnost desferrioxaminu projít přes cytoplazmatickou membránu, a proto nitrobuněčné železo téměř nevázal. Ostatní ligandy kromě EDTA byly chelatačně účinné přičemž nejvíce chelatovaly SIH a Dp44mT. Při sledování produkce ROS v roztoku komplexu EDTA a Dp44mT ukázaly potenciál působit prooxidačně, zatímco komplexy ostatních látek působily spíše antioxidačně. Při esaji v buňkách ovšem výsledky tak jednoznačné nebyly.

Naše studie ukazuje, že chelátory železa mají potenciál chránit srdeční buňky před oxidačním stresem. Je ale potřeba racionálně zvolit vhodnou látku a dávkové rozmezí pro optimální účinky. Ze studovaných látek projevil nejlepší poměr účinku a vlastní toxicity chelátor SIH (Bendova *et al.* 2010).

4.7 Katalytické inhibitory topoizomerázy II rozdílně moduluji toxicitu antracyklinů vůči srdečním a nádorovým buňkám

Vávrová A, Jansová H, Macková E, Macháček M, Hašková P, Tichotová L, Štěrba M, Šimůnek T. Catalytic inhibitors of topoisomerase II differently modulate the toxicity of anthracyclines in cardiac and cancer cells. *PLoS One*. 2013; **8**(10):e76676.

IF₂₀₁₂ = 3,730

Antracyklinová antibiotika jsou široce používanou skupinou cytostatik. Jsou to topoizomerázové jedy, které způsobují dvojité zlomy DNA u rychle proliferujících

buněk (Brunton *et al.* 2011). Jejich hlavním nežádoucím účinkem je však výše zmíněná kardiotoxicita. Dlouho se mělo za to, že je kardiotoxicita způsobena vytvořením redoxaktivního komplexu antracyklinového antibiotika s atomem železa a katalýzou vzniku ROS, které vyvolaly oxidační poškození kardiomyocytů (Ferreira *et al.* 2008). Tuto teorii podporoval i fakt, že jediná registrovaná látka pro prevenci antracyklinové kardiotoxicity je dexrazoxan, který je v buňce štěpen na látku ADR-925, schopnou chelatovat železo (Popelova *et al.* 2009). V současné době je ale více podporována teorie, kdy je protektivní působení dexrazoxanu způsobeno katalytickou inhibicí topoizomerázy II (Vejpongsa *et al.* 2014), což vede k obavám o snížení protinádorového působení antracyklinů při použití dexrazoxanu. Tato studie byla proto zaměřená na sledování kardioprotektivního působení katalytických inhibitorů topoizomerázy II, dexrazoxanu, jeho analogu sobuzoxanu a derivátu kyseliny barbiturové merbaronu, proti toxicitě způsobené antracykliny, doxorubicinem a daunorubicinem, a peroxidem vodíku na primární linii potkaních neonatálních ventrikulárních kardiomyocytů (NVCM) a zároveň na stanovení antiproliferační aktivity těchto látek a jejich kombinací na rakovinnou linii lidské promyelocytární leukémie HL-60.

NVCM buňky byly preinkubovány 3 hodiny s různými koncentracemi dexrazoxanu, pak byly na další 3 hodiny přidány antracykliny nebo pexoxid vodíku po této inkubaci bylo médium u antracyklinů nahrazeno čerstvým kultivačním médiem a buňky byly inkubovány po dalších 48 hodin. Po vyhodnocení měření aktivity laktátdehydrogenázy uvolněné z poškozených kardiomyocytů bylo patrné, že dexrazoxan byl schopen snížit poškození kardiomyocytů do 1,4 μM koncentrace doxorubicinu a do 1,2 μM koncentrace daunorubicinu. Dexrazoxan však nepředcházel poškození způsobenému peroxidem vodíku. Podobné pokusy jsme provedli i s preinkubací se sobuzoxanem a merbaronem, přičemž obě látky ukázaly potenciál chránit kardiomyocyty před antracyklinovou toxicitou, ale nepůsobily protektivně proti peroxidu vodíku. Tyto výsledky byly potvrzeny i aktivací kaskády kaspáz, která je součástí buněčné smrti, apoptózy. Dalším důkazem kardioprotekce mechanismem inhibice topoizomerázy II spíše než chelatací železa a zamezení vzniku ROS byla signifikantně nezměněná hladina jak oxidovaného tak redukovaného glutathionu v NVCM buňkách při inkubaci s antracyklinem a dexrazoxanem nebo pouze s antracyklinem. Navíc prověřením schopností dexrazoxanu, sobuzoxanu a merbaronu

chelátovat železo z LIP kardiomyoblastové buněčné linie H9c2 ukázalo, že schopnost chelátovat železo má ze zkoušených látek jen dexrazoxan.

Při proliferační studii na HL-60 buňkách byly katalytické inhibitory topoizomerázy II a antracykliny kombinovány v násobcích svých IC_{50} koncentrací po dobu 72 hodin podle metody Chou-Talalay s vyhodnocováním MTT testem. Byly provedeny současné inkubace nebo tříhodinová preinkubace s katalytickým inhibitorem topoizomerázy II a poté přidání antracyklinu. V případě dexrazoxanu byla studována i šestihodinová preinkubace nebo poměr daunorubicin:dexrazoxan 1:20, který je používán v klinické léčbě. Kombinace sobuzoxanu a merbaronu s oběma antracykliny byly silně synergické v celé škále dávkového rozmezí. Kombinace dexrazoxanu s antracykliny však ve vysokých dávkách přecházely ze silné synergie k mírně až středně antagonistickému účinku. Klinicky používaná kombinace daunorubicin:dexrazoxan 1:20 však byla synergická v celé škále koncentrací. Synergický účinek na rakovinných buňkách HL-60 byl potvrzen i měřením aktivace kaspáz, kdy kombinace látek způsobovaly jejich silnější aktivaci než jednotlivé látky. Dále byly provedeny analýzy buněčných cyklů HL-60 buněk inkubovaných s jednotlivými látkami nebo jejich kombinacemi v koncentracích odpovídajících hodnotám IC_{50} . Doxorubicin samotný způsobil kumulaci buněk v G_2/M fázi buněčného cyklu a výskyt mnohojaderných buněk, dexrazoxan způsobil nárůst buněk v sub G_1 fázi (apoptóza), sobuzoxan způsobil jen minimální změnu tvaru buněčného cyklu, ale merbaron způsobil ještě vyšší kumulaci buněk v G_2/M fázi než doxorubicin. Kombinace dexrazoxanu a sobuzoxanu s doxorubicinem vedla k podobné kumulaci buněk v G_2/M fázi a k zásadnímu nárůstu polyploidních buněk, na druhé straně kombinace merbaronu s doxorubicinem se výrazně nelišila od účinku samotného merbaronu.

Výsledky této studie ukazují, že pro protekci srdečních buněk před poškozením antracyklinovou toxicitou je podstatná schopnost dexrazoxanu katalyticky inhibovat topoizomerázu II, spíše než jeho železo-chelatační účinnost. Zároveň jsme prokázali, že katalytické inhibitory topoizomerázy II působí synergicky proti proliferaci rakovinných buněk HL-60 (Vavrova *et al.* 2013).

5 Souhrnná diskuse

Chelátory železa by se v budoucnu mohly zařadit mezi nová léčiva rakovinných onemocnění. Svědčí o tom fakt, že některé chelátory železa jsou již v této indikaci v raných fázích klinických studií (Yu *et al.* 2006, Hatcher *et al.* 2008). Proto je tato práce zaměřena na studium strukturních obměn některých chelátorů železa a na jejich farmakologické a toxikologické vlastnosti, což je klíčové pro vývoj nových specifických chemoterapeutik.

V první části této práce jsme studovali analogy chelátoru SIH (Mackova *et al.* 2012). Zjistili jsme, že nejvyšší vliv na zvýšení stability ve vodném prostředí i antiproliferační aktivity mělo zavedení alkylového řetězce do sousedství hydrazonové vazby (Hruskova *et al.* 2011). Čím delší pak řetězec byl, tím vyšší byla antiproliferační aktivita látek a zároveň se zvyšovala i selektivita jejich působení. Tento efekt mohl být způsoben zvýšením lipofility, které usnadňuje průchod látek do buněk, což bylo u jiných chelátorů železa spjato se zvýšením antiproliferačních účinků (Landschulz *et al.* 1984, Lovejoy *et al.* 2012). Větvení alkylového řetězce v sousedství hydrazonové vazby v α -poloze však vedlo ke sterickému bránění chelatačního místa molekuly a tím ke ztrátě biologických účinků. Ke ztrátě chelatační aktivity vedla také redukce hydrazonové vazby, jenž se ukázala být pro chelatační působení nezbytnou. Když jsme se pokusili zvýšit lipofilitu zavedením halogenu (bromu nebo chloru) na aromatické jádro v ketonické části molekuly, došli jsme k látkám s poměrně vysokým antiproliferačním působením, avšak s ne příliš vyhraněnou specifitou. Podobný efekt mělo i zavedení methoxy skupiny na aromatické jádro. Když jsme šli opačným směrem a zavedli jsme hydroxy skupinu na aromatické jádro v ketonické části, získali jsme látky s vyšší toxicitou k nenádorovým buňkám než k nádorovým. Jako zajímavá se ukázala nitro skupina na aromatickém jádře v ketonické části. Látka s nitro skupinou měla vysokou specifitu antiproliferačního působení a proto byla použita i do kombinační studie (Mackova *et al.* 2012).

Druhou částí této práce byla zmíněná kombinační studie (Potuckova *et al.* 2014). Z rešerže literatury jsme zjistili, že žádná komplexní práce, která by kombinovala chelátory železa s různými vlastnostmi a klinicky používaná cytostatika s různými mechanismy účinku zatím provedena nebyla. Bylo však publikováno několik doporučení pro současné podávání chelátorů železa s cytostatiky, která zvyšovala hladinu železa v séru a v myokardu (Millart *et al.* 1993, Carmine *et al.* 1995). Během

naší *in vitro* studie jsme zjistili, že ne všechny kombinace cytostatika a chelátoru železa jsou pro současnou léčbu vhodná. Nutné je ovšem podotknout, že jsme nezkoušeli postupné podávání látek, které by možná mělo lepší účinek (Zoli *et al.* 2005), ale v komplexním měřítku by enormně zvýšilo náročnost studie. Nejlepších synergických vlastností s testovanými chemoterapeutiky v naší studii dosáhly chelátory NHAPI a Dp44mT. Chelátor Dp44mT dosahoval synergických účinků i jako komplex se železem či mědí, zatímco komplex NHAPI se železem působil s chemoterapeutiky většinou antagonisticky. Tyto výsledky mohou být vysvětleny prooxidačním působením kovových komplexů chelátoru Dp44mT (Noulsri *et al.* 2009, Jansson *et al.* 2010), zatímco u železitého komplexu NHAPI prooxidační působení prokázáno nebylo (Mackova *et al.* 2012). Nejlepší z kombinací v této studii byla kombinace chelátorů SIH, NHAPI a Dp44mT s antiestrogenem, tamoxifenem (Potuckova *et al.* 2014). Silně synergický účinek zmíněných látek je potvrzením již dříve zaznamenaného spojení metabolismu železa v buňkách rakoviny prsu a jejich estrogenní stimulací (Vyhlidal *et al.* 2002).

V třetí části této práce jsme se zabývali hodnocením nových thiosemikarbazonů s ketonickou částí odvozenou od di-2-pyridylketonu, chinolin-2-karbaldehydu, chinolin-8-karbaldehydu, chinoxalin-2-karbaldehydu a salicylaldehydu a s thiosemikarbazidovou částí obsahující šestičlenný heterocyklus nebo methyl a cyklohexyl. V této studii se ukázalo, že thiosemikarbazony odvozené od salicylaldehydu jsou nejvíce chelatačně účinné, což se shoduje s daty o SIH (aroylhydrazon odvozený od stejného ketonu) (Simunek *et al.* 2005, Glickstein *et al.* 2006). Antiproliferační účinnost těchto látek byla však v porovnání s ostatními v této studii jen malá. Látky s hydrofilnějším ketonem, obsahujícím hydroxy skupinu nebo chinoxalin, měli střední antiproliferační aktivitu. Nejvíce antiproliferačně účinné se ukázaly látky s di-2-pyridylketonovou částí nebo s chinolinem, které byly schopny katalyzovat vznik ROS a jejichž dříve připravené deriváty byly již studovány pro vysokou antiproliferační aktivitu (Richardson *et al.* 2006, Serda *et al.* 2012).

Charakterizace metabolismu a biologických aktivit metabolických produktů je velmi důležitou částí výzkumu látek, které mají potenciál stát se léčivem. O nadějně specificky antiproliferačně působící látce ze skupiny thiosemikarbazonů, Bp4eT, je již známo relativně mnoho (Kalinowski *et al.* 2007, Yu *et al.* 2012), její metabolismus byl však objasněn teprve nedávno (Stariat *et al.* 2012). Ve čtvrté části této práce se proto zabýváme studiem chelatační a biologické aktivity chelátoru Bp4eT a jeho metabolitů.

Během těchto studií jsme na několika buněčných liniích prokázali vysokou a specifickou antiproliferační účinnost parentního chelátorů, ale také jistou rezistenci buněčné linie plicního adenokarcinomu A549 k této látce. U chelátoru Bp4eT byla prokázána schopnost způsobit kumulaci buněk v S fázi buněčného cyklu a navodit buněčnou smrt apoptózou. Oba metabolity Bp4eT se ukázaly jako chelatačně neaktivní, což vedlo ke ztrátě antiproliferačního i toxického působení. Můžeme tedy říci, že se chelátor Bp4eT metabolizuje na antiproliferačně neúčinné a zároveň netoxické metabolity, což dává předpoklady pro příznivý bezpečnostní profil této látky.

Jak je známo, některé cytostatické látky mohou způsobovat jako nežádoucí účinek kardiotoxicitu, která je spojována s oxidačním stresem (Kappus 1987, Schimmel *et al.* 2004). Některé chelátory železa mají schopnost zabraňovat vzniku ROS pomocí Fentonovy a Haber-Weissovy reakce (Simunek *et al.* 2005). V další části této práce jsme se proto zaměřili na použití klinicky používaných a vybraných experimentálních chelátorů železa pro prevenci oxidačního poškození srdečních buněk (Bendova *et al.* 2010). Chelátor EDTA neprokázal žádný protektivní účinek, což bylo pravděpodobně způsobeno jeho vysokou redoxní aktivitou prokázanou v roztoku. Extracelulární chelátor desferrioxamin poskytoval protekci ve velmi vysokých dávkách, které nejsou v plazmě dosahovány (Summers *et al.* 1979), jeho celkové působení bylo ale antioxidační. Další dva klinicky používané chelátory deferasirox a deferipron a experimentální chelátor PIH ukázaly schopnost chránit před oxidačním stresem v nižších koncentracích, působily antioxidačně, ale jejich vlastní toxicita se překrývala s koncentracemi jejich protektivního účinku. Chelátor s vysokou antiproliferační účinností a se schopností tvořit redoxně aktivní komplexy se železem, Dp44mT, prokázal protektivní vlastnosti v poměrně úzkém dávkovém rozmezí. Nejlepších výsledků dosáhl antioxidačně působící chelátor SIH, který prokazoval vlastní toxicitu až ve vyšších koncentracích, než které byly potřeba k protekci srdečních buněk před oxidačním stresem (Bendova *et al.* 2010).

V poslední části této práce jsme se zabývali konkrétním příkladem kardiotoxicity způsobené léčbou antracykliny. Tato léčba způsobuje akutní i chronické poškození srdce, které je tradičně v literatuře spojováno s tvorbou ROS (Ferreira *et al.* 2008). Jediným klinicky používaným léčivem pro prevenci tohoto poškození je katalytický inhibitor topoizomerázy II a zároveň prekursor chelátoru železa ADR-925, dexrazoxan. Dlouho se považovala za mechanismus jeho protektivního působení právě chelatace železa pomocí ADR-925. V současné době se od této teorie ustupuje

(Popelova *et al.* 2009) a upřednostňuje se teorie protekce katalytickou inhibicí topoizomerázy II, na kterou působí i antracykliny (Vejpongsa *et al.* 2014). Naše studie se soustředila na předpoklad, že pokud působí katalytická inhibice topoizomerázy II kardioprotekci před antracykliny, měly by protektivně působit i jiné katalytické inhibitory topoizomerázy II, než jen dexrazoxan. Tento předpoklad se ukázal jako správný, když katalytické inhibitory sobuzoxan a merbaron byly schopny poskytovat podobnou protekci před antracyklinovou toxicitou jako dexrazoxan. Tyto látky ovšem nebyly schopny ochránit buňky před oxidačním stresem způsobeným peroxidem vodíku (Vavrova *et al.* 2013), což by umožňovaly látky chelatující železo (Bendova *et al.* 2010). Dále jsme studovali možnost blokování antiproliferačního účinku antracyklinů, působících jako topoizomerázový jed, na rakovinné buňky současným podáním katalytických inhibitorů topoizomerázy II. V kombinační studii antracyklinů a katalytických inhibitorů topoizomerázy II se však blokáda antiproliferačního účinku nepotvrdila. Naopak většina kombinací byla synergická v celém dávkovém rozmezí (Vavrova *et al.* 2013). Tento výsledek může být vysvětlen různou distribucí izoform topoizomerázy II v různých tkáních. Srdeční tkáň obsahuje více topoizomerázy II β , na kterou cílí katalytické inhibitory topoizomerázy II, a u rakovinných buněk zas převládá topoizomeráza II α , která je cílem antiproliferačního působení antracyklinů (Vejpongsa *et al.* 2014).

Jak je známo, k vývoji jednoho účinného léčiva uvedeného do klinického používání musí být prozkoumáno tisíce struktur (Matter *et al.* 2001). Během této práce jsme popsali několik klíčových závislostí a souvislostí, které jsou důležité pro racionální design a syntézu nových antiproliferačně aktivních a zároveň specifických látek s aroylhydrazonovou ale i thiosemikarbazonovou strukturou. Dále jsme také pomohli objasnit přispění chelátorů železa ke snížení některých nežádoucích účinků, které se projevují při použití chemoterapie rakovinných onemocnění.

6 Závěry

- Ve studii antiproliferačních účinků nových analogů chelátoru SIH se jako nejvíce antiproliferačně aktivní látky projevily deriváty SIH s delším alkylovým řetězcem v sousedství hydrazonové vazby a látka s nitroskupinou na aromatickém jádře ketonické části.
- Při kombinační studii společného podávání chelátorů železa a klinicky používaných antineoplastických chemoterapeutik se jako nejvhodnější látky pro kombinaci s chelátory železa projevily antracyklinivé antibiotikum doxorubicin a antagonist estrogenových receptorů tamoxifen. Nejlepší kombinační výsledky ze studovaných chelátorů pak měly chelátory NHAPI a Dp44mT.
- Během studie biologických účinků nových thiosemikarbazonových chelátorů železa jsme zjistili, že nejvíce antiproliferačně aktivní látky z nově připravených thiosemikarbazonů jsou chelátory, jejichž kovové komplexy katalyzují vznik ROS. Dále jsme potvrdili, že chelátory železa odvozené od salicylaldehydu mají nejvyšší schopnost mobilizovat nitrobuněčné železo.
- Prokázali jsme, že vysoce antiproliferačně účinný thiosemikarbazonový chelátor Bp4eT se metabolizuje na antiproliferačně neúčinné a zároveň netoxické produkty.
- Studie kardioprotektivních účinků a redoxních vlastností klinicky používaných a experimentálních chelátorů železa ukázala, že všechny testované látky, kromě chelátoru EDTA, projevily schopnost chránit buňky před oxidačním stresem. Nejvhodnější poměr protektivního účinku a vlastní toxicity měl chelátor SIH.
- Z výsledků studie kardioprotektivních účinků inhibitoru topoizomerázy II a prekursoru chelátoru železa ADR-925, dexrazoxanu, vyplývá, že kardioprotektivní účinek dexrazoxanu při léčbě antracykliny je způsoben spíše katalytickou inhibicí topoizomerázy II než chelatací železa. Současné podávání katalytických inhibitorů topoizomerázy II s antracykliny pak mělo synergický antiproliferační účinek na leukemické buňky.

7 Podíl předkladatelky na publikacích zahrnutých v disertační práci

Macková E, Hrušková K, Bendová P, Vávrová A, Jansová H, Hašková P, Kovaříková P, Vávrová K, Šimůnek T. Methyl and ethyl ketone analogs of salicylaldehyde isonicotinoyl hydrazone: novel iron chelators with selective antiproliferative action. *Chem Biol Interact.* 2012; **197**(2-3): 69-79. IF₂₀₁₂ = 2,967

- Kultivace nádorových buněčných linií MCF-7 a HL-60
- Studium antiproliferační aktivity nových analogů SIH
- Analýzy prováděné na průtokovém cytometru (stanovení apoptózy pomocí anexinu-V a propidium jodidu, stanovení potenciálu vnitřní mitochondriální membrány sondou JC-1, stanovení progresu buněčného cyklu)
- Stanovení enzymové aktivity kaspáz
- Test oxidace askorbátu
- Hlavní podíl na analýze dat a textu publikace

Potůčková E, Hrušková K, Špírková IA, Pravidíková K, Kolbabová L, Hergeselová T, Hašková P, Jansová H, Macháček M, Jirkovská A, Richardson V, Lane DJR, Kalinowski DS, Richardson DR, Vávrová K, Šimůnek T. Structure-activity relationships of novel salicylaldehyde isonicotinoyl hydrazone (SIH) analogs: iron chelation, anti-oxidant and cytotoxic properties.

- Kultivace buněčné linie MCF-7
- Stanovení chelatační aktivity látek v roztoku a v buňkách MCF-7
- Stanovení schopnosti nových chelátorů mobilizovat železo ⁵⁹Fe z buněk MCF-7 a zabraňovat vstřebávání železa ⁵⁹Fe z Tf
- Test oxidace askorbátu
- Hlavní podíl na analýze dat a textu publikace

Potůčková E, Jansová H, Macháček M, Vávrová A, Hašková P, Tichotová T, Richardson V, Kalinowski DS, Richardson DR, Šimůnek T. Quantitative analysis of the anti-proliferative activity of combinations of selected iron-chelating agents and clinically used anti-neoplastic drugs. *PLoS One*. 2014; **9**(2): e88754. IF₂₀₁₂ = 3,730

- Kultivace buněčných linií MCF-7, T47D a MDA-MB-231
- Provádění proliferačních experimentů kombinační studie
- Měření elektrické impedance pro sledování proliferace buněk v čase
- Analýzy prováděné na průtokovém cytometru (stanovení potenciálu vnitřní mitochondriální membrány sondou JC-1, stanovení progresu buněčného cyklu)
- Hlavní podíl na analýze dat a textu publikace

Serda M, Kalinowski DS, Rasko N, Potůčková E, Mrozek-Wilczkiewicz A, Musiol R, Małecki JG, Sajewicz M, Ratuszna A, Muchowicz A, Gołąb J, Šimůnek T, Richardson DR, Polanski J. Exploring the anti-cancer activity of novel thiosemicarbazones generated through the combination of retro-fragments.

- Kultivace buněčné linie SK-N-MC
- Stanovení schopnosti nových chelátorů mobilizovat železo ⁵⁹Fe z buněk SK-N-MC a zabraňovat vstřebávání železa ⁵⁹Fe z Tf
- Test oxidace askorbátu

Potůčková E, Roh J, Macháček M, Stariat J, Šesták V, Jansová H, Hašková P, Jirkovská A, Vávrová K, Kovaříková P, Richardson DR, Šimůnek T. *In vitro* characterization of pharmacological properties of the anticancer iron chelator Bp4eT and its phase I metabolites.

- Kultivace nádorových buněčných linií MCF-7, HL-60, HCT116, A549 a nenádorových linií H9c2 a 3T3
- Studium antiproliferačních a toxických účinků Bp4eT a jeho metabolitů
- Stanovení chelatační aktivity látek v buňkách MCF-7

- Stanovení schopnosti Bp4eT a jeho metabolitů mobilizovat železo ^{59}Fe z MCF-7 buněk a zabránit vstřebávání železa ^{59}Fe z Tf
- Analýza progresu buněčného cyklu prováděná na průtokovém cytometru
- Stanovení enzymové aktivity kaspáz
- Test oxidace askorbátu
- Hlavní podíl na analýze dat a textu publikace

Bendová P, Macková E, Hašková P, Vávrová A, Jirkovský E, Štěrba M, Popelová O, Kalinowski DS, Kovaříková P, Vávrová K, Richardson DR, Šimůnek T. Comparison of clinically used and experimental iron chelators for protection against oxidative stress-induced cellular injury. *Chem Res Toxicol.* 2010; **23**(6):1105-14.

IF₂₀₁₀ = 4,148

- Test oxidace askorbátu
- Podíl na analýze dat a textu publikace

Vávrová A, Jansová H, Macková E, Macháček M, Hašková P, Tichotová L, Štěrba M, Šimůnek T. Catalytic inhibitors of topoisomerase II differently modulate the toxicity of anthracyclines in cardiac and cancer cells. *PLoS One.* 2013; **8**(10):e76676.

IF₂₀₁₂ = 3,730

- Kultivace buněčné linie HL-60
- Analýzy progresu buněčného cyklu prováděné na průtokovém cytometru
- Analýza dat z průtokové cytometrie

8 Seznam zkratek

2API	(<i>E</i>)- <i>N'</i> -[1-(pyridin-2-yl)ethyliden]isonikotinohydrazid
7HII	(<i>E</i>)- <i>N'</i> -(7-hydroxy-2,3-dihydro-1 <i>H</i> -inden-1-yliden)isonikotinohydrazid
Bp44mT	2-benzoylpyridin-4,4-dimethyl-3-thiosemikarbazon
Bp4eA	<i>N</i> ³ -ethyl- <i>N'</i> ¹ -[fenyl(pyridin-2-yl)methylen]formamidrazon
Bp4eS	2-benzoylpyridin-4-ethyl-3-semikarbazon
Bp4eT	2-benzoylpyridin-4-ethyl-3-thiosemikarbazon
CDK	cyklin dependentní kináza
DCYTB	duodenální cytochrom B
DMT1	transportér divalentních iontů
Dp44mT	di-2-pyridylketon-4,4-dimethyl-3-thiosemikarbazon
DpC	di-2-pyridylketon-4-cyklohexyl-4-methyl-3-thiosemikarbazon
EDTA	kyselina ethylendiamintetraoctová
FDA	americká agentura pro schvalování léčiv ke klinickému použití
HAPI	(<i>E</i>)- <i>N'</i> -(1-(2-hydroxyfenyl)ethyliden)isonikotinohydrazid
HER2	receptor lidského epidermálního růstového faktoru 2
HIF	faktor indukovaný hypoxií
HPPI	(<i>E</i>)- <i>N'</i> -(1-(2-hydroxyfenyl)propyliden)isonikotinohydrazid
IC ₅₀	koncentrace látky inhibující buněčnou proliferaci na 50% kontroly
IRE	vazné místo pro IRP na mRNA
IRP	proteiny regulující železo
LIP	rezervoár volného železa
NHAPI	(<i>E</i>)- <i>N'</i> -(1-(2-hydroxy-5-nitrofenyl)ethyliden)isonikotinohydrazid
NIH	2-hydroxy-1-naftylaldehyd isonikotinoyl hydrazon
PIH	pyridoxal isonikotinoyl hydrazon
ROS	reaktivní formy kyslíku
SIH	salicylaldehyd isonikotinoyl hydrazon
Tf	transferrin
TfR	transferrinový receptor
VEGF-A	vaskulární endoteliální růstový faktor A

9 Seznam použité literatury

- Abeyasinghe RD, Greene BT, Haynes R, Willingham MC, Turner J, Planalp RP, Brechbiel MW, Torti FM, Torti SV. p53-independent apoptosis mediated by tachpyridine, an anti-cancer iron chelator. *Carcinogenesis* 2001; **22**(10): 1607-1614.
- Aisen P, Listowsky I. Iron transport and storage proteins. *Annu Rev Biochem* 1980; **49**: 357-393.
- Anderegg G, Raber M. Metal-Complex Formation of a New Siderophore Desferrithiocin and of 3 Related Ligands. *Journal of the Chemical Society-Chemical Communications* 1990; (17): 1194-1196.
- Anderson LJ, Wonke B, Prescott E, Holden S, Walker JM, Pennell DJ. Comparison of effects of oral deferiprone and subcutaneous desferrioxamine on myocardial iron concentrations and ventricular function in beta-thalassaemia. *Lancet* 2002; **360**(9332): 516-520.
- Arredondo M, Nunez MT. Iron and copper metabolism. *Mol Aspects Med* 2005; **26**(4-5): 313-327.
- Baker E, Richardson D, Gross S, Ponka P. Evaluation of the iron chelation potential of hydrazones of pyridoxal, salicylaldehyde and 2-hydroxy-1-naphthylaldehyde using the hepatocyte in culture. *Hepatology* 1992; **15**(3): 492-501.
- Beinert H, Kennedy MC, Stout CD. Aconitase as Ironminus signSulfur Protein, Enzyme, and Iron-Regulatory Protein. *Chem Rev* 1996; **96**(7): 2335-2374.
- Bekri S, Kispal G, Lange H, Fitzsimons E, Tolmie J, Lill R, Bishop DF. Human ABC7 transporter: gene structure and mutation causing X-linked sideroblastic anemia with ataxia with disruption of cytosolic iron-sulfur protein maturation. *Blood* 2000; **96**(9): 3256-3264.
- Belletti B, Vaidya JS, D'Andrea S, Entschladen F, Roncadin M, Lovat F, Berton S, Perin T, Candiani E, Reccanello S, Veronesi A, Canzonieri V, Trovo MG, Zaenker KS, Colombatti A, Baldassarre G, Massarut S. Targeted intraoperative

- radiotherapy impairs the stimulation of breast cancer cell proliferation and invasion caused by surgical wounding. *Clin Cancer Res* 2008; **14**(5): 1325-1332.
- Bendova P, Mackova E, Haskova P, Vavrova A, Jirkovsky E, Sterba M, Popelova O, Kalinowski DS, Kovarikova P, Vavrova K, Richardson DR, Simunek T. Comparison of clinically used and experimental iron chelators for protection against oxidative stress-induced cellular injury. *Chem Res Toxicol* 2010; **23**(6): 1105-1114.
- Berdoukas V, Chouliaras G, Moraitis P, Zannikos K, Berdoussi E, Ladis V. The efficacy of iron chelator regimes in reducing cardiac and hepatic iron in patients with thalassaemia major: a clinical observational study. *J Cardiovasc Magn Reson* 2009; **11**: 20.
- Bergeron RJ, Streiff RR, Creary EA, Daniels RD, Jr., King W, Luchetta G, Wiegand J, Moerker T, Peter HH. A comparative study of the iron-clearing properties of desferrithiocin analogues with desferrioxamine B in a Cebus monkey model. *Blood* 1993; **81**(8): 2166-2173.
- Bergeron RJ, Wiegand J, Bharti N, McManis JS. Substituent effects on desferrithiocin and desferrithiocin analogue iron-clearing and toxicity profiles. *J Med Chem* 2012; **55**(16): 7090-7103.
- Bernabe-Pineda M, Ramirez-Silva MT, Romero-Romo MA, Gonzalez-Vergara E, Rojas-Hernandez A. Spectrophotometric and electrochemical determination of the formation constants of the complexes Curcumin-Fe(III)-water and Curcumin-Fe(II)-water. *Spectrochim Acta A Mol Biomol Spectrosc* 2004; **60**(5): 1105-1113.
- Berndt C, Kurz T, Selenius M, Fernandes AP, Edgren MR, Brunk UT. Chelation of lysosomal iron protects against ionizing radiation. *Biochem J* 2010; **432**(2): 295-301.
- Blackwell KL, Burstein HJ, Storniolo AM, Rugo H, Sledge G, Koehler M, Ellis C, Casey M, Vukelja S, Bischoff J, Baselga J, O'Shaughnessy J. Randomized study of Lapatinib alone or in combination with trastuzumab in women with ErbB2-

- positive, trastuzumab-refractory metastatic breast cancer. *J Clin Oncol* 2010; **28**(7): 1124-1130.
- Borsari M, Gabbi C, Ghelfi F, Grandi R, Saladini M, Severi S ,Borella F. Silybin, a new iron-chelating agent. *J Inorg Biochem* 2001; **85**(2-3): 123-129.
- Brunton L, Chabner B ,Knollman B. General Principles of Cancer Chemotherapy. *Goodman & Gilman's - The Pharmacological Basis of Therapeutics 12th edition*. 2011, McGraw-Hill.
- Buss JL, Torti FM ,Torti SV. The role of iron chelation in cancer therapy. *Current Medicinal Chemistry* 2003; **10**(12): 1021-1034.
- Cancer Genome Atlas N. Comprehensive molecular portraits of human breast tumours. *Nature* 2012; **490**(7418): 61-70.
- Cappellini MD, Cohen A, Piga A, Bejaoui M, Perrotta S, Agaoglu L, Aydinok Y, Kattamis A, Kilinc Y, Porter J, Capra M, Galanello R, Fattoum S, Drelichman G, Magnano C, Verissimo M, Athanassiou-Metaxa M, Giardina P, Kourakli-Symeonidis A, Janka-Schaub G, Coates T, Vermynen C, Olivieri N, Thuret I, Opitz H, Ressayre-Djaffer C, Marks P ,Alberti D. A phase 3 study of deferasirox (ICL670), a once-daily oral iron chelator, in patients with beta-thalassemia. *Blood* 2006; **107**(9): 3455-3462.
- Carmine TC, Evans P, Bruchelt G, Evans R, Handgretinger R, Niethammer D ,Halliwell B. Presence of iron catalytic for free radical reactions in patients undergoing chemotherapy: implications for therapeutic management. *Cancer Lett* 1995; **94**(2): 219-226.
- Clarke M, Collins R, Darby S, Davies C, Elphinstone P, Evans E, Godwin J, Gray R, Hicks C, James S, MacKinnon E, McGale P, McHugh T, Peto R, Taylor C, Wang Y ,Early Breast Cancer Trialists' Collaborative G. Effects of radiotherapy and of differences in the extent of surgery for early breast cancer on local recurrence and 15-year survival: an overview of the randomised trials. *Lancet* 2005; **366**(9503): 2087-2106.

- Cohen AR, Galanello R, Piga A, De Sanctis V, Tricta F. Safety and effectiveness of long-term therapy with the oral iron chelator deferiprone. *Blood* 2003; **102**(5): 1583-1587.
- Cui W, Gu F, Hu KQ. Effects and mechanisms of silibinin on human hepatocellular carcinoma xenografts in nude mice. *World J Gastroenterol* 2009; **15**(16): 1943-1950.
- Cui Y, Vogt S, Olson N, Glass AG, Rohan TE. Levels of zinc, selenium, calcium, and iron in benign breast tissue and risk of subsequent breast cancer. *Cancer Epidemiol Biomarkers Prev* 2007; **16**(8): 1682-1685.
- ČR Mz. Vyhláška o stanovení obsahu a časového rozmezí preventivních prohlídek. 2009. **3/2010 Sb.**
- Dautry-Varsat A, Ciechanover A, Lodish HF. pH and the recycling of transferrin during receptor-mediated endocytosis. *Proc Natl Acad Sci U S A* 1983; **80**(8): 2258-2262.
- Dawson JH, Sono M. Cytochrome.P-450 and Chloroperoxidase - Thiolate-Ligated Heme Enzymes - Spectroscopic Determination of Their Active-Site Structures and Mechanistic Implications of Thiolate Ligation. *Chemical Reviews* 1987; **87**(5): 1255-1276.
- DeSantis C, Ma J, Bryan L, Jemal A. Breast cancer statistics, 2013. *CA Cancer J Clin* 2014; **64**(1): 52-62.
- Dezza L, Cazzola M, Danova M, Carlo-Stella C, Bergamaschi G, Brugnattelli S, Invernizzi R, Mazzini G, Riccardi A, Ascari E. Effects of desferrioxamine on normal and leukemic human hematopoietic cell growth: in vitro and in vivo studies. *Leukemia* 1989; **3**(2): 104-107.
- Donfrancesco A, Deb G, Dominici C, Pileggi D, Castello MA, Helson L. Effects of a single course of deferoxamine in neuroblastoma patients. *Cancer Res* 1990; **50**(16): 4929-4930.

- Donovan A, Brownlie A, Zhou Y, Shepard J, Pratt SJ, Moynihan J, Paw BH, Drejer A, Barut B, Zapata A, Law TC, Brugnara C, Lux SE, Pinkus GS, Pinkus JL, Kingsley PD, Palis J, Fleming MD, Andrews NC, Zon LI. Positional cloning of zebrafish ferroportin1 identifies a conserved vertebrate iron exporter. *Nature* 2000; **403**(6771): 776-781.
- Dunn LL, Suryo Rahmanto Y, Richardson DR. Iron uptake and metabolism in the new millennium. *Trends Cell Biol* 2007; **17**(2): 93-100.
- Elliott RL, Elliott MC, Wang F, Head JF. Breast carcinoma and the role of iron metabolism. A cytochemical, tissue culture, and ultrastructural study. *Ann N Y Acad Sci* 1993; **698**: 159-166.
- Fairweather-Tait SJ, Wawer AA, Gillings R, Jennings A, Myint PK. Iron status in the elderly. *Mech Ageing Dev* 2013.
- Fattman CL, Allan WP, Hasinoff BB, Yalowich JC. Collateral sensitivity to the bisdioxopiperazine dexrazoxane (ICRF-187) in etoposide (VP-16)-resistant human leukemia K562 cells. *Biochem Pharmacol* 1996; **52**(4): 635-642.
- Ferreira AL, Matsubara LS, Matsubara BB. Anthracycline-induced cardiotoxicity. *Cardiovasc Hematol Agents Med Chem* 2008; **6**(4): 278-281.
- Ferris CD, Jaffrey SR, Sawa A, Takahashi M, Brady SD, Barrow RK, Tysoe SA, Wolosker H, Baranano DE, Dore S, Poss KD, Snyder SH. Haem oxygenase-1 prevents cell death by regulating cellular iron. *Nat Cell Biol* 1999; **1**(3): 152-157.
- Fisher B, Costantino JP, Wickerham DL, Redmond CK, Kavanah M, Cronin WM, Vogel V, Robidoux A, Dimitrov N, Atkins J, Daly M, Wieand S, Tan-Chiu E, Ford L, Wolmark N. Tamoxifen for prevention of breast cancer: report of the National Surgical Adjuvant Breast and Bowel Project P-1 Study. *J Natl Cancer Inst* 1998; **90**(18): 1371-1388.
- Fleming MD. The regulation of hepcidin and its effects on systemic and cellular iron metabolism. *Hematology Am Soc Hematol Educ Program* 2008: 151-158.

- Fleming RE ,Sly WS. Mechanisms of iron accumulation in hereditary hemochromatosis. *Annu Rev Physiol* 2002; **64**: 663-680.
- Ford SJ, Obeidy P, Lovejoy DB, Bedford M, Nichols L, Chadwick C, Tucker O, Lui GY, Kalinowski DS, Jansson PJ, Iqbal TH, Alderson D, Richardson DR ,Tselepis C. Deferasirox (ICL670A) effectively inhibits oesophageal cancer growth in vitro and in vivo. *Br J Pharmacol* 2013; **168**(6): 1316-1328.
- Geyer CE, Forster J, Lindquist D, Chan S, Romieu CG, Pienkowski T, Jagiello-Gruszfeld A, Crown J, Chan A, Kaufman B, Skarlos D, Campone M, Davidson N, Berger M, Oliva C, Rubin SD, Stein S ,Cameron D. Lapatinib plus capecitabine for HER2-positive advanced breast cancer. *N Engl J Med* 2006; **355**(26): 2733-2743.
- Gharagozloo M, Khoshdel Z ,Amirghofran Z. The effect of an iron (III) chelator, silybin, on the proliferation and cell cycle of Jurkat cells: a comparison with desferrioxamine. *Eur J Pharmacol* 2008; **589**(1-3): 1-7.
- Glickstein H, El RB, Link G, Breuer W, Konijn AM, Hershko C, Nick H ,Cabantchik ZI. Action of chelators in iron-loaded cardiac cells: Accessibility to intracellular labile iron and functional consequences. *Blood* 2006; **108**(9): 3195-3203.
- Gobin J ,Horwitz MA. Exochelins of Mycobacterium tuberculosis remove iron from human iron-binding proteins and donate iron to mycobactins in the M. tuberculosis cell wall. *J Exp Med* 1996; **183**(4): 1527-1532.
- Goldhirsch A, Glick JH, Gelber RD, Coates AS ,Senn HJ. Meeting highlights: International Consensus Panel on the Treatment of Primary Breast Cancer. Seventh International Conference on Adjuvant Therapy of Primary Breast Cancer. *J Clin Oncol* 2001; **19**(18): 3817-3827.
- Goldhirsch A, Ingle JN, Gelber RD, Coates AS, Thurlimann B, Senn HJ ,Panel m. Thresholds for therapies: highlights of the St Gallen International Expert Consensus on the primary therapy of early breast cancer 2009. *Ann Oncol* 2009; **20**(8): 1319-1329.

- Greenberg PL. Myelodysplastic syndromes: iron overload consequences and current chelating therapies. *J Natl Compr Canc Netw* 2006; **4**(1): 91-96.
- Guo B, Phillips JD, Yu Y ,Leibold EA. Iron regulates the intracellular degradation of iron regulatory protein 2 by the proteasome. *J Biol Chem* 1995; **270**(37): 21645-21651.
- Guo Q, Zhao B, Li M, Shen S ,Xin W. Studies on protective mechanisms of four components of green tea polyphenols against lipid peroxidation in synaptosomes. *Biochim Biophys Acta* 1996; **1304**(3): 210-222.
- Gutteridge JM. Iron promoters of the Fenton reaction and lipid peroxidation can be released from haemoglobin by peroxides. *FEBS Lett* 1986; **201**(2): 291-295.
- Hann HW, Stahlhut MW, Rubin R ,Maddrey WC. Antitumor effect of deferoxamine on human hepatocellular carcinoma growing in athymic nude mice. *Cancer* 1992; **70**(8): 2051-2056.
- Hatcher H, Planalp R, Cho J, Torti FM ,Torti SV. Curcumin: from ancient medicine to current clinical trials. *Cell Mol Life Sci* 2008; **65**(11): 1631-1652.
- Heinz U, Hegetschweiler K, Acklin P, Faller B, Lattmann R ,Schnebli HP. 4-[3,5-bis(2-hydroxyphenyl)-1,2,4-triazol-1-yl]benzoic acid: A novel efficient and selective iron(III) complexing agent. *Angewandte Chemie-International Edition* 1999; **38**(17): 2568-2570.
- Hentze MW, Muckenthaler MU ,Andrews NC. Balancing acts: molecular control of mammalian iron metabolism. *Cell* 2004; **117**(3): 285-297.
- Hentze MW, Muckenthaler MU, Galy B ,Camaschella C. Two to tango: regulation of Mammalian iron metabolism. *Cell* 2010; **142**(1): 24-38.
- Hong CC, Ambrosone CB, Ahn J, Choi JY, McCullough ML, Stevens VL, Rodriguez C, Thun MJ ,Calle EE. Genetic variability in iron-related oxidative stress pathways (Nrf2, NQO1, NOS3, and HO-1), iron intake, and risk of postmenopausal breast cancer. *Cancer Epidemiol Biomarkers Prev* 2007; **16**(9): 1784-1794.

- Horackova M, Ponka P ,Byczko Z. The antioxidant effects of a novel iron chelator salicylaldehyde isonicotinoyl hydrazone in the prevention of H₂O₂ injury in adult cardiomyocytes. *Cardiovasc Res* 2000; **47**(3): 529-536.
- Hruskova K, Kovarikova P, Bendova P, Haskova P, Mackova E, Stariat J, Vavrova A, Vavrova K ,Simunek T. Synthesis and initial in vitro evaluations of novel antioxidant aroylhydrazone iron chelators with increased stability against plasma hydrolysis. *Chem Res Toxicol* 2011; **24**(3): 290-302.
- Huang X. Does iron have a role in breast cancer? *Lancet Oncol* 2008; **9**(8): 803-807.
- Huang ZX, May PM, Quinlan KM, Williams DR ,Creighton AM. Metal binding by pharmaceuticals. Part 2. Interactions of Ca(II), Cu(II), Fe(II), Mg(II), Mn(II) and Zn(II) with the intracellular hydrolysis products of the antitumour agent ICRF 159 and its inactive homologue ICRF 192. *Agents Actions* 1982; **12**(4): 536-542.
- Chen Y, Jungsuwadee P, Vore M, Butterfield DA ,St Clair DK. Collateral damage in cancer chemotherapy: oxidative stress in nontargeted tissues. *Mol Interv* 2007; **7**(3): 147-156.
- Chenoufi N, Drenou B, Loreal O, Pigeon C, Brissot P ,Lescoat G. Antiproliferative effect of deferiprone on the Hep G2 cell line. *Biochem Pharmacol* 1998; **56**(4): 431-437.
- Chou TC ,Talalay P. Quantitative analysis of dose-effect relationships: the combined effects of multiple drugs or enzyme inhibitors. *Adv Enzyme Regul* 1984; **22**: 27-55.
- Ionescu JG, Novotny J, Stejskal V, Latsch A, Blaurock-Busch E ,Eisenmann-Klein M. Increased levels of transition metals in breast cancer tissue. *Neuro Endocrinol Lett* 2006; **27 Suppl 1**: 36-39.
- Iwai K, Drake SK, Wehr NB, Weissman AM, LaVaute T, Minato N, Klausner RD, Levine RL ,Rouault TA. Iron-dependent oxidation, ubiquitination, and degradation of iron regulatory protein 2: implications for degradation of oxidized proteins. *Proc Natl Acad Sci U S A* 1998; **95**(9): 4924-4928.

- Jacobs A, Jones B, Ricketts C, Bulbrook RD, Wang DY. Serum ferritin concentration in early breast cancer. *Br J Cancer* 1976; **34**(3): 286-290.
- Jacobs BP, Dennehy C, Ramirez G, Sapp J, Lawrence VA. Milk thistle for the treatment of liver disease: a systematic review and meta-analysis. *Am J Med* 2002; **113**(6): 506-515.
- Jansson PJ, Hawkins CL, Lovejoy DB, Richardson DR. The iron complex of Dp44mT is redox-active and induces hydroxyl radical formation: An EPR study. *Journal of Inorganic Biochemistry* 2010; **104**(11): 1224-1228.
- Jemal A, Bray F, Center MM, Ferlay J, Ward E, Forman D. Global cancer statistics. *CA Cancer J Clin* 2011; **61**(2): 69-90.
- Jomova K, Valko M. Advances in metal-induced oxidative stress and human disease. *Toxicology* 2011; **283**(2-3): 65-87.
- Kakhlon O, Cabantchik ZI. The labile iron pool: characterization, measurement, and participation in cellular processes(1). *Free Radic Biol Med* 2002; **33**(8): 1037-1046.
- Kalinowski DS, Richardson DR. The evolution of iron chelators for the treatment of iron overload disease and cancer. *Pharmacol Rev* 2005; **57**(4): 547-583.
- Kalinowski DS, Sharpe PC, Bernhardt PV, Richardson DR. Design, synthesis, and characterization of new iron chelators with anti-proliferative activity: structure-activity relationships of novel thiohydrazone analogues. *J Med Chem* 2007; **50**(24): 6212-6225.
- Kallianpur AR, Lee SA, Gao YT, Lu W, Zheng Y, Ruan ZX, Dai Q, Gu K, Shu XO, Zheng W. Dietary animal-derived iron and fat intake and breast cancer risk in the Shanghai Breast Cancer Study. *Breast Cancer Res Treat* 2008; **107**(1): 123-132.
- Kappus H. Oxidative stress in chemical toxicity. *Arch Toxicol* 1987; **60**(1-3): 144-149.
- Kehrer JP. The Haber-Weiss reaction and mechanisms of toxicity. *Toxicology* 2000; **149**(1): 43-50.

- Kicic A, Chua AC ,Baker E. Desferrithiocin is a more potent antineoplastic agent than desferrioxamine. *Br J Pharmacol* 2002; **135**(6): 1393-1402.
- King MC, Marks JH, Mandell JB ,New York Breast Cancer Study G. Breast and ovarian cancer risks due to inherited mutations in BRCA1 and BRCA2. *Science* 2003; **302**(5645): 643-646.
- Klimtova I, Simunek T, Mazurova Y, Kaplanova J, Sterba M, Hrdina R, Gersl V, Adamcova M ,Ponka P. A study of potential toxic effects after repeated 10-week administration of a new iron chelator--salicylaldehyde isonicotinoyl hydrazone (SIH) to rabbits. *Acta Medica (Hradec Kralove)* 2003; **46**(4): 163-170.
- Knox JJ, Hotte SJ, Kollmannsberger C, Winquist E, Fisher B ,Eisenhauer EA. Phase II study of Triapine in patients with metastatic renal cell carcinoma: a trial of the National Cancer Institute of Canada Clinical Trials Group (NCIC IND.161). *Invest New Drugs* 2007; **25**(5): 471-477.
- Kosters JP ,Gotzsche PC. Regular self-examination or clinical examination for early detection of breast cancer. *Cochrane Database Syst Rev* 2003; (2): CD003373.
- Kovacevic Z, Chikhani S, Lovejoy DB ,Richardson DR. Novel thiosemicarbazone iron chelators induce up-regulation and phosphorylation of the metastasis suppressor N-myc down-stream regulated gene 1: a new strategy for the treatment of pancreatic cancer. *Mol Pharmacol* 2011a; **80**(4): 598-609.
- Kovacevic Z, Kalinowski DS, Lovejoy DB, Yu Y, Suryo Rahmanto Y, Sharpe PC, Bernhardt PV ,Richardson DR. The medicinal chemistry of novel iron chelators for the treatment of cancer. *Curr Top Med Chem* 2011b; **11**(5): 483-499.
- Kunnumakkara AB, Diagaradjane P, Anand P, Harikumar KB, Deorukhkar A, Gelovani J, Guha S, Krishnan S ,Aggarwal BB. Curcumin sensitizes human colorectal cancer to capecitabine by modulation of cyclin D1, COX-2, MMP-9, VEGF and CXCR4 expression in an orthotopic mouse model. *Int J Cancer* 2009; **125**(9): 2187-2197.
- Kwiatkowski JL. Real-world use of iron chelators. *Hematology Am Soc Hematol Educ Program* 2011; **2011**: 451-458.

- Landschulz W, Thesleff I, Ekblom P. A lipophilic iron chelator can replace transferrin as a stimulator of cell proliferation and differentiation. *J Cell Biol* 1984; **98**(2): 596-601.
- Laskey J, Webb I, Schulman HM, Ponka P. Evidence that transferrin supports cell proliferation by supplying iron for DNA synthesis. *Exp Cell Res* 1988; **176**(1): 87-95.
- Latunde-Dada GO, Simpson RJ, McKie AT. Recent advances in mammalian haem transport. *Trends Biochem Sci* 2006; **31**(3): 182-188.
- Le NT, Richardson DR. The role of iron in cell cycle progression and the proliferation of neoplastic cells. *Biochim Biophys Acta* 2002; **1603**(1): 31-46.
- Leidgens S, Bullough KZ, Shi H, Li F, Shakoury-Elizeh M, Yabe T, Subramanian P, Hsu E, Natarajan N, Nandal A, Stemmler TL, Philpott CC. Each member of the poly-r(C)-binding protein 1 (PCBP) family exhibits iron chaperone activity toward ferritin. *J Biol Chem* 2013; **288**(24): 17791-17802.
- Li L, Gao Y, Zhang L, Zeng J, He D, Sun Y. Silibinin inhibits cell growth and induces apoptosis by caspase activation, down-regulating survivin and blocking EGFR-ERK activation in renal cell carcinoma. *Cancer Lett* 2008; **272**(1): 61-69.
- Liu ZD, Hider RC. Design of iron chelators with therapeutic application. *Coordination Chemistry Reviews* 2002; **232**(1-2): 151-171.
- Liuzzi JP, Aydemir F, Nam H, Knutson MD, Cousins RJ. Zip14 (Slc39a14) mediates non-transferrin-bound iron uptake into cells. *Proc Natl Acad Sci U S A* 2006; **103**(37): 13612-13617.
- Lovejoy DB, Sharp DM, Seebacher N, Obeidy P, Prichard T, Stefani C, Basha MT, Sharpe PC, Jansson PJ, Kalinowski DS, Bernhardt PV, Richardson DR. Novel second-generation di-2-pyridylketone thiosemicarbazones show synergism with standard chemotherapeutics and demonstrate potent activity against lung cancer xenografts after oral and intravenous administration in vivo. *J Med Chem* 2012; **55**(16): 7230-7244.

- Lui GY, Obeidy P, Ford SJ, Tselepis C, Sharp DM, Jansson PJ, Kalinowski DS, Kovacevic Z, Lovejoy DB, Richardson DR. The iron chelator, deferasirox, as a novel strategy for cancer treatment: oral activity against human lung tumor xenografts and molecular mechanism of action. *Mol Pharmacol* 2013; **83**(1): 179-190.
- Ma B, Goh BC, Tan EH, Lam KC, Soo R, Leong SS, Wang LZ, Mo F, Chan AT, Zee B, Mok T. A multicenter phase II trial of 3-aminopyridine-2-carboxaldehyde thiosemicarbazone (3-AP, Triapine) and gemcitabine in advanced non-small-cell lung cancer with pharmacokinetic evaluation using peripheral blood mononuclear cells. *Invest New Drugs* 2008; **26**(2): 169-173.
- Ma CX, Ellis MJ. The Cancer Genome Atlas: clinical applications for breast cancer. *Oncology (Williston Park)* 2013; **27**(12): 1263-1269, 1274-1269.
- Mackova E, Hruskova K, Bendova P, Vavrova A, Jansova H, Haskova P, Kovarikova P, Vavrova K, Simunek T. Methyl and ethyl ketone analogs of salicylaldehyde isonicotinoyl hydrazone: novel iron chelators with selective antiproliferative action. *Chem Biol Interact* 2012; **197**(2-3): 69-79.
- Mandel S, Amit T, Reznichenko L, Weinreb O, Youdim MB. Green tea catechins as brain-permeable, natural iron chelators-antioxidants for the treatment of neurodegenerative disorders. *Mol Nutr Food Res* 2006; **50**(2): 229-234.
- Matter H, Baringhaus KH, Naumann T, Klabunde T, Pirard B. Computational approaches towards the rational design of drug-like compound libraries. *Comb Chem High Throughput Screen* 2001; **4**(6): 453-475.
- McKie AT. The role of Dcytb in iron metabolism: an update. *Biochem Soc Trans* 2008; **36**(Pt 6): 1239-1241.
- McKie AT, Barrow D, Latunde-Dada GO, Rolfs A, Sager G, Mudaly E, Mudaly M, Richardson C, Barlow D, Bomford A, Peters TJ, Raja KB, Shirali S, Hediger MA, Farzaneh F, Simpson RJ. An iron-regulated ferric reductase associated with the absorption of dietary iron. *Science* 2001; **291**(5509): 1755-1759.

- Merlot AM, Pantarat N, Lovejoy DB, Kalinowski DS ,Richardson DR. Membrane transport and intracellular sequestration of novel thiosemicarbazone chelators for the treatment of cancer. *Mol Pharmacol* 2010; **78**(4): 675-684.
- Millart H, Kantelip JP, Platonoff N, Descous I, Trenque T, Lamiable D ,Choisy H. Increased iron content in rat myocardium after 5-fluorouracil chronic administration. *Anticancer Res* 1993; **13**(3): 779-783.
- Miller K, Wang M, Gralow J, Dickler M, Cobleigh M, Perez EA, Shenkier T, Cella D ,Davidson NE. Paclitaxel plus bevacizumab versus paclitaxel alone for metastatic breast cancer. *N Engl J Med* 2007; **357**(26): 2666-2676.
- Mims MP ,Prchal JT. Divalent metal transporter 1. *Hematology* 2005; **10**(4): 339-345.
- Moller S, Jensen MB, Ejlersen B, Bjerre KD, Larsen M, Hansen HB, Christiansen P, Mouridsen HT ,Danish Breast Cancer Cooperative G. The clinical database and the treatment guidelines of the Danish Breast Cancer Cooperative Group (DBCG); its 30-years experience and future promise. *Acta Oncol* 2008; **47**(4): 506-524.
- Murren J, Modiano M, Clairmont C, Lambert P, Savaraj N, Doyle T ,Sznol M. Phase I and pharmacokinetic study of triapine, a potent ribonucleotide reductase inhibitor, administered daily for five days in patients with advanced solid tumors. *Clin Cancer Res* 2003; **9**(11): 4092-4100.
- Nakai Y, Inoue K, Abe N, Hatakeyama M, Ohta KY, Otagiri M, Hayashi Y ,Yuasa H. Functional characterization of human proton-coupled folate transporter/heme carrier protein 1 heterologously expressed in mammalian cells as a folate transporter. *J Pharmacol Exp Ther* 2007; **322**(2): 469-476.
- Neilands JB. Siderophores: structure and function of microbial iron transport compounds. *J Biol Chem* 1995; **270**(45): 26723-26726.
- Nemeth E, Tuttle MS, Powelson J, Vaughn MB, Donovan A, Ward DM, Ganz T ,Kaplan J. Hepcidin regulates cellular iron efflux by binding to ferroportin and inducing its internalization. *Science* 2004; **306**(5704): 2090-2093.

- Nordlund P, Sjöberg BM, Eklund H. Three-dimensional structure of the free radical protein of ribonucleotide reductase. *Nature* 1990; **345**(6276): 593-598.
- Noulsri E, Richardson DR, Lerdwana S, Fucharoen S, Yamagishi T, Kalinowski DS, Pattanapanyasat K. Antitumor activity and mechanism of action of the iron chelator, Dp44mT, against leukemic cells. *Am J Hematol* 2009; **84**(3): 170-176.
- Nyholm S, Mann GJ, Johansson AG, Bergeron RJ, Graslund A, Thelander L. Role of ribonucleotide reductase in inhibition of mammalian cell growth by potent iron chelators. *J Biol Chem* 1993; **268**(35): 26200-26205.
- Ohgami RS, Campagna DR, Greer EL, Antiochos B, McDonald A, Chen J, Sharp JJ, Fujiwara Y, Barker JE, Fleming MD. Identification of a ferrireductase required for efficient transferrin-dependent iron uptake in erythroid cells. *Nat Genet* 2005; **37**(11): 1264-1269.
- Ohyashiki JH, Kobayashi C, Hamamura R, Okabe S, Tauchi T, Ohyashiki K. The oral iron chelator deferasirox represses signaling through the mTOR in myeloid leukemia cells by enhancing expression of REDD1. *Cancer Sci* 2009; **100**(5): 970-977.
- Oliveira F, Rocha S, Fernandes R. Iron Metabolism: From Health to Disease. *J Clin Lab Anal* 2014.
- Olivieri NF, Brittenham GM. Iron-chelating therapy and the treatment of thalassemia. *Blood* 1997; **89**(3): 739-761.
- Olivieri NF, Brittenham GM, McLaren CE, Templeton DM, Cameron RG, McClelland RA, Burt AD, Fleming KA. Long-term safety and effectiveness of iron-chelation therapy with deferiprone for thalassemia major. *N Engl J Med* 1998; **339**(7): 417-423.
- Pahl PM, Horwitz LD. Cell permeable iron chelators as potential cancer chemotherapeutic agents. *Cancer Invest* 2005; **23**(8): 683-691.

- Pahl PM, Horwitz MA, Horwitz KB, Horwitz LD. Desferri-exochelin induces death by apoptosis in human breast cancer cells but does not kill normal breast cells. *Breast Cancer Res Treat* 2001; **69**(1): 69-79.
- Pantopoulos K, Hentze MW. Nitric oxide signaling to iron-regulatory protein: direct control of ferritin mRNA translation and transferrin receptor mRNA stability in transfected fibroblasts. *Proc Natl Acad Sci U S A* 1995; **92**(5): 1267-1271.
- Paradkar PN, Zumbrennen KB, Paw BH, Ward DM, Kaplan J. Regulation of mitochondrial iron import through differential turnover of mitoferrin 1 and mitoferrin 2. *Mol Cell Biol* 2009; **29**(4): 1007-1016.
- Pennell DJ, Porter JB, Cappellini MD, El-Beshlawy A, Chan LL, Aydinok Y, Elalfy MS, Sutcharitchan P, Li CK, Ibrahim H, Viprakasit V, Kattamis A, Smith G, Habr D, Domokos G, Roubert B, Taher A. Efficacy of deferasirox in reducing and preventing cardiac iron overload in beta-thalassemia. *Blood* 2010; **115**(12): 2364-2371.
- Peslova G, Petrak J, Kuzelova K, Hrdy I, Halada P, Kuchel PW, Soe-Lin S, Ponka P, Sutak R, Becker E, Huang ML, Suryo Rahmanto Y, Richardson DR, Vyoral D. Hepcidin, the hormone of iron metabolism, is bound specifically to alpha-2-macroglobulin in blood. *Blood* 2009; **113**(24): 6225-6236.
- Petruzelka L, Novotny J. Doporučené postupy pro praktické lékaře - Karcinom prsu. 2002 Purkyně Čl. JE.
- Piga A, Gaglioti C, Fogliacco E, Tricta F. Comparative effects of deferiprone and deferoxamine on survival and cardiac disease in patients with thalassemia major: a retrospective analysis. *Haematologica* 2003; **88**(5): 489-496.
- Pinnix ZK, Miller LD, Wang W, D'Agostino R, Jr., Kute T, Willingham MC, Hatcher H, Tesfay L, Sui G, Di X, Torti SV, Torti FM. Ferroportin and iron regulation in breast cancer progression and prognosis. *Sci Transl Med* 2010; **2**(43): 43ra56.
- Ponka P, Borova J, Neuwirt J, Fuchs O. Mobilization of iron from reticulocytes. Identification of pyridoxal isonicotinoyl hydrazone as a new iron chelating agent. *FEBS Lett* 1979; **97**(2): 317-321.

- Popelova O, Sterba M, Haskova P, Simunek T, Hroch M, Guncova I, Nachtigal P, Adamcova M, Gersl V, Mazurova Y. Dexrazoxane-afforded protection against chronic anthracycline cardiotoxicity in vivo: effective rescue of cardiomyocytes from apoptotic cell death. *Br J Cancer* 2009; **101**(5): 792-802.
- Potuckova E, Jansova H, Machacek M, Vavrova A, Haskova P, Tichotova L, Richardson V, Kalinowski DS, Richardson DR, Simunek T. Quantitative analysis of the anti-proliferative activity of combinations of selected iron-chelating agents and clinically used anti-neoplastic drugs. *PLoS One* 2014; **9**(2): e88754.
- Princiotto JV, Zapolski EJ. Difference between the two iron-binding sites of transferrin. *Nature* 1975; **255**(5503): 87-88.
- Rao VA, Klein SR, Agama KK, Toyoda E, Adachi N, Pommier Y, Shacter EB. The iron chelator Dp44mT causes DNA damage and selective inhibition of topoisomerase IIalpha in breast cancer cells. *Cancer Res* 2009; **69**(3): 948-957.
- Richardson DR. Friedreich's ataxia: iron chelators that target the mitochondrion as a therapeutic strategy? *Expert Opin Investig Drugs* 2003; **12**(2): 235-245.
- Richardson DR, Kalinowski DS, Lau S, Jansson PJ, Lovejoy DB. Cancer cell iron metabolism and the development of potent iron chelators as anti-tumour agents. *Biochim Biophys Acta* 2009; **1790**(7): 702-717.
- Richardson DR, Lane DJ, Becker EM, Huang ML, Whitnall M, Suryo Rahmanto Y, Sheftel AD, Ponka P. Mitochondrial iron trafficking and the integration of iron metabolism between the mitochondrion and cytosol. *Proc Natl Acad Sci U S A* 2010; **107**(24): 10775-10782.
- Richardson DR, Ponka P. The molecular mechanisms of the metabolism and transport of iron in normal and neoplastic cells. *Biochim Biophys Acta* 1997; **1331**(1): 1-40.
- Richardson DR, Sharpe PC, Lovejoy DB, Senaratne D, Kalinowski DS, Islam M, Bernhardt PV. Dipyrindyl thiosemicarbazone chelators with potent and selective

- antitumor activity form iron complexes with redox activity. *J Med Chem* 2006; **49**(22): 6510-6521.
- Richardson DR, Tran EH ,Ponka P. The potential of iron chelators of the pyridoxal isonicotinoyl hydrazone class as effective antiproliferative agents. *Blood* 1995; **86**(11): 4295-4306.
- Ryan P ,Hynes MJ. The kinetics and mechanisms of the complex formation and antioxidant behaviour of the polyphenols EGCg and ECG with iron(III). *J Inorg Biochem* 2007; **101**(4): 585-593.
- Samuni AM, Krishna MC, DeGraff W, Russo A, Planalp RP, Brechbiel MW ,Mitchell JB. Mechanisms underlying the cytotoxic effects of Tachpyr--a novel metal chelator. *Biochim Biophys Acta* 2002; **1571**(3): 211-218.
- Sartorelli AC, Agrawal KC, Tsiftoglou AS ,Moore EC. Characterization of the biochemical mechanism of action of alpha-(N)-heterocyclic carboxaldehyde thiosemicarbazones. *Adv Enzyme Regul* 1976; **15**: 117-139.
- Serda M, Kalinowski DS, Mrozek-Wilczkiewicz A, Musiol R, Szurko A, Ratuszna A, Pantarat N, Kovacevic Z, Merlot AM, Richardson DR ,Polanski J. Synthesis and characterization of quinoline-based thiosemicarbazones and correlation of cellular iron-binding efficacy to anti-tumor efficacy. *Bioorg Med Chem Lett* 2012; **22**(17): 5527-5531.
- Sharpe PC, Richardson DR, Kalinowski DS ,Bernhardt PV. Synthetic and natural products as iron chelators. *Curr Top Med Chem* 2011; **11**(5): 591-607.
- Shayeghi M, Latunde-Dada GO, Oakhill JS, Laftah AH, Takeuchi K, Halliday N, Khan Y, Warley A, McCann FE, Hider RC, Frazer DM, Anderson GJ, Vulpe CD, Simpson RJ ,McKie AT. Identification of an intestinal heme transporter. *Cell* 2005; **122**(5): 789-801.
- Shindelman JE, Ortmeyer AE ,Sussman HH. Demonstration of the transferrin receptor in human breast cancer tissue. Potential marker for identifying dividing cells. *Int J Cancer* 1981; **27**(3): 329-334.

- Shindo M, Torimoto Y, Saito H, Motomura W, Ikuta K, Sato K, Fujimoto Y, Kohgo Y. Functional role of DMT1 in transferrin-independent iron uptake by human hepatocyte and hepatocellular carcinoma cell, HLF. *Hepatol Res* 2006; **35**(3): 152-162.
- Schimmel KJ, Richel DJ, van den Brink RB, Guchelaar HJ. Cardiotoxicity of cytotoxic drugs. *Cancer Treat Rev* 2004; **30**(2): 181-191.
- Siegel R, Naishadham D, Jemal A. Cancer statistics, 2013. *CA Cancer J Clin* 2013; **63**(1): 11-30.
- Simonart T, Boelaert JR, Mosselmans R, Andrei G, Noel JC, De Clercq E, Snoeck R. Antiproliferative and apoptotic effects of iron chelators on human cervical carcinoma cells. *Gynecol Oncol* 2002; **85**(1): 95-102.
- Simunek T, Boer C, Bouwman RA, Vlasblom R, Versteilen AM, Sterba M, Gersl V, Hrdina R, Ponka P, de Lange JJ, Paulus WJ, Musters RJ. SIH--a novel lipophilic iron chelator--protects H9c2 cardiomyoblasts from oxidative stress-induced mitochondrial injury and cell death. *J Mol Cell Cardiol* 2005; **39**(2): 345-354.
- Simunek T, Sterba M, Popelova O, Kaiserova H, Adamcova M, Hroch M, Haskova P, Ponka P, Gersl V. Anthracycline toxicity to cardiomyocytes or cancer cells is differently affected by iron chelation with salicylaldehyde isonicotinoyl hydrazone. *Br J Pharmacol* 2008; **155**(1): 138-148.
- Singh RP, Raina K, Sharma G, Agarwal R. Silibinin inhibits established prostate tumor growth, progression, invasion, and metastasis and suppresses tumor angiogenesis and epithelial-mesenchymal transition in transgenic adenocarcinoma of the mouse prostate model mice. *Clin Cancer Res* 2008; **14**(23): 7773-7780.
- Singletary SE, Connolly JL. Breast cancer staging: working with the sixth edition of the AJCC Cancer Staging Manual. *CA Cancer J Clin* 2006; **56**(1): 37-47; quiz 50-31.
- Smith IE, Dowsett M. Aromatase inhibitors in breast cancer. *N Engl J Med* 2003; **348**(24): 2431-2442.

- Solomon EI, Brunold TC, Davis MI, Kemsley JN, Lee SK, Lehnert N, Neese F, Skulan AJ, Yang YS, Zhou J. Geometric and electronic structure/function correlations in non-heme iron enzymes. *Chem Rev* 2000; **100**(1): 235-350.
- Sorlie T, Tibshirani R, Parker J, Hastie T, Marron JS, Nobel A, Deng S, Johnsen H, Pesich R, Geisler S, Demeter J, Perou CM, Lonning PE, Brown PO, Borresen-Dale AL, Botstein D. Repeated observation of breast tumor subtypes in independent gene expression data sets. *Proc Natl Acad Sci U S A* 2003; **100**(14): 8418-8423.
- Stariat J, Sestak V, Vavrova K, Nobilis M, Kollarova Z, Klimes J, Kalinowski DS, Richardson DR, Kovarikova P. LC-MS/MS identification of the principal in vitro and in vivo phase I metabolites of the novel thiosemicarbazone anti-cancer drug, Bp4eT. *Anal Bioanal Chem* 2012; **403**(1): 309-321.
- Summers MR, Jacobs A, Tudway D, Perera P, Ricketts C. Studies in desferrioxamine and ferrioxamine metabolism in normal and iron-loaded subjects. *Br J Haematol* 1979; **42**(4): 547-555.
- Swain SM, Whaley FS, Gerber MC, Weisberg S, York M, Spicer D, Jones SE, Wadler S, Desai A, Vogel C, Speyer J, Mittelman A, Reddy S, Pendergrass K, Velez-Garcia E, Ewer MS, Bianchini JR, Gams RA. Cardioprotection with dexrazoxane for doxorubicin-containing therapy in advanced breast cancer. *J Clin Oncol* 1997; **15**(4): 1318-1332.
- Taketani S, Adachi Y, Kohno H, Ikehara S, Tokunaga R, Ishii T. Molecular characterization of a newly identified heme-binding protein induced during differentiation of urine erythroleukemia cells. *J Biol Chem* 1998; **273**(47): 31388-31394.
- Tanaka H, Arakawa H, Yamaguchi T, Shiraishi K, Fukuda S, Matsui K, Takei Y, Nakamura Y. A ribonucleotide reductase gene involved in a p53-dependent cell-cycle checkpoint for DNA damage. *Nature* 2000; **404**(6773): 42-49.
- Thangapazham RL, Passi N, Maheshwari RK. Green tea polyphenol and epigallocatechin gallate induce apoptosis and inhibit invasion in human breast cancer cells. *Cancer Biol Ther* 2007; **6**(12): 1938-1943.

- Torti FM ,Torti SV. Regulation of ferritin genes and protein. *Blood* 2002; **99**(10): 3505-3516.
- Torti SV, Torti FM, Whitman SP, Brechbiel MW, Park G ,Planalp RP. Tumor cell cytotoxicity of a novel metal chelator. *Blood* 1998; **92**(4): 1384-1389.
- Tyagi A, Singh RP, Ramasamy K, Raina K, Redente EF, Dwyer-Nield LD, Radcliffe RA, Malkinson AM ,Agarwal R. Growth inhibition and regression of lung tumors by silibinin: modulation of angiogenesis by macrophage-associated cytokines and nuclear factor-kappaB and signal transducers and activators of transcription 3. *Cancer Prev Res (Phila)* 2009; **2**(1): 74-83.
- Vaidya JS, Baum M, Tobias JS, Wenz F, Massarut S, Keshtgar M, Hilaris B, Saunders C, Williams NR, Brew-Graves C, Corica T, Roncadin M, Kraus-Tiefenbacher U, Sutterlin M, Bulsara M ,Joseph D. Long-term results of targeted intraoperative radiotherapy (Targit) boost during breast-conserving surgery. *Int J Radiat Oncol Biol Phys* 2011; **81**(4): 1091-1097.
- Vaidya JS, Joseph DJ, Tobias JS, Bulsara M, Wenz F, Saunders C, Alvarado M, Flyger HL, Massarut S, Eiermann W, Keshtgar M, Dewar J, Kraus-Tiefenbacher U, Sutterlin M, Esserman L, Holtveg HM, Roncadin M, Pigorsch S, Metaxas M, Falzon M, Matthews A, Corica T, Williams NR ,Baum M. Targeted intraoperative radiotherapy versus whole breast radiotherapy for breast cancer (TARGIT-A trial): an international, prospective, randomised, non-inferiority phase 3 trial. *Lancet* 2010; **376**(9735): 91-102.
- Vandewalle B, Hornez L, Revillion F ,Lefebvre J. Secretion of transferrin by human breast cancer cells. *Biochem Biophys Res Commun* 1989; **163**(1): 149-154.
- Vavrova A, Jansova H, Mackova E, Machacek M, Haskova P, Tichotova L, Sterba M ,Simunek T. Catalytic inhibitors of topoisomerase II differently modulate the toxicity of anthracyclines in cardiac and cancer cells. *PLoS One* 2013; **8**(10): e76676.
- Vejpongsa P ,Yeh ET. Topoisomerase 2beta: a promising molecular target for primary prevention of anthracycline-induced cardiotoxicity. *Clin Pharmacol Ther* 2014; **95**(1): 45-52.

- Veronesi U, Cascinelli N, Mariani L, Greco M, Saccozzi R, Luini A, Aguilar M, Marubini E. Twenty-year follow-up of a randomized study comparing breast-conserving surgery with radical mastectomy for early breast cancer. *N Engl J Med* 2002; **347**(16): 1227-1232.
- Vogel CL, Cobleigh MA, Tripathy D, Gutheil JC, Harris LN, Fehrenbacher L, Slamon DJ, Murphy M, Novotny WF, Burchmore M, Shak S, Stewart SJ, Press M. Efficacy and safety of trastuzumab as a single agent in first-line treatment of HER2-overexpressing metastatic breast cancer. *J Clin Oncol* 2002; **20**(3): 719-726.
- Vulpe CD, Kuo YM, Murphy TL, Cowley L, Askwith C, Libina N, Gitschier J, Anderson GJ. Hephaestin, a ceruloplasmin homologue implicated in intestinal iron transport, is defective in the sla mouse. *Nat Genet* 1999; **21**(2): 195-199.
- Vyhlidal C, Li X, Safe S. Estrogen regulation of transferrin gene expression in MCF-7 human breast cancer cells. *J Mol Endocrinol* 2002; **29**(3): 305-317.
- Wallander ML, Leibold EA, Eisenstein RS. Molecular control of vertebrate iron homeostasis by iron regulatory proteins. *Biochim Biophys Acta* 2006; **1763**(7): 668-689.
- Weiss G, Loyevsky M, Gordeuk VR. Dexrazoxane (ICRF-187). *Gen Pharmacol* 1999; **32**(1): 155-158.
- Whitnall M, Howard J, Ponka P, Richardson DR. A class of iron chelators with a wide spectrum of potent antitumor activity that overcomes resistance to chemotherapeutics. *Proc Natl Acad Sci U S A* 2006; **103**(40): 14901-14906.
- Wood JC, Kang BP, Thompson A, Giardina P, Harmatz P, Glynos T, Paley C, Coates TD. The effect of deferasirox on cardiac iron in thalassemia major: impact of total body iron stores. *Blood* 2010; **116**(4): 537-543.
- Yeh KY, Yeh M, Glass J. Heparin regulation of ferroportin 1 expression in the liver and intestine of the rat. *Am J Physiol Gastrointest Liver Physiol* 2004; **286**(3): G385-394.

- Yu Y, Kovacevic Z ,Richardson DR. Tuning cell cycle regulation with an iron key. *Cell Cycle* 2007; **6**(16): 1982-1994.
- Yu Y, Suryo Rahmanto Y ,Richardson DR. Bp44mT: an orally active iron chelator of the thiosemicarbazone class with potent anti-tumour efficacy. *Br J Pharmacol* 2012; **165**(1): 148-166.
- Yu Y, Wong J, Lovejoy DB, Kalinowski DS ,Richardson DR. Chelators at the cancer coalface: desferrioxamine to Triapine and beyond. *Clin Cancer Res* 2006; **12**(23): 6876-6883.
- Yuan J, Lovejoy DB ,Richardson DR. Novel di-2-pyridyl-derived iron chelators with marked and selective antitumor activity: in vitro and in vivo assessment. *Blood* 2004; **104**(5): 1450-1458.
- Zaveri NT. Green tea and its polyphenolic catechins: medicinal uses in cancer and noncancer applications. *Life Sci* 2006; **78**(18): 2073-2080.
- Zoli W, Ulivi P, Tesei A, Fabbri F, Rosetti M, Maltoni R, Giunchi DC, Ricotti L, Briigliadori G, Vannini I ,Amadori D. Addition of 5-fluorouracil to doxorubicin-paclitaxel sequence increases caspase-dependent apoptosis in breast cancer cell lines. *Breast Cancer Res* 2005; **7**(5): R681-689.

10 Přehled publikační činnosti

Potůčková E, Jansová H, Macháček M, Vávrová A, Hašková P, Tichotová T, Richardson V, Kalinowski DS, Richardson DR, Šimůnek T. Quantitative analysis of the anti-proliferative activity of combinations of selected iron-chelating agents and clinically used anti-neoplastic drugs. *PLoS One*. 2014; **9**(2): e88754. IF₂₀₁₂ = 3,730

Vávrová A, Jansová H, Macková E, Macháček M, Hašková P, Tichotová L, Štěrba M, Šimůnek T. Catalytic inhibitors of topoisomerase II differently modulate the toxicity of anthracyclines in cardiac and cancer cells. *PLoS One*. 2013; **8**(10): e76676. IF₂₀₁₂ = 3,730

Macková E, Hrušková K, Bendová P, Vávrová A, Jansová H, Hašková P, Kovaříková P, Vávrová K, Šimůnek T. Methyl and ethyl ketone analogs of salicylaldehyde isonicotinoyl hydrazone: novel iron chelators with selective antiproliferative action. *Chem Biol Interact*. 2012; **197**(2-3): 69-79. IF₂₀₁₂ = 2,967

Hašková P, Koubková L, Vávrová A, Macková E, Hrušková K, Kovaříková P, Vávrová K, Šimůnek T. Comparison of various iron chelators used in clinical practice as protecting agents against catecholamine-induced oxidative injury and cardiotoxicity. *Toxicology*. 2011; **289**(2-3): 122-131. IF₂₀₁₁ = 3,681

Hrušková K, Kovaříková P, Bendová P, Hašková P, Macková E, Stariat J, Vávrová A, Vávrová K, Šimůnek T. Synthesis and Initial in Vitro Evaluations of Novel Antioxidant Aroylhydrazone Iron Chelators with Increased Stability against Plasma Hydrolysis. *Chem Res Toxicol*. 2011; **24**(3): 290-302. IF₂₀₁₁ = 3,779

Hašková P, Kovaříková P, Koubková L, Vávrová A, Macková E, Šimůnek T. Iron chelation with salicylaldehyde isonicotinoyl hydrazone protects against catecholamine autoxidation and cardiotoxicity. *Free Radic Biol Med*. 2011; **50**(4): 537-549. IF₂₀₁₁ = 5,423

- Bendová P, Macková E, Hašková P, Vávrová A, Jirkovský E, Štěrbá M, Popelová O, Kalinowski DS, Kovaříková P, Vávrová K, Richardson DR, Šimůnek T. Comparison of clinically used and experimental iron chelators for protection against oxidative stress-induced cellular injury. *Chem Res Toxicol*. 2010; **23**(6): 1105-1114. IF₂₀₁₀ = 4,148
- Mladěnka P, Zatloukalová L, Šimůnek T, Bobrovová Z, Semecký V, Nachtigal P, Hašková P, Macková E, Vávrová J, Holečková M, Palička V, Hrdina R. Direct administration of rutin does not protect against catecholamine cardiotoxicity. *Toxicology*. 2009; **255**(1-2): 25-32. IF₂₀₀₉ = 3,241

11 Prezentace na konferencích

Potůčková E, Macháček M, Tichotová L, Richardson DR, Šimůnek T. Quantitative analysis of the anti-proliferative activity of combinations of iron-chelating agents NHAPI and Dp44mT with the estrogen receptor antagonist tamoxifen. *4. Postgraduální & 2. postdoktorandská vědecká konference Farmaceutické fakulty UK* 28.-29.4.2014, Hradec Králové, Česká republika; sborník abstraktů str. 158.

Macková-Potůčková E, Roh J, Stariat J, Šesták V, Hašková P, Kovaříková P., Richardson DR, Šimůnek T. *In vitro* characterization of Dp44mT and Bp4eT metabolic products. *Tenth International ISSX meeting* 29.9.-3.10.2013, Toronto, Ontario, Kanada; sborník abstraktů str. 152-153.

Macková E, Jansová H, Hašková P, Tichotová L, Šimůnek T. The quantitative assessment of combinations of the novel iron chelator (*E*)-*N'*-[1-(2-hydroxy-5-nitrophenyl)ethylinden] isonicotinoylhydrazide and the anti-estrogen tamoxifen on MCF-7 breast adenocarcinoma cell line. *Fifth Congress of the International Bioiron Society (IBIS), BioIron 2013* 14.-18.4.2013, Londýn, Velká Británie; sborník abstraktů str. 240.

Macková E, Jansová H, Šimůnek T. The assessment of combination of iron chelators and clinically used anticancer agents in MCF-7 breast adenocarcinoma cell line. *Trace Elements in Biology and Medicine (FASEB)* 10.-15.6.2012, Steamboat Springs, Kolorado, USA; sborník abstraktů „Poster #19“

Macková E, Hrušková K, Bendová P, Vávrová K, Šimůnek T. Antiproliferative action of methyl and ethyl ketone analogs of salicylaldehyde isonicotinoyl hydrazine. *2. Postgraduální vědecká konference Farmaceutické fakulty UK* 31.1.-1.2.2012, Hradec Králové, Česká republika.

Macková E, Hrušková K, Bendová P, Vávrová K, Šimůnek T. Assessment of antiproliferative action of novel aroylhydrazone iron chelating agents – ketone analogs of salicylaldehyde isonicotinoyl hydrazone. *Mitochondria, Apoptosis and Cancer Conference 2011* 27.-29.10.2011, Singapur; sborník abstraktů str. 61.

Macková E, Hrušková K, Bendová P, Vávrová K, Šimůnek T. Study of antiproliferative activity of novel ketone analogs of Salicylaldehyde isonicotinoyl hydrazone. *61. česko-slovenské farmakologické dny* 14.-16.9.2011, Brno, Česká republika; sborník abstraktů str. 95.

Macková E, Hašková P, Koubková L, Mladěnka P, Šimůnek T. *In vitro* assessment of rutin against catecholamine-mediated cardiotoxicity. *9th New Frontiers in Basic Cardiovascular Research Meeting* 14. -17.10.2010, Toulouse, Francie; sborník abstraktů str. 87.

Ocenění za nejlepší posterovou prezentaci v sekci „Calcium, Mitochondria and Autonomic Nervous System“

12 Přílohy

Příloha I

Macková E, Hrušková K, Bendová P, Vávrová A, Jansová H, Hašková P, Kovaříková P, Vávrová K, Šimůnek T. Methyl and ethyl ketone analogs of salicylaldehyde isonicotinoyl hydrazone: novel iron chelators with selective antiproliferative action. *Chem Biol Interact.* 2012; **197**(2-3): 69-79. IF₂₀₁₂ = 2,967

Příloha II

Potůčková E, Hrušková K, Špírková IA, Pravidíková K, Kolbabová L, Hergeselová T, Hašková P, Jansová H, Macháček M, Jirkovská A, Richardson V, Lane DJR, Kalinowski DS, Richardson DR, Vávrová K, Šimůnek T. Structure-activity relationships of novel salicylaldehyde isonicotinoyl hydrazone (SIH) analogs: iron chelation, anti-oxidant and cytotoxic properties.

Structure-activity relationships of novel salicylaldehyde isonicotinoyl hydrazone (SIH) analogs: iron chelation, anti- oxidant and cytotoxic properties

**Eliška Potůčková¹, Kateřina Hrušková¹, Iva A. Špírková¹, Kateřina Pravdíkova¹,
Lucie Kolbabová¹, Tereza Hergeselová¹, Pavlína Hašková¹, Hana Jansová¹,
Miloslav Macháček¹, Anna Jirkovská¹, Vera Richardson², Darius J. R. Lane²,
Danuta S. Kalinowski², Des R. Richardson², Kateřina Vávrová^{1,*}, Tomáš
Šimůnek^{1,*}**

¹*Charles University in Prague, Faculty of Pharmacy in Hradec Králové, Czech Republic.*

²*Molecular Pharmacology and Pathology Program, Bosch Institute and Department of Pathology, University of Sydney, Sydney, Australia.*

***Authors for correspondence:**

Dr. Tomáš Šimůnek

Charles University in Prague, Faculty of Pharmacy

Department of Biochemical Sciences

Heyrovského 1203

500 05 Hradec Králové

Czech Republic

Tel.: +420-495-067-422; Fax: +420-495-067-168

E-mail: Tomas.Simunek@faf.cuni.cz

Dr. Kateřina Vávrová

Charles University in Prague, Faculty of Pharmacy

Department of Inorganic and Organic Chemistry

Heyrovského 1203

500 05 Hradec Králové

Czech Republic

Tel.: +420-495-067-497; Fax: +420-495-067-168

E-mail: Katerina.Vavrova@faf.cuni.cz

Abstract

Salicylaldehyde isonicotinoyl hydrazone (SIH) is a lipophilic, tridentate iron chelator with marked anti-oxidant and modest cytotoxic activity against neoplastic cells. However, it has poor stability in an aqueous environment due to the rapid hydrolysis of its hydrazone bond. In this study, a series of new SIH analogs (based on previously described aromatic ketones with improved hydrolytic stability) were synthesized. Their structure-activity relationships were assessed with respect to their iron chelation efficacy, redox effects and cytotoxic activity against MCF-7 breast adenocarcinoma cells. Furthermore, studies assessed the cytotoxicity of these chelators and their ability to afford protection against hydrogen peroxide-induced oxidative injury in H9c2 cardiomyoblast cells. The ligands with a reduced hydrazone bond, or the presence of bulky alkyl substituents near the hydrazone bond, showed severely limited biological activity. The introduction of a bromine substituent increased ligand-induced cytotoxicity to both cancer cells and H9c2 cardiomyoblasts. A similar effect was observed when the phenolic ring was exchanged with pyridine (*i.e.*, changing the ligating site from *O, N, O* to *N, N, O*), which led to pro-oxidative effects. In contrast, compounds with long, flexible alkyl chains adjacent to the hydrazone bond exhibited specific cytotoxic effects against MCF-7 breast adenocarcinoma cells and low toxicity against H9c2 cardiomyoblasts. Hence, this study highlights important structure-activity relationships and provides insight into the further development of aroylhydrazone iron chelators with more potent and selective anti-neoplastic effects.

Keywords:

Iron chelator; Aroylhydrazone; Salicylaldehyde isonicotinoyl hydrazone (SIH); Anti-neoplastic agent; Anti-oxidant.

Abbreviations:

2API, (*E*)-*N'*-[1-(pyridin-2-yl)ethylidene]isonicotinoylhydrazide; BHAPI, (*E*)-*N'*-[1-(5-bromo-2-hydroxyphenyl)ethylidene]isonicotinoylhydrazide; BHPPI, (*E*)-*N'*-[1-(5-bromo-2-hydroxyphenyl)propylidene]isonicotinoylhydrazide; CHAPI, (*E*)-*N'*-[1-(5-chloro-2-hydroxyphenyl)ethylidene]isonicotinoylhydrazide; EC₅₀, half-maximal effective concentration; IC₅₀, half-maximal inhibitory concentration; H16, (*E*)-*N'*-(1-(2-hydroxyphenyl)-2-methylpropylidene)isonicotinoylhydrazide; H17, (*E*)-*N'*-[1-(2-hydroxyphenyl)butylidene]isonicotinoylhydrazide; H18, (*E*)-*N'*-(1-(2-hydroxyphenyl)-3-methylbutylidene)isonicotinoylhydrazide; H28, (*E*)-*N'*-[cyclohexyl(2-hydroxyphenyl)methylene]isonicotinoylhydrazide; HAPI, (*E*)-*N'*-[1-(2-hydroxyphenyl)ethylidene]isonicotinoylhydrazide; 7HII, (*E*)-*N'*-(7-hydroxy-2,3-dihydro-1*H*-inden-1-ylidene)isonicotinoylhydrazide; HPPI, (*E*)-*N'*-[1-(2-hydroxyphenyl)propylidene]isonicotinoylhydrazide; IBE, iron binding equivalent; LIP, labile iron pool; PCIH, 2-pyridylcarboxaldehyde isonicotinoyl hydrazone; redHAPI, *N'*-[1-(2-hydroxyphenyl)ethyl]isonicotinoylhydrazide; redHPPI, *N'*-[1-(2-hydroxyphenyl)propyl]isonicotinoylhydrazide; redSIH, *N'*-(2-hydroxybenzyl)isonicotinoylhydrazide; SIH, *N'*-salicylaldehyde isonicotinoyl hydrazone; Tf, transferrin; TfR1, transferrin receptor 1.

1 Introduction

Iron is a crucial component of various molecules involved in oxygen transport, cellular respiration, metabolism and division [1-3]. The majority of cellular iron acquired by tumor cells is stored in ferritin [4,5], with smaller amounts being utilized for cellular metabolism, such as the synthesis of heme or iron-sulfur clusters [6,7]. Intracellular iron is also found within a poorly defined “labile iron pool” (LIP), in which iron is thought to be in transit between proteins and could be bound by low-molecular weight (M_r) ligands or specifically transported by putative iron-chaperone proteins, such as poly(rC)-binding proteins 1-4 [8,9].

When intracellular iron content is depleted, the synthesis of new iron-dependent proteins and enzymes, and the processes they regulate (*e.g.*, cellular growth and proliferation), can be inhibited [10,11]. On the other hand, when iron is present in excess, iron-mediated oxidative stress can lead to the damage of proteins, lipids and nucleic acids and can be cytotoxic. In fact, “free” or labile redox-active iron can catalyze the Fenton and Haber-Weiss-type reactions that generate highly toxic reactive oxygen species (ROS) [2,4]. Classical iron chelators used in the clinics, such as desferrioxamine (DFO), deferiprone, and deferasirox, sequester iron and are primarily used to manage disorders with increased systemic iron levels, such as that caused by repeated blood transfusions in β -thalassemia major patients [12-14]. More recently, iron chelators have been also studied in pathological conditions associated with oxidative stress unrelated to iron-overload diseases [15].

Cancer cells require more iron than their neoplastic counterparts in order to support their increased rates of proliferation [1]. Indeed, iron is a key cofactor of ribonucleotide reductase, an enzyme that catalyzes the rate-limiting step in DNA synthesis [16,17]. Cancer cells up-regulate transferrin (Tf) receptor 1 (TfR1) expression on their surface to increase iron uptake from the iron transport protein, Tf [18,19]. Some cancer cells also express hepcidin, a hormone that induces the internalization of the iron-export protein, ferroportin 1, leading to a reduction in iron efflux from cells [19,20]. Iron chelators induce iron depletion with subsequent G₁-S cell cycle arrest and apoptosis [21] and they are increasingly studied as potential anti-neoplastic agents, with several in pre-clinical or clinical development [13,22,23].

N'-Salicylaldehyde isonicotinoyl hydrazone (SIH, Fig. 1) is a well-established tridentate iron chelator, which forms 2:1 complexes with both Fe³⁺ and Fe²⁺ ions

[24,25]. SIH has been shown to: (1) protect various cell types against oxidative stress-inducing agents [15,26,27]; (2) prevent the cardiotoxicity of anthracycline-based antineoplastic agents both *in vitro* and *in vivo* [28]; and (3) act as a potential radio-protective, anti-viral and anti-cancer agent [29-31]. SIH has low *in vitro* and *in vivo* toxicity and good tolerability, even following prolonged administration to animals [32]. Recently, a series of new analogs of SIH were developed that have markedly enhanced hydrolytic stability compared to SIH and retain their ability to protect cells against oxidative injury [33]. In addition, these agents have increased cytotoxic activity compared to SIH [31]. The lead ligands identified in this series included (*E*)-*N'*-[1-(2-hydroxyphenyl)ethylidene]isonicotinoylhydrazide (HAPI; Fig. 1) and (*E*)-*N'*-[1-(2-hydroxyphenyl)propylidene]isonicotinoylhydrazide (HPPI; Fig. 1), which possess either a methyl or ethyl group, respectively, in proximity to the hydrazone bond [31].

To further analyze their structure-activity relationships, in the present study, we designed and synthesized derivatives of SIH, HAPI and HPPI (Fig. 1). The first modification was the reduction of the hydrazone bond leading to *N'*-(2-hydroxybenzyl)isonicotinoylhydrazide (redSIH; Fig. 1), *N'*-[1-(2-hydroxyphenyl)ethyl]isonicotinoylhydrazide (redHAPI; Fig. 1) and *N'*-[1-(2-hydroxyphenyl)propyl]isonicotinoylhydrazide (redHPPI; Fig. 1). These compounds were specifically synthesized to probe the importance of the hydrazone bond for the anti-oxidative and/or cytotoxic activity that has been associated with various aroylhydrazones [34-36].

We also studied the effects of bromination at position 5 of the phenolic ring of HAPI and HPPI, leading to (*E*)-*N'*-[1-(5-bromo-2-hydroxyphenyl)ethylidene]isonicotinoylhydrazide (BHAPI; Fig. 1) and (*E*)-*N'*-[1-(5-bromo-2-hydroxyphenyl)propylidene]isonicotinoylhydrazide (BHPPI; Fig. 1), respectively. The effect of halogenation was examined since a previous study demonstrated the high cytotoxic activity of a chloro-substituted ligand [31]. An analog, in which the phenolic ring of HAPI was exchanged for pyridine, was also prepared ((*E*)-*N'*-[1-(pyridin-2-yl)ethylidene]isonicotinoylhydrazide; 2API; Fig. 1) to assess the effects on its properties of changing the ligating groups from *O*, *N*, *O* to *N*, *N*, *O*.

The 2API ligand is a methyl analog of the previously reported iron chelator, 2-pyridylcarboxaldehyde isonicotinoyl hydrazone (PCIH), which was developed for the treatment of iron overload disease [37,38]. An analog of HAPI with a 2C side chain as a part of an indane ring was also synthesized, leading to (*E*)-*N'*-(7-hydroxy-2,3-dihydro-

1*H*-inden-1-ylidene)isonicotinoylhydrazide (7HII; Fig. 1). Analogs of HAPI and HPPI with varying alkyl groups adjacent to the hydrazone bond were also prepared, including derivatives containing an isopropyl substituent ((*E*)-*N'*-(1-(2-hydroxyphenyl)-2-methylpropylidene)isonicotinoylhydrazide; H16; Fig. 1), propyl substituent ((*E*)-*N'*-[1-(2-hydroxyphenyl)butylidene]isonicotinoylhydrazide; H17; Fig. 1), isobutyl substituent ((*E*)-*N'*-(1-(2-hydroxyphenyl)-3-methylbutylidene)isonicotinoylhydrazide; H18; Fig. 1), or cyclohexyl ring ((*E*)-*N'*-[cyclohexyl(2-hydroxyphenyl)methylene]isonicotinoylhydrazide; H28; Fig. 1).

To characterize these new ligands, we examined their: (1) iron chelating and redox properties; (2) protective potential against oxidative injury induced by exposure of H9c2 rat embryonic cardiomyoblast cells to hydrogen peroxide (H₂O₂); (3) cytotoxic activity using neoplastic MCF-7 breast adenocarcinoma cells; and (4) selectivity by comparing their cytotoxic effects to the non-tumorigenic, cardiomyoblast cell line, H9c2. These studies are important for dissecting structure-activity relationships that are essential for the development of more effective ligands.

2 Materials and methods

2.1 Syntheses of chelators

2.1.1 General procedures

All chemicals were purchased from Sigma-Aldrich (St. Louis, MO, USA). Thin layer chromatography was performed on TLC sheets (silica gel 60 F254) from Merck (Darmstadt, Germany). Microwave reactions were conducted in a Milestone Micro-SYNTH Ethos 1600 URM apparatus. Melting points were measured on a Kofler apparatus and are uncorrected. All products were characterized by NMR (Varian Mercury Vx BB 300 or VNMR S500 NMR spectrometers). Chemical shifts were reported as δ values in parts per million (ppm) and were indirectly referenced to tetramethylsilane (TMS) *via* the solvent signal. All assignments were based on 1D experiments. Elemental analysis was measured on a CHNS-OCE FISIONS EA 1110 apparatus.

2.1.2 Syntheses of chelators

***N'*-Salicylaldehyde isonicotinoyl hydrazone (SIH).** SIH was synthesized as described previously [39]. Yellow crystalline solid. mp 232-234°C. ¹H NMR (300 MHz, DMSO-*d*₆): δ 12.29 (s, 1H, OH), 11.02 (s, 1H, NH), 8.80 (d, *J* = 4.4 Hz, 2H, Py), 8.68 (s, 1H, CH), 7.85 (d, *J* = 4.4 Hz, 2H, Py), 7.61 (dd, *J* = 7.7, 1.5 Hz, 1H, Ph), 7.36 - 7.28 (m, 1H, Ph), 6.95 - 6.88 (m, 2H, Ph). ¹³C NMR (75 MHz, DMSO-*d*₆): δ 163.1, 157.5, 150.4, 148.9, 141.2, 131.7, 129.2, 121.5, 119.5, 116.4.

***N'*-(2-hydroxybenzyl)isonicotinoylhydrazide (redSIH).** SIH (0.69 g, 2.8 mmol) was dissolved in 96% (v/v) ethanol (50 mL) and NaBH₃CN (0.36 g, 5.7 mmol) was added. The reaction mixture was adjusted to a pH of 3-5 using a 10% (v/v) solution of HCl in methanol. The reaction mixture was stirred at room temperature (RT) overnight and was then neutralized with a solution of sodium bicarbonate to pH 7. The reaction mixture was evaporated to dryness and was then partitioned against water and EtOAc. The combined organic layers were dried with anhydrous Na₂SO₄ and evaporated under reduced pressure. The product was purified with column chromatography on silica using hexane/EtOAc (1:1) as a mobile phase. The product was isolated as a white crystalline solid. Yield 0.17 g (24%). mp 143-146°C. ¹H NMR (300 MHz, DMSO-*d*₆): δ 10.43 (s, 1H, OH), 9.61 (s, 1H, NH), 8.70 (d, *J* = 5.1 Hz, 2H, Py),

7.74 - 7.65 (m, 2H, Py), 7.20 (dd, $J = 7.5, 1.7$ Hz, 1H, Ph), 7.12 - 7.02 (m, 1H, Ph), 6.84 - 6.67 (m, 2H, Ph), 5.65 (s, 1H, NH), 3.95 (d, $J = 6.0$ Hz, 2H, CH₂). ¹³C NMR (75 MHz, DMSO-*d*₆): δ 163.5, 156.1, 150.4, 140.3, 130.1, 128.5, 124.1, 121.3, 118.9, 115.3, 50.7. Anal. Calcd. for C₁₃H₁₃N₃O₂: C, 64.19; H, 5.39; N, 17.27; Found: C, 64.50; H, 5.26; N, 17.56.

***N'*-[1-(2-Hydroxyphenyl)ethyl]isonicotinoylhydrazide (redHAPI).** The initial chelator, (*E*)-*N'*-[1-(2-hydroxyphenyl)ethylidene]isonicotinoylhydrazide (HAPI), was synthesized as described previously [33]. The reduced analog, redHAPI, was prepared from HAPI as described above for redSIH. The product was isolated as a yellow solid. Yield 0.18 g (26%). mp 131-134°C. ¹H NMR (500 MHz, DMSO-*d*₆): δ 10.29 (s, 1H, OH), 9.63 (s, 1H, NH), 8.70 (m, 2H, Py), 7.68 (d, $J = 4.8$ Hz, 2H, Py), 7.29 (dd, $J = 7.8, 1.7$ Hz, 1H, Ph), 7.11 - 7.00 (m, 1H, Ph), 6.82 - 6.69 (m, 2H, Ph), 5.57 (s, 1H, NH), 4.53 - 4.27 (m, 1H, CH), 1.28 (d, $J = 6.6$ Hz, 3H, CH₃). ¹³C NMR (125 MHz, DMSO-*d*₆): δ 164.1, 155.4, 150.4, 140.3, 129.1, 127.9, 127.3, 124.9, 119.1, 115.6, 54.3, 19.7. Anal. Calcd. for C₁₄H₁₅N₃O₂: C, 65.36; H, 5.88; N, 16.33; Found: C, 64.98; H, 6.04; N, 16.53.

***N'*-[1-(2-Hydroxyphenyl)propyl]isonicotinoylhydrazide (redHPPI).** The initial chelator, (*E*)-*N'*-[1-(2-hydroxyphenyl)propylidene]isonicotinoylhydrazide (HPPI), was synthesized as described previously [33]. The reduced analog, redHPPI was prepared from HPPI as described above for redSIH. The product was obtained as a yellow solid. Yield 0.29 g (42%). mp 115-118°C. ¹H NMR (500 MHz, DMSO-*d*₆): δ 10.21 (s, 1H, NH), 9.58 (s, 1H, NH), 8.90 - 8.55 (m, 2H, Py), 7.83 - 7.55 (m, 2H, Py), 7.27 (dd, $J = 7.6, 1.7$ Hz, 1H, Ph), 7.10 (m, 1H, Ph), 6.82 - 6.68 (m, 2H, Py), 5.62 (s, 1H, OH), 4.21 (t, $J = 6.6$ Hz, 1H, CH), 1.81 - 1.60 (m, 2H, CH₂), 1.14 (t, $J = 7.6$ Hz, 3H, CH₃). ¹³C NMR (125 MHz, DMSO-*d*₆): δ 163.8, 155.8, 150.3, 140.3, 128.4, 127.8, 124.9, 118.9, 115.6, 60.6, 26.0, 10.7. Anal. Calcd. for C₁₅H₁₇N₃O₂: C, 66.40; H, 6.32; N, 15.49; Found: C, 66.42; H, 6.45; N, 15.55.

(*E*)-*N'*-[1-(5-Bromo-2-hydroxyphenyl)ethylidene]isonicotinoylhydrazide (BHAPI). Isoniazid (0.21 g, 1.5 mmol), 5-bromo-2-hydroxyacetophenone (0.32 g, 1.5 mmol) and acetic acid (0.25 mL) were dissolved in methanol (5 mL) and stirred for 2 h under reflux in the microwave reactor described above. The reaction mixture was then cooled to 4°C and the resulting precipitate was collected by filtration, washed with

water and methanol and dried over P₂O₅ to give 0.2 g (39%) of the product as a yellow crystalline solid. mp 225-227 °C. ¹H NMR (500 MHz, DMSO-*d*₆): δ 13.27 (s, 1H, OH), 11.66 (s, 1H, NH), 8.82 - 8.76 (m, 2H, Py), 7.86 - 7.79 (m, 2H, Py), 7.76 (d, *J* = 2.3 Hz, 1H, Ph), 7.45 (dd, *J* = 8.8, 2.2 Hz, 1H, Ph), 6.90 (d, *J* = 8.7 Hz, 1H, Ph), 2.49 (s, 3H, CH₃). ¹³C NMR (125 MHz, DMSO-*d*₆): δ 163.3, 158.1, 158.0, 150.4, 140.1, 134.1, 131.0, 122.2, 121.5, 119.8, 109.9, 14.7. Anal. Calcd. for C₁₄H₁₄BrN₃O₂: C, 50.32; H, 3.62; N, 12.57; Found: C 50.71; H, 3.99; N, 12.88.

(*E*)-*N'*-[1-(5-Bromo-2-hydroxyphenyl)propylidene]isonicotinoylhydrazide (BHPPI). Isoniazid (0.2 g, 1.4 mmol), 5-bromo-2-hydroxypropiophenone (0.33 g, 1.4 mmol) and acetic acid (0.25 mL) were dissolved in methanol (5 mL) and stirred overnight under reflux. After cooling the reaction mixture to 4°C, the resulting precipitate was collected by filtration, washed with water and methanol and dried over P₂O₅ to give 0.32 g (64%) of the product as a yellow crystalline solid. mp 239-242°C. ¹H NMR (500 MHz, DMSO-*d*₆): δ 13.33 (s, 1H, OH), 11.69 (s, 1H, NH), 8.79 (d, *J* = 5.0 Hz, 2H, Py), 7.86 - 7.81 (m, 3H, Py, Ph), 7.45 (dd, *J* = 8.8, 2.4 Hz, 1H, Ph), 6.92 (d, *J* = 8.7 Hz, 1H, Ph), 3.01 (q, *J* = 7.6 Hz, 2H, CH₂), 1.09 (t, *J* = 7.0 Hz, 3H, CH₃). ¹³C NMR (125 MHz, DMSO-*d*₆): δ 163.8, 161.2, 158.5, 150.3, 140.3, 134.0, 130.5, 122.4, 120.2, 120.1, 109.9, 19.7, 11.4. Anal. Calcd. for: C₁₅H₁₆BrN₃O₂: C, 51.74; H, 4.05; N, 12.07; Found: C, 51.41; H, 4.26; N, 11.74.

(*E*)-*N'*-[1-(Pyridin-2-yl)ethylidene]isonicotinoylhydrazide (2API). Isoniazid (0.57 g, 4.1 mmol), 2-acetylpyridine (0.5 g, 3.4 mmol) and acetic acid (0.25 mL) were dissolved in methanol (10 mL) and stirred overnight under reflux. After cooling the reaction mixture to 4°C, the resulting precipitate was collected by filtration, washed with water and methanol and dried over P₂O₅ to give 0.37 g (37%) of the product as a white crystalline solid. mp 166°C. ¹H NMR (500 MHz, DMSO-*d*₆): δ 11.10 (s, 1H, NH), 8.77 (d, *J* = 5.1 Hz, 2H, Py), 8.62 (d, *J* = 5.3 Hz, 1H, Py'), 8.12 (d, *J* = 8.2 Hz, 1H, Py'), 7.90 - 7.40 (m, 1H, Py'), 7.83 - 7.77 (m, 2H, Py), 7.47 - 7.40 (m, 1H, Py'), 2.47 (s, 3H, CH₃). ¹³C NMR (125 MHz, DMSO-*d*₆): δ 163.0, 155.1, 150.3, 149.7, 141.2, 136.9, 124.7, 122.2, 121.2, 13.1. Anal. Calcd. for C₁₃H₁₂N₄O: C, 64.99; H, 5.03; N, 23.32; Found: C, 65.33; H, 5.31; N, 23.43.

(*E*)-*N'*-(7-Hydroxy-2,3-dihydro-1*H*-inden-1-ylidene)isonicotinoylhydrazide

(7HII). Isoniazid (0.46 g, 3.4 mmol), 7-hydroxy-2,3-dihydro-1*H*-inden-1-one (0.5 g, 3.4 mmol) and acetic acid (0.25 mL) were dissolved in methanol (10 mL) and stirred overnight under reflux. After cooling the reaction mixture to 4°C, the resulting precipitate was collected by filtration and washed with water and methanol. The solid was suspended in toluene and was stirred for 30 min. This solution was filtered to obtain 0.37 g (66%) of the product as a yellow crystalline solid. mp 232-236°C. ¹H NMR (500 MHz, DMSO-*d*₆): δ 11.30 (s, 1H, NH), 10.15 (s, 1H, OH), 8.80 - 8.70 (m, 2H, Py), 7.84 - 7.74 (m, 2H, Py), 7.30 (dd, *J* = 7.8, 1.3 Hz, 1H, Ph), 6.89 (d, *J* = 7.4 Hz, 1H, Ph), 6.75 (d, *J* = 8.1 Hz, 1H, Ph), 3.13 - 3.00 (m, 4H, 2xCH₂). ¹³C NMR (125 MHz, DMSO-*d*₆): δ 167.9, 162.5, 155.5, 150.3, 150.0, 140.8, 133.1, 122.6, 122.1, 116.6, 113.0, 28.7, 28.1. Anal. Calcd. for C₁₅H₁₃N₃O₂: C, 67.40; H, 4.90; N, 15.72; Found: C, 67.02; H, 5.13; N, 15.87.

(*E*)-*N'*-(1-(2-Hydroxyphenyl)-2-methylpropylidene)isonicotinoylhydrazide

(H16). To prepare H16, 1-(2-hydroxyphenyl)-2-methylpropan-1-one was first synthesized: 2-hydroxybenzotrile (0.36 g, 3 mmol) was dissolved in dry THF (5 mL) and a solution of isopropylmagnesium chloride in THF (2 M, 6.1 mL, 1.2 mmol) was added and the reaction mixture refluxed for 2 h. The reaction mixture was cooled in an ice bath, 10 mL of cold water was carefully added and cold concentrated H₂SO₄ added dropwise to obtain an acidic pH. The reaction mixture was then heated for 1 h at 80°C and, after cooling to RT, it was extracted twice with diethyl ether. The combined organic layer was dried with anhydrous Na₂SO₄ and evaporated under reduced pressure. The product was purified by column chromatography on silica using hexane/EtOAc (40:1) as the mobile phase. The product was obtained as a yellow oil. Yield 0.45 g (91%). ¹H NMR (300 MHz, CDCl₃): δ 12.52 (s, 1H, OH), 7.79 (dd, *J* = 8.1, 1.6 Hz, 1H, Ph), 7.53 - 7.40 (m, 1H, Ph), 7.04 - 6.84 (m, 2H, Ph), 3.70 - 3.54 (m, 1H, CH), 1.43 - 1.14 (m, 6H, 2xCH₃). ¹³C NMR (75 MHz, CDCl₃): δ 210.9, 163.1, 136.2, 129.8, 118.8, 118.7, 118.1, 34.9, 29.7, 19.3.

1-(2-Hydroxyphenyl)-2-methylpropan-1-one (0.29 g, 1.8 mmol), isoniazid (0.24 g, 1.8 mmol) and acetic acid (0.25 mL) were dissolved in methanol (5 mL) and heated at 110°C in an autoclave for 48 h. After cooling to RT, water was added dropwise until the solution turned cloudy and the mixture was left to crystallize at 4°C for 24 h. The precipitate was collected by filtration, washed with water and methanol and dried over

P₂O₅ to yield 0.07 g (14%) of H16 as a white crystalline solid. mp 228-235°C. ¹H NMR (300 MHz, DMSO-*d*₆): δ 10.08 (s, 1H, NH), 8.66 (m, 2H, Py), 7.66 (m, 2H, Py), 7.43 (d, *J* = 7.7 Hz, 1H, Ph), 7.35 - 7.22 (m, 1H, Ph), 7.13 (d, *J* = 7.7 Hz, 1H, Ph), 7.03 - 6.79 (m, 1H, Ph), 3.07 - 2.80 (m, 1H, CH), 1.42 - 0.78 (m, 6H, 2xCH₃). ¹³C NMR (75 MHz, DMSO-*d*₆): δ 163.7, 163.3, 153.9, 150.4, 141.4, 130.9, 128.8, 121.2, 120.7, 119.7, 116.2, 35.9, 20.1. Anal. Calcd. for C₁₆H₁₇N₃O₂: C, 67.83; H, 6.05; N, 14.83; Found: C, 67.44; H, 6.37; N, 14.83.

(*E*)-*N'*-[1-(2-Hydroxyphenyl)butylidene]isonicotinoylhydrazide (H17). To prepare H17, 1-(2-hydroxyphenyl)butan-1-one was first synthesized: Magnesium (0.3 g, 12 mmol) was suspended in dry THF (5 mL), and propylbromide (1.5 g, 12 mmol) was added dropwise and the mixture refluxed for 2 h until the magnesium dissolved. After cooling the reaction mixture to RT, 2-hydroxybenzotrile (0.36 g, 3 mmol) dissolved in dry THF (5 mL) was added dropwise and the reaction refluxed for 2 h. The reaction mixture was cooled in an ice bath, 10 mL of cold water was carefully added and cold concentrated H₂SO₄ added dropwise to obtain an acidic pH. The reaction mixture was then heated for 1 h at 80°C and, after cooling to RT, it was extracted twice with diethyl ether. The combined organic layer was dried with anhydrous Na₂SO₄ and evaporated under reduced pressure. The product was purified by column chromatography on silica (gradient; hexane to hexane/EtOAc 40:1). The product was obtained as a yellow oil. Yield: 0.41 g (82%). ¹H NMR (300 MHz, CDCl₃): δ 7.90 - 7.67 (m, 1H, Ph), 7.57 - 7.36 (m, 1H, Ph), 7.05 - 6.76 (m, 2H, Ph), 2.79 (t, *J* = 7.3 Hz, 2H, CH₂), 1.69 - 1.43 (m, 2H, CH₂), 1.03 (t, *J* = 7.4 Hz, 3H, CH₃). ¹³C NMR (75 MHz, CDCl₃): δ 206.8, 162.5, 136.2, 130.0, 119.4, 118.8, 118.5, 40.2, 17.9, 13.8.

1-(2-Hydroxyphenyl)-butan-1-one (0.39 g, 2.4 mmol), isoniazid (0.33 g, 2.4 mmol) and acetic acid (0.25 mL) were dissolved in methanol (5 mL) and heated at 110°C in an autoclave for 72 h. After cooling to RT, water was added dropwise until the solution turned cloudy and the mixture was left to crystallize at 4°C for 24 h. The precipitate was collected by filtration, washed with water and methanol and dried over P₂O₅ to yield 0.08 g (12%) of the product as a white crystalline solid. mp 189-192°C. ¹H NMR (500 MHz, DMSO-*d*₆): δ 8.79 (d, *J* = 5.3, 2H, Py), 7.89 - 7.72 (m, 2H, Py), 7.63 (dd, *J* = 8.1, 1.6 Hz, 1H, Ph), 7.30 (ddd, *J* = 8.4, 7.1, 1.5 Hz, 1H, Ph), 7.00 - 6.79 (m, 2H, Ph), 3.06 - 2.86 (m, 2H, CH₂), 1.73 - 1.44 (m, 2H, CH₂), 0.99 (t, *J* = 7.3 Hz, 3H, CH₃). ¹³C NMR (125 MHz, DMSO-*d*₆): δ 163.6, 161.7, 159.4, 150.3, 140.5, 131.6,

128.7, 122.3, 118.8, 118.3, 117.8, 27.9, 20.3, 13.9. Anal. Calcd. for C₁₆H₁₇N₃O₂: C, 67.83; H, 6.05; N, 14.83; Found: C, 67.42; H, 6.41; N, 14.55.

(*E*)-*N'*-(1-(2-Hydroxyphenyl)-3-methylbutylidene)isonicotinoylhydrazide

(H18). To prepare H18, 1-(2-hydroxyphenyl)-3-methylbutan-1-one was first synthesized: Magnesium (0.41 g, 16.9 mmol) was suspended in dry THF (5 mL), and isobutylbromide (2.31 g, 16.7 mmol) was added dropwise and the mixture refluxed for 2 h until the magnesium dissolved. After cooling the reaction mixture to RT, 2-hydroxybenzotrile (0.33 g, 2.8 mmol) dissolved in dry THF (5 mL) was added dropwise and the reaction refluxed for 2 h. The reaction mixture was cooled in an ice bath, 10 mL of cold water was carefully added and cold concentrated H₂SO₄ added dropwise to obtain an acidic pH. The reaction mixture was then heated for 1 h at 80°C and, after cooling to RT, it was extracted twice with diethyl ether. The combined organic layer was dried with anhydrous Na₂SO₄ and evaporated under reduced pressure. The product was purified by column chromatography on silica using hexane/EtOAc (40:1) as the mobile phase. The product was a yellow oil. Yield 0.45 g (91%). ¹H NMR (300 MHz, CDCl₃): δ 12.48 (s, 1H, OH), 7.89 - 7.63 (m, 1H, Ph), 7.59 - 7.40 (m, 1H, Ph), 7.08 - 6.83 (m, 2H, Ph), 2.92 - 2.74 (m, 2H, CH₂), 2.38 - 2.22 (m, 1H, CH), 1.13 - 0.94 (m, 6H, 2xCH₃). ¹³C NMR (75 MHz, CDCl₃): δ 206.7, 162.6, 136.2, 130.1, 119.6, 118.8, 118.5, 47.1, 25.5, 22.7.

1-(2-Hydroxyphenyl)-3-methylbutan-1-one (0.2 g, 1.1 mmol), isoniazid (0.12 g, 1.1 mmol) and acetic acid (0.25 mL) were dissolved in methanol (5 mL) and heated at 110°C in an autoclave for 72 h. After cooling to RT, water was added dropwise until the solution turned cloudy and the mixture was left to crystallize at 4°C. The precipitate was then collected by filtration, washed with water and methanol and dried over P₂O₅. The overall yield of the white crystalline product was 0.06 g (19%). mp 144-146°C. ¹H NMR (500 MHz, DMSO-*d*₆): δ 13.27 (s, 1H, OH), 11.61 (s, 1H, NH), 8.82 - 8.77 (m, 2H, Py), 7.81 - 7.73 (m, 2H, Py), 7.65 (dd, *J* = 8.0, 1.7 Hz, 1H, Ph), 7.42 - 7.19 (m, 1H, Ph), 6.97 - 6.86 (m, 2H, Ph), 2.99 (d, *J* = 7.4 Hz, 2H, CH₂), 2.02 - 1.93 (m, 1H, CH), 0.95 (d, *J* = 6.6 Hz, 6H, 2xCH₃). ¹³C NMR (125 MHz, DMSO-*d*₆): δ 163.3, 161.5, 159.2, 150.4, 140.4, 131.6, 129.0, 122.2, 118.7, 117.8, 34.3, 27.6, 22.2. Anal. Calcd. for C₁₇H₁₉N₃O₂: C, 68.67; H, 6.44; N, 14.13; Found: C, 68.28; H, 6.69; N, 13.85.

(E)-N'-[Cyclohexyl(2-hydroxyphenyl)methylene]isonicotinoylhydrazide

(H28). To prepare H28, cyclohexyl(2-hydroxyphenyl)methanone was synthesized: Magnesium (0.36 g, 15 mmol) was suspended in dry THF (5 mL) and cyclohexylbromide (2.4 g, 15 mmol) was added dropwise. This reaction mixture was refluxed for 2 h until the magnesium dissolved. After cooling the reaction mixture to RT, 2-hydroxybenzotrile (0.29 g, 2.4 mmol) dissolved in dry THF (5 mL) was added dropwise and the reaction refluxed for 3 h. The reaction mixture was cooled in an ice bath, 10 mL of cold water was added carefully and then cold concentrated H₂SO₄ was added dropwise to obtain an acidic pH. The reaction mixture was then heated overnight at 80°C and, after cooling to RT, it was extracted twice with diethyl ether. The combined organic layer was dried with anhydrous Na₂SO₄ and evaporated under reduced pressure. The product was purified by column chromatography on silica (gradient; hexane to hexane/EtOAc 40:1). The product was obtained as a yellow oil. Yield 0.49 g (97%). ¹H NMR (300 MHz, CDCl₃) δ 12.58 (s, 1H, OH), 7.88 - 7.69 (m, 1H, Ph), 7.55 - 7.32 (m, 1H, Ph), 7.07 - 6.95 (m, 2H, Ph), 3.43 - 3.12 (m, 1H, Cy), 2.03 - 1.06 (m, 10H, Cy). ¹³C NMR (75 MHz, CDCl₃): δ 210.1, 163.1, 136.1, 129.8, 118.7, 118.7, 118.2, 45.2, 29.5, 25.8, 25.7.

Cyclohexyl(2-hydroxyphenyl)methanone (0.19 g, 0.93 mmol), isoniazid (0.13 g, 0.93 mmol) and acetic acid (0.20 mL) were dissolved in methanol (5 mL) and heated at 110°C in an autoclave for 4 days. After cooling to RT, water was added dropwise until the solution turned cloudy and the mixture was left to crystallize at 4°C for 24 h. The precipitate was collected by filtration, washed with methanol and dried over P₂O₅ to give 0.046 g (15%) of the product as a white solid. mp 251-253°C. ¹H NMR (300 MHz, DMSO-*d*₆): δ 9.27 (s, 1H, NH), 8.70 - 8.63 (m, 2H, Py), 7.86 - 7.70 (m, 2H, Py), 7.51 - 7.34 (m, 1H, Ph), 7.33 - 7.19 (m, 1H, Ph), 7.17 - 7.02 (m, 1H, Ph), 7.02 - 6.78 (m, 1H, Ph), 2.69 - 2.34 (m, 1H, Cy), 1.92 - 1.00 (m, 10H, Cy). ¹³C NMR (75 MHz, DMSO-*d*₆): δ 163.0, 161.3, 150.4, 141.4, 130.8, 128.8, 121.2, 120.8, 119.7, 116.2, 30.3, 29.9, 26.0, 25.8. Anal. Calcd. for C₁₉H₂₁N₃O₂: C, 70.57; H, 6.55; N, 12.99; Found: C, 70.36; H, 6.91; N, 13.03.

2.2 Biological studies

2.2.1 Chemicals

Constituents for various buffers as well as other chemicals (*e.g.*, various iron salts) were purchased from Sigma-Aldrich, Merck or Penta (Prague, Czech Republic) and were of the highest pharmaceutical or analytical grade available.

2.2.2 Cell cultures

The MCF-7 human breast adenocarcinoma cell line was purchased from the European Collection of Cell Cultures (ECACC; Salisbury, UK), and the H9c2 cardiomyoblast cell line, derived from embryonic rat heart tissue, was obtained from the American Type Culture Collection (ATCC; Manassas, VA, USA). Cells were cultured in Dulbecco's modified Eagle's medium (DMEM; Lonza, Verviers, Belgium) with (H9c2) or without (MCF-7) phenol red and were supplemented with 10% (v/v) heat-inactivated fetal bovine serum (FBS; Lonza), 1% penicillin/streptomycin solution (Lonza) and 10 mM HEPES buffer (pH 7.0 - 7.6; Sigma-Aldrich). Both cell lines were cultured in 75 cm² tissue culture flasks (TPP, Trasadingen, Switzerland) at 37°C in a humidified atmosphere of 5% CO₂. Sub-confluent cells (70-80% confluency) were sub-cultured every 3-4 days.

2.2.3 Determination of iron chelating efficacy in solution

To assess the iron chelation efficiency of the newly synthesized agents in solution, their ability to remove iron from the iron-calcein complex was examined [40]. Calcein is a fluorescent probe that readily forms iron complexes [40]. Upon formation of the iron-calcein complex, the fluorescence of calcein is quenched. The addition of another chelating agent to the iron-calcein complex leads to the removal of iron from this complex, resulting in the formation of the new iron-chelator complex. The removal of iron from the iron-calcein complex is accompanied by an increase in fluorescence intensity, due to the formation of free calcein. Thus, the measurement of calcein fluorescence intensity was used to examine the iron chelation efficacy of the novel chelators [40].

A complex of calcein (free acid, 20 nM; Molecular Probes, Eugene, OR, USA) with iron derived from ferrous ammonium sulfate (200 nM) was prepared in HBS buffer (150 mM NaCl, 40 mM HEPES, pH 7.2). Calcein and ferrous ammonium sulfate were

continuously stirred for 45 min in the dark, after which >90% of the fluorescence was quenched. Then, 995 μL of the complex was pipetted into a stirred cuvette and baseline measurements were acquired. After 100 s, 5 μL of the novel chelator solution was added, yielding a final chelator concentration of 5 μM . Fluorescence intensity change was measured as a function of time at RT using a Perkin Elmer LS50B fluorimeter (Perkin Elmer, Waltham, MA, USA) at $\lambda_{\text{ex}} = 486 \text{ nm}$ and $\lambda_{\text{em}} = 517 \text{ nm}$ for 350 s. The iron chelation efficiency in solution was expressed as a percentage of the efficiency of the reference chelator, SIH (100%).

2.2.4 Calcein-AM assay to assess the cell membrane permeability and access to the labile iron pool

These experiments were performed according to Glickstein *et al.* [41] with slight modifications. MCF-7 cells were seeded in 96-well plates (10,000 cells per well). Cells were loaded with iron using the iron donor, ferric ammonium citrate (530 $\mu\text{g}/\text{mL}$), 24 h prior to the experiment, and the cells then washed. To prevent potential interference (especially with regard to various trace elements), the medium was replaced with the ADS buffer (prepared using Millipore water supplemented with 116 mM NaCl, 5.3 mM KCl, 1 mM CaCl₂, 1.2 mM MgSO₄, 1.13 mM NaH₂PO₄, 5 mM D-glucose, and 20 mM HEPES, pH 7.4). Cells were then loaded with the membrane-permeant, calcein green acetoxymethyl ester (calcein-AM; 2 μM ; Molecular Probes) for 30 min/37°C, and then washed. Cellular esterases cleave the acetoxymethyl groups to form the cell membrane-impermeant compound, calcein green, whose fluorescence is quenched upon binding iron. Intracellular fluorescence ($\lambda_{\text{ex}} = 488 \text{ nm}$; $\lambda_{\text{em}} = 530 \text{ nm}$) was then measured as a function of time (1 min before and 10 min after the addition of chelator) at 37°C using a Tecan Infinite 200 M plate reader (Tecan Group, Männedorf, Switzerland). The iron chelation efficiency in cells was expressed as a percentage of the efficiency of the reference chelator, SIH (100%).

2.2.5 Preparation of ⁵⁹Fe₂-transferrin

Human Tf (Sigma-Aldrich) was labeled with Fe or ⁵⁹Fe (PerkinElmer) to produce Fe₂-Tf or ⁵⁹Fe₂-Tf, respectively, with a final specific activity of 500 pCi/pmol Fe, as previously described [34,42]. Unbound ⁵⁹Fe was removed by exhaustive vacuum

dialysis against an excess of 0.15 M NaCl buffered at pH 7.4 with 1.4 % (w/v) NaHCO₃ by standard methods [34,42].

2.2.5.1 The effect of chelators on mobilizing cellular ⁵⁹Fe

The ability of the novel ligands to mobilize ⁵⁹Fe from MCF-7 cells was examined by conducting ⁵⁹Fe efflux experiments using established techniques [34,43]. In brief, after pre-labeling cells with ⁵⁹Fe₂-Tf (0.75 μM) for 3 h/37°C, the cell cultures were washed four times with ice-cold PBS and then subsequently incubated with each chelator (25 μM) for 3 h/37°C. The overlying media containing released ⁵⁹Fe was then carefully separated from the cells using a Pasteur pipette. Radioactivity was measured in both the cell pellet and supernatant using a γ-scintillation counter (Wallac Wizard 3, Turku, Finland).

2.2.5.2 The effect of the chelators on the prevention of cellular ⁵⁹Fe uptake from ⁵⁹Fe₂-Tf

The ability of the chelators to prevent cellular ⁵⁹Fe uptake from ⁵⁹Fe₂-Tf was examined using standard methods [44,45]. In brief, MCF-7 cells were incubated with ⁵⁹Fe₂-Tf (0.75 μM) for 3 h/37°C in the presence of the assessed chelators (25 μM). The cells were then washed four times with ice-cold PBS and the internalized ⁵⁹Fe was determined *via* established methods by incubating the cell monolayer for 30 min/4°C with the general protease, Pronase (1 mg/mL; Sigma-Aldrich). The cells were then removed from the monolayer with a plastic spatula and centrifuged for 1 min/12,000 x g. The supernatant represents membrane-bound, Pronase-sensitive ⁵⁹Fe that was released by the protease, while the Pronase-insensitive fraction represents internalized ⁵⁹Fe [34,44,45]. The amount of internalized ⁵⁹Fe was expressed as a percentage of the ⁵⁹Fe internalized by untreated control cells (100%).

2.2.6 Ascorbate oxidation assay for analysis of redox activity of iron complexes

The ability of the iron complexes of the novel ligands to mediate the oxidation of a physiological substrate, ascorbate, was examined using an established protocol [44,46]. In brief, L-ascorbic acid (100 μM) was prepared immediately prior to the experiment and was incubated either alone or in the presence of Fe³⁺ (10 μM; as FeCl₃)

in a 50-fold molar excess (500 μM) of citrate and chelators (1-60 μM). Chelators were assayed at iron-binding equivalents (IBE) of 0.1 (excess of iron), 1 (iron-chelator complexes with a fully saturated coordination sphere) and 3 (excess of free chelator). The iron chelators, ethylenediaminetetraacetic acid (EDTA) and DFO, were used as positive and negative controls, respectively, as their redox activity has been well characterized [47]. The decrease in absorbance at 265 nm, which is the absorption maximum of ascorbate, was measured using the plate reader described previously after 10 and 40 min of incubation at RT. The decrease in absorbance between the two time points was calculated and expressed as a percentage of the control in the absence of the chelators (100%).

2.2.7 Protection against oxidative injury and assessment of cytotoxicity

For these experiments, cells were seeded in 96-well plates (TPP) at a density of 10,000 cells/well (H9c2 rat cardiomyoblast) or 5,000 cells/well (MCF-7). H9c2 cells were seeded in the plates 48 h prior to addition of the studied ligands and 24 h prior to the experiments, the medium was changed to serum- and pyruvate-free DMEM (Sigma-Aldrich). The ability of the ligands to protect against oxidative injury was assessed by a simultaneous 24 h incubation with H_2O_2 (200 μM) in the presence and absence of varying concentrations of the chelators. The inherent cytotoxicity of the ligands was studied using the H9c2 cell line after a 72 h incubation. For proliferation studies, MCF-7 cells were seeded 24 h prior to addition of the chelators. The cytotoxic effects of the various iron chelators were then studied at different concentrations after a 72 h incubation. To dissolve the lipophilic agents, dimethyl sulfoxide (DMSO; Sigma-Aldrich) was utilized leading to a final DMSO concentration of 0.1% (v/v) in the culture medium of all groups. At this concentration, DMSO had no effect on cytotoxicity (data not shown). The viability of the H9c2 and MCF-7 cells was determined using the neutral red (NR; Sigma) uptake assay, which is based on the ability of viable cells to incorporate NR into lysosomes [33,48]. The optical density of soluble NR was measured at $\lambda = 540$ nm using the Tecan Infinite 200M plate reader. The viability or proliferation of the experimental groups was expressed as a percentage of the untreated controls (100%). Control experiments using viable cell counts demonstrated a direct correlation to NR uptake.

2.3 Data analysis and statistics

The values of the molecular weights (MW) and n-octanol/water coefficients ($\log P_{\text{calc}}$; Table 1) were calculated using ChemBioOffice Ultra 11.0 software (CambridgeSoft, Cambridge, MA, USA). The $\log P_{\text{calc}}$ is expressed as an average of the results of Crippen's [49], Viswanadhan's [50], and Broto's [51] method. SigmaStat for Windows 3.5 (Systat Software, San Jose, CA, USA) statistical software was used for data analyses. The data are expressed as the mean \pm S.D. of at least 3 experiments. Statistical significance was determined using a one-way ANOVA with a Bonferroni *post-hoc* test (comparisons of multiple groups against the relevant control). The results were considered to be statistically significant when $p < 0.05$. The EC_{50} (half-maximal effective concentration) and IC_{50} (half-maximal inhibitory concentration) values were calculated using CalcuSyn 2.0 software (Biosoft, Cambridge, UK).

3 Results

3.1 Determination of the iron chelating efficacy in solution and in MCF-7 cells

To assess the iron chelation efficacy of the ligands in solution, the iron complexes of the weak iron chelator, calcein, were used. In this assay, the examined chelators compete with calcein for iron and the fluorescence of the free, dequenched calcein is proportional to their chelation efficacy in comparison to calcein. The iron chelation efficacy of the novel ligands was expressed as a percentage of the efficiency of the parent chelator, SIH (100%).

The reduction of the hydrazone bond in redSIH, redHAPI and redHPPI resulted in significantly ($p < 0.001$) reduced iron chelating efficacies in solution (Fig. 2A). The brominated ligands, BHAPI and BHPPI, and the alkylated analogs, 7HII, H17 and H18 exhibited iron chelating activity similar to the reference agent, SIH (Fig. 2A). The 2-acetylpyridine derivative, 2API, was observed to have poor iron chelating efficacy in this assay relative to SIH. However, this may be due to the ability of the iron complex of 2API to oxidize calcein [52], as the iron complex of 2API was identified to act as a pro-oxidant (see below), and thus, resulted in decreased calcein fluorescence. Additionally, low chelation efficacy was also observed for the ligands, H16 and H28 (Fig. 2A), that possess an isopropyl or cyclohexyl group, respectively, adjacent to the hydrazone bond.

The ability of the ligands to permeate the cell membrane to gain access to the LIP was examined using the calcein-AM assay in iron-loaded MCF-7 cells (Fig. 2B). In these studies, the iron chelation efficacy of the synthesized ligands was expressed as a percentage of the efficiency of the parent chelator, SIH (100%).

The ability of the chelators, BHPPI, 7HII and H17 to permeate the cell membrane and to bind iron from the calcein-AM detectable LIP did not significantly ($p > 0.05$) differ from that of SIH (Fig. 2B). This was well correlated with their high chelation efficacy in solution (Fig. 2A). The ligands, redSIH, BHAPI, 2API, H18 and H28, exhibited moderate (50-80% relative to SIH), but significantly ($p < 0.05 - 0.001$) decreased iron chelation efficacy in MCF-7 cells relative to SIH (Fig. 2B). In contrast, redHAPI, redHPPI and H16 displayed the poorest ability (<50% relative to SIH) to access and bind iron from the LIP (Fig. 2B) and this was in good correlation to their chelation activity in solution (Fig. 2A).

3.2 The effect of the chelators on the mobilization of cellular ⁵⁹Fe and prevention of cellular ⁵⁹Fe uptake from ⁵⁹Fe₂-Tf

To examine the ability of the novel ligands to mobilize intracellular ⁵⁹Fe from MCF-7 cells, ⁵⁹Fe efflux experiments were performed using established techniques [34,43]. The novel ligands were compared to control medium containing no added chelator and also to the parent analog, SIH (Fig. 3A). The control medium showed limited ability to mobilize cellular ⁵⁹Fe, resulting in the release of 8% of cellular ⁵⁹Fe (Fig. 3A). In contrast, SIH displayed high ⁵⁹Fe mobilization efficacy, mediating the release of 55% of cellular ⁵⁹Fe (Fig. 3A). The ligands, BHAPI, BHPPI, 2API, 7HII, H17 and H18 were highly effective in mediating ⁵⁹Fe mobilization and resulted in the release of 43-58% of cellular ⁵⁹Fe (Fig. 3A). The agents, redSIH and H28 demonstrated significantly ($p < 0.001$) increased ⁵⁹Fe mobilization compared to the control. However, their ⁵⁹Fe mobilization efficacy was approximately half that of SIH (Fig. 3A). The ⁵⁹Fe mobilization efficacy of redHAPI, redHPPI and H16 were poor and comparable to the untreated control (Fig. 3A). In general, the results of this assay correlated well with the observed iron-chelation efficacies of these analogs in solution (Fig. 2A) and in the cell-based calcein-AM assay (Fig. 2B). The only notable exception being 2API, which demonstrated high activity at mobilizing cellular ⁵⁹Fe (Fig. 3A), which was in contrast to the iron chelation assay in solution (Fig. 2A). As noted previously, this could be due to its pro-oxidative effects on calcein [52].

As the iron chelation efficacy and cytotoxic activity of a ligand are due to both its ability to mobilize cellular Fe, but also, inhibit Fe uptake from Tf [34], the ability of the chelators to prevent the cellular uptake of ⁵⁹Fe from ⁵⁹Fe₂-Tf was determined and expressed as a percentage of the untreated control (Fig. 3B). As observed in the ⁵⁹Fe mobilization experiments, the parent chelator, SIH, demonstrated high ⁵⁹Fe chelation efficacy and inhibited ⁵⁹Fe uptake to 15% of the control (Fig. 3B).

Importantly, those ligands that showed high ⁵⁹Fe mobilization efficacy (Fig. 3A) were also highly effective at inhibiting the uptake of ⁵⁹Fe from ⁵⁹Fe₂-Tf (Fig. 3B). For example, the ligands, BHAPI, BHPPI, 2API, 7HII, H17 and H18, that demonstrated high ⁵⁹Fe mobilization activity, were able to limit ⁵⁹Fe uptake to 10 - 26% of the control (Fig. 3B). In contrast, the compounds, redSIH, redHAPI, redHPPI, H16, and H28,

showed limited ability to prevent ^{59}Fe uptake, inhibiting it to >70% of the control (Fig. 3B).

3.3 Examination of the ability of the iron-chelator complexes to catalyze the oxidation of ascorbate

It has been previously observed that the cytotoxic effects of some iron chelators is due not only to their ability to bind cellular iron, but also to form redox-active iron complexes [12,44,53]. Thus, we examined whether the iron complexes of our novel ligands were able to redox cycle by assessing their ability to mediate the oxidation of ascorbate by standard methods [44,46]. The ability of the iron complexes to catalyze the oxidation of ascorbate was expressed as a percentage of the control (ascorbate with “free” Fe^{3+}).

The chelators, DFO and EDTA, were used as negative (anti-oxidative) and positive (pro-oxidative) controls, respectively [44,47]. As previously observed, the Fe complex of DFO demonstrated a typical anti-oxidative profile [54], resulting in decreased levels of ascorbate oxidation at an IBE of 3 (excess DFO) than at an IBE of 0.1 (excess iron; Fig. 4). In contrast, the iron complex of EDTA exhibited a pro-oxidative effect and mediated higher levels of ascorbate oxidation at an IBE of 3 relative to that at 0.1 (Fig. 4). In fact, at an IBE of 3, the iron complex of EDTA increased the oxidation of ascorbate to 924% of the control.

The iron complex of the parent chelator, SIH, exhibited anti-oxidant activity similar to that of the iron complex of DFO (Fig. 4). All of the iron complexes of the novel ligands, with the exception of 2API, demonstrated neither anti-oxidant nor pro-oxidative effects and were comparable to the control. The iron complex of the pyridine derivative, 2API, was the only Fe complex that showed pro-oxidative effects and significantly ($p < 0.001$) increased ascorbate oxidation to 256% relative to the control at an IBE of 3 (Fig. 4).

3.4 Prevention of oxidative injury induced by hydrogen peroxide

The ability of the ligands to act as protective agents in a model of oxidative stress was then examined by assessing the cellular viability of H9c2 cardiomyoblast cells upon a 24 h co-incubation of the chelators with H_2O_2 (200 μM). These results are

shown in Fig. 5 and summarized in Table 2. In these experiments, the EC₅₀ value is calculated which represents the concentration that reduced the cytotoxicity induced by hydrogen peroxide (200 μM) to 50% of the untreated control after a 24 h/37°C incubation with H9c2 cells. SIH was used as a positive control and resulted in an EC₅₀ value of 7.63 ± 1.38 μM (Table 2).

Of all the novel ligands synthesized, the analog that displayed the highest level of cytoprotective activity was 7HII, with an EC₅₀ value of 2.68 ± 1.30 μM (Table 2). In fact, 7HII demonstrated significantly ($p < 0.001$) greater protection against hydrogen peroxide-induced cytotoxicity than the parent chelator, SIH. Although the iron chelators, BHAPI, BHPPI, 2API, H17 and H18 also prevented peroxide-induced cytotoxicity (EC₅₀: 8.48-42.57 μM), their EC₅₀ values were higher than that of SIH. The ligands, redSIH, redHAPI, redHPPI, H16 and H28 did not display protective activity against peroxide-induced cytotoxicity in the concentration range examined.

3.5 Cytotoxicity studies in H9c2 cardiomyoblast cells

The selectivity of the novel ligands was then examined after a 72 h incubation with the non-tumorigenic H9c2 cardiomyoblast cell line (Fig. 6; Table 2). The parent chelator, SIH, was examined as a control and demonstrated an IC₅₀ value of 49.47 ± 1.77 μM (Table 2).

Of the synthesized analogs, redHAPI, redHPPI, H16 and H28 were the least toxic agents, with IC₅₀ values >80 μM. The ligands, redSIH and H17, showed comparable cytotoxicity to H9c2 cardiomyoblasts as the parent chelator, SIH. The other studied ligands, BHAPI, BHPPI, 2API, 7HII, H18, were more toxic than the chelator, SIH, with IC₅₀ values ranging from 0.62 μM to 7.40 μM. The most cytotoxic agent was 7HII with an IC₅₀ value of 0.62 ± 0.17 μM (Table 2; Fig. 6).

3.6 Cytotoxic effects of SIH derivatives on MCF-7 cells

The cytotoxic effects of the SIH derivatives were studied in MCF-7 breast adenocarcinoma cells following a 72 h incubation. The parent chelator, SIH, was used as a control and demonstrated moderate cytotoxic activity (IC₅₀: 4.21 ± 1.05 μM; Table 2; Fig. 7), similar to that previously observed [31].

The analogs containing a reduced hydrazone bond (redSIH, redHAPI and redHPPI) or an isopropyl group adjacent to this bond (H16) exhibited poor cytotoxic

activity ($IC_{50} >100 \mu\text{M}$). The chelator, H28, with a bulky cyclohexyl group in close proximity to the hydrazone bond demonstrated intermediate cytotoxic effects, with an IC_{50} of $42.41 \pm 3.15 \mu\text{M}$. The remaining agents, BHAPI, BHPPI, 2API, 7HII, H17 and H18, showed increased cytotoxic activity (IC_{50} : 0.38-2.92 μM ; Table 2) relative to SIH (Table 2). The greatest level of cytotoxic activity was observed with the indanone derivative, 7HII ($IC_{50} = 0.38 \pm 0.11 \mu\text{M}$).

To provide insight into the selectivity of the cytotoxic effects of the novel ligands, which is crucial for potential anti-cancer agents, their IC_{50} values in H9c2 cells and their IC_{50} values in MCF-7 cells were compared by calculating a “selectivity ratio”, namely $IC_{50} \text{ H9c2} / IC_{50} \text{ MCF-7 cells}$ (Table 2). SIH had a selectivity ratio of 11.75. The analogs, redSIH and redHAPI, with reduced hydrazone bonds had lower IC_{50} values in H9c2 cardiomyoblasts than in MCF-7 cancer cells, indicating greater cytotoxic activity in the former. Relative to SIH, this resulted in a marked decrease in the selectivity ratio to 0.14 and 0.63, respectively (Table 2). The ligands, redHPPI, 2API, 7HII and H28, showed somewhat similar cytotoxic activity in both the MCF-7 and H9c2 cell-types leading to selectivity ratios that were far less than SIH, and which ranged between 1.05 and 2.01. On the other hand, the bromine-substituted chelators (BHAPI and BHPPI) demonstrated selective activity against MCF-7 breast cancer cells relative to the H9c2 cell-type, although their selectivity ratios were approximately half that observed for SIH, *viz.*, 6.59 and 7.60, respectively (Table 2). The analogs that demonstrated the greatest selectivity profile against MCF-7 cells relative to H9c2 cells were the propyl (H17) and isobutyl (H18) derivatives of SIH, which were more active than SIH itself, demonstrating selectivity ratios of 14.36 and 15.10, respectively (Table 2).

4 Discussion

Aroylhydrazones represent an intriguing group of chelators that exhibit a variety of biological effects associated with their ability to influence cellular iron levels [27,33,55]. The aim of the present study was to synthesize and evaluate the biological activity of a series of new analogs of the well-established iron-binding ligand, SIH, with respect to their: (1) cytotoxic effects; (2) ability to protect cells against oxidative injury; and (3) cytotoxicity to H9c2 non-tumorigenic cardiomyoblast cells. The iron chelation activity, ability to mobilize cellular ^{59}Fe , efficacy to inhibit ^{59}Fe uptake from $^{59}\text{Fe}_2\text{-Tf}$, and the redox activity of the iron complexes of the novel analogs were also determined, as these properties are crucial factors involved in their biological activity [34,35]. The primary goal was to further characterize the structure-activity relationships of SIH-related aroylhydrazones for the future rational design of compounds with therapeutic potential.

4.1 Reduction of the hydrazone bond

First, we probed the role of the hydrazone bond itself, as it is prone to hydrolysis and is a site of instability in this class of compounds [56]. Previous studies suggested that compounds with a reduced hydrazone bond retained their chelation properties [57]. Thus, we examined the effect of the reduction of the hydrazone bond of the chelators, SIH, HAPI and HPPI, as these ligands previously exhibited cardioprotective [33] and cytotoxic [31] activity.

The results of the present study revealed that the reduced analogs were relatively non-toxic against both tumorigenic MCF7 cells and non-tumorigenic H9c2 cardiomyoblasts (Table 2). The cytotoxicity of redHAPI and redHPPI were approximately one order of magnitude lower than those of the parent chelators (HAPI and HPPI, respectively) [31,33], while the cytotoxic activity of redSIH towards H9c2 cells was similar to that of SIH (Table 2). Reduction of the hydrogen bond in redSIH, redHAPI and redHPPI led to a marked decrease in their selectivity ratios (0.14 - 1.14) relative to SIH (11.75; Table 2). In fact, these agents containing a reduced hydrazone bond had the lowest selectivity ratios of all analogues examined in this investigation. Furthermore, these latter compounds totally lost the ability to protect H9c2 cells against oxidative stress relative to SIH (Table 2) [33]. This lack of protection against oxidative stress is likely due to their limited iron chelation (Fig. 2) and ^{59}Fe mobilization efficacy

(Fig. 3A). Of the reduced analogs, only redSIH retained limited chelation activity (Figs. 2 and 3). Therefore, the presence of the hydrazone bond is an important criterion for the cardioprotective and cytotoxic effects of these aroylhydrazones. The loss of iron chelation efficacy of the reduced analogs may be a result of the altered molecular spatial arrangement of the ligating groups due to the free rotation of the single C-N bond, or the decreased electron density on the chelating nitrogen due to its transition from sp^2 to sp^3 orbital hybridization.

4.2 Bromination of the phenyl ring

The introduction of a halogen into the structure of a molecule enhances its lipophilicity (Table 1), which can potentially facilitate its permeation into cells. The halogen substitution, due to its inductive electron-withdrawing effects, may also influence the stability of the hydrazone bond and the ability of the compound to chelate metal ions. Indeed, a previously synthesized chlorinated HAPI derivative (*i.e.*, (*E*)-*N'*-[1-(5-chloro-2-hydroxyphenyl)ethylidene]isonicotinoylhydrazide; CHAPI), showed greater hydrolytic stability than HAPI and moderate cytotoxic activity ($IC_{50} = 0.65 \pm 0.07 \mu\text{M}$ against MCF-7 cells) [31]. Therefore, the brominated analog, BHAPI, bearing a bromine instead of chlorine, and its homolog, BHPPI (Fig. 1), were prepared to evaluate the influence of halogenation on the cardioprotective and cytotoxic activity of these chelators. Both BHAPI and BHPPI showed comparable iron chelation efficacy to SIH in solution, as well as in cells (Fig. 2). The cytotoxic activity of these brominated analogs against MCF-7 cells was greater than that found for SIH (Table 2). Further, both BHAPI and BHPPI showed greater cytotoxic activity against MCF-7 breast cancer cells relative to non-tumorigenic, H9c2 cardiomyoblasts, although their selectivity ratios were approximately half that observed for SIH (Table 2). In addition, BHAPI and BHPPI were less effective than SIH when assessing the ability of these agents to prevent the cytotoxicity induced by H_2O_2 in H9c2 cardiomyoblasts (Table 2). Similar results were observed for the chlorine derivative, CHAPI [33]. Thus, the exchange of chlorine for bromine did not significantly alter the biological activity of such aroylhydrazones.

4.3 Exchange of phenol for pyridine

The ligand, 2API, which contains a pyridine nitrogen as a donor atom instead of the phenolic oxygen, was prepared to examine the effect of alterations of the donor atom set from *O, N, O* to *N, N, O* on their biological activity. The cytotoxic activity of 2API was similar in MCF-7 breast cancer cells and non-tumorigenic H9c2 cells, with the selectivity ratio decreasing markedly (to 1.05) relative to that observed with SIH (11.75; Table 2). This observation may be explained by the redox activity of 2API, as it was the only analog that exhibited significant pro-oxidative activity in the ascorbate oxidation assay (Fig. 4). In fact, previous studies reported the reversible $\text{Fe}^{2+/3+}$ redox couple of the iron complex of 2API [58] and the current investigation demonstrates its ability to oxidize ascorbate.

The iron chelation efficacy and ^{59}Fe mobilization activity of 2API in cells was marked, with the ligand being generally comparable to SIH (Figs. 2B, 3A, 3B). In contrast, the iron chelation activity of 2API in solution did not correlate with the results of cellular experiments (Fig. 2A), which may be explained by the pro-oxidative effects of 2API. It is possible the ability of the 2API iron complex to redox cycle may have interfered in the solution-based calcein assay, as it is known that the fluorescence of free calcein decreases in an oxidative environment [52]. Whereas the unaltered sensitivity of the calcein-AM assay in cells (Fig. 2B) with regards to 2API, may be due to the redox buffering capacity provided by glutathione and other intracellular anti-oxidative systems [59] that maintain calcein sensitivity. In summary, the alteration of the donor atom set from *O, N, O* to *N, N, O* in 2API resulted in the formation of a redox active iron complex with decreased selectivity against MCF-7 breast cancer cells.

4.4 Branching, prolongation or cyclization of the alkyl chain adjacent to the hydrazone bond

In a previous investigation, we found that the presence of an alkyl chain adjacent to the hydrazone bond did not significantly increase the cytotoxic activity of the ketone-derived hydrazones, HAPI and HPPI, compared to SIH [31]. In the current study, we synthesized the analogs, 7HII, H16, H17, H18 and H28, to evaluate the influence of alkyl chain length and branching on biological activity.

The 7-hydroxyindanone derivative, 7HII, contains an extra five-membered ring relative to SIH and showed comparable iron chelating and ^{59}Fe mobilization efficacy

(Figs. 2, 3). The cyclization of the alkyl chain, and hence, its increased rigidity, improved its ability to protect cells against oxidative stress compared to SIH, with 7HII being the most effective ligand screened in this regard (Table 2). However, this structural change in 7HII resulted in significantly higher cytotoxicity towards H9c2 cells and a marked drop in the selectivity ratio relative to SIH (Table 2). Therefore, this structural modification resulted in unfavorable biological activity.

The ligand, H16, bears an additional isopropyl chain at the α -position from the hydrazone bond relative to SIH (Fig. 1). This modification was intended to: (1) protect the hydrazone bond against hydrolysis [60]; and (2) increase lipophilicity, which is known to enhance cellular permeability of aroylhydrazone ligands [34]. However, this structural modification in H16 resulted in a marked loss of its iron chelation activity relative to SIH, which may be due to steric hindrance around the hydrazone bond mediated by the bulky branched isopropyl group that potentially reduces binding to iron. Notably, consistent with the loss of iron-binding, the cytotoxic activity of H16 was very low in H9c2 and MCF-7 cells and did not show any protective effects against H₂O₂ (Table 2).

To examine whether the effect of the isopropyl chain of H16 was caused by steric hindrance close to the hydrazone bond, compound H17, with an unbranched propyl chain, was prepared. Interestingly, the iron chelation and ⁵⁹Fe mobilization efficacy of H17 was similar to SIH, with the compound showing selective cytotoxic activity against MCF-7 cancer cells relative to non-tumorigenic H9c2 cardiomyoblasts [31,33]. In fact, the selectivity ratio of H17 (14.36) was greater than that found for SIH (11.75), demonstrating its potential. We were also interested to examine whether H18, with an isobutyl substituent adjacent to the hydrazone bond (Fig. 1), would retain the favorable activity of H17. In contrast to H16, H18 is branched at the β -position in relation to the imine carbon and led to the ligand maintaining its iron chelation efficacy in solution and also in cells relative to SIH (Figs. 2, 3). This structural change increased the cytotoxic activity of H18 against both MCF-7 tumor cells and H9c2 cardiomyoblasts relative to SIH and H17 (Table 2). However, notably, H18 had the best selectivity ratio of all the studied compounds (*i.e.*, 15.10).

To further examine the structure-activity relationships of bulky substituents close to the hydrazone bond, compound H28, with a cyclohexyl group, was prepared. As in the case of H16, this modification markedly decreased the iron chelation efficacy of H28 (Figs. 2, 3). Furthermore, in comparison with H16, the cytotoxic activity of H28

was greater in both MCF-7 and H9c2 cells, leading to an unfavorable selectivity ratio of 2.01 which was much less than SIH. In addition, the cardioprotective activity of H28 against H₂O₂ was completely abolished, which is consistent with the low iron chelation efficacy of H28.

Thus, the alkyl chain on the imine carbon markedly influenced the activity of such hydrazones. Prolonged linear or iso-branched alkyl groups increased their anti-cancer potential, while branching or cyclization in close proximity to the hydrazone bond dramatically decreased their chelation ability and, consequently, decreased their cytotoxic activity against MCF-7 cells and their ability to protect H9c2 cells against oxidative injury.

4.5 Conclusions

In this study, we identified several structural parameters important for the design of aroylhydrazone iron chelator. First, the hydrazone bond is essential for chelation activity. Second, halogenation (with bromine) of the phenyl ring does not have any beneficial effect due to increased non-selective cytotoxic activity against non-tumorigenic H9c2 cardiomyoblasts. Third, exchange of the chelating phenolic hydroxyl for a pyridine nitrogen resulted in increased non-selective cytotoxic activity that is likely due to the formation of redox active iron complexes. Finally, and most significantly, the exchange of the aldimine hydrogen in SIH for a longer unbranched or iso-branched alkyl group is a favorable modification to increase the anti-cancer potential of such hydrazones. The most promising compounds identified in this study are the propyl-containing analog, H17, and isobutyl-containing derivative, H18, that possessed the highest selectivity ratios. These compounds warrant further investigation.

Acknowledgements

This study was supported by the Charles University in Prague (projects GAUK 299511, SVV 260065 and 260062), the Czech Science Foundation (grant 13-15008S), and the European Social Fund and the State Budget of the Czech Republic (Operational Program CZ.1.07/2.3.00/30.0061). This work was also funded by a Project Grant from the National Health and Medical Research Council (NHMRC) Australia to D.R.R. [Grant 632778]; a NHMRC Senior Principal Research Fellowship to D.R.R. [Grant 571123]; and a Cancer Institute New South Wales Early Career Development Fellowship to D.S.K. [Grant 08/ECF/1–30]. D.J.R.L thanks the Cancer Institute New South Wales for an Early Career Fellowship [10/ECF/2–18] and the NHMRC of Australia for an Early Career Postdoctoral Fellowship [1013810].

Conflict of Interest Disclosure

The authors declare no competing financial interests.

References

1. Wang J, Pantopoulos K (2011) Regulation of cellular iron metabolism. *Biochem J* 434: 365-381.
2. Lawen A, Lane DJ (2013) Mammalian iron homeostasis in health and disease: uptake, storage, transport, and molecular mechanisms of action. *Antioxid Redox Signal* 18: 2473-2507.
3. Dunn LL, Suryo Rahmanto Y, Richardson DR (2007) Iron uptake and metabolism in the new millennium. *Trends Cell Biol* 17: 93-100.
4. Hentze MW, Muckenthaler MU, Andrews NC (2004) Balancing acts: molecular control of mammalian iron metabolism. *Cell* 117: 285-297.
5. Richardson DR, Baker E (1991) The release of iron and transferrin from the human melanoma cell. *Biochim Biophys Acta* 1091: 294-302.
6. Napier I, Ponka P, Richardson DR (2005) Iron trafficking in the mitochondrion: novel pathways revealed by disease. *Blood* 105: 1867-1874.
7. Richardson DR, Lane DJ, Becker EM, Huang ML, Whitnall M, et al. (2010) Mitochondrial iron trafficking and the integration of iron metabolism between the mitochondrion and cytosol. *Proc Natl Acad Sci U S A* 107: 10775-10782.
8. Arredondo M, Nunez MT (2005) Iron and copper metabolism. *Mol Aspects Med* 26: 313-327.
9. Leidgens S, Bullough KZ, Shi H, Li F, Shakoury-Elizeh M, et al. (2013) Each member of the poly-r(C)-binding protein 1 (PCBP) family exhibits iron chaperone activity toward ferritin. *J Biol Chem* 288: 17791-17802.
10. Cooper CE, Lynagh GR, Hoyes KP, Hider RC, Cammack R, et al. (1996) The relationship of intracellular iron chelation to the inhibition and regeneration of human ribonucleotide reductase. *J Biol Chem* 271: 20291-20299.
11. Lane DJ, Mills TM, Shafie NH, Merlot AM, Saleh Moussa R, et al. (2014) Expanding horizons in iron chelation and the treatment of cancer: Role of iron in

the regulation of ER stress and the epithelial-mesenchymal transition. *Biochim Biophys Acta* 1845: 166-181.

12. Kalinowski DS, Richardson DR (2005) The evolution of iron chelators for the treatment of iron overload disease and cancer. *Pharmacol Rev* 57: 547-583.
13. Merlot AM, Kalinowski DS, Richardson DR (2013) Novel chelators for cancer treatment: where are we now? *Antioxid Redox Signal* 18: 973-1006.
14. Richardson DR, Kalinowski DS, Lau S, Jansson PJ, Lovejoy DB (2009) Cancer cell iron metabolism and the development of potent iron chelators as anti-tumour agents. *Biochim Biophys Acta* 1790: 702-717.
15. Bendova P, Mackova E, Haskova P, Vavrova A, Jirkovsky E, et al. (2010) Comparison of clinically used and experimental iron chelators for protection against oxidative stress-induced cellular injury. *Chem Res Toxicol* 23: 1105-1114.
16. Torti SV, Torti FM (2013) Iron and cancer: more ore to be mined. *Nat Rev Cancer* 13: 342-355.
17. Kolberg M, Strand KR, Graff P, Andersson KK (2004) Structure, function, and mechanism of ribonucleotide reductases. *Biochim Biophys Acta* 1699: 1-34.
18. Walker RA, Day SJ (1986) Transferrin receptor expression in non-malignant and malignant human breast tissue. *J Pathol* 148: 217-224.
19. Jiang XP, Elliott RL, Head JF (2010) Manipulation of iron transporter genes results in the suppression of human and mouse mammary adenocarcinomas. *Anticancer Res* 30: 759-765.
20. Pinnix ZK, Miller LD, Wang W, D'Agostino R, Jr., Kute T, et al. (2010) Ferroportin and iron regulation in breast cancer progression and prognosis. *Sci Transl Med* 2: 43ra56.
21. Le NT, Richardson DR (2002) The role of iron in cell cycle progression and the proliferation of neoplastic cells. *Biochim Biophys Acta* 1603: 31-46.

22. Whitnall M, Howard J, Ponka P, Richardson DR (2006) A class of iron chelators with a wide spectrum of potent antitumor activity that overcomes resistance to chemotherapeutics. *Proc Natl Acad Sci U S A* 103: 14901-14906.
23. Lovejoy DB, Sharp DM, Seebacher N, Obeidy P, Prichard T, et al. (2012) Novel second-generation di-2-pyridylketone thiosemicarbazones show synergism with standard chemotherapeutics and demonstrate potent activity against lung cancer xenografts after oral and intravenous administration in vivo. *J Med Chem* 55: 7230-7244.
24. Vitolo LMW, Hefter GT, Clare BW, Webb J (1990) Iron Chelators of the Pyridoxal Isonicotinoyl Hydrazone Class .2. Formation-Constants with Iron(III) and Iron(II). *Inorganica Chimica Acta* 170: 171-176.
25. Dubois JE, Fakhrayan H, Doucet JP, Chahine JME (1992) Kinetic and Thermodynamic Study of Complex-Formation between Iron(II) and Pyridoxal Isonicotinoylhydrazone and Other Synthetic Chelating-Agents. *Inorganic Chemistry* 31: 853-859.
26. Horackova M, Ponka P, Byczko Z (2000) The antioxidant effects of a novel iron chelator salicylaldehyde isonicotinoyl hydrazone in the prevention of H₂O₂ injury in adult cardiomyocytes. *Cardiovasc Res* 47: 529-536.
27. Simunek T, Boer C, Bouwman RA, Vlasblom R, Versteilen AM, et al. (2005) SIH-- a novel lipophilic iron chelator--protects H9c2 cardiomyoblasts from oxidative stress-induced mitochondrial injury and cell death. *J Mol Cell Cardiol* 39: 345-354.
28. Simunek T, Sterba M, Popelova O, Kaiserova H, Adamcova M, et al. (2008) Anthracycline toxicity to cardiomyocytes or cancer cells is differently affected by iron chelation with salicylaldehyde isonicotinoyl hydrazone. *Br J Pharmacol* 155: 138-148.
29. Berndt C, Kurz T, Selenius M, Fernandes AP, Edgren MR, et al. (2010) Chelation of lysosomal iron protects against ionizing radiation. *Biochem J* 432: 295-301.

30. Fillebeen C, Pantopoulos K (2010) Iron inhibits replication of infectious hepatitis C virus in permissive Huh7.5.1 cells. *J Hepatol* 53: 995-999.
31. Mackova E, Hruskova K, Bendova P, Vavrova A, Jansova H, et al. (2012) Methyl and ethyl ketone analogs of salicylaldehyde isonicotinoyl hydrazone: novel iron chelators with selective antiproliferative action. *Chem Biol Interact* 197: 69-79.
32. Klimentova I, Simunek T, Mazurova Y, Kaplanova J, Sterba M, et al. (2003) A study of potential toxic effects after repeated 10-week administration of a new iron chelator--salicylaldehyde isonicotinoyl hydrazone (SIH) to rabbits. *Acta Medica (Hradec Kralove)* 46: 163-170.
33. Hruskova K, Kovarikova P, Bendova P, Haskova P, Mackova E, et al. (2011) Synthesis and initial in vitro evaluations of novel antioxidant aroylhydrazone iron chelators with increased stability against plasma hydrolysis. *Chem Res Toxicol* 24: 290-302.
34. Richardson DR, Tran EH, Ponka P (1995) The potential of iron chelators of the pyridoxal isonicotinoyl hydrazone class as effective antiproliferative agents. *Blood* 86: 4295-4306.
35. Chaston TB, Lovejoy DB, Watts RN, Richardson DR (2003) Examination of the antiproliferative activity of iron chelators: multiple cellular targets and the different mechanism of action of triapine compared with desferrioxamine and the potent pyridoxal isonicotinoyl hydrazone analogue 311. *Clin Cancer Res* 9: 402-414.
36. Chaston TB, Richardson DR (2003) Redox chemistry and DNA interactions of the 2-pyridyl-carboxaldehyde isonicotinoyl hydrazone class of iron chelators: Implications for toxicity in the treatment of iron overload disease. *J Biol Inorg Chem* 8: 427-438.
37. Becker EM, Lovejoy DB, Greer JM, Watts R, Richardson DR (2003) Identification of the di-pyridyl ketone isonicotinoyl hydrazone (PKIH) analogues as potent iron chelators and anti-tumour agents. *Br J Pharmacol* 138: 819-830.

38. Richardson DR, Ponka P (1994) The iron metabolism of the human neuroblastoma cell: lack of relationship between the efficacy of iron chelation and the inhibition of DNA synthesis. *J Lab Clin Med* 124: 660-671.
39. Edward JT, Gauthier M, Chubb FL, Ponka P (1988) Synthesis of New Acylhydrazones as Iron-Chelating Compounds. *Journal of Chemical and Engineering Data* 33: 538-540.
40. Esposito BP, Epsztejn S, Breuer W, Cabantchik ZI (2002) A review of fluorescence methods for assessing labile iron in cells and biological fluids. *Anal Biochem* 304: 1-18.
41. Glickstein H, El RB, Link G, Breuer W, Konijn AM, et al. (2006) Action of chelators in iron-loaded cardiac cells: Accessibility to intracellular labile iron and functional consequences. *Blood* 108: 3195-3203.
42. Richardson DR, Milnes K (1997) The potential of iron chelators of the pyridoxal isonicotinoyl hydrazone class as effective antiproliferative agents II: the mechanism of action of ligands derived from salicylaldehyde benzoyl hydrazone and 2-hydroxy-1-naphthylaldehyde benzoyl hydrazone. *Blood* 89: 3025-3038.
43. Baker E, Richardson D, Gross S, Ponka P (1992) Evaluation of the iron chelation potential of hydrazones of pyridoxal, salicylaldehyde and 2-hydroxy-1-naphthylaldehyde using the hepatocyte in culture. *Hepatology* 15: 492-501.
44. Richardson DR, Sharpe PC, Lovejoy DB, Senaratne D, Kalinowski DS, et al. (2006) Dipyriddy thiosemicarbazone chelators with potent and selective antitumor activity form iron complexes with redox activity. *J Med Chem* 49: 6510-6521.
45. Becker E, Richardson DR (1999) Development of novel aroylhydrazone ligands for iron chelation therapy: 2-pyridylcarboxaldehyde isonicotinoyl hydrazone analogs. *J Lab Clin Med* 134: 510-521.
46. Mladenka P, Kalinowski DS, Haskova P, Bobrovova Z, Hrdina R, et al. (2009) The novel iron chelator, 2-pyridylcarboxaldehyde 2-thiophenecarboxyl hydrazone, reduces catecholamine-mediated myocardial toxicity. *Chem Res Toxicol* 22: 208-217.

47. Chaston TB, Watts RN, Yuan J, Richardson DR (2004) Potent antitumor activity of novel iron chelators derived from di-2-pyridylketone isonicotinoyl hydrazone involves fenton-derived free radical generation. *Clin Cancer Res* 10: 7365-7374.
48. Repetto G, del Peso A, Zurita JL (2008) Neutral red uptake assay for the estimation of cell viability/cytotoxicity. *Nat Protoc* 3: 1125-1131.
49. Ghose AK, Crippen GM (1987) Atomic physicochemical parameters for three-dimensional-structure-directed quantitative structure-activity relationships. 2. Modeling dispersive and hydrophobic interactions. *J Chem Inf Comput Sci* 27: 21-35.
50. Viswanadhan VNG, A. K.; Revankar, G. R.; Robins, R. K. (1989) Atomic physicochemical parameters for three dimensional structure directed quantitative structure-activity relationships. 4. Additional parameters for hydrophobic and dispersive interactions and their application for an automated superposition of certain naturally occurring nucleoside antibiotics. *J Chem Inf Comput Sci* 29: 163-172.
51. Broto PM, G.; Vandycke, C. (1984) Molecular Structures: Perception, Autocorrelation Descriptor and SAR Studies. System of Atomic Contributions for the Calculation of the *n*-Octanol/Water Partition Coefficients. *Eur J Med Chem Chim Theor* 19: 71-78.
52. Zhang XZ, Li M, Cui Y, Zhao J, Cui ZG, et al. (2012) Electrochemical Behavior of Calcein and the Interaction Between Calcein and DNA. *Electroanalysis* 24: 1878-1886.
53. Yuan J, Lovejoy DB, Richardson DR (2004) Novel di-2-pyridyl-derived iron chelators with marked and selective antitumor activity: in vitro and in vivo assessment. *Blood* 104: 1450-1458.
54. Gutteridge JM, Richmond R, Halliwell B (1979) Inhibition of the iron-catalysed formation of hydroxyl radicals from superoxide and of lipid peroxidation by desferrioxamine. *Biochem J* 184: 469-472.

55. Ponka P, Borova J, Neuwirt J, Fuchs O (1979) Mobilization of iron from reticulocytes. Identification of pyridoxal isonicotinoyl hydrazone as a new iron chelating agent. *FEBS Lett* 97: 317-321.
56. Kalia J, Raines RT (2008) Hydrolytic stability of hydrazones and oximes. *Angew Chem Int Ed Engl* 47: 7523-7526.
57. Sunami S, Nishimura T, Nishimura I, Ito S, Arakawa H, et al. (2009) Synthesis and biological activities of topoisomerase I inhibitors, 6-arylmethylamino analogues of edotecarin. *J Med Chem* 52: 3225-3237.
58. Bernhardt PV, Wilson GJ, Sharpe PC, Kalinowski DS, Richardson DR (2008) Tuning the antiproliferative activity of biologically active iron chelators: characterization of the coordination chemistry and biological efficacy of 2-acetylpyridine and 2-benzoylpyridine hydrazone ligands. *J Biol Inorg Chem* 13: 107-119.
59. Sies H (1993) Strategies of antioxidant defense. *Eur J Biochem* 215: 213-219.
60. Richardson D, Vitolo LW, Baker E, Webb J (1989) Pyridoxal isonicotinoyl hydrazone and analogues. Study of their stability in acidic, neutral and basic aqueous solutions by ultraviolet-visible spectrophotometry. *Biol Met* 2: 69-76.

Tables

Table 1. Molecular weights (MW) and calculated n-octanol/water coefficients (log P_{calc}) of the studied analogs. The MW and log P_{calc} values were calculated using ChemBioOffice Ultra 11.0 software. The log P_{calc} is expressed as an average of the results of Crippen's and Viswanadhan's fragmentations and Broto's method.

Chelator	MW (g/mol)	log P_{calc}
SIH	241	1.5
redSIH	243	1.0
redHAPI	257	1.4
redHPPI	271	1.9
BHAPI	334	2.1
BHPPI	348	2.6
2API	240	0.7
7HII	267	1.4
H16	283	2.2
H17	283	2.2
H18	297	2.5
H28	323	3.1

Table 2. Protective and cytotoxic effects of the synthesized SIH derivatives and their calculated “selectivity ratios”. The EC₅₀ values (concentration that reduced the cytotoxicity induced by H₂O₂ (200 μM) to 50% of the untreated control) were calculated after a 24 h incubation with non-tumorigenic H9c2 cardiomyoblasts. The IC₅₀ values (concentration that reduced the cellular viability or proliferation to 50% of the untreated control) were calculated after a 72 h incubation with H9c2 cardiomyoblasts or MCF-7 breast cancer cells. Selectivity ratios were calculated *via* IC₅₀ H9c2 cells/IC₅₀ MCF-7 cells. Mean ± SD; *n* ≥ 4 experiments. N/A - the EC₅₀ value was not achieved within the studied concentration range (no protection).

Chelator	EC₅₀ H9c2 (μM)	IC₅₀ H9c2 (μM)	IC₅₀ MCF-7 (μM)	Selectivity Ratio
SIH	7.63 ± 1.38	49.47 ± 1.77	4.21 ± 1.05	11.75
redSIH	N/A	39.59 ± 5.11	279.97 ± 53.17	0.14
redHAPI	N/A	83.96 ± 2.76	133.47 ± 28.76	0.63
redHPPI	N/A	226.12 ± 6.31	197.86 ± 13.09	1.14
BHAPI	30.34 ± 7.23	6.99 ± 0.82	1.06 ± 0.46	6.59
BHPPI	17.18 ± 4.39	6.31 ± 0.59	0.83 ± 0.50	7.60
2API	8.48 ± 3.11	3.07 ± 0.55	2.92 ± 0.67	1.05
7HII	2.68 ± 1.30	0.62 ± 0.17	0.38 ± 0.11	1.63
H16	N/A	>100	153.67 ± 24.20	-
H17	42.57 ± 7.94	32.60 ± 1.09	2.27 ± 0.14	14.36
H18	27.76 ± 3.90	7.40 ± 2.13	0.49 ± 0.18	15.10
H28	N/A	85.37 ± 12.90	42.41 ± 3.15	2.01

Figure Legends

Figure 1. Line drawings of the chemical structures of the iron chelators, SIH, HAPI and HPPI, and their novel analogs.

Figure 2. Iron chelation properties of the novel analogs in solution (A) and in MCF-7 cells (B). (A) The chelation dynamics of the new agents in solution were observed for 360 s using the calcein assay, and the agent was applied at $t = 100$ s. The fluorescence intensity of free calcein at $t = 360$ s was expressed as a percentage of that observed using the reference iron chelator, SIH. (B) The ability of the analogs to chelate “free” iron from the LIP in MCF-7 cells was measured using the calcein-AM assay. The fluorescence intensity of free calcein at $t = 600$ s was expressed as a percentage of that observed in the presence of SIH. Results are Mean \pm SD ($n \geq 3$ experiments). Statistical significance (ANOVA): # $p < 0.05$, ## $p < 0.01$, ### $p < 0.001$ compared to the reference chelator, SIH.

Figure 3. The effect of SIH and its analogs on ^{59}Fe mobilization from pre-labeled MCF-7 cells (A) and on internalized ^{59}Fe uptake from $^{59}\text{Fe}_2$ -transferrin (Tf) by MCF-7 cells (B). (A) The ability of the ligands to promote ^{59}Fe mobilization from MCF-7 cells was performed by first prelabeling the cells with ^{59}Fe -Tf (0.75 μM) for 3 h/37°C, followed by washing and then reincubation for 3 h/37°C with either control medium alone, or control medium containing the chelator (25 μM). (B) Inhibition of ^{59}Fe uptake from $^{59}\text{Fe}_2$ -Tf by MCF-7 cells by chelators was performed by incubating cells for 3 h/37°C with $^{59}\text{Fe}_2$ -Tf (0.75 μM) in the presence or absence of the chelator (25 μM). Results are Mean \pm SD ($n \geq 3$ experiments). Statistical significance (ANOVA): * $p < 0.05$, ** $p < 0.01$, *** $p < 0.001$ compared to the control (untreated) group, and # $p < 0.05$, ## $p < 0.01$, ### $p < 0.001$ compared to the reference chelator, SIH.

Figure 4. Effects of SIH and its analogs on iron-induced oxidation of ascorbic acid in a buffered solution (pH 7.4). Chelators were assayed at iron binding equivalents (IBE) of 0.1 (excess of Fe), 1 (iron-chelator complexes with a fully filled coordination sphere) and 3 (excess of free chelator). DFO and EDTA were used as negative and positive control chelators, respectively. The results are expressed as a percentage of the

control group in the absence of chelator (100%). Results are Mean \pm SD ($n \geq 3$ experiments). Statistical significance (ANOVA): * $p < 0.05$, ** $p < 0.01$, *** $p < 0.001$ as compared to the control group (iron with ascorbate).

Figure 5. Protective effects of the chelator, SIH (A), and the new analogues (B-L). The ability of the SIH derivatives to protect H9c2 cardiomyoblast cells against oxidative injury were evaluated using a 24 h/37°C incubation of the cells with H₂O₂ (200 μ M) and the novel analogs (0.3-1000 μ M). Results are Mean \pm SD ($n \geq 4$ experiments). Statistical significance (ANOVA): * $p < 0.05$, ** $p < 0.01$, *** $p < 0.001$ compared to the control (untreated) group, and # $p < 0.05$, ## $p < 0.01$, ### $p < 0.001$ compared to the H₂O₂ group.

Figure 6. Cytotoxic effects of the chelator, SIH (A), and the new analogues (B-L), using non-tumorigenic H9c2 cardiomyoblasts. The effect of the analogs (0.3-500 μ M) on the cellular viability of H9c2 cardiomyoblasts were performed using a 72 h/37°C incubation. Results are Mean \pm SD ($n \geq 4$ experiments). Statistical significance (ANOVA): * $p < 0.05$, ** $p < 0.01$, *** $p < 0.001$ as compared to the control (untreated) group.

Figure 7. Cytotoxic effects of the chelator, SIH (A), and the new analogues (B-L) against MCF-7 breast cancer cells. For the determination of their cytotoxic activity, MCF-7 breast adenocarcinoma cells were incubated with the analogs (0.3-3000 μ M) for 72 h/37°C. Results are Mean \pm SD ($n \geq 4$ experiments). Statistical significance (ANOVA): * $p < 0.05$, ** $p < 0.01$, *** $p < 0.001$ as compared to the control (untreated) group.

Figure 1

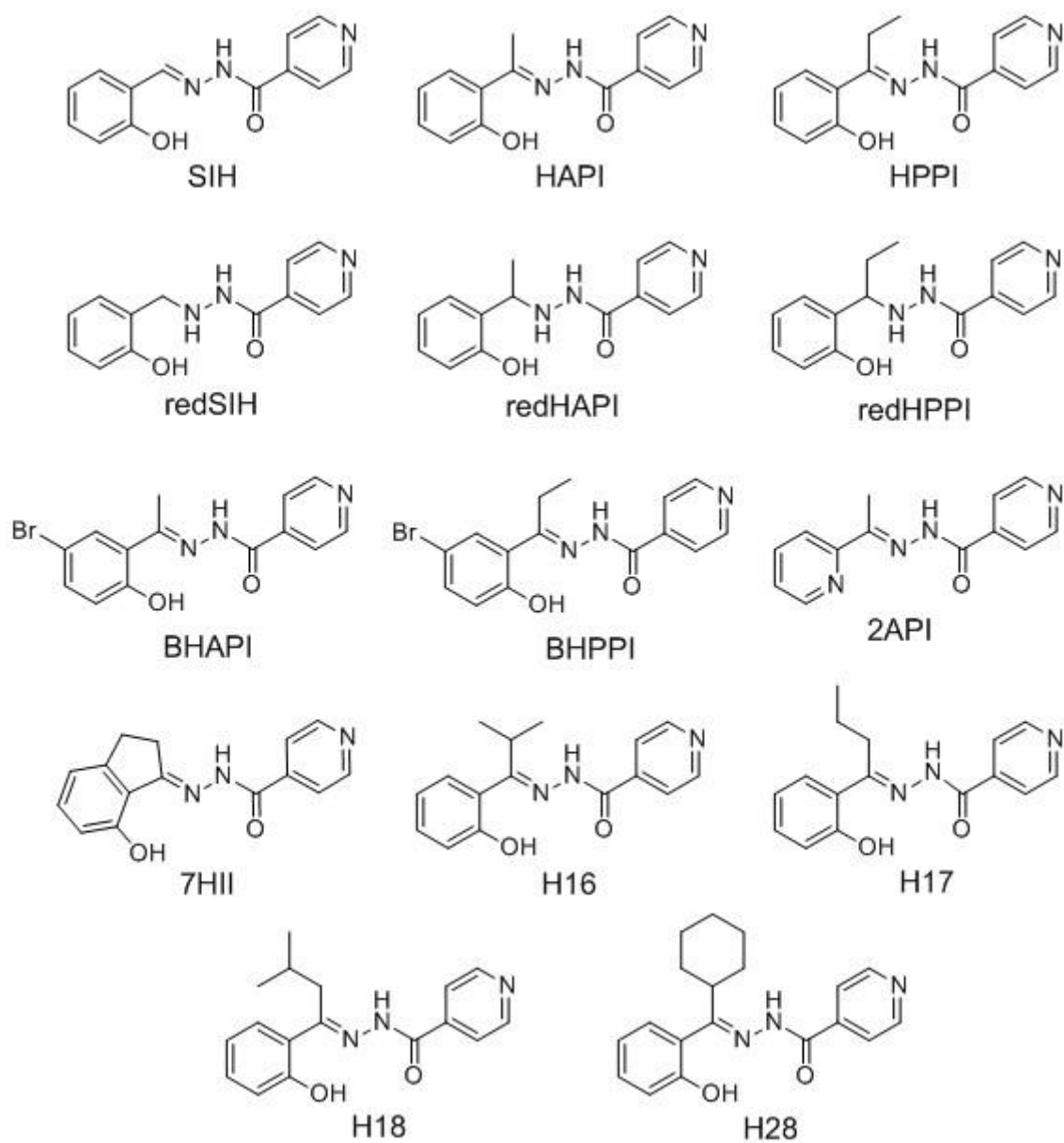


Figure 2

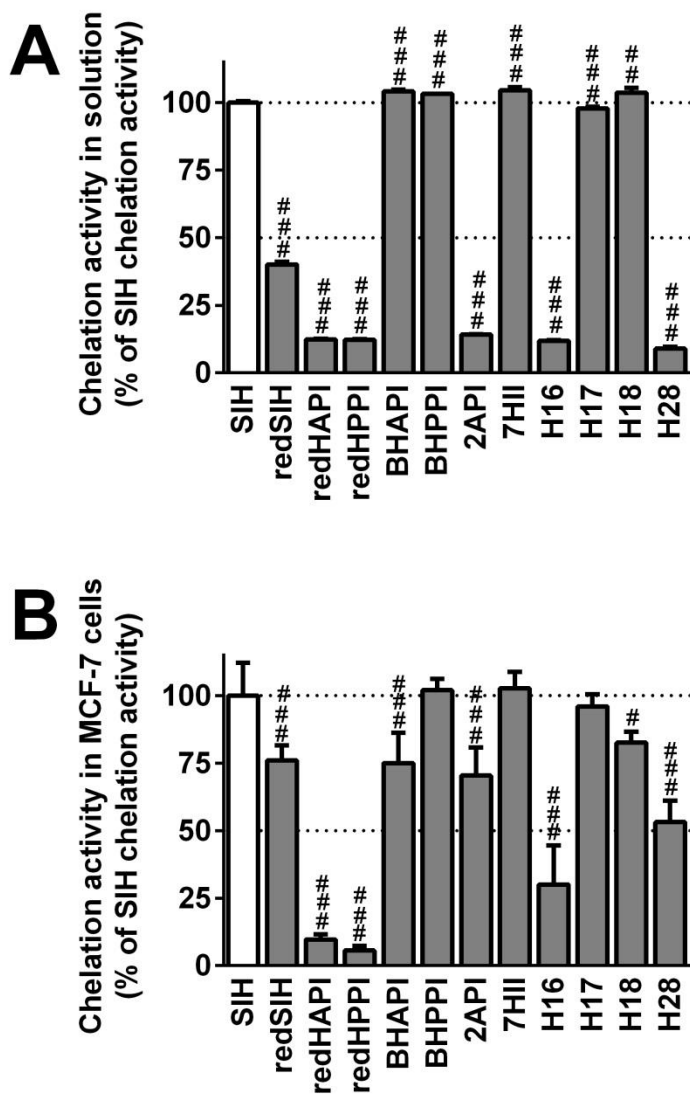


Figure 3



Figure 4

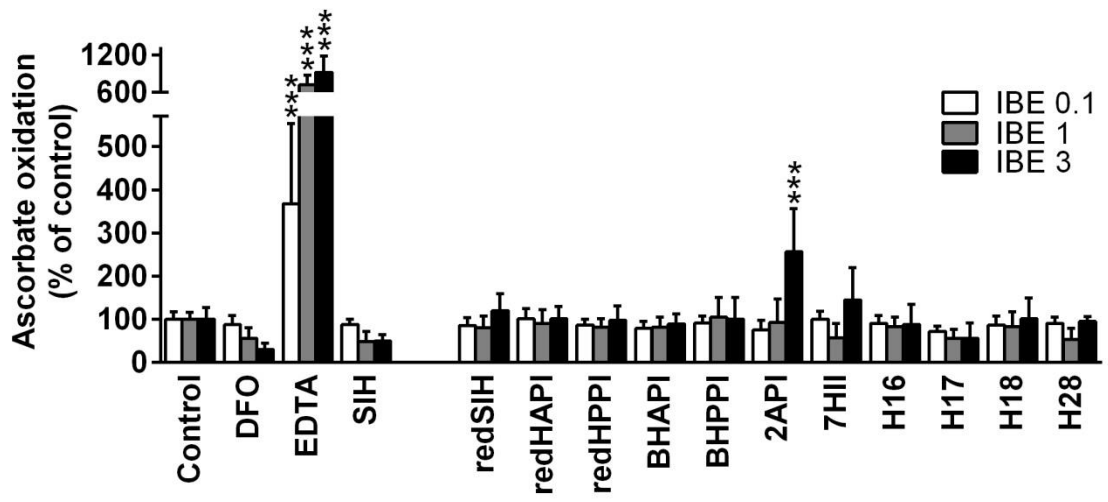


Figure 5

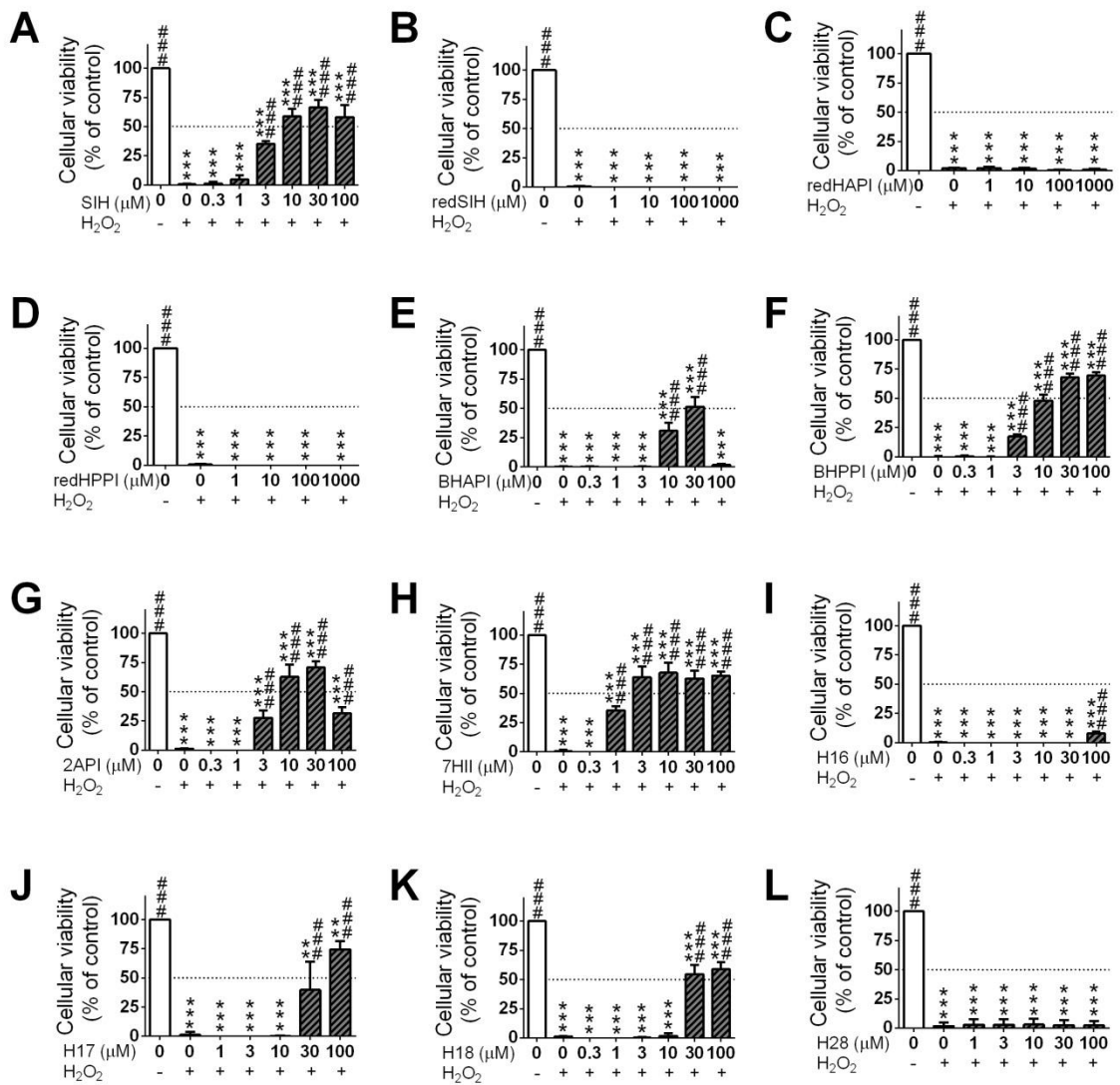


Figure 6

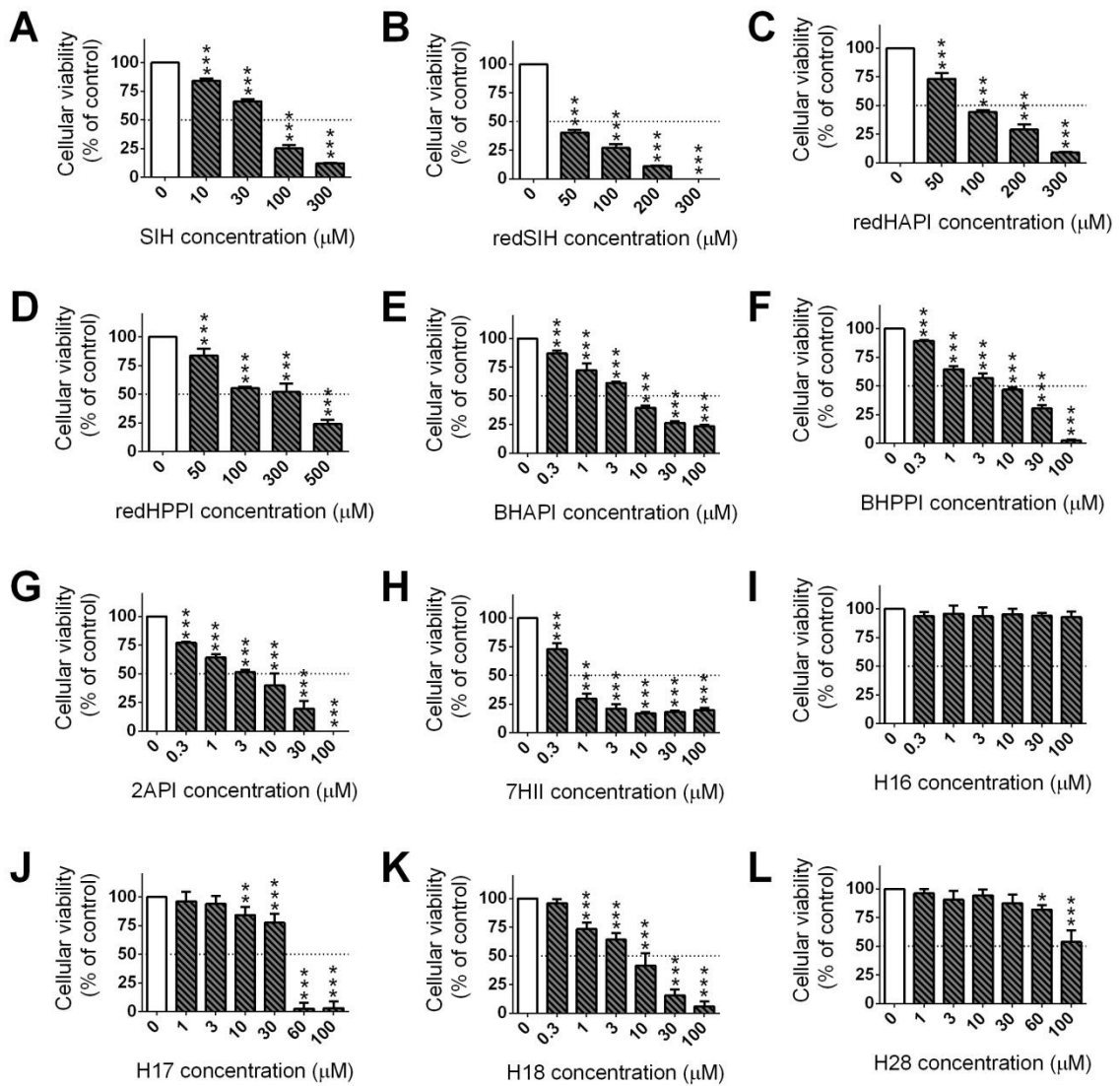
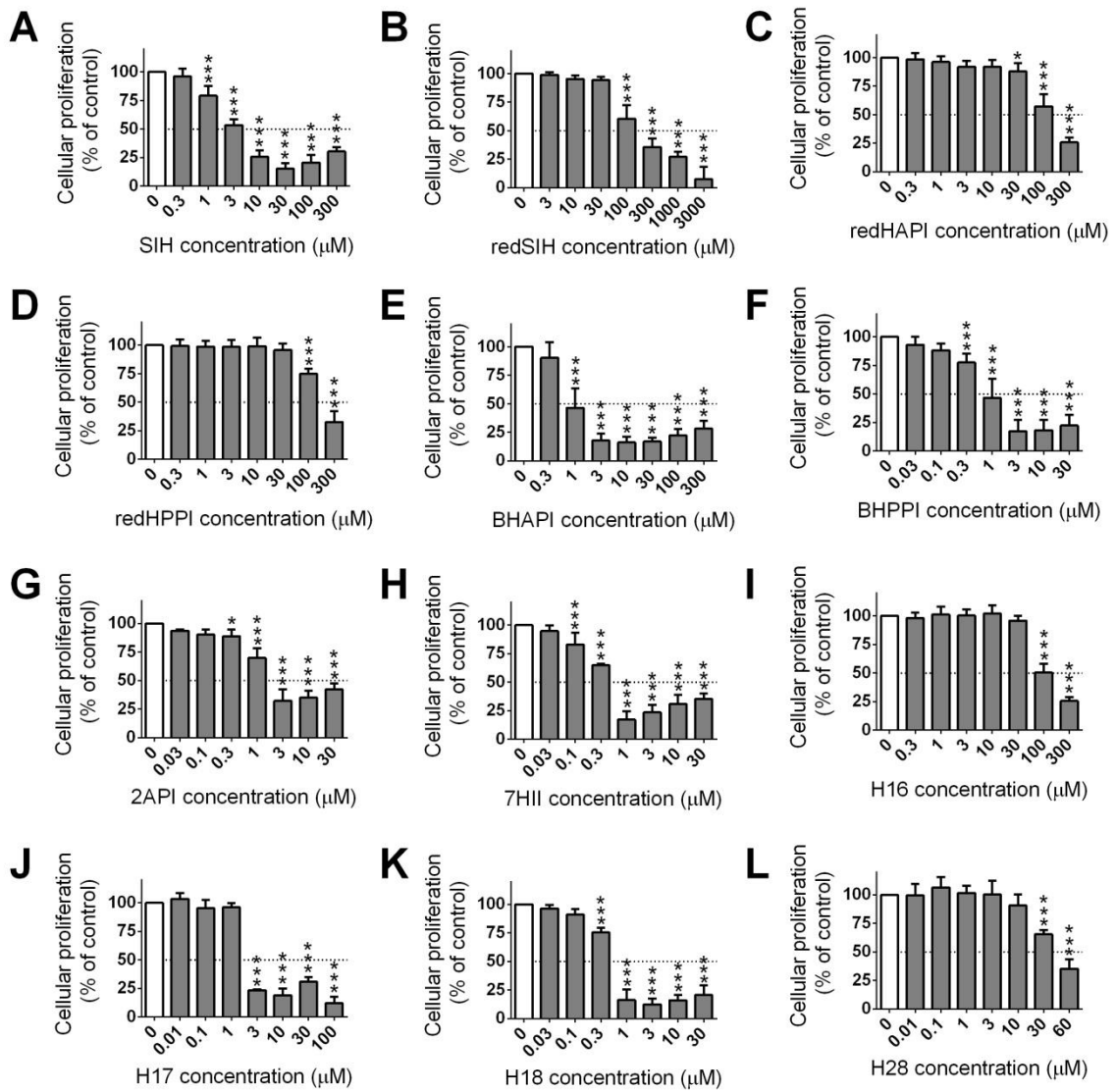


Figure 7



Příloha III

Potůčková E, Jansová H, Macháček M, Vávrová A, Hašková P, Tichotová T, Richardson V, Kalinowski DS, Richardson DR, Šimůnek T. Quantitative analysis of the anti-proliferative activity of combinations of selected iron-chelating agents and clinically used anti-neoplastic drugs. *PLoS One*. 2014; **9**(2): e88754. IF₂₀₁₂ = 3,730

Příloha IV

Serda M, Kalinowski DS, Rasko N, Potůčková E, Mrozek-Wilczkiewicz A, Musiol R, Małecki JG, Sajewicz M, Ratuszna A, Muchowicz A, Gołąb J, Šimůnek T, Richardson DR, Polanski J. Exploring the anti-cancer activity of novel thiosemicarbazones generated through the combination of retro-fragments.

Exploring the anti-cancer activity of novel thiosemicarbazones generated through the combination of retro-fragments

Maciej Serda^{1†}, Danuta S. Kalinowski^{2†}, Nathalie Rasko², Eliška Potůčková³, Anna Mrozek-Wilczkiewicz⁴, Robert Musiol¹, Jan G. Małecki¹, Mieczysław Sajewicz¹, Alicja Ratuszna⁴, Angelika Muchowicz⁵, Jakub Gołąb^{5,6}, Tomáš Šimůnek³, Des R. Richardson^{2*}, Jarosław Polanski^{1*}

¹*Institute of Chemistry, University of Silesia, PL-40-006 Katowice, Poland*

²*Department of Pathology and Bosch Institute, University of Sydney, Sydney, New South Wales 2006, Australia*

³*Department of Biochemical Sciences, Charles University in Prague, Faculty of Pharmacy in Hradec Králové, Czech Republic*

⁴*A.Chełkowski Institute of Physics and Silesian Interdisciplinary Centre for Education and Research, University of Silesia, PL-40-007 Katowice, Poland*

⁵*Department of Immunology, Medical University of Warsaw, PL-02-097 Warsaw, Poland*

⁶*Institute of Physical Chemistry, Polish Academy of Sciences, Department 3, PL-01-224 Warsaw, Poland.*

[†] *M.S. and D.S.K. contributed as equal first authors.*

*e-mail: polanski@us.edu.pl

Short title: Anti-cancer activity of novel thiosemicarbazones

Abstract

Thiosemicarbazones (TSCs) are an exciting class of chelators that show a diverse range of biological activity, including anti-fungal, anti-viral and anti-cancer effects. Our previous studies have demonstrated the potent *in vivo* anti-tumor activity of novel TSCs and their ability to overcome resistance to clinically used chemotherapeutics. In the current study, several novel classes of TSCs were designed using a combination of retro-fragments that appear in other TSC precursors. Additionally, di-substitution at the terminal N4 atom, which was previously identified to be critical for potent anti-cancer activity, was preserved through the incorporation of an N4-based piperazine or morpholine ring. The anti-proliferative activity of the novel TSCs were examined in a variety of cancer and normal cell-types. In particular, compounds **1d** and **3c** demonstrated the greatest promise as anti-cancer agents with potent and selective anti-proliferative effects. Structure-activity relationship studies revealed that the chelators that utilized “soft” donor atoms, such as nitrogen and sulfur, resulted in potent anti-cancer activity. Indeed, the *N,N,S* donor atom set was crucial for the formation of redox active iron complexes that were able to mediate the oxidation of ascorbate. This further highlights the important role of ROS generation in mediating potent anti-cancer effects. Significantly, this study identified the potent and selective anti-cancer activity of **1d** and **3c** that warrant further examination.

1. Introduction

Iron is an essential element that is necessary for a number of cellular processes, such as cellular proliferation [1,2,3]. In fact, the iron-containing enzyme, ribonucleotide reductase, is involved in the rate-limiting step of DNA synthesis and is responsible for the conversion of ribonucleotides to their deoxyribonucleotide counterparts [4,5]. Importantly, alterations in the iron metabolism of cancer cells relative to their normal counterparts have highlighted the potential of iron chelation therapy to act as a novel treatment avenue. Cancer cells demonstrate a higher requirement for iron than normal cells and this is emphasized by the increased expression of the transferrin receptor 1 (TfR1), that takes up iron from the iron transport protein, transferrin (Tf), on the cell surface [6,7,8]. Additionally, the expression of iron-dependent ribonucleotide reductase is markedly higher in tumor cells than normal cells [9]. These factors render tumor cells more sensitive to iron chelation.

Although iron chelators (e.g., desferrioxamine; DFO) have been clinically applied for the treatment of iron overload disease [1,3], novel thiosemicarbazone (TSC) chelators have been widely investigated as potential anti-cancer agents [10,11,12,13,14,15,16,17,18,19,20,21]. Although the molecular mechanisms involved in the activity of TSCs have not been completely elucidated, a number of modes of action have been reported [3,15,21,22,23]. This includes: (1) the inhibition of cellular iron uptake from Tf [10,13,18]; (2) the mobilization of iron from cells [10,13,18]; (3) the inhibition of the ribonucleotide reductase activity [24,25]; (4) the up-regulation of the metastasis suppressor protein, N-myc downstream regulated gene 1 [26,27,28,29]; and (5) the formation redox active metal complexes that produce reactive oxygen species (ROS) [10,15,21,23,30]. This latter mechanism is significant, especially as studies have demonstrated the important role of ROS generation in increasing the activity of chelators against tumor cells [10,15,21].

The TSC, 3-aminopyridine-2-carboxaldehyde thiosemicarbazone (Triapine®; Fig. 1), has been examined in >20 Phase I and II clinical trials as a novel cancer chemotherapeutic [11,31,32,33,34,35,36,37,38,39,40,41]. Although clinical trials using Triapine® have generally demonstrated limited anti-tumor activity [36,37,38,40], other studies show positive results in locally advanced cervical and vaginal cancers when co-administered with cisplatin and radiochemotherapy [33,34]. Notable side effects observed upon Triapine® administration include methemoglobin formation and hypoxia

[35,39,41] and has necessitated the development of other selective TSCs with potent anti-cancer activity.

Several classes of TSCs have been developed as potential anti-proliferative agents (Fig. 1), a number of which show potent and selective anti-tumor activity both in vitro [10,15,21,42] and in vivo [12,21,26,42]. For example, a five day treatment of mice with di-2-pyridylketone 4,4-dimethyl-3-thiosemicarbazone (Dp44mT; Fig. 1) at 0.4 mg/kg reduced the growth of a murine M109 lung carcinoma to 47% of the control [21]. Additionally, Dp44mT showed potent and selective anti-tumor activity in vitro and in vivo against human tumor xenografts [42] and was able form redox active metal complexes that generate reactive oxygen species (ROS) [15,21,30]. Although this TSC demonstrated great potential, it demonstrated cardiac fibrosis at high, non-optimal doses [42]. Thus, further investigations into Dp44mT analogs were necessary and have resulted in the development of di-2-pyridylketone 4-cyclohexyl-4-methyl-3-thiosemicarbazone (DpC; Fig. 1) [12,26]. DpC has demonstrated selective in vitro and in vivo anti-tumor activity by both the intravenous [26] and oral routes [12] and is currently being prepared for clinical trials. Recently, other TSCs have also been shown to have a novel application as photodynamic therapy enhancers [43].

We have previously examined a variety of quinolone-based TSCs that demonstrate in vitro anti-proliferative activity [16]. In the current study, we synthesized 6 series of novel hybrid TSCs that were designed by the combination of TSC fragments present in previously reported analogs [16,44]. Previous studies indicated that di-substitution at the terminal (N4) nitrogen is crucial for modulating anti-cancer activity [12,21]. In the presented study, we have preserved di-substitution at the N4 atom through the construction of an N4-based piperazine or morpholine ring, a fragment that is known in several active TSCs [45,46]. The anti-proliferative activity and selectivity of these novel TSCs was examined in vitro against human cancer cell-types and normal human dermal fibroblast (NHDF) cells. Those series that demonstrated the ability to form redox active iron complexes and mediate the oxidation of ascorbate showed potent anti-proliferative activity, highlighting the importance of ROS formation in their anti-cancer activity.

2. Materials and Methods

The reagents were purchased from Sigma-Aldrich (St. Louis, MO, USA), ACROS Organics (Belgium) or Princeton Chemicals Ltd (Luton, Bedfordshire, UK). Silica gel 60, 0.040-0.063 mm (Merck, Darmstadt, Germany) was used for column chromatography. Thin layer chromatography (TLC) experiments were performed on alumina-backed silica gel 40 F₂₅₄ plates (Merck). The plates were illuminated under UV (254 nm) and evaluated in iodine vapor. The melting points were determined on Optimelt MPA100 instrument (SRS, USA) and are uncorrected. High resolution-mass spectrometry (HRMS) analysis was performed for all new compounds on a Finnigan MAT95 spectrometer (Thermo Fisher Scientific, Bremen, Germany) or on Mariner ESI-TOF spectrometer (Applied Biosystems, USA). The purity for all novel compounds was determined using a Gynkotek HPLC Modular System equipped with a DAAD detector UVD340U at 250 nm.

All ¹H- and ¹³C-NMR spectra were recorded on a Bruker AM-400 spectrometer (399.95 MHz for ¹H; 99.99 MHz for ¹³C; BrukerBioSpin Corp., Germany). Chemical shifts are reported in ppm against the internal standard, Si(CH₃)₄. Easily exchangeable signals were omitted when diffuse. Syntheses were performed on a CEM-DISCOVERY microwave reactor (CEM Corporation, Matthews, NC, USA) with temperature and pressure control.

Log*P*_{calc} values were calculated using ChemDraw 12 (Perkin-Elmer, Waltham, MA, USA) by obtaining the Crippen's fragmentation [47], Viswanadhan's fragmentation [48] and Broto's method [49] data and calculating the average log*P*_{calc}.

2.1. Synthesis of Thiosemicarbazide Precursors (a-f)

2.1.1. General method I (Scheme 1)

N-alkyl or *N*-aryl piperazine (6 mmol) was added to a solution of 1,1'-thiocarbonyldiimidazole (6 mmol; 1.068 g) in 25 mL of dichloromethane and the reaction mixture was stirred for 24 h at room temperature. The organic solvent was separated and extracted 3 times using water, then dried over anhydrous magnesium sulfate, filtered and concentrated to provide the crude piperazine derivatives. These crude products were used in the next step without further purification. These intermediates were added to a solution of hydrazine hydrate in 25 mL of ethanol at

room temperature. The reaction mixture was refluxed for 3 h and cooled to obtain a white precipitate which was collected *via* filtration as the final product. All obtained thiosemicarbazides were crystallized from methanol. See Supporting Information for structural characterization details.

2.1.2. General method II (Scheme 2)

Carbon disulfide (CS₂) (0.2 mol, 12.06 mL) was added dropwise over 15 min to *N*-methylcyclohexylamine (0.2 mol, 26.3 mL) in NaOH solution (0.8 M, 250 mL). The reaction mixture was intensively stirred for 20 min and then sodium chloroacetate (0.2 mol) was added to the solution and was allowed to stir for 15 h. Concentrated HCl (20 mL) was triturated to give the carboxymethylthiocarbamate intermediate as a white precipitate. The obtained carboxymethylthiocarbamate intermediate (0.08 mol) was reacted with hydrazine hydrate (0.08 mol) in water (10 mL). This reaction mixture was gently refluxed for 2 h to give white crystals of the thiosemicarbazide. The final product was crystallized from methanol-water (1/1, v/v).

2.2. Preparation of TSC Derivatives (Scheme 3)

The heteroaromatic thiosemicarbazones analogs were synthesized by reacting the respective heteroaromatic ketone or carbaldehyde and thiosemicarbazide under microwave irradiation. Equimolar quantities of the appropriate thiosemicarbazide (0.5 mmol) and carbonyl compound (0.5 mmol) were dissolved in 4 mL of EtOH with the addition of 0.1 mL of acetic acid as catalyst. The resulting mixture was heated in a microwave reactor at 83°C/30 min (max. microwave power 50 W). After cooling, the precipitated solid was filtered and washed with ether. The final product was purified using a simple crystallization (from ethanol or methanol) or column chromatography. See Supporting Information for structural characterization details.

2.3. HPLC Purity Data

The final purity of the thiosemicarbazones was determined using the following general conditions: HPLC Gynkotek; Pump T580; Autosampler GINA50; Detector DAAD UVD340U; Column: Hilic Kinetex 100A, Phenomenex; Flow: 0.5 mL/min (0-1

min), 0.5-1.2 mL/min (1-3 min), 1.2 mL/min (3-7 min), 1.2-0.5 mL/min (7-8 min), 90% CH₂Cl₂, 10% CH₃OH; UV at 250 nm; Software: Chromeleon.

2.4. Cell Culture

The human cancer cell types (neuroepithelioma (SK-N-MC), colon cancer (HCT116 with wild-type (p53^{+/+}) and null (p53^{-/-}) p53), Burkitt's lymphoma (Raji) and cervical carcinoma (HeLa)) and normal human dermal fibroblast (NHDF) were obtained from the American Type Culture Collection (ATCC).

The SK-N-MC cells were cultured in minimum essential medium (MEM; Gibco) containing 10% (v/v) Fetal Bovine Serum (FBS), 1 mM sodium pyruvate (Gibco), 1% (v/v) non-essential amino acids (Gibco), 2 mM L-glutamine (Gibco), 100 U/mL penicillin (Gibco), 100 µg/mL streptomycin (Gibco) and 0.28 µg/mL fungizone (Squibb Pharmaceuticals). The HCT116 and NHDF cells were grown in Dulbecco's modified Eagle's medium (DMEM; Sigma) supplemented with 12% (v/v) heat-inactivated FBS (HCT116; Gibco) and 15% (v/v) FBS (NHDF; Gibco), 100 µg/mL of gentamicin (Polfa), 100 µg/mL of streptomycin (Polfa) and 100 U/mL of penicillin (Polfa). The Raji and HeLa cells were cultured in Roswell Park Memorial Institute medium (RPMI-1640; Sigma) with the addition of 10% (v/v) heat-inactivated FBS (Invitrogen) and an antibiotic/antimycotic solution (Sigma). All cell lines were cultured under standard conditions at 37°C in a humidified atmosphere at 5% CO₂ and were passaged every 3-4 days as required.

2.5. Proliferation Assay

The cells were seeded in 96-well plates (SK-N-MC: 1.5 x 10⁴ cells/well; HeLa: 5.0 x 10³ cells/well; Raji: 3.0 x 10³ cells/well; HCT116: 3.5 x 10³ cells/well; NHDF: 3.0 x 10³ cells/well) 24 h prior to the addition of the novel compounds. The assays were performed following a 96 h (HCT 116, NHDF) or 72 h (SK-N-MC, Raji, HeLa) incubation with varying concentrations of the agents. Additionally, DFO and Dp44mT were included as positive controls. Chelator stock solutions were prepared in DMSO and diluted in media so that the final [DMSO] < 0.05%. The results were expressed as a percentage of the control and the resulting IC₅₀ values were calculated (using GraphPad Prism 5). The IC₅₀ was defined as the concentration necessary to reduce the absorbance

to 50% of the untreated control. Each individual compound was tested in triplicate in a single experiment, with each experiment being repeated three times. After incubation of HCT 116 and NHDF cells with the tested compounds, 20 μL of the CellTiter 96[®] AQueous One Solution - MTS (Promega) solution was added to each well (with 100 μL of DMEM without phenol red) and incubated for 1 h at 37°C. The optical density of the samples were analyzed at 490 nm. MTT (3-[4,5-dimethylthiazol-2-yl]-2,5-diphenyltetrazolium bromide) was used to evaluate their anti-proliferative effects in SK-N-MC and Raji cells. Following the incubation with the investigated compounds, 10 μL of MTT (5 mg/mL in PBS; Sigma) was added to each well. After a 2 (SK-N-MC) or 4 h (Raji) incubation, the plates were centrifuged, and the cells were lysed with 100 μL of 10% SDS-50% isobutanol in 0.01 M HCl (SK-N-MC) or DMSO (Raji). The absorbance was measured at 570 nm. The anti-proliferative effects of these novel agents on HeLa cells were estimated using crystal violet staining (0.5% crystal violet solution for 10 min). Finally, the wells were rinsed with water and the cells were lysed with 2% SDS. The optical density of the samples were analyzed at 595 nm.

2.6. Labeling of Transferrin with ⁵⁹Fe

The iron transport protein, Tf (Sigma), was labeled with ⁵⁹Fe (PerkinElmer Life and Analytical Sciences, Boston, MA) to form ⁵⁹Fe₂-Tf using standard methods [6,7]. Unbound ⁵⁹Fe was removed by passage through a Sephadex G25 column and was followed by exhaustive dialysis [6,7].

2.6.1. Effect of the Chelators on Mobilizing Cellular ⁵⁹Fe

To examine the ability of the novel chelators to mobilize ⁵⁹Fe from SK-N-MC cells, ⁵⁹Fe efflux experiments were performed using established techniques [50,51]. The monolayer of SK-N-MC cells was prelabeled for 3 h at 37°C in MEM containing ⁵⁹Fe₂-Tf (0.75 μM). Cells were then washed four times with ice-cold PBS and incubated for a further 3 h at 37°C with medium alone (the control) or medium containing the chelator (25 μM). After this incubation, the overlying medium that contained the released ⁵⁹Fe was separated from the cells using a Pasteur pipette. Radioactivity was measured in both the cells and supernatant using a γ -scintillation counter (Wallac Wizard 3, Turku, Finland). In these studies, the novel ligands were compared to the previously

characterized chelators, DFO and Dp44mT, as their ability to mobilize cellular ^{59}Fe has been extensively examined in these cells [10,12,17,18,51].

2.6.2. Effect of Chelators at Preventing Cellular ^{59}Fe Uptake

The ability of the chelators to prevent the cellular uptake of ^{59}Fe from $^{59}\text{Fe}_2\text{-Tf}$ was examined using standard methods [10,14,17,18,51]. A monolayer of SK-N-MC cells was incubated with medium containing $^{59}\text{Fe}_2\text{-Tf}$ (0.75 μM) and the chelator (25 μM) for 3 h at 37°C. The medium was then removed and the cells were washed four times with ice-cold PBS. The cells were then incubated for 30 min at 4°C with the general protease, Pronase (1 mg/mL; Sigma), to remove membrane-bound ^{59}Fe . The cells were removed using a plastic spatula and centrifuged at 14000 rpm/1 min to separate internalized from membrane-bound ^{59}Fe . The cell pellet was resuspended in 1 mL of PBS and the internalized ^{59}Fe was measured on a γ -scintillation counter. Internalized ^{59}Fe uptake was calculated as a percentage of the control (medium alone). Again, the novel ligands were compared to DFO and Dp44mT as their ability to inhibit cellular ^{59}Fe uptake has been extensively characterized in these cells [10,14,17,18,51].

2.7. Ascorbate Oxidation Assay

The ability of the iron complexes of the novel ligands to mediate the oxidation of the physiological substrate, ascorbate, was examined using established methods [10,18,22,52,53]. Ascorbic acid (100 μM) was prepared immediately prior to each experiment and was incubated in the presence of Fe^{III} (10 μM ; as FeCl_3), the chelator (1–60 μM) and a 50-fold molar excess of citrate (500 μM). The absorbance at 265 nm was measured after 10 and 40 min and the difference in absorbance at these time points was calculated. The results of these experiments were expressed as iron-binding equivalents (IBE) due to the different denticity of the chelators examined. The chelators, Dp44mT, DFO and ethylenediaminetetraacetic acid (EDTA) were used as controls as the ability of their iron complexes to oxidize ascorbate has been previously examined [10,15,52,53].

2.8. Statistical Analysis

Data was expressed as mean \pm S.D. of at least 3 experiments. Statistical analyses were performed using Prism v6 (GraphPad Software, Inc., La Jolla, CA) implementing a one-way ANOVA.

3. Results and Discussion

3.1. Drug Design

Upon comparison of compounds that have become pharmaceuticals relative to those that have failed during drug development, molecular properties such as molecular weight (MW) and $\text{Log}P_{\text{calc}}$ (calculated octanol-water partition coefficient) have been revealed to be key factors in the attrition of drug candidates [54,55]. In general, the average MW and $\text{Log}P_{\text{calc}}$ of successful drugs that are launched on the market are 300–450 Da and 2–4, respectively [56,57]. Thus, the challenge for successful drug discovery lies in balancing these properties [54]. With this in mind, Triapine[®] (MW: 195 Da; $\text{Log}P_{\text{calc}}$: 0.761) represents an interesting lead molecule with a considerable reserve in MW and $\text{Log}P_{\text{calc}}$ for modification. Similarly, highly active TSCs that maintain their MW and $\text{Log}P_{\text{calc}}$ below 450 Da and 4.5, respectively, also have substantial promise as drug candidates.

Identifying functional fragments for drug design is a complex problem that involves a variety of different approaches, including both an experimental and theoretical basis. The latter can consist of a variety of methods among which are those that attempt to identify advantageous substructures, scaffolds and/or linkers on the basis of previously reported active compounds. Alternatively, the fragmentation of organic molecules into smaller moieties is an important method in retrosynthetic analysis and has inspired a variety of pseudo-retrosynthetic approaches [58]. This has identified fragments that may be useful for drug design. For example, the di-2-pyridyl [12,15,21,59], quinolinyl [60], piperazinyl [60,61,62], morpholinyl [63] and quinoxalinyl [64] motifs are common fragments in other anti-cancer agents, which we currently incorporated into the design of our novel TSCs.

In the current study, the main rationale underlying our approach was that the newly synthesized TSCs would preserve the potent anti-cancer activity of their TSC precursors, while retaining appropriate MW and $\text{Log}P_{\text{calc}}$ values to show substantial promise as drug candidates for pharmaceutical development. We used a combination of retro-fragments that appear in other TSC precursors [15,16,21,44,59] and other anti-cancer agents [60,61,62,63,64]. Additionally, di-substitution at the terminal N4 atom was preserved through the construction of an N4-based piperazine or morpholine ring

(Scheme 4), a moiety that is observed in several active TSCs [45,46]. Although the novel TSCs containing piperazine or morpholine fragments have higher MW and $\text{Log}P_{\text{calc}}$ values than their precursors, these properties still lie within the optimal values for these parameters that is MW and $\text{Log}P_{\text{calc}}$ below 450 Da and 4.5, respectively.

3.2. Synthesis of Novel Ligands

The thiosemicarbazide precursors, **a-f** (Scheme 4), were synthesized from commercially available reagents in a two-step process that gave moderate to high yields (47–95%). The treatment of bis(imidazole)thioketone with the appropriate piperazine, followed by the reaction with hydrazine hydrate gave the *N*-substituted piperazine-based thiosemicarbazides in a high yield (Supporting Information). The final thiosemicarbazone series, **1-6** (Scheme 4), were synthesized in moderate to high yield (58–96%) by Schiff-base condensation of the appropriate ketone/aldehyde with the prepared thiosemicarbazides. The purity of the thiosemicarbazones was confirmed by HPLC and were >95% (Supporting Information).

3.3. Anti-Proliferative Activity of the Novel Thiosemicarbazones Against a Variety of Cancer Cell-Types

The ability of the novel thiosemicarbazone series **1-6** to inhibit the cellular proliferation of tumor cells was examined in a variety of cancer cell-types (Table 1), including human p53 wild-type and null colon cancer (HCT116 p53^{+/+} and HCT116 p53^{-/-}, respectively), Burkitt's lymphoma (Raji), human cervical carcinoma (HeLa) and neuroepithelioma (SK-N-MC) cancer cells. The ability of these novel agents to selectively target cancer cells was assessed by examining their effects on the cellular proliferation of a mortal cell-type, namely normal human dermal fibroblast (NHDF) cells. The effects of these novel ligands were compared to the following chelators that were used as positive controls: (1) DFO, that is clinically used for iron overload disease [1,3] and (2) Dp44mT, a chelator with potent anti-proliferative activity *in vitro* and *in vivo* [15,21].

As expected, the control chelator, DFO, demonstrated poor anti-proliferative effects in all cancer and normal cell-types, with IC_{50} values ranging between 4.74 to >25 μM (Table 1). In contrast, Dp44mT showed selective and potent anti-cancer

activity with IC_{50} values of 0.002–0.04 μM , but was markedly less effective in mortal NHDF cells (IC_{50} : 15.38 μM ; Table 1).

The p53 protein, which acts as a tumor suppressor and regulates processes such as DNA repair and cell cycle control, is lost in >50% of human cancers [65]. Furthermore, a lack of p53 expression in some cancers aids the progression of tumor cells and promotes resistance against chemotherapeutics [66]. The development of agents that target both with wild-type and null p53 tumors are vital, particularly considering the high prevalence of p53 mutations in advanced cancers [42,67]. Thus, we examined the anti-proliferative activity of the novel TSC series **1–6** against human HCT116 p53^{+/+} and HCT116 p53^{-/-} colon cancer cells (Table 1) after a 96 h incubation. Importantly, the anti-proliferative effects of the novel TSCs showed the same general pattern of activity against HCT116 p53^{+/+} and HCT116 p53^{-/-} cells, irrespective of p53 status (Table 1). This is in agreement with our previous studies that demonstrated that the anti-proliferative activity of other closely-related TSCs was independent of p53 status [16].

Of all the series of TSCs synthesized in this study, those analogs derived from di-2-pyridyl (**1a–e**) demonstrated the most potent anti-proliferative activity in HCT116 p53^{+/+} and p53^{-/-} cells, resulting in IC_{50} values ranging from 0.0008–0.04 μM (Table 1). While the analogs derived from quinolin-2-yl (**2a–f**) and 8-hydroxyquinolin-2-yl (**3a–f**) demonstrated moderate anti-proliferative effects (IC_{50} : 0.026–3.55 and 0.004–9.25 μM , respectively). Those chelators derived from the 7-hydroxyquinolin-8-yl (**4a–f**), quinoxalin-2-yl (**5a–f**) and salicylic (**6a–f**) moieties showed poor anti-cancer activity (IC_{50} : 1.02 – >25 μM) in HCT116 p53^{+/+} and p53^{-/-} cells (Table 1).

A similar trend in the anti-proliferative activity of the novel TSCs was observed in Raji, HeLa and SK-N-MC cells after a 72 h incubation (Table 1). Those chelators containing the di-2-pyridyl moiety (**1a–e**) were the most potent anti-cancer (IC_{50} : 0.003–2.21 μM) analogs examined. Similarly to the HCT116 data, compounds from series **2** generally displayed moderate anti-proliferative activity (IC_{50} : 0.04–5.14 μM) in Raji, HeLa and SK-N-MC cells, while series **3**, **4**, **5** and **6** generally showed moderate to poor anti-cancer effects (Table 1).

No correlation was evident between the anti-cancer activity of the ligands and their $\log P_{\text{calc}}$ values, suggesting that other factors besides their ability to transverse the cellular membrane were critical in their anti-proliferative effects.

3.4. Anti-Proliferative Activity of the Novel Thiosemicarbazones Against Normal Cells

Importantly, the selectivity of the novel TSCs was examined in mortal cells, namely NHDF cells, after a 96 h incubation. Of all the analogs examined, **1b**, **1d**, **2b**, **2f** and **3c** showed the greatest anti-proliferative activity in the majority of cancer cell-types (Table 1). Thus, to examine the selectivity of the 5 best TSCs identified above, namely **1b**, **1d**, **2b**, **2f** and **3c**, a therapeutic index was calculated by dividing the NHDF cell IC_{50} by the IC_{50} of the neoplastic HCT116 p53^{+/+} or HCT116 p53^{-/-} cell-types (Table 2). Notably, the selectivity index of Dp44mT comparing NHDFs to HCT116 p53^{+/+} or HCT116 p53^{-/-} cell-types was marked, being 7690 and 3076, respectively.

Of the 5 most potent anti-cancer TSCs described herein, the greatest therapeutic indices were identified for **1d** and **3c** and were 18-2650, respectively (Table 2). Compounds **1d** and **3c** showed potent anti-cancer activity (IC_{50} : 0.002–0.017 μ M) in HCT116 cells, but their anti-proliferative activity was greatly reduced in NHDF cells (IC_{50} : 0.16–10.6 μ M).

In contrast, analogs **1b**, **2b** and **2f** demonstrated poor selectivity with IC_{50} values of 0.0008–0.09 μ M in HCT116 cells and 0.0017–0.03 μ M in mortal NHDF cells (Table 1). In fact, compounds **2b** and **2f** generally showed greater anti-proliferative effects in mortal NHDF cells relative to HCT116 cells, resulting in therapeutic indices of 0.4–0.8 (Table 2). Compound **1b** demonstrated limited selectivity and resulted in a therapeutic index of 2 in mortal NHDF cells relative to HCT116 cells. Hence, of all the analogs examined, compounds **1d** and **3c** demonstrated the greatest promise as anti-cancer agents with potent and selective anti-proliferative effects.

3.5. Ability of Novel Thiosemicarbazones to Mobilize Cellular ⁵⁹Fe

As the ability of chelators to bind cellular iron can play a role in their anti-proliferative effects [51], we examined the ability of these novel ligands (25 μ M) to mobilize cellular ⁵⁹Fe from prelabeled SK-N-MC cells (Fig. 2). The chelator-mediated release of intracellular ⁵⁹Fe was compared to the positive controls, DFO and Dp44mT (Fig. 2), as their ability to mobilize ⁵⁹Fe has been extensively characterized in these cells [10,17,18,52,53]. As previously observed [10,17,18,52,53], the control medium

alone resulted in the release of very little ^{59}Fe , namely $4 \pm 1\%$ of cellular ^{59}Fe (Fig. 2). The chelators, DFO and Dp44mT, significantly ($p < 0.001$) increased the mobilization of cellular ^{59}Fe to 11 ± 2 and $35 \pm 2\%$, respectively, relative to the control medium (Fig. 2).

Compounds of series **1**, **3**, **4** and **6** generally displayed high efficacy at mobilizing cellular ^{59}Fe (Fig. 2). In particular, the ligands, **1c**, **1e**, **3b-3f**, **4c**, and **6b-6f** all demonstrated comparable ^{59}Fe mobilization efficacy to that of Dp44mT, resulting in the efflux of 31-39% of cellular ^{59}Fe . Apart from **1b**, all ligands of series **1**, **3**, **4** and **6** were significantly ($p < 0.001$) more effective than DFO in mediating the release of cellular ^{59}Fe . Interestingly, ligands of series **1** and **4** demonstrated a similar pattern in terms of their ability to mobilize cellular ^{59}Fe (Fig. 2A,D). For example, ligands of series **1** and **4** containing the more hydrophilic fragments, **a**, **c** and **e**, showed increased efficacy at mobilizing cellular ^{59}Fe relative to those containing the more lipophilic fragments **b**, **d** and **f** (Fig. 2A,D). Of all the ligands examined, chelators of series **3** and **6** demonstrated the greatest efficacy as ^{59}Fe mobilization agents, mediating the release of 25-39% of cellular ^{59}Fe (Fig. 2C,F).

In contrast, the series based on quinolin-2-yl (**2**) and quinoxalin-2-yl (**5**) generally demonstrated poor ability to mobilize cellular ^{59}Fe and resulted in the release of 5-28% of cellular ^{59}Fe (Fig. 2B,E). All ligands of series **2** and **5** were significantly ($p < 0.001$) less effective than Dp44mT in mediating the release of cellular ^{59}Fe . In fact, ligand **2a** demonstrated comparable ^{59}Fe mobilization efficacy to that of the control medium (Fig. 2B), while **2b**, **2d**, **2f** and **5f** showed comparable release of ^{59}Fe relative to DFO (Fig. 2B,E).

Importantly, a strong correlation ($R^2 = 0.911$) between $\log P_{\text{calc}}$ and ^{59}Fe mobilization efficacy was only observed for ligands of series **1**, suggesting that their lipophilic/hydrophilic balance played a role in their ability to permeate the cellular membrane to reach intracellular ^{59}Fe . Interestingly, the more hydrophobic ligands of series **1** were less effective than their more hydrophilic counterparts, suggesting that the more hydrophobic ligands or their resultant ^{59}Fe complexes were sequestered in cellular membranes. No correlation was observed between the anti-proliferative activity of these novel ligands and their ability to mobilize cellular ^{59}Fe in SK-N-MC cells, indicating that other factors besides ^{59}Fe mobilization were responsible for their anti-cancer effects.

3.6. Ability of Novel Thiosemicarbazones to Inhibit the Cellular Uptake of ^{59}Fe from $^{59}\text{Fe}_2\text{-Tf}$

The anti-proliferative activity and iron chelation efficacy of a ligand is dependent not only on its ability to mobilize cellular iron, but also on its ability to prevent the cellular uptake of iron from $\text{Fe}_2\text{-Tf}$ [51]. Thus, the ability of the novel ligands (25 μM) to inhibit the cellular uptake of ^{59}Fe from $^{59}\text{Fe}_2\text{-Tf}$ was assessed in SK-N-MC cells (Fig. 3), as the ability of iron chelators to inhibit ^{59}Fe uptake in these cells is well characterized [10,14,52,53]. As utilized in the ^{59}Fe efflux experiments, the chelators, DFO and Dp44mT, were included as positive controls as their ability to inhibit ^{59}Fe from $^{59}\text{Fe}_2\text{-Tf}$ has been extensively assessed [10,14,17,18,51,52,53]. The results were expressed as a percentage of the ^{59}Fe uptake observed with control medium (Fig. 3).

Although DFO was able to significantly ($p < 0.001$) inhibit ^{59}Fe uptake from $^{59}\text{Fe}_2\text{-Tf}$ relative to the control, it only reduced ^{59}Fe uptake to 83% of the control medium (Fig. 3). In contrast, Dp44mT significantly ($p < 0.001$) and markedly prevented the uptake of ^{59}Fe , reducing it to 6% of the control (Fig. 3), as previously observed [10,52].

In general, those analogs that displayed high efficacy at mobilizing cellular ^{59}Fe (Fig. 2) also potently inhibited the cellular uptake of ^{59}Fe from $^{59}\text{Fe}_2\text{-Tf}$ (Fig. 3), with a linear correlation ($R^2 = 0.81$) evident between these 2 factors. Generally, the ligands of series **1**, **3**, **4** and **6** potently inhibited the uptake of ^{59}Fe from $^{59}\text{Fe}_2\text{-Tf}$ and were significantly ($p < 0.001$) more effective than DFO (Fig. 3A,C,D,F). In fact, the ligands, **1c**, **3f**, **5c**, **6c** and **6f** demonstrated comparable inhibition of cellular ^{59}Fe uptake to that of Dp44mT, resulting in 3.6-11.5% of cellular ^{59}Fe uptake relative to the control (Fig. 3). Interestingly, those ligands containing the more hydrophilic fragment, **c**, were generally the most effective chelators of each series (Fig. 3).

Similarly to the ^{59}Fe efflux experiments, those ligands based on the quinolin-2-yl (**2**) and quinoxalin-2-yl (**5**) moieties generally showed poor ability to prevent the uptake of ^{59}Fe from $^{59}\text{Fe}_2\text{-Tf}$ (Fig. 3B,E). Indeed, compound **2a** showed comparable ability to inhibit ^{59}Fe uptake to the control medium, while compounds **2d**, **2f** and **5f** demonstrated comparable inhibition of ^{59}Fe uptake to that of DFO (Fig. 3B,E). All analogs of series **2**

and **5**, except **5c**, were significantly ($p < 0.001$) less effective than Dp44mT at inhibiting cellular ^{59}Fe uptake.

No strong structure-activity relationships were observed between the ability of the ligands to prevent cellular ^{59}Fe uptake and $\log P_{\text{calc}}$ or anti-proliferative activity in SK-N-MC cells, suggesting other factors besides inhibition of ^{59}Fe uptake played a role in their anti-cancer activity.

3.7. Ability of the Iron Complexes of Novel Thiosemicarbazone to Mediate the Oxidation of Ascorbate

The ability of the iron complexes of the novel ligands to catalyze the oxidation of the physiological substrate, ascorbate, was important to assess as redox cycling may play an critical role in their anti-proliferative activity [10,15,18,52,53]. Thus, the oxidation of ascorbate mediated by the iron complexes of series **1-6** were examined in comparison to the iron complexes of the control compounds, DFO, EDTA and Dp44mT, as their ability to oxidize ascorbate is well characterized [10,15,52,53,68]. The results were expressed as a percentage of the control (no chelator) at IBEs of 0.1 (excess “free” iron), 1 (iron-chelator complexes with a fully filled coordination sphere) and 3 (excess free chelator), due to the different denticity of the chelators examined (Fig. 4).

As previously observed, the redox-inactive iron complex of DFO resulted in limited ascorbate oxidation (Fig. 4) [15,68]. In fact, the iron complex of DFO acted in a protective manner, significantly ($p < 0.05$) inhibiting the oxidation of ascorbate at IBEs of 1 and 3 to 23% and 47%, respectively, relative to the control (Fig. 4). In contrast, the iron complex of the positive control, EDTA, significantly ($p < 0.001$) increased ascorbate oxidation at IBEs of 0.1, 1 and 3 to 208%, 449% and 936%, respectively, in comparison to the control (Fig. 4). This is in agreement with our previous studies that showed the ability of the iron complex of EDTA to mediate ascorbate oxidation [10,15,52,53]. Additionally, the iron complex of Dp44mT also mediated the oxidation of ascorbate, significantly ($p < 0.01-0.001$) increasing it to 129%, 203% and 196% at IBEs of 0.1, 1 and 3, respectively, relative to the control (Fig. 4), as previously demonstrated [10,15,52,53].

The resultant iron complexes of the ligands of series **1** and **2** generally enhanced ascorbate oxidation, with compounds **1b**, **1d**, **1e**, **2a** and **2e** significantly ($p < 0.05-0.001$) increasing the oxidation of ascorbate to 200-265% relative to the control at an IBE of 3 (Fig. 4A,B). In fact, all iron chelator complexes of series **1** and **2**, except for **2f**, showed comparable levels of ascorbate oxidation to that of the iron complex of Dp44mT at an IBE of 3 (Fig 4A,B). These data suggest that the ligands of series 1 and 2 form iron complexes that are redox active.

In contrast, the iron chelator complexes of ligands from series **3**, **4**, **5** and **6** generally did not enhance ascorbate oxidation, with the majority acting in a protective manner (Fig. 4C,D,E,F). Although the iron complexes of **3a** and **5e** mediated significantly ($p < 0.01-0.001$) increased levels of ascorbate oxidation, the majority of the iron complexes of series **3**, **4**, **5** and **6** resulted in comparable ability to catalyze ascorbate oxidation relative to the control at an IBE of 3. In fact, the iron complexes of **5d**, **5f**, **6a**, **6d** and **6f** significantly ($p < 0.05$) decreased levels of ascorbate oxidation relative to the control at an IBE of 3. Additionally, all iron complexes of series **3**, **4**, **5** and **6**, apart from **3a**, **4a**, **4e** and **5e**, mediated comparable levels of ascorbate oxidation to that of DFO at an IBE of 3, resulting in 4-111% of ascorbate oxidation relative to the control (Fig. 4C,D,E,F). Thus, the majority of the iron complexes of series **3**, **4**, **5** and **6** acted in a protective manner, suggesting the formation of redox inactive iron complexes.

3.8. Structure-Activity Relationships Linking Anti-Proliferative Activity, Ascorbate Oxidation and Donor Atom Identity

In the current study, series **1** analogs based on the di-2-pyridyl moiety (Scheme 4) generally demonstrated the greatest anti-proliferative activity of all the series of ligands examined (Table 1). Series **1** ligands, that utilize the *N,N,S* donor atom set, showed high iron chelation efficacy (Figs. 2A,3A) and their iron complexes generally resulted in the increased oxidation of ascorbate (Fig. 4A). This data suggest that the potent anti-proliferative activity of series **1** stemmed from their ability to effectively chelate cellular iron and result in the formation of redox active iron complexes that mediate oxidative damage. This is in agreement with our previous studies on other di-2-pyridyl-based thiosemicarbazones, such as Dp44mT and DpC [12,15], and di-2-pyridyl-

based thiohydrazones [52], which also utilize the *N,N,S* donor atom set and demonstrate potent anti-cancer activity *via* the formation of redox active complexes. The use of “soft” donor atoms, such as nitrogen and sulfur, play a critical role in facilitating reversible Fe^{III/II} redox reactions that are important for potent anti-cancer effects [12,15,52].

The ligands of series **2**, based on the quinolin-2-yl moiety (Scheme 4), also utilized the *N,N,S* donor atom set and their resultant iron complexes generally increased levels of ascorbate oxidation (Fig. 4B). This suggested that, similarly to series **1**, ligands of series **2** may form redox active iron complexes. However, in contrast to series **1**, series **2** compounds demonstrated poor iron chelation efficacy and may be a contributing factor in the moderate anti-proliferative activity observed for series **2** relative to series **1** (Table 1). This is consistent with our previous studies, in which the presence of the quinolin-2-yl moiety in 2-quinolinecarboxaldehyde isonicotinoyl hydrazones [59] and other quinoline-based thiosemicarbazones [16] were found to have poor iron mobilization efficacy and anti-proliferative effects in SK-N-MC cells. Our current data support these previous findings, suggesting that the quinolin-2-yl moiety confers poor anti-proliferative and iron chelation efficacy when the quinoline nitrogen acts as a donor atom [16,59].

Series **3** analogs, that differ from series **2** by the addition of a hydroxy group at position 8 of the quinoline ring (Scheme 4), generally demonstrated moderate to poor anti-proliferative effects (Table 1). In contrast to series **2** that showed poor iron mobilization efficacy and the ability to mediate ascorbate oxidation, series **3** ligands displayed high iron chelation efficacy (Figs. 2C,3C) and their iron complexes generally did not enhance the oxidation of ascorbate (Fig. 4C). In fact, the majority of series **3** iron complexes acted in a protective manner and inhibited ascorbate oxidation (Fig. 4C). It is probable that series **3** ligands can bind iron either in a tridentate manner, using the *N,N,S* donor atom set similarly to series **2**, or in a bidentate system similar to that of the structurally-related chelator, clioquinol [69] that utilizes the quinoline nitrogen and 8-hydroxy oxygen as donor atoms [70]. Due to the contrasting activity of series **3** relative to series **2** with regards to anti-proliferative effects (Table 1), iron chelation efficacy (Figs. 2&3) and ascorbate oxidation (Fig. 4), this suggests that the series **3** analogs may act as bidentate ligands that utilize the 8-hydroxyl oxygen and quinoline nitrogen as donor atoms. Significantly, the use of the “hard” oxygen donor atom in

series **3** may result in the formation of redox inactive iron complexes that cannot oxidize ascorbate and consequently show poor anti-proliferative activity [1,52].

Those ligands based on the 7-hydroxyquinolin-8-yl (series **4**) moiety bind iron in an analogous manner to that of the 2-hydroxynaphthaldehyde thiosemicarbazone [71] or 2-hydroxy-1-naphthaldehyde thiobenzoyl hydrazone (H₂NTBH; [52]) chelators and utilize the *O,N,S* donor atom set [16]. Similarly, those chelators of series **6**, based on the salicylic moiety, also bind iron *via* the *O,N,S* donor atom set in a similar manner to salicylaldehyde thiobenzoyl hydrazone (H₂STBH; [52]). Although the series **4** and **6** analogs demonstrated high iron mobilization efficacy (Figs. 2&3), these ligands showed poor anti-proliferative effects (Table 1) and their iron complexes did not mediate or prevented the oxidation of ascorbate (Fig. 4). This is in agreement with our previous studies in which the *O,N,S*-thiohydrazones, H₂STBH or H₂NTBH, mediated high iron chelation efficacy, but showed poor anti-proliferative activity and the inability of their iron complexes to mediate the oxidation of ascorbate [52]. Importantly, these results suggest that iron complexes of series **4** and **6** ligands cannot mediate the formation of ROS, which greatly reduces their anti-proliferative effects.

The analogs based on quinoxalin-2-yl (**5a-f**) utilize the *N,N,S* donor atoms and differ from series **2** by an additional non-coordinating nitrogen located at position 4 of the quinoline moiety (Scheme 4). This structural modification resulted in a large decrease in anti-proliferative activity of series **5** relative to series **2** (Table 1), although both series showed poor iron mobilization efficacy (Figs. 2&3). Importantly, the iron complexes of series **5** acted in a protective manner and inhibited the oxidation of ascorbate, while iron complexes of series **2** were able to promote ascorbate oxidation (Fig. 4). This further highlights the critical role of the formation of redox active iron complexes in the anti-proliferative of novel thiosemicarbazones [10,15,21,52]. Significantly, our previous studies on methyl pyrazinylketone isonicotinoyl hydrazone (MPIH) analogs demonstrated that the incorporation of a second, non-coordinating, electron-withdrawing nitrogen in the aromatic ring played a major role in the formation of redox-inactive iron complexes that prevented the formation of ROS [53,72]. Similarly to series **5**, the iron complexes of the MPIH series prevented the oxidation of ascorbate [53]. Thus, the replacement of the quinoline moiety of series **2** with the quinoxaline group of series **5** resulted in decreased anti-proliferative activity due to the formation of redox-inactive iron complexes.

3.9. Conclusion

In the current study, several novel classes of TSCs were designed that retained the appropriate MW and $\text{Log}P_{\text{calc}}$ values to show promise as drug candidates for pharmaceutical development. A combination of retro-fragments that appear in other TSC precursors were utilized and di-substitution at the terminal N4 atom was preserved through the incorporation of an N4-based piperazine or morpholine ring. The selectivity and anti-cancer activity of the novel TSCs were examined in a variety of cancer cell-types. In particular, of all the compounds examined, **1d** and **3c** demonstrated the greatest promise as anti-cancer agents with potent and selective anti-proliferative effects. Structure-activity relationship studies revealed that the combination of the donor atoms used, rather than the identity of fragments **a-f**, played a crucial role in their anti-cancer activity. Indeed, the chelators that utilized “soft” donor atoms, such as nitrogen and sulfur, formed redox active iron complexes that were able to mediate the oxidation of ascorbate. This further highlights the important role of ROS generation in mediating potent anti-cancer effects. Significantly, this study identified potent and selective anti-cancer chelators that warrant further *in vivo* examination.

Supporting Information

Chemical characterization of thiosemicarbazides and thiosemicarbazones, X-ray data for selected thiosemicarbazones and thiosemicarbazides, HPLC purity data and isosbestic curves.

Acknowledgment

We appreciated the financial support of TWING and DoktorIS PhD scholarships, NCN (DEC-2011/01/N/NZ4/01166 and N405/068440), and the National Centre for Research and Development, Warsaw (ORGANOMET No: PBS2/A5/40/2014 grants). This work was also supported by a Project Grant from the National Health and Medical Research Council (NHMRC) Australia to DRR [Grant 632778]; and DSK [Grant 1048972]; a NHMRC Senior Principal Research Fellowship to DRR [Grant 571123]; and a Helen and Robert Ellis Fellowship to DSK from the Sydney Medical School Foundation of The University of Sydney. EP and TS also appreciate the support of a Czech Science Foundation Grant [13-15008S].

Author Contributions

Designed the experiments: JP, RM, MS, DSK, EP, TS, DRR; Performed the experiments: AMW, NR, MS, AM, DSK, EP; Analyzed the data: JP, RM, DRR, DSK, JGM, AM, MS, NR, EP; Supervised PhD Students: AR, JP, DRR, JG, DSK, TS; Wrote the paper: JP, JG, RM, MS, AMW, DSK, DRR; Drug design and chemistry: MS, RM, JP; Biology: SK-N-MC cells and ⁵⁹Fe assays: NR, EP, TS, DRR, DSK; HCT 116 and NHDF: AMW, RM, AR, Raji, HeLa: AM, JG; Ascorbate Oxidation assay: EP, TS; X-Ray: JGM, HPLC: MS.

Abbreviations

DFO, desferrioxamine; Dp44mT, di-2-pyridylketone 4,4-dimethyl-3-thiosemicarbazone; DpC, di-2-pyridylketone 4-cyclohexyl-4-methyl-3-thiosemicarbazone; EDTA, ethylenediaminetetraacetic acid; H₂NTBH, 2-hydroxy-1-naphthaldehyde thiobenzoyl hydrazone; H₂STBH, salicylaldehyde thiobenzoyl

hydrazone; HCT116, human colon carcinoma; HeLa, human cervical cancer cells; IBE, iron-binding equivalent; MPIH, methyl pyrazinylketone isonicotinoyl hydrazone; MW, molecular weight; NHDF, human normal dermal fibroblasts; Raji, human Burkitt's lymphoma; ROS, reactive oxygen species; Tf, transferrin; TfR1, transferrin receptor 1; TSC,thiosemicarbazone.

References

1. Kalinowski DS, Richardson DR (2005) The evolution of iron chelators for the treatment of iron overload disease and cancer. *Pharmacol Rev* 57: 547-583.
2. Lieu PT, Heiskala M, Peterson PA, Yang Y (2001) The roles of iron in health and disease. *Mol Aspects Med* 22: 1-87.
3. Merlot AM, Kalinowski DS, Richardson DR (2013) Novel chelators for cancer treatment: where are we now? *Antioxid Redox Signal* 18: 973-1006.
4. Kolberg M, Strand KR, Graff P, Andersson KK (2004) Structure, function, and mechanism of ribonucleotide reductases. *Biochim Biophys Acta* 1699: 1-34.
5. Thelander L, Reichard P (1979) Reduction of ribonucleotides. *Annu Rev Biochem* 48: 133-158.
6. Richardson D, Baker E (1992) Two mechanisms of iron uptake from transferrin by melanoma cells. The effect of desferrioxamine and ferric ammonium citrate. *J Biol Chem* 267: 13972-13979.
7. Richardson DR, Baker E (1990) The uptake of iron and transferrin by the human malignant melanoma cell. *Biochim Biophys Acta* 1053: 1-12.
8. Trinder D, Zak O, Aisen P (1996) Transferrin receptor-independent uptake of differic transferrin by human hepatoma cells with antisense inhibition of receptor expression. *Hepatology* 23: 1512-1520.
9. Elford HL, Freese M, Passamani E, Morris HP (1970) Ribonucleotide reductase and cell proliferation. I. Variations of ribonucleotide reductase activity with tumor growth rate in a series of rat hepatomas. *J Biol Chem* 245: 5228-5233.
10. Kalinowski DS, Yu Y, Sharpe PC, Islam M, Liao YT, et al. (2007) Design, synthesis, and characterization of novel iron chelators: structure-activity relationships of the 2-benzoylpyridine thiosemicarbazone series and their 3-nitrobenzoyl analogues as potent antitumor agents. *J Med Chem* 50: 3716-3729.

11. Kunos C, Radivoyevitch T, Abdul-Karim FW, Fanning J, Abulafia O, et al. (2012) Ribonucleotide reductase inhibition restores platinum-sensitivity in platinum-resistant ovarian cancer: a Gynecologic Oncology Group Study. *J Transl Med* 10: 79.
12. Lovejoy DB, Sharp DM, Seebacher N, Obeidy P, Prichard T, et al. (2012) Novel second-generation di-2-pyridylketone thiosemicarbazones show synergism with standard chemotherapeutics and demonstrate potent activity against lung cancer xenografts after oral and intravenous administration in vivo. *J Med Chem* 55: 7230-7244.
13. Lukmantara AY, Kalinowski DS, Kumar N, Richardson DR (2013) Synthesis and biological evaluation of substituted 2-benzoylpyridine thiosemicarbazones: novel structure-activity relationships underpinning their anti-proliferative and chelation efficacy. *Bioorg Med Chem Lett* 23: 967-974.
14. Richardson DR, Kalinowski DS, Richardson V, Sharpe PC, Lovejoy DB, et al. (2009) 2-Acetylpyridine thiosemicarbazones are potent iron chelators and antiproliferative agents: redox activity, iron complexation and characterization of their antitumor activity. *J Med Chem* 52: 1459-1470.
15. Richardson DR, Sharpe PC, Lovejoy DB, Senaratne D, Kalinowski DS, et al. (2006) Dipyridyl thiosemicarbazone chelators with potent and selective antitumor activity form iron complexes with redox activity. *J Med Chem* 49: 6510-6521.
16. Serda M, Kalinowski DS, Mrozek-Wilczkiewicz A, Musiol R, Szurko A, et al. (2012) Synthesis and characterization of quinoline-based thiosemicarbazones and correlation of cellular iron-binding efficacy to anti-tumor efficacy. *Bioorg Med Chem Lett* 22: 5527-5531.
17. Stefani C, Jansson PJ, Gutierrez E, Bernhardt PV, Richardson DR, et al. (2013) Alkyl substituted 2'-benzoylpyridine thiosemicarbazone chelators with potent and selective anti-neoplastic activity: novel ligands that limit methemoglobin formation. *J Med Chem* 56: 357-370.

18. Stefani C, Punnia-Moorthy G, Lovejoy DB, Jansson PJ, Kalinowski DS, et al. (2011) Halogenated 2'-benzoylpyridine thiosemicarbazone (XBpT) chelators with potent and selective anti-neoplastic activity: relationship to intracellular redox activity. *J Med Chem* 54: 6936-6948.
19. Yu Y, Kalinowski DS, Kovacevic Z, Siafakas AR, Jansson PJ, et al. (2009) Thiosemicarbazones from the old to new: iron chelators that are more than just ribonucleotide reductase inhibitors. *J Med Chem* 52: 5271-5294.
20. Yu Y, Suryo Rahmanto Y, Richardson DR (2012) Bp44mT: an orally active iron chelator of the thiosemicarbazone class with potent anti-tumour efficacy. *Br J Pharmacol* 165: 148-166.
21. Yuan J, Lovejoy DB, Richardson DR (2004) Novel di-2-pyridyl-derived iron chelators with marked and selective antitumor activity: in vitro and in vivo assessment. *Blood* 104: 1450-1458.
22. Chaston TB, Lovejoy DB, Watts RN, Richardson DR (2003) Examination of the antiproliferative activity of iron chelators: multiple cellular targets and the different mechanism of action of triapine compared with desferrioxamine and the potent pyridoxal isonicotinoyl hydrazone analogue 311. *Clin Cancer Res* 9: 402-414.
23. Lovejoy DB, Jansson PJ, Brunk UT, Wong J, Ponka P, et al. (2011) Antitumor activity of metal-chelating compound Dp44mT is mediated by formation of a redox-active copper complex that accumulates in lysosomes. *Cancer Res* 71: 5871-5880.
24. Shao J, Zhou B, Di Bilio AJ, Zhu L, Wang T, et al. (2006) A Ferrous-Triapine complex mediates formation of reactive oxygen species that inactivate human ribonucleotide reductase. *Mol Cancer Ther* 5: 586-592.
25. Zhu L, Zhou B, Chen X, Jiang H, Shao J, et al. (2009) Inhibitory mechanisms of heterocyclic carboxaldehyde thiosemicarbazones for two forms of human ribonucleotide reductase. *Biochem Pharmacol* 78: 1178-1185.

26. Kovacevic Z, Chikhani S, Lovejoy DB, Richardson DR (2011) Novel thiosemicarbazone iron chelators induce up-regulation and phosphorylation of the metastasis suppressor N-myc down-stream regulated gene 1: a new strategy for the treatment of pancreatic cancer. *Mol Pharmacol* 80: 598-609.
27. Kovacevic Z, Chikhani S, Lui GY, Sivagurunathan S, Richardson DR (2013) The iron-regulated metastasis suppressor NDRG1 targets NEDD4L, PTEN, and SMAD4 and inhibits the PI3K and Ras signaling pathways. *Antioxid Redox Signal* 18: 874-887.
28. Kovacevic Z, Sivagurunathan S, Mangs H, Chikhani S, Zhang D, et al. (2011) The metastasis suppressor, N-myc downstream regulated gene 1 (NDRG1), upregulates p21 via p53-independent mechanisms. *Carcinogenesis* 32: 732-740.
29. Le NT, Richardson DR (2004) Iron chelators with high antiproliferative activity up-regulate the expression of a growth inhibitory and metastasis suppressor gene: a link between iron metabolism and proliferation. *Blood* 104: 2967-2975.
30. Bernhardt PV, Sharpe PC, Islam M, Lovejoy DB, Kalinowski DS, et al. (2009) Iron chelators of the dipyriddyketone thiosemicarbazone class: precomplexation and transmetalation effects on anticancer activity. *J Med Chem* 52: 407-415.
31. Feun L, Modiano M, Lee K, Mao J, Marini A, et al. (2002) Phase I and pharmacokinetic study of 3-aminopyridine-2-carboxaldehyde thiosemicarbazone (3-AP) using a single intravenous dose schedule. *Cancer Chemother Pharmacol* 50: 223-229.
32. Karp JE, Giles FJ, Gojo I, Morris L, Greer J, et al. (2008) A phase I study of the novel ribonucleotide reductase inhibitor 3-aminopyridine-2-carboxaldehyde thiosemicarbazone (3-AP, Triapine) in combination with the nucleoside analog fludarabine for patients with refractory acute leukemias and aggressive myeloproliferative disorders. *Leuk Res* 32: 71-77.
33. Kunos CA, Radivoyevitch T, Waggoner S, Debernardo R, Zanotti K, et al. (2013) Radiochemotherapy plus 3-aminopyridine-2-carboxaldehyde thiosemicarbazone

(3-AP, NSC #663249) in advanced-stage cervical and vaginal cancers. *Gynecol Oncol* 130: 75-80.

34. Kunos CA, Waggoner S, von Gruenigen V, Eldermire E, Pink J, et al. (2010) Phase I trial of pelvic radiation, weekly cisplatin, and 3-aminopyridine-2-carboxaldehyde thiosemicarbazone (3-AP, NSC #663249) for locally advanced cervical cancer. *Clin Cancer Res* 16: 1298-1306.
35. Ma B, Goh BC, Tan EH, Lam KC, Soo R, et al. (2008) A multicenter phase II trial of 3-aminopyridine-2-carboxaldehyde thiosemicarbazone (3-AP, Triapine) and gemcitabine in advanced non-small-cell lung cancer with pharmacokinetic evaluation using peripheral blood mononuclear cells. *Invest New Drugs* 26: 169-173.
36. Mackenzie MJ, Saltman D, Hirte H, Low J, Johnson C, et al. (2007) A Phase II study of 3-aminopyridine-2-carboxaldehyde thiosemicarbazone (3-AP) and gemcitabine in advanced pancreatic carcinoma. A trial of the Princess Margaret hospital Phase II consortium. *Invest New Drugs* 25: 553-558.
37. Nutting CM, van Herpen CM, Miah AB, Bhide SA, Machiels JP, et al. (2009) Phase II study of 3-AP Triapine in patients with recurrent or metastatic head and neck squamous cell carcinoma. *Ann Oncol* 20: 1275-1279.
38. Ocean AJ, Christos P, Sparano JA, Matulich D, Kaubish A, et al. (2010) Phase II trial of the ribonucleotide reductase inhibitor 3-aminopyridine-2-carboxaldehydethiosemicarbazone plus gemcitabine in patients with advanced biliary tract cancer. *Cancer Chemother Pharmacol* 68: 379-388.
39. Odenike OM, Larson RA, Gajria D, Dolan ME, Delaney SM, et al. (2008) Phase I study of the ribonucleotide reductase inhibitor 3-aminopyridine-2-carboxaldehyde-thiosemicarbazone (3-AP) in combination with high dose cytarabine in patients with advanced myeloid leukemia. *Invest New Drugs* 26: 233-239.
40. Wadler S, Makower D, Clairmont C, Lambert P, Fehn K, et al. (2004) Phase I and pharmacokinetic study of the ribonucleotide reductase inhibitor, 3-

aminopyridine-2-carboxaldehyde thiosemicarbazone, administered by 96-hour intravenous continuous infusion. *J Clin Oncol* 22: 1553-1563.

41. Yen Y, Margolin K, Doroshow J, Fishman M, Johnson B, et al. (2004) A phase I trial of 3-aminopyridine-2-carboxaldehyde thiosemicarbazone in combination with gemcitabine for patients with advanced cancer. *Cancer Chemother Pharmacol* 54: 331-342.
42. Whitnall M, Howard J, Ponka P, Richardson DR (2006) A class of iron chelators with a wide spectrum of potent antitumor activity that overcomes resistance to chemotherapeutics. *Proc Natl Acad Sci U S A* 103: 14901-14906.
43. Mrozek-Wilczkiewicz A, Serda M, Musiol R, Malecki G, Szurko A, et al. (2014) Iron chelators in photodynamic therapy revisited: Synergistic effect by novel highly active thiosemicarbazones. *ACS Med Chem Lett* In press.
44. Serda M, Mrozek-Wilczkiewicz A, Jampilek J, Pesko M, Kralova K, et al. (2012) Investigation of the biological properties of (hetero)aromatic thiosemicarbazones. *Molecules* 17: 13483-13502.
45. Hu WX, Zhou W, Xia CN, Wen X (2006) Synthesis and anticancer activity of thiosemicarbazones. *Bioorg Med Chem Lett* 16: 2213-2218.
46. Stanojkovic TP, Kovala-Demertzi D, Primikyri A, Garcia-Santos I, Castineiras A, et al. (2010) Zinc(II) complexes of 2-acetyl pyridine 1-(4-fluorophenyl)-piperazinyl thiosemicarbazone: Synthesis, spectroscopic study and crystal structures - potential anticancer drugs. *J Inorg Biochem* 104: 467-476.
47. Ghose AK, Crippen GM (1987) Atomic physicochemical parameters for three-dimensional-structure-directed quantitative structure-activity relationships. 2. Modeling dispersive and hydrophobic interactions. *J Chem Inf Comput Sci* 27: 21-35.
48. Viswanadhan VN, Ghose AK, Revankar GR, Robins RK (1987) Atomic physicochemical parameters for 3-dimensional-structure directed quantitative structure-activity relationships 4. Additional parameters for hydrophobic and

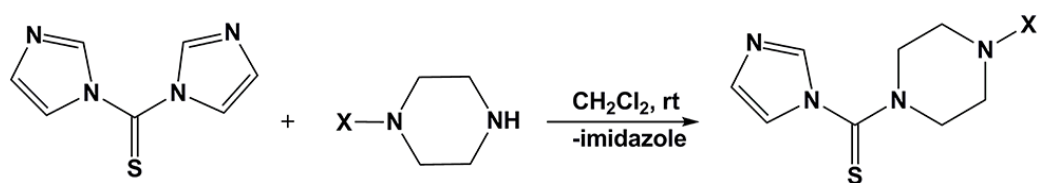
- dispersive interactions and their application for an automated superposition of certain naturally-occurring nucleoside antibiotics. *J Chem Inf Comput Sci* 29: 163–172.
49. Broto P, Moreau G, Vandycke C (1984) Molecular structures: Perception, autocorrelation descriptor and SAR studies. System of atomic contributions for the calculation of the n-octanol/water partition coefficients. *Eur J Med Chem Chim Theor* 19: 71-78.
 50. Baker E, Richardson D, Gross S, Ponka P (1992) Evaluation of the iron chelation potential of hydrazones of pyridoxal, salicylaldehyde and 2-hydroxy-1-naphthylaldehyde using the hepatocyte in culture. *Hepatology* 15: 492-501.
 51. Richardson DR, Tran EH, Ponka P (1995) The potential of iron chelators of the pyridoxal isonicotinoyl hydrazone class as effective antiproliferative agents. *Blood* 86: 4295-4306.
 52. Kalinowski DS, Sharpe PC, Bernhardt PV, Richardson DR (2007) Design, synthesis, and characterization of new iron chelators with anti-proliferative activity: structure-activity relationships of novel thiohydrazone analogues. *J Med Chem* 50: 6212-6225.
 53. Kalinowski DS, Sharpe PC, Bernhardt PV, Richardson DR (2008) Structure-activity relationships of novel iron chelators for the treatment of iron overload disease: the methyl pyrazinylketone isonicotinoyl hydrazone series. *J Med Chem* 51: 331-344.
 54. Hann MM, Keseru GM (2012) Finding the sweet spot: the role of nature and nurture in medicinal chemistry. *Nat Rev Drug Discov* 11: 355-365.
 55. Meanwell NA (2011) Improving drug candidates by design: a focus on physicochemical properties as a means of improving compound disposition and safety. *Chem Res Toxicol* 24: 1420-1456.
 56. Gleeson MP (2008) Generation of a set of simple, interpretable ADMET rules of thumb. *J Med Chem* 51: 817-834.

57. Hann MM (2011) Molecular obesity, potency and other addictions in drug discovery. *Med Chem Commun* 2: 349-355.
58. Proschak E, Tanrikulu Y, Schneider G (2008) Chapter 7: Fragment-based de novo design of drug-like molecules. In: Varnek A, Tropsha A, editors. *Cheminformatics approaches to virtual screening*. Cambridge: Royal Society of Chemistry. pp. 217-239.
59. Becker EM, Lovejoy DB, Greer JM, Watts R, Richardson DR (2003) Identification of the di-pyridyl ketone isonicotinoyl hydrazone (PKIH) analogues as potent iron chelators and anti-tumour agents. *Br J Pharmacol* 138: 819-830.
60. Wang Y, Ai J, Chen Y, Wang L, Liu G, et al. (2011) Synthesis and c-Met kinase inhibition of 3,5-disubstituted and 3,5,7-trisubstituted quinolines: identification of 3-(4-acetylpiperazin-1-yl)-5-(3-nitrobenzylamino)-7-(trifluoromethyl)quinoline as a novel anticancer agent. *J Med Chem* 54: 2127-2142.
61. Chetan B, Bunha M, Jagrat M, Sinha BN, Saiko P, et al. (2010) Design, synthesis and anticancer activity of piperazine hydroxamates and their histone deacetylase (HDAC) inhibitory activity. *Bioorg Med Chem Lett* 20: 3906-3910.
62. Hou X, Ge Z, Wang T, Guo W, Cui J, et al. (2006) Dithiocarbamic acid esters as anticancer agent. Part 1: 4-substituted-piperazine-1-carbodithioic acid 3-cyano-3,3-diphenyl-propyl esters. *Bioorg Med Chem Lett* 16: 4214-4219.
63. Yu K, Toral-Barza L, Shi C, Zhang WG, Lucas J, et al. (2009) Biochemical, cellular, and in vivo activity of novel ATP-competitive and selective inhibitors of the mammalian target of rapamycin. *Cancer Res* 69: 6232-6240.
64. Gao H, Yamasaki EF, Chan KK, Shen LL, Snapka RM (2003) DNA sequence specificity for topoisomerase II poisoning by the quinoxaline anticancer drugs XK469 and CQS. *Mol Pharmacol* 63: 1382-1388.
65. Silva JL, Gallo CV, Costa DC, Rangel LP (2014) Prion-like aggregation of mutant p53 in cancer. *Trends Biochem Sci* In Press April 25, 2014.

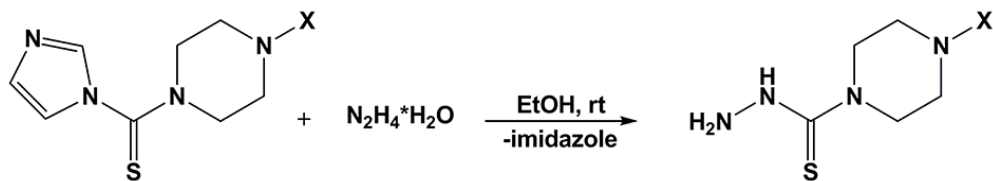
66. Breen L, Heenan M, Amberger-Murphy V, Clynes M (2007) Investigation of the role of p53 in chemotherapy resistance of lung cancer cell lines. *Anticancer Res* 27: 1361-1364.
67. Whibley C, Pharoah PD, Hollstein M (2009) p53 polymorphisms: cancer implications. *Nat Rev Cancer* 9: 95-107.
68. Mladenka P, Kalinowski DS, Haskova P, Bobrovova Z, Hrdina R, et al. (2009) The novel iron chelator, 2-pyridylcarboxaldehyde 2-thiophenecarboxyl hydrazone, reduces catecholamine-mediated myocardial toxicity. *Chem Res Toxicol* 22: 208-217.
69. Deraeve C, Pitie M, Meunier B (2006) Influence of chelators and iron ions on the production and degradation of H₂O₂ by beta-amyloid-copper complexes. *J Inorg Biochem* 100: 2117-2126.
70. Di Vaira M, Bazzicalupi C, Orioli P, Messori L, Bruni B, et al. (2004) Clioquinol, a drug for Alzheimer's disease specifically interfering with brain metal metabolism: Structural characterization of its zinc(II) and copper(II) complexes. *Inorg Chem* 43: 3795-3797.
71. Lovejoy DB, Richardson DR (2002) Novel "hybrid" iron chelators derived from aroylhydrazones and thiosemicarbazones demonstrate selective antiproliferative activity against tumor cells. *Blood* 100: 666-676.
72. Bernhardt PV, Wilson GJ, Sharpe PC, Kalinowski DS, Richardson DR (2008) Tuning the antiproliferative activity of biologically active iron chelators: characterization of the coordination chemistry and biological efficacy of 2-acetylpyridine and 2-benzoylpyridine hydrazone ligands. *J Biol Inorg Chem* 13: 107-119.

Schemes

Scheme 1.

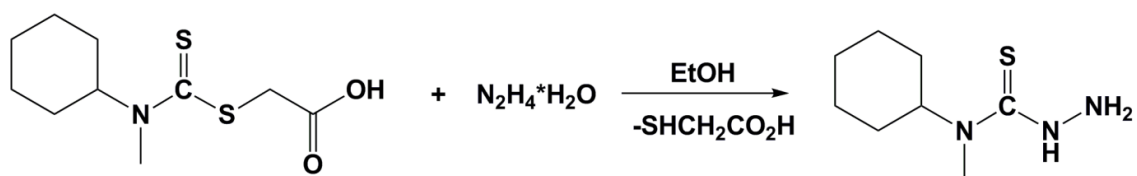
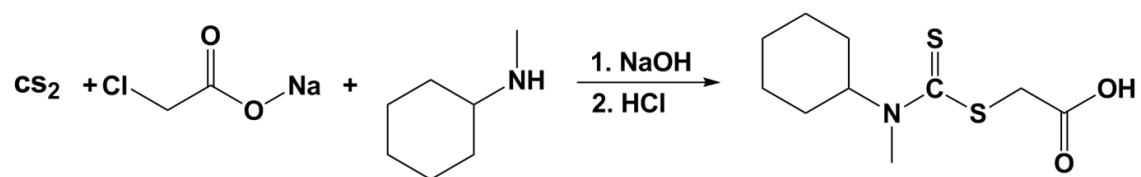


X= alkyl, aryl

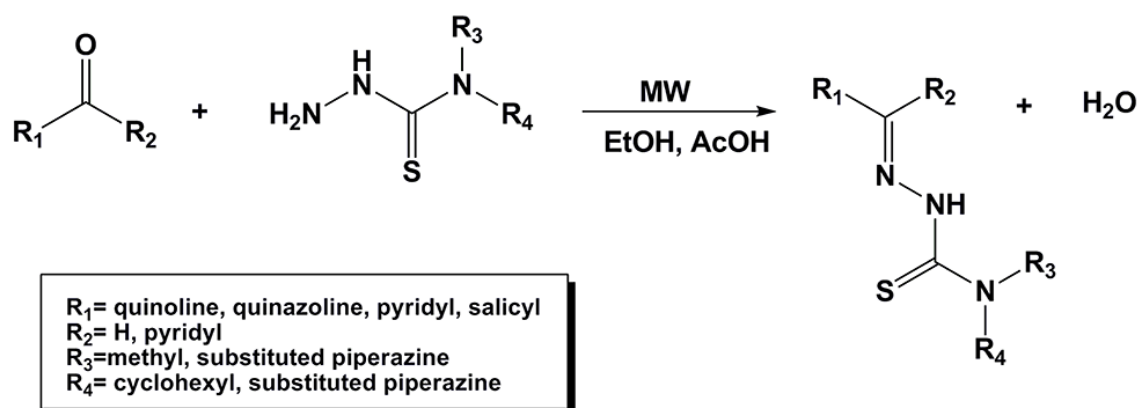


X= alkyl, aryl

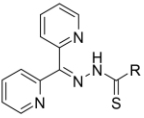
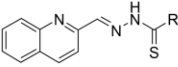
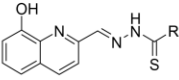
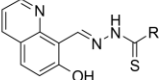
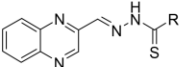
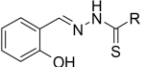
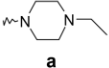
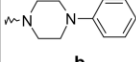
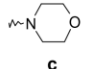
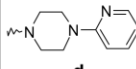
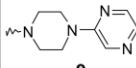
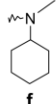
Scheme 2.



Scheme 3.



Scheme 4.

R =	 Series 1	 Series 2	 Series 3	 Series 4	 Series 5	 Series 6
 a	1a	2a	3a	4a	5a	6a
 b	1b	2b	3b	4b	5b	6b
 c	1c	2c	3c	4c	5c	6c
 d	1d	2d	3d	4d	5d	6d
 e	1e	2e	3e	4e	5e	6e
 f	-	2f	3f	4f	5f	6f

Tables

Table 1. Anti-proliferative activity (IC₅₀ values) of the new thiosemicarbazones in comparison to DFO and Dp44mT in several tumor cell-types and normal human dermal fibroblast (NHDF) cells. Results are mean ± SD (3 experiments).

Chelator	IC ₅₀ (μM)					
	HCT116 p53 ^{+/+}	HCT116 p53 ^{-/-}	Raji	HeLa	SK-N-MC	NHDF
DFO	>25	>25	4.74 ± 1.80	14.34 ± 0.96	15.06 ± 5.2	>25
Dp44mT	0.002 ± 0.001	0.005 ± 0.002	0.007 ± 0.001	0.04 ± 0.01	0.012 ± 0.001	15.38 ± 5.06
1a	0.020 ± 0.002	0.040 ± 0.003	0.08 ± 0.02	0.48 ± 0.31	0.18 ± 0.09	0.017 ± 0.004
1b	0.0008 ± 0.0001	0.0008 ± 0.0001	0.0003 ± 0.00003	0.57 ± 0.16	0.05 ± 0.01	0.0017 ± 0.0007
1c	0.014 ± 0.005	0.014 ± 0.006	0.003 ± 0.004	2.21 ± 0.47	1.21 ± 0.35	0.016 ± 0.006
1d	0.002 ± 0.008	0.009 ± 0.001	0.0013 ± 0.0001	0.03 ± 0.02	0.02 ± 0.01	0.16 ± 0.04
1e	0.038 ± 0.003	0.031 ± 0.003	0.04 ± 0.02	0.72 ± 0.07	0.07 ± 0.05	0.014 ± 0.003
2a	1.44 ± 0.69	3.55 ± 1.23	0.06 ± 0.02	0.43 ± 0.16	2.54 ± 0.86	9.62 ± 1.80
2b	0.042 ± 0.003	0.09 ± 0.04	0.04 ± 0.01	0.20 ± 0.07	0.33 ± 0.02	0.033 ± 0.007
2c	1.49 ± 0.02	1.56 ± 1.12	0.06 ± 0.01	1.75 ± 0.33	1.40 ± 0.69	3.27 ± 0.88
2d	0.39 ± 0.15	0.27 ± 0.16	0.05 ± 0.02	5.14 ± 2.87	0.52 ± 0.16	0.032 ± 0.008
2e	0.088 ± 0.044	0.48 ± 0.15	0.29 ± 0.11	1.56 ± 0.44	0.48 ± 0.10	9.44 ± 3.84
2f	0.026 ± 0.001	0.035 ± 0.003	0.81 ± 0.10	0.94 ± 0.45	0.82 ± 0.19	0.015 ± 0.005
3a	9.25 ± 1.42	8.83 ± 0.63	0.20 ± 0.02	3.41 ± 1.46	0.82 ± 0.61	15.8 ± 4.6
3b	4.18 ± 1.46	4.67 ± 2.04	0.19 ± 0.02	8.45 ± 2.09	>6.25	8.88 ± 1.07
3c	0.004 ± 0.002	0.017 ± 0.006	0.02 ± 0.01	0.18 ± 0.07	>6.25	10.6 ± 3.5

3d	8.41 ± 1.78	8.46 ± 0.25	0.12 ± 0.04	6.59 ± 0.13	>6.25	10.2 ± 2.4
3e	0.05 ± 0.03	5.01 ± 2.55	0.04 ± 0.02	2.39 ± 0.02	>6.25	12.1 ± 3.6
3f	3.11 ± 1.92	4.35 ± 1.35	0.01 ± 0.04	2.57 ± 0.46	>6.25	5.36 ± 1.99
4a	20.2 ± 0.3	20.3 ± 0.9	3.35 ± 1.11	11.3 ± 1.6	5.09 ± 0.47	12.1 ± 4.2
4b	7.45 ± 0.66	8.88 ± 2.53	2.23 ± 1.20	4.38 ± 0.95	4.46 ± 0.78	10.1 ± 1.2
4c	20.1 ± 0.3	19.8 ± 4.9	3.53 ± 1.87	10.2 ± 1.2	4.97 ± 0.95	>25
4d	9.15 ± 1.19	6.84 ± 5.48	1.55 ± 0.40	2.73 ± 0.55	4.54 ± 1.60	10.1 ± 2.7
4e	10.1 ± 0.7	9.44 ± 1.35	4.55 ± 2.52	3.49 ± 0.04	4.17 ± 1.44	9.56 ± 1.44
4f	19.0 ± 0.5	18.9 ± 3.6	0.46 ± 0.23	13.3 ± 1.0	>6.25	9.18 ± 3.68
5a	6.15 ± 1.28	8.72 ± 1.64	0.11 ± 0.02	1.12 ± 0.03	ND	2.73 ± 1.77
5b	3.92 ± 0.74	2.24 ± 1.47	0.50 ± 0.05	6.05 ± 2.73	3.44 ± 1.12	9.61 ± 0.90
5c	2.03 ± 1.24	5.84 ± 1.65	0.24 ± 0.04	0.86 ± 0.09	2.87 ± 1.25	11.6 ± 1.8
5d	9.4 ± 0.8	9.41 ± 1.04	0.49 ± 0.09	1.78 ± 0.77	2.33 ± 0.09	7.13 ± 0.82
5e	5.73 ± 0.75	8.49 ± 3.05	0.27 ± 0.01	3.77 ± 1.71	1.98 ± 0.68	15.8 ± 5.1
5f	1.24 ± 0.45	1.02 ± 0.54	0.72 ± 0.29	4.09 ± 2.07	2.04 ± 0.34	0.50 ± 0.21
6a	>25	>25	10.2 ± 6.6	22.1 ± 5.4	>6.25	>25
6b	6.9 ± 2.3	8.86 ± 1.46	1.96 ± 0.85	5.80 ± 0.48	5.13 ± 0.51	13.5 ± 4.8
6c	15.4 ± 1.7	16.4 ± 3.1	3.79 ± 0.08	18.2 ± 1.3	>6.25	>25
6d	9.7 ± 2.5	10.6 ± 1.2	2.60 ± 0.33	16.4 ± 4.5	5.42 ± 0.64	18.4 ± 1.9
6e	10.9 ± 0.7	10.7 ± 1.0	9.83 ± 2.05	19.2 ± 2.5	>6.25	>25
6f	>25	>25	0.69 ± 0.51	10.1 ± 3.6	>6.25	>25

Table 2. The selectivity of Dp44mT relative to the 5 most potent anti-cancer TSCs, namely **1b**, **1d**, **2b**, **2f** and **3c**, was examined by determining their therapeutic indices. This was calculated by dividing the NHDF cell IC₅₀ by the IC₅₀ of the neoplastic HCT116 p53^{+/+} or HCT116 p53^{-/-} cell-types after a 96 h incubation.

Chelator	Therapeutic index	
	NHDF vs. HCT116 p53 ^{+/+}	NHDF vs. HCT116 p53 ^{-/-}
Dp44mT	7690	3076
1b	2	2
1d	80	18
2b	0.8	0.4
2f	0.6	0.4
3c	2650	624

Figures Legends

Figure 1. Chemical structures of the chelators, Triapine[®], di-2-pyridylketone 4,4-dimethyl-3-thiosemicarbazone (Dp44mT), di-2-pyridylketone 4-cyclohexyl-4-methyl-3-thiosemicarbazone (DpC), 2-acetylpyridine (*N*(4)-(2-pyridyl)-piperazin-1-yl) thiosemicarbazone, 2-benzoylpyridine 4,4-dimethyl-3-thiosemicarbazone (Bp44mT) and quinoline thiosemicarbazone (QT).

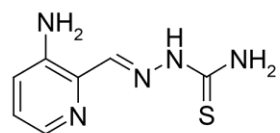
Figure 2. Effect of (A) series 1, (B) series 2, (C) series 3, (D) series 4, (E) series 5 and (F) series 6 chelators, relative to DFO and Dp44mT, on ⁵⁹Fe mobilization from prelabeled SK-N-MC cells. Cells were incubated for 3 h/37°C with ⁵⁹Fe-transferrin (0.75 μM), washed 4 times with ice-cold PBS and then reincubated for 3 h/37°C in the presence or absence of the chelators (25 μM). Release of ⁵⁹Fe was then assessed using a γ-scintillation counter. Results are mean ± SD (three experiments).

Figure 3. Effect of (A) series 1, (B) series 2, (C) series 3, (D) series 4, (E) series 5 and (F) series 6 chelators, relative to DFO and Dp44mT, on ⁵⁹Fe uptake from ⁵⁹Fe-transferrin by SK-N-MC cells. Cells were incubated for 3 h/37°C with ⁵⁹Fe-transferrin (0.75 μM) in the presence or absence of the chelators (25 μM). At the end of this incubation, cells were washed 4 times with ice-cold PBS. Internalization of ⁵⁹Fe was assessed by incubation for 30 min/4°C with the protease, Pronase (1 mg/mL). Cellular ⁵⁹Fe was then assessed using a γ-scintillation counter. Results are mean ± SD (three experiments).

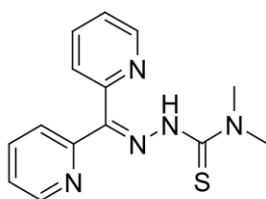
Figure 4. Effect of the iron complexes of (A) series 1, (B) series 2, (C) series 3, (D) series 4, (E) series 5 and (F) series 6 chelators, relative to DFO, Dp44mT and EDTA, on ascorbate oxidation. Chelators at iron-binding equivalent (IBE) ratios of 0.1, 1, and 3 were incubated in the presence of Fe^{III} (10 μM) and ascorbate (100 μM). The UV-vis absorbance at 265 nm was recorded after 10 and 40 min, and the difference between the time points was calculated. Results are mean ± SD (three experiments).

Figures

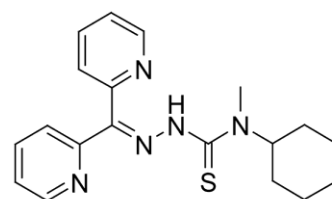
Figure 1.



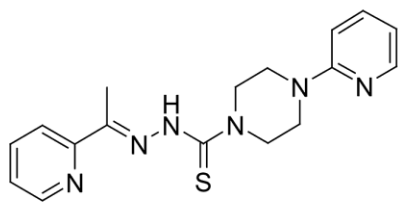
Triapine



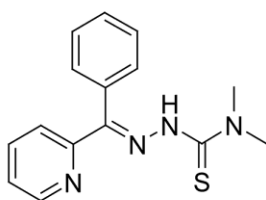
Dp44mT



DpC



Bp44mT



QT

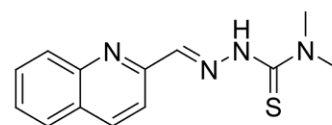


Figure 2.

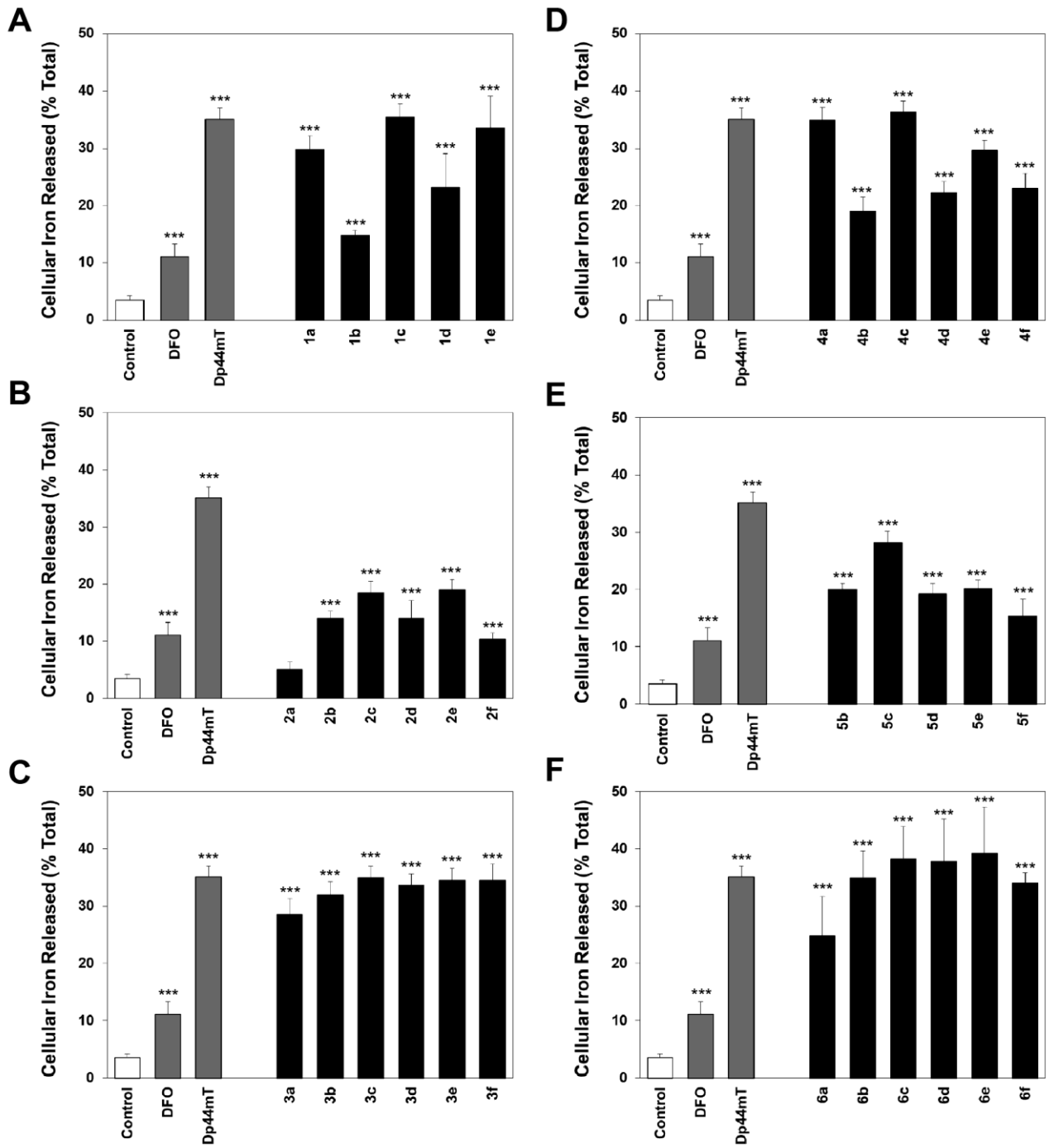


Figure 3.

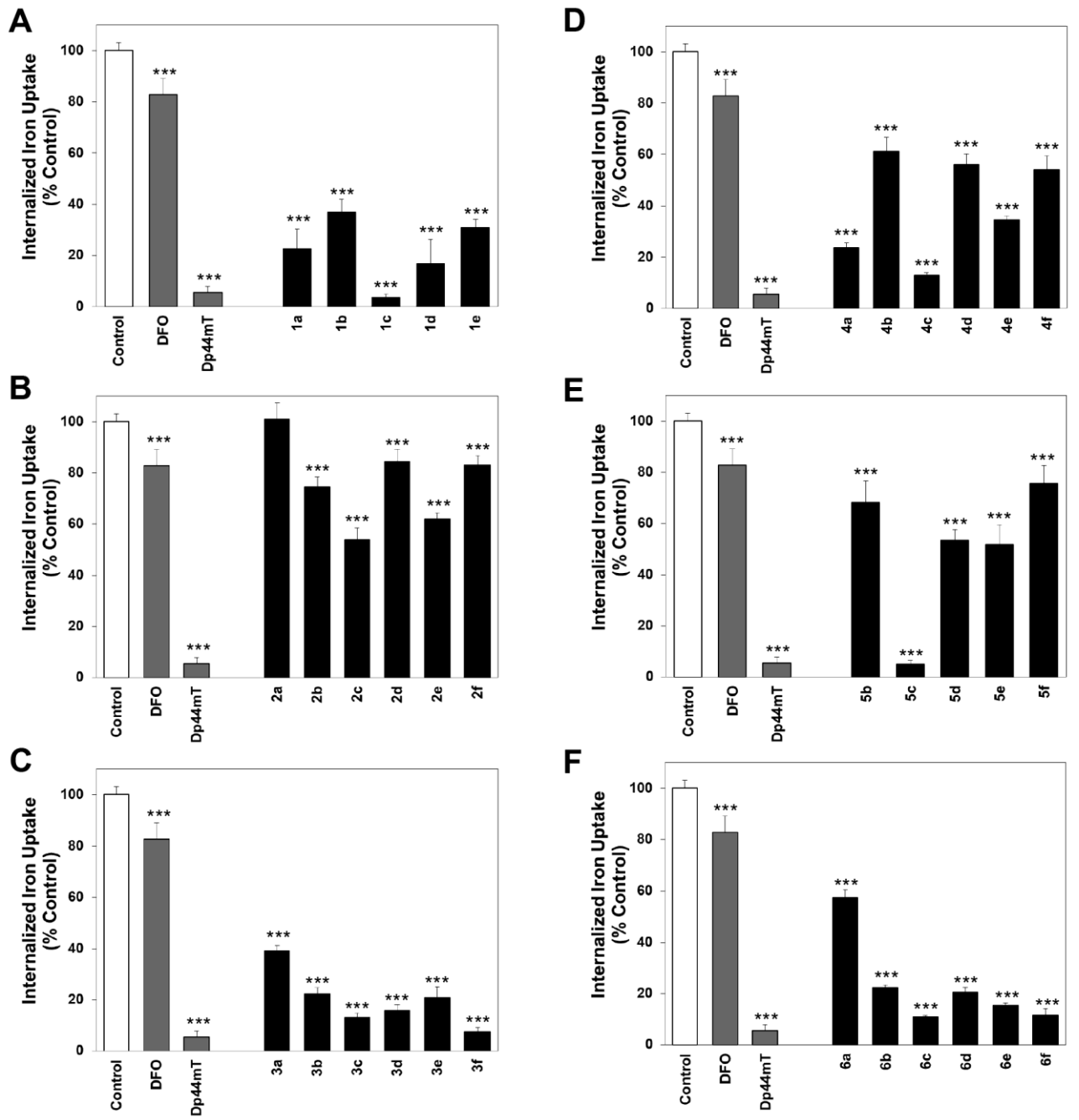
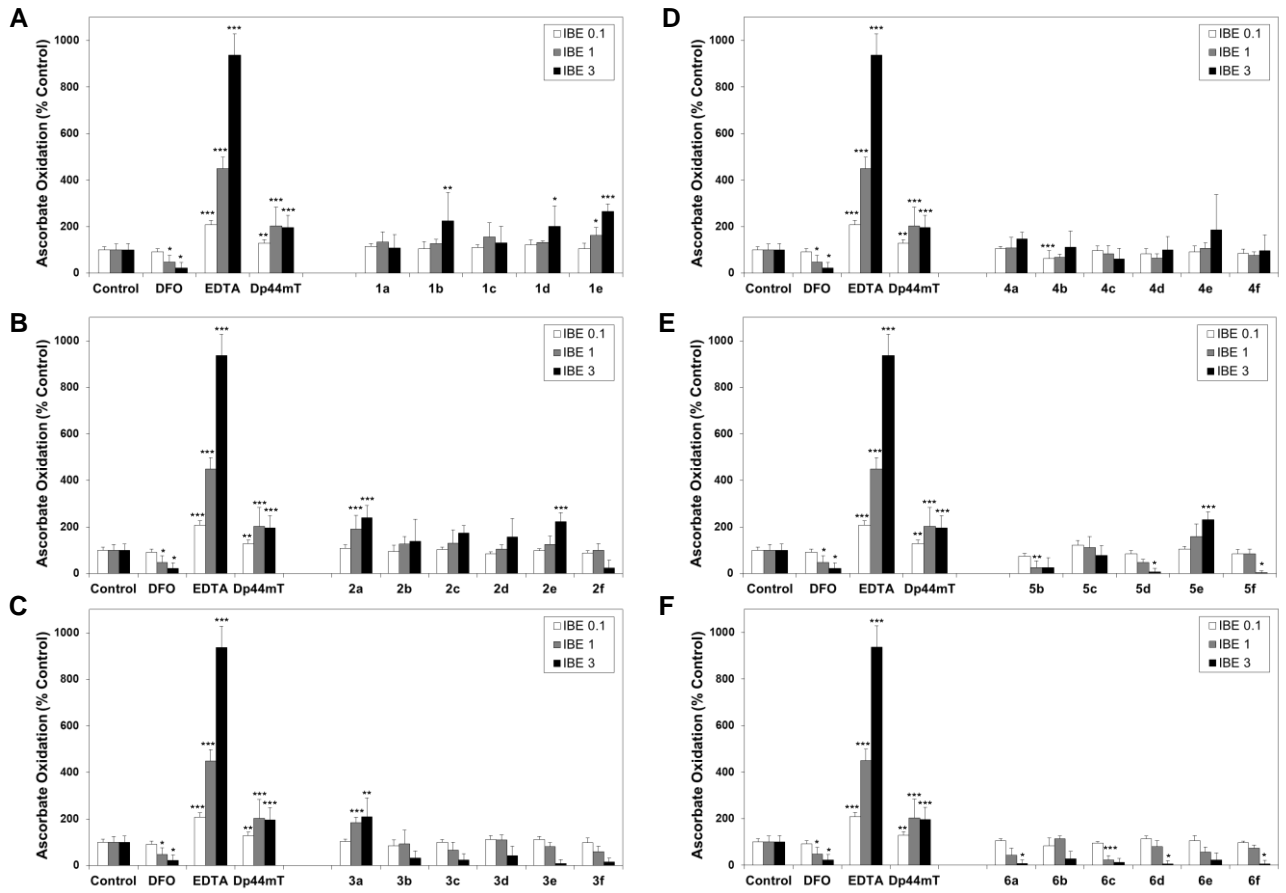


Figure 4.



Supporting information

Exploring the anti-cancer activity of novel thiosemicarbazones generated through the combination of retro-fragments

Maciej Serda^{1†}, Danuta S. Kalinowski^{2†}, Nathalie Rasko², Eliška Potůčková³, Anna Mrozek-Wilczkiewicz⁴, Robert Musiol¹, Jan G. Małecki¹, Mieczysław Sajewicz¹, Alicja Ratuszna⁴, Angelika Muchowicz⁵, Jakub Gołąb^{5,6}, Tomáš Šimůnek³, Des R. Richardson^{2*}, Jarosław Polanski^{1*}

¹*Institute of Chemistry, University of Silesia, PL-40-006 Katowice, Poland*

²*Department of Pathology and Bosch Institute, University of Sydney, Sydney, New South Wales 2006, Australia*

³*Department of Biochemical Sciences, Charles University in Prague, Faculty of Pharmacy in Hradec Králové, Czech Republic*

⁴*A.Chelkowski Institute of Physics and Silesian Interdisciplinary Centre for Education and Research, University of Silesia, PL-40-007 Katowice, Poland*

⁵*Department of Immunology, Medical University of Warsaw, PL-02-097 Warsaw, Poland*

⁶*Institute of Physical Chemistry, Polish Academy of Sciences, Department 3, PL-01-224 Warsaw, Poland.*

[†] *M.S. and D.S.K. contributed as equal first authors.*

S1 Chemistry

S1.1 Chemical characterization of thiosemicarbazides and thiosemicarbazones
S1.2 X-ray data for selected thiosemicarbazones and thiosemicarbazides

S1.3 HPLC purity data

S1.4 Isosbestic curves

S2 References

S1 Chemistry

General reagents were purchased from Sigma-Aldrich (St. Louis, MO, USA), ACROS Organics (Belgium) or Princeton Chemicals Ltd (Luton, Bedfordshire, UK). Silica gel 60 (0.040-0.063 mm; Merck, Darmstadt, Germany) was used for column chromatography. Thin layer chromatography (TLC) was performed on alumina-backed silica gel 40 F₂₅₄ plates (Merck). The plates were illuminated under UV (254 nm) and evaluated in iodine vapor. The melting points were determined on Optimelt MPA100 instrument (SRS, USA) and are uncorrected. Syntheses were performed on a CEM-DISCOVERY microwave reactor (CEM Corporation, Matthews, NC, USA) with temperature and pressure control. High resolution-mass spectrometry (HRMS) analysis was performed for all new compounds on a Finnigan MAT95 spectrometer (Thermo Fisher Scientific, Bremen, GmbH) or on Mariner ESI-TOF spectrometer (Applied Biosystems, USA). The purity of all novel compounds was assessed using a Gynkotek HPLC Modular System equipped with a DAAD UVD340U detector at 250 nm.

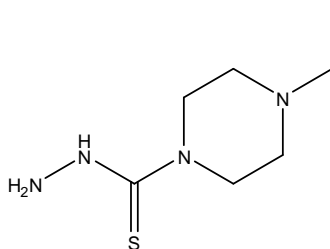
All ¹H NMR spectra were recorded on a Bruker AM-400 spectrometer (399.95 MHz for ¹H; 99.99 MHz for ¹³C; BrukerBioSpin Corp., Germany). Chemical shifts are reported in ppm against the internal standard, Si(CH₃)₄. Easily exchangeable signals were omitted when diffuse.

Log*P*_{calc} values were calculated using ChemDraw 12 (Perkin-Elmer, Waltham, MA, USA) by obtaining Crippen's fragmentation [1], Viswanadhan's fragmentation [2] and Broto's method [3] data and then calculating the average log*P*_{calc}.

S1.1 Chemical Characterization of Thiosemicarbazides and Thiosemicarbazones

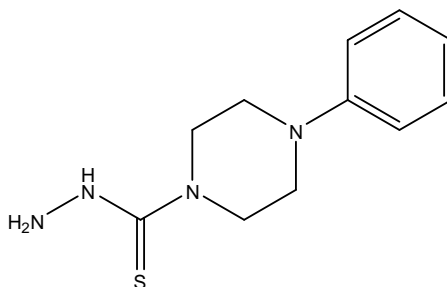
The thiosemicarbazides (**a-f**) and their thiosemicarbazones (Series **1-6**) were prepared according to Schemes 1-3. The characterization of all novel products is described below.

4-Ethylpiperazine-1-carbothiohydrazide (a)



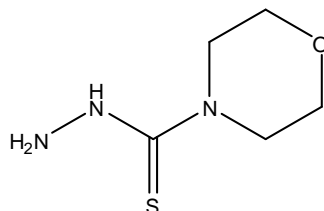
Yield: 47%. Purity: 98.67%. $^1\text{H-NMR}$ (d_6 -DMSO, 400 MHz, ppm): 3.71-3.68 (m, 4H, CH_2), 2.35-2.29 (m, 6H, CH_2), 1.00 (t, 3H, $J = 7.2$ Hz). $^{13}\text{C-NMR}$ (d_6 -DMSO, 100 MHz, ppm): 183.0, 52.45, 51.86, 47.75, 12.35. MP: 137-138°C (ethanol). HRMS-ESI-TOF: 189.1171 $[\text{M} + \text{H}]^+$ ($\text{C}_7\text{H}_{17}\text{N}_4\text{S}$; Exact Mass: 189.1174). $\text{Log}P_{\text{calc}}$: 0.57.

4-Phenylpiperazine-1-carbothiohydrazide (b)



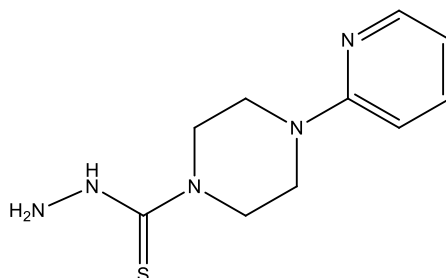
Yield: 58%. MP: 161-162°C (ethanol) [176-177°C (dioxane) [4]]. $\text{Log}P_{\text{calc}}$: 1.472.

Morpholine-4-carbothiohydrazide (c)



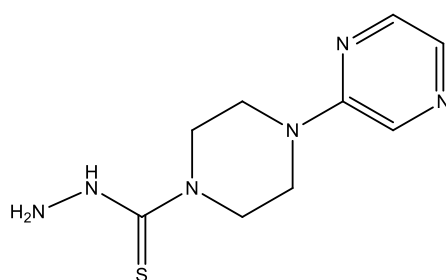
Yield: 76%. MP: 170-171°C (ethanol) [170-171°C; [5]] $\text{Log}P_{\text{calc}}$: -0.52.

4-(Pyridin-2-yl)piperazine-1-carbothiohydrazide (d)



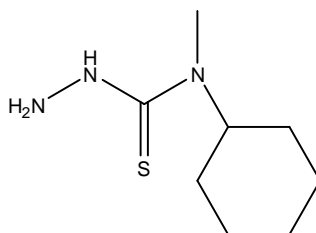
Yield: 95%. MP: 177-178°C (ethanol) [179-180°C; [4]]. $\text{Log}P_{\text{calc}}$: 0.524.

4-(Pyrazin-2-yl)piperazine-1-carbothiohydrazide (e)



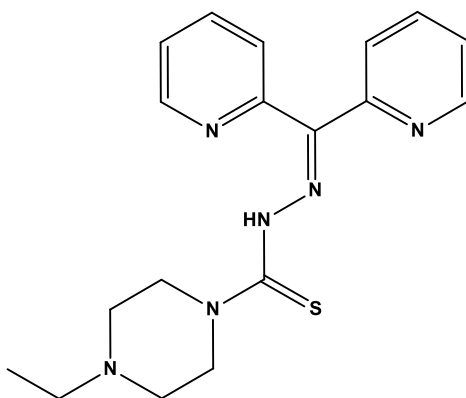
Yield: 95%. Purity: 96.98% (250 nm). $^1\text{H-NMR}$ (d_6 -DMSO, 400 MHz, ppm): 9.17 (bs, 1H, NH), 8.31 (bs, 1H, pyrazine), 8.09 (bs, 1H, pyrazine), 7.86 (bs, 1H, pyrazine), 4.83 (bs, 2H, NH), 3.89 (m, 4H, CH_2), 3.61 (m, 4H, CH_2). $^{13}\text{C-NMR}$ (d_6 -DMSO, 100 MHz, ppm): 183.0, 154.7, 141.9, 133.1, 131.7, 47.0, 43.7. MP: 167-168°C (ethanol). HRMS-ESI-TOF: 239.1080 [$\text{M} + \text{H}$] $^+$ ($\text{C}_9\text{H}_{15}\text{N}_6\text{S}$; Exact Mass: 239.1079). $\text{Log}P_{\text{calc}}$: -0.24.

N-Cyclohexyl-N-methylhydrazinecarbothioamide (f)



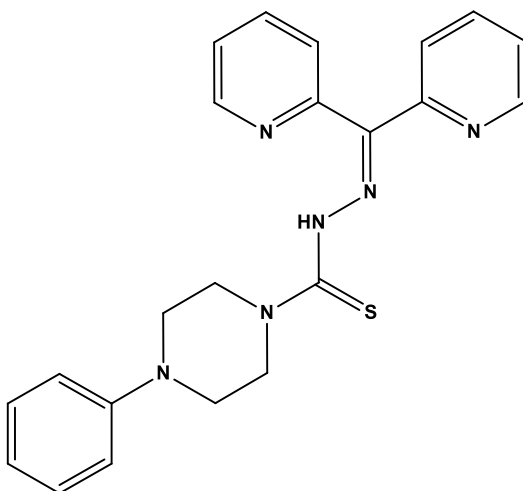
Yield: 66%. MP: 138-139°C (ethanol) [140°C; [6]] $\text{Log}P_{\text{calc}}$: 1.733.

(Z)-N'-(Di(pyridin-2-yl)methylene)-4-ethylpiperazine-1-carbothiohydrazide (1a)



Yield: 62%. Purity: 97.32%. $^1\text{H-NMR}$ (d_6 -DMSO, 400 MHz, ppm): 14.47 (bs, 1H, NH), 8.85 (d, 1H, $J= 3,6$ Hz), 8.60 (d, 1H, $J= 3.6$ Hz), 8.01-7.91 (m, 3H), 7.59 (m, 2H), 7.58 (m, 1H), 4.00 (m, 4H, CH_2 , piperazine), 2.50 (m, 6H, CH_2 , piperazine), 1.06 (t, 3H, $J= 6.8$ Hz, CH_3). $^{13}\text{C-NMR}$ (d_6 -DMSO, 100 MHz, ppm): 180.8, 148.9, 148.3, 138.3, 127.4, 125.1, 124.2, 56.5, 52.4, 51.7, 12.4. MP: 144-145°C. $R_f= 0.52$ [dichloromethane:ethanol 16:1 (v/v)]. HRMS-EI: 354.1626 ($\text{C}_{18}\text{H}_{22}\text{N}_6\text{S}$; Exact Mass: 354.1627). $\text{Log}P_{\text{calc}}$: 1.842.

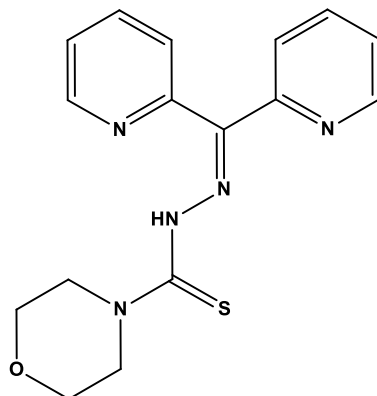
N'-(Di(pyridin-2-yl)methylene)-4-phenylpiperazine-1-carbothiohydrazide (1b)



Yield: 78%. Purity: 98.65%. $^1\text{H-NMR}$ (d_6 -DMSO, 400 MHz, ppm): 14.59 (bs, 1H, NH), 8.89 (d, 1H, $J= 3.9$ Hz), 8.60 (d, 1H, $J= 4.0$ Hz, pyridine), 8.01-7.91 (m, 3H), 7.60 (m, 2H), 7.49 (m, 1H), 7.25 (t, 2H, $J= 7.7$ Hz), 6.96 (d, 2H, $J= 8.2$ Hz), 6.81 (t, 1H, $J= 7.2$ Hz), 4.17 (m, 4H, CH_2 , piperazine), 3.34 (m, 4H, CH_2 , piperazine). $^{13}\text{C-NMR}$ (d_6 -DMSO, 100 MHz, ppm): 180.7, 150.8, 148.7, 148.4, 138.3, 137.7, 129.5, 127.3,

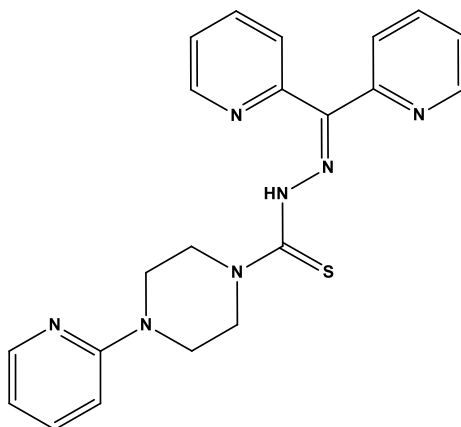
125.1, 119.4, 115.7, 49.6, 48.1. MP: 151-152°C. R_f = 0.28 [dichloromethane:methanol 40:1 (v/v)]. HRMS-EI: 402.1628 (C₂₂H₂₂N₆S; Exact Mass: 402.1627). $\text{Log}P_{\text{calc}}$: 2.744.

***N'*-(Di(pyridin-2-yl)methylene)morpholine-4-carbothiohydrazide (1c)**



Yield: 78%. Purity: 96.32%. ¹H-NMR (*d*₆-DMSO, 400 MHz, ppm): 14.50 (bs, 1H, NH), 8.85 (d, 1H, *J*= 3,7 Hz), 8.61 (d, 1H, *J*= 3.5 Hz), 8.01-7.91 (m, 3H), 7.58 (m, 2H), 7.49 (m, 1H), 4.00 (m, 4H, CH₂); 3.71 (m, 4H, CH₂). ¹³C-NMR (*d*₆-DMSO, 100 MHz, ppm): 180.2, 148.3, 148.4, 138.7, 127.5, 125.1, 124.0, 68.5, 52.6. MP: 124-125°C. R_f = 0.57 [dichloromethane:ethyl acetate 8:1 (v/v)]. HRMS-EI: 327.1158 (C₁₆H₁₇N₅OS; Exact Mass: 327.1154). $\text{Log}P_{\text{calc}}$: 0.752.

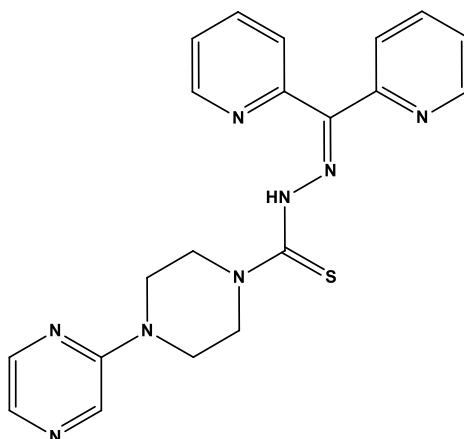
***(Z)*-N'-(Di(pyridin-2-yl)methylene)-4-(pyridin-2-yl)piperazine-1-carbothiohydrazide (1d)**



Yield: 74%. Purity: 95.62%. ¹H-NMR (*d*₆-DMSO, 400 MHz, ppm): 14.65 (bs, 1H, NH), 8.90 (d, 1H, *J*= 5.2 Hz, pyridine), 8.62 (d, 1H, *J*= 4.4 Hz, pyridine), 8.15 (dd, 1H, *J*₁= 4.6 Hz, *J*₂= 1.5 Hz, pyridine), 8.05-7.93 (m, 3H, pyridine), 7.62-7.55 (m, 3H, pyridine), 7.49 (t, 1H, *J*= 7.2 Hz, pyridine), 6.82 (d, 1H, *J*= 8.6 Hz, pyridine), 6.68 (dd,

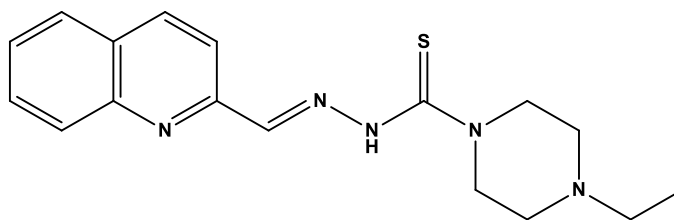
1H, $J_1 = 6.8$ Hz, $J_2 = 5.2$ Hz, pyridine), 4.15 (m, 4H, CH₂, piperazine), 3.72 (m, 4H, CH₂, piperazine). ¹³C-NMR (*d*₆-DMSO, 100 MHz, ppm): 180.7, 158.9, 148.9, 148.4, 148.0, 138.3, 137.8, 127.3, 125.1, 124.2, 113.5, 107.3, 49.0, 44.2. MP: 143-144°C. HRMS-ESI-TOF: 404.1652 [M + H]⁺ (C₂₁H₂₂N₇S; Exact Mass: 404.1657). Log*P*_{calc}: 1.796.

***N'*-(Di(pyridin-2-yl)methylene)-4-(pyrazin-2-yl)piperazine-1-carbothiohydrazide (1e)**



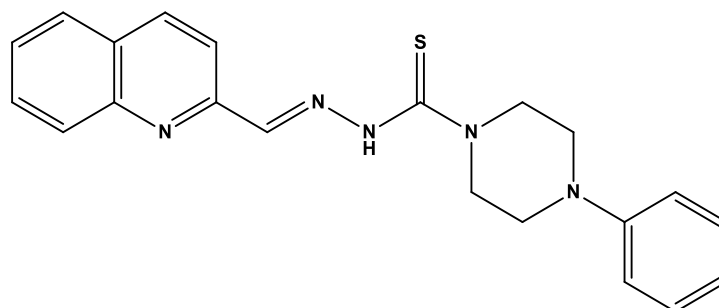
Yield: 66%. Purity: 95.45%. ¹H-NMR (*d*₆-DMSO, 400 MHz, ppm): 14.66 (bs, 1H, NH), 8.89 (d, 1H, $J = 4.7$ Hz, pyridine), 8.62 (d, 1H, $J = 4.0$ Hz), 8.31 (bs, 1H, pyrazine), 8.12 (bs, 1H, pyrazine), 8.06 – 7.91 (m, 3H, pyridine), 7.88 (d, 1H, $J = 2.2$ Hz, pyrazine), 7.61 (t, 2H, $J = 6.4$ Hz, pyridine), 7.49 (t, 1H, $J = 5.6$ Hz, pyridine), 4.18 (m, 4H, CH₂, piperazine), 3.80 (m, 4H, CH₂, piperazine). ¹³C-NMR (*d*₆-DMSO, 100 MHz, ppm): 180.7, 154.5, 149.4, 148.9, 148.4, 141.9, 138.2, 137.8, 127.3, 125.1, 124.2, 48.8, 43.5. MP: 175-176°C. HRMS-ESI-TOF: 405.1606 [M + H]⁺ (C₂₀H₂₁N₈S; Exact Mass: 405.1610). Log*P*_{calc}: 1.031.

(*E*)-4-Ethyl-*N'*-(quinolin-2-ylmethylene)piperazine-1-carbothiohydrazide (2a)



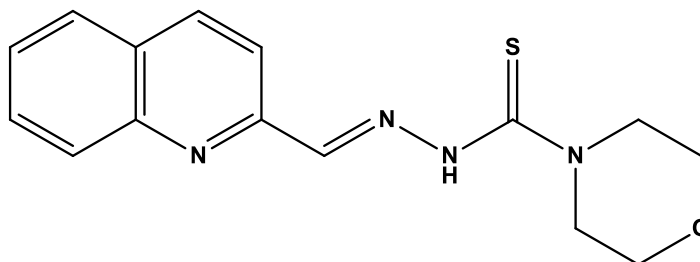
Yield: 78%. Purity: 96.67%. ¹H-NMR (*d*₆-DMSO, 400 MHz, ppm): 8.39 (d, 1H, *J* = 8.7 Hz, quinoline), 8.32 (s, 1H, CH), 8.03-7.98 (m, 3H, quinoline), 7.77 (t, 1H, *J* = 8.4 Hz, quinoline), 7.62 (t, 1H, *J* = 7.8 Hz, quinoline), 3.97 (m, 4H, CH₂, piperazine), 2.51 (m, 6H, CH₂, piperazine, CH₂-CH₃), 1.04 (t, 3H, *J* = 7.2 Hz, CH₂-CH₃). ¹³C-NMR (*d*₆-DMSO, 100 MHz, ppm): 181.1, 154.3, 147.8, 144.2, 137.1, 130.5, 129.2, 128.5, 128.2, 127.6, 117.7, 52.6, 51.8, 50.5, 12.3. MP: 168-169°C. *R*_f = 0.48 [dichloromethane:ethanol 10:1 (v/v)]. HRMS-ESI-TOF: 350.1414 [M + Na]⁺ (C₁₇H₂₁N₅SNa; Exact Mass: 350.1415). Log*P*_{calc}: 2.883.

(*E*)-4-Phenyl-*N'*-(quinolin-2-ylmethylene)piperazine-1-carbothiohydrazide (2b)



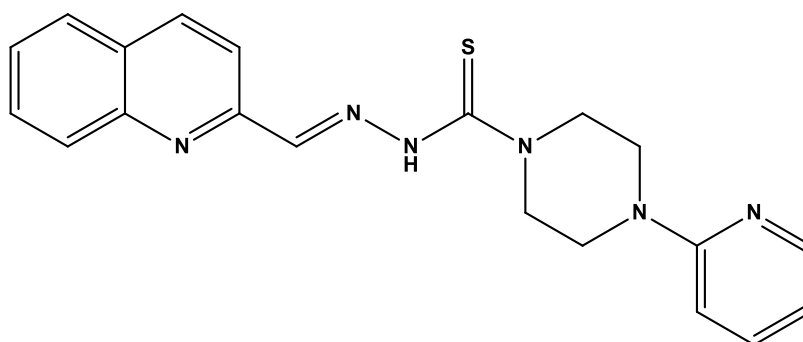
Yield: 81%. Purity: 98.00%. ¹H-NMR (*d*₆-DMSO, 400 MHz, ppm): 11.66 (bs, 1H, NH), 8.39 (d, 1H, *J* = 8.7 Hz, quinoline), 8.35 (s, 1H, CH), 8.03 (d, 2H, *J* = 8.5 Hz, quinoline), 7.99 (d, 1H, *J* = 8.0 Hz, quinoline), 7.79 (t, 1H, *J* = 7.6 Hz, quinoline), 7.62 (t, 1H, *J* = 7.8 Hz, quinoline), 7.25 (t, 2H, *J* = 7.8 Hz, phenyl), 6.99 (d, 2H, *J* = 8.1 Hz, phenyl), 6.82 (t, 1H, *J* = 7.1 Hz, phenyl), 4.14 (m, 4H, CH₂, piperazine), 3.32 (m, 4H, CH₂, piperazine). ¹³C-NMR (*d*₆-DMSO, 100 MHz, ppm): 181.2, 154.3, 150.9, 147.9, 144.4, 137.1, 130.5, 129.5, 129.3, 128.5, 128.2, 127.6, 119.6, 117.8, 116.0, 50.3, 48.5. MP: 162-163°C. HRMS-ESI-TOF: 376.1591 [M + H]⁺ (C₂₁H₂₂N₅S; Exact Mass: 376.1596). Log*P*_{calc}: 3.785.

(*E*)-*N'*-(Quinolin-2-ylmethylene)morpholine-4-carbothiohydrazide (2c)



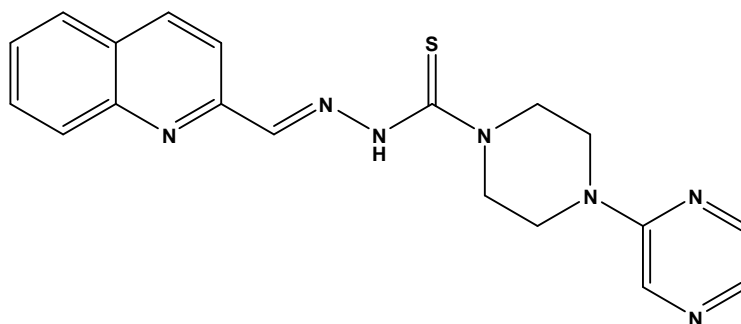
Yield: 85%. Purity: 97.42%. $^1\text{H-NMR}$ (d_6 -DMSO, 400 MHz, ppm): 11.61 (bs, 1H, NH), 8.38 (d, 1H, $J = 8.7$ Hz, quinoline), 8.32 (s, 1H, CH), 8.01 (m, 3H, quinoline), 7.80 (t, 1H, $J = 8.0$ Hz, quinoline), 7.64 (t, 1H, $J = 6.4$ Hz, quinoline), 3.99 (m, 4H, piperazine), 3.72 (m, 4H, piperazine). $^{13}\text{C-NMR}$ (d_6 -DMSO, 100 MHz, ppm): 181.4, 154.3, 147.8, 144.4, 137.1, 130.5, 129.3, 128.4, 128.2, 127.6, 117.7, 66.5, 51.2. MP: 145-146°C. HRMS-EI: 300.1034 ($\text{C}_{15}\text{H}_{16}\text{N}_4\text{OS}$; Exact Mass: 300.1045). $\text{Log}P_{\text{calc}}$: 1.793.

(*E*)-4-(Pyridin-2-yl)-*N'*-(quinolin-2-ylmethylene)piperazine-1-carbothiohydrazide (2d)



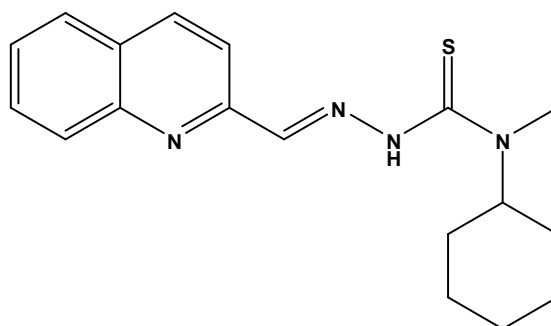
Yield: 69%. Purity: 97.87%. $^1\text{H-NMR}$ (d_6 -DMSO, 400 MHz, ppm): 11.50 (bs, 1H, NH), 8.38 (m, 2H, quinoline, pyridine), 8.16 (d, 1H, $J = 4.0$ Hz, pyridine), 8.03 (d, 2H, $J = 8.6$ Hz, quinoline), 7.98 (d, 1H, $J = 8.0$ Hz, quinoline), 7.79 (t, 1H, $J = 7.2$ Hz, quinoline), 7.64-7.56 (m, 2H, quinoline, pyridine), 6.85 (d, 1H, $J = 8.8$ Hz, pyridine), 6.68 (t, 1H, $J = 5.2$ Hz, pyridine), 4.12 (m, 4H, piperazine), 3.71 (m, 4H, piperazine). $^{13}\text{C-NMR}$, (d_6 -DMSO, 100 MHz, ppm): 181.5, 159.0, 154.3, 148.0, 147.9, 144.5, 138.0, 137.1, 130.4, 129.3, 128.4, 128.2, 127.6, 117.8, 113.6, 107.5, 50.2, 44.7. MP: 133-134°C. HRMS-ESI-TOF: 377.1549 [$\text{M} + \text{H}$] $^+$ ($\text{C}_{20}\text{H}_{21}\text{N}_6\text{S}$; Exact Mass: 377.1548). $\text{Log}P_{\text{calc}}$: 2.837.

(E)-4-(Pyrazin-2-yl)-N'-(quinolin-2-ylmethylene)piperazine-1-carbothiohydrazide
(2e)



Yield: 96%. Purity: 98.98%. $^1\text{H-NMR}$ (d_6 -DMSO, 400 MHz, ppm): 11.77 (bs, 1H, NH), 8.39 (d, 1H, $J= 8.7$ Hz), 8.35 (m, 2H, CH, pyrazine), 8.13 (m, 1H), 8.03 (m, 2H), 8.00 (d, 1H, $J= 7.8$ Hz), 7.89 (d, 1H, $J= 2.4$ Hz), 7.79 (t, 1H, $J= 7.0$ Hz), 7.63 (t, 1H, $J= 7.9$ Hz), 4.13 (m, 4H, piperazine), 3.78 (m, 4H, piperazine). $^{13}\text{C-NMR}$ (d_6 -DMSO, 100 MHz, ppm): 181.3, 154.7, 154.3, 147.9, 144.4, 141.9, 137.1, 133.1, 131.7, 130.5, 129.3, 128.5, 128.2, 127.6, 117.8, 49.9, 44.0. MP: 188-189° C. HRMS-ESI-TOF: 378.1498 $[\text{M} + \text{H}]^+$ ($\text{C}_{19}\text{H}_{20}\text{N}_7\text{S}$; Exact Mass: 378.1501). $\text{Log}P_{\text{calc}}$: 2.072.

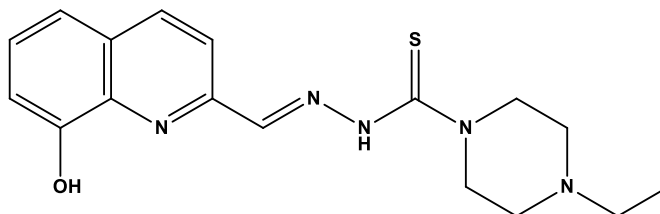
(E)-N-Cyclohexyl-N-methyl-2-(quinolin-2-ylmethylene)hydrazinecarbothioamide
(2f)



Yield: 58%. Purity: 99.12%. $^1\text{H-NMR}$ (d_6 -DMSO, 400 MHz, ppm): 11.25 (bs, 1H, NH), 8.39 (m, 2H, CH, quinoline), 8.03-7.98 (m, 3H, quinoline), 7.78 (t, 1H, $J= 8.0$ Hz, quinoline), 7.62 (t, 1H, $J= 7.6$ Hz, quinoline), 4.74 (bs, 1H, C_1 -cyclohexyl), 3.14 (s, 3H, CH_3), 1.80 (m, 4H, cyclohexyl), 1.58 (m, 3H, cyclohexyl), 1.30 (m, 2H, cyclohexyl), 1.15 (t, 1H, $J= 12.0$ Hz, cyclohexyl). $^{13}\text{C-NMR}$ (d_6 -DMSO, 100 MHz, ppm): 181.1, 154.5, 147.9, 144.2, 137.0, 130.5, 129.2, 128.4, 128.1, 127.5, 117.7, 61.2,

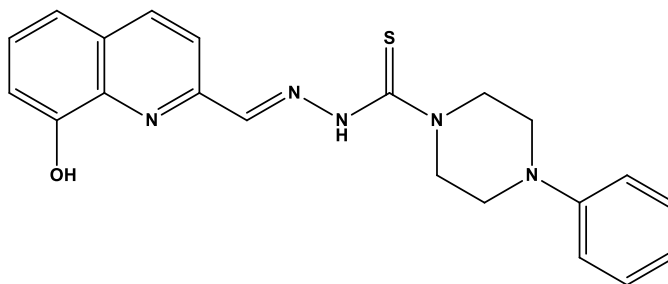
39.8, 34.9, 29.7, 25.8, 25.7, 25.4. MP: 125-126°C. HRMS-EI: 326.1564 (C₁₈H₂₂N₄S; Exact Mass: 326.1565). Log*P*_{calc}: 4.145.

(Z)-4-Ethyl-N'-((8-hydroxyquinolin-2-yl)methylene)piperazine-1-carbothiohydrazide (3a)



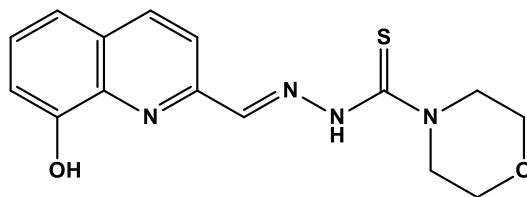
Yield: 74%. Purity: 95.03%. ¹H-NMR (*d*₆-DMSO, 400 MHz, ppm): 15.29 (bs, 1H, NH), 8.33 (s, 1H, CH), 8.30 (d, 1H, *J* = 8.4 Hz, quinoline), 7.97 (d, 1H, *J* = 8.4 Hz, quinoline), 7.44 (t, 1H, *J* = 7.6 Hz), 7.38 (d, 1H, *J* = 7.2 Hz), 7.11 (d, 1H, *J* = 7.4 Hz), 3.95 (m, 4H, piperazine), 2.50 (m, 6H, piperazine, CH₂), 1.04 (t, 3H, *J* = 6.8 Hz). ¹³C-NMR (*d*₆-DMSO, 100 MHz, ppm): 181.2, 153.8, 152.3, 144.0, 138.6, 136.9, 129.1, 128.5, 118.2, 117.9, 112.6, 52.7, 51.7, 50.5, 12.4. MP: 167-168°C. HRMS-ESI-TOF: 366.1362 [M + Na]⁺ (C₁₇H₂₁N₅OSNa; Exact Mass: 366.1365). Log*P*_{calc}: 2.931.

(E)-N'-((8-Hydroxyquinolin-2-yl)methylene)-4-phenylpiperazine-1-carbothiohydrazide (3b)



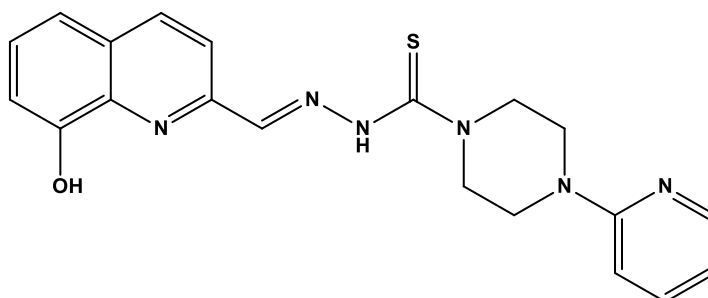
Yield: 67%. Purity: 96.59%. ¹H-NMR (*d*₆-DMSO, 400 MHz, ppm): 11.71 (bs, 1H, NH), 9.83 (bs, 1H, OH), 8.38 (bs, 1H, CH), 8.32 (d, 1H, *J* = 8.7 Hz, quinoline), 8.01 (d, 1H, *J* = 8.7 Hz, quinoline), 7.44 (m, 1H, quinoline), 7.39 (m, 1H), 7.25 (t, 2H, *J* = 7.9 Hz, phenyl), 7.13 (d, 1H, *J* = 7.1 Hz), 6.99 (d, 2H, *J* = 8.2 Hz, phenyl), 6.82 (t, 1H, *J* = 7.1 Hz, phenyl), 4.13 (m, 4H, piperazine), 3.32 (m, 4H, piperazine). ¹³C-NMR (*d*₆-DMSO, 100 MHz, ppm): 181.3, 153.8, 152.3, 151.0, 144.2, 138.6, 137.0, 129.5, 129.2, 128.6, 119.6, 118.3, 117.9, 115.9, 112.7, 50.4, 48.6. MP: 175-176°C. HRMS-ESI-TOF: 392.1540 [M + H]⁺ (C₂₁H₂₂N₅OS; Exact Mass: 392.1545). Log*P*_{calc}: 3.833.

(E)-N'-((8-Hydroxyquinolin-2-yl)methylene)morpholine-4-carbothiohydrazide (3c)



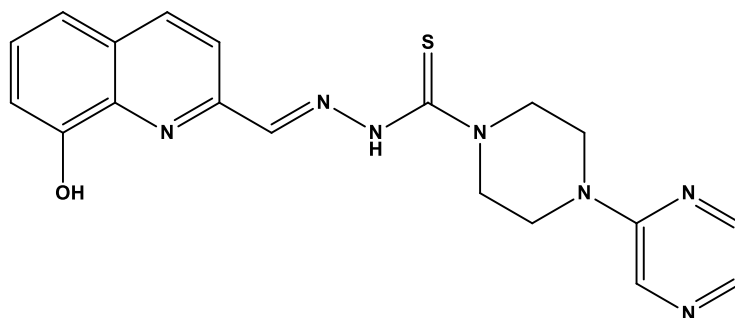
Yield: 76%. Purity: 95.77%. $^1\text{H-NMR}$ (d_6 -DMSO, 400 MHz, ppm): 11.66 (bs, 1H, NH), 9.81 (bs, 1H, OH), 8.35 (s, 1H, CH), 8.30 (d, 1H, $J = 8.7$ Hz, quinoline), 7.97 (d, 1H, $J = 8.7$ Hz, quinoline), 7.45 (t, 1H, $J = 7.7$ Hz, quinoline), 7.39 (d, 1H, $J = 7.6$ Hz, quinoline), 7.12 (d, 1H, $J = 7.1$ Hz, quinoline), 3.98 (m, 4H, piperazine), 3.72 (m, 4H, piperazine). $^{13}\text{C-NMR}$ (d_6 -DMSO, 100 MHz, ppm): 181.4, 153.8, 152.2, 144.3, 138.6, 137.0, 129.1, 128.6, 118.3, 117.9, 112.6, 66.5, 51.2. MP: 181-182°C. HRMS-EI: 316.0984 ($\text{C}_{15}\text{H}_{16}\text{N}_4\text{O}_2\text{S}$; Exact Mass: 316.0994). $\text{Log}P_{\text{calc}}$: 1.841.

(E)-N'-((8-Hydroxyquinolin-2-yl)methylene)-4-(pyridin-2-yl)piperazine-1-carbothiohydrazide (3d)



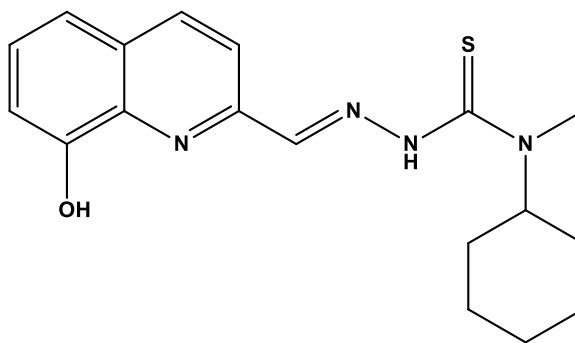
Yield: 77%. Purity: 99.25%. $^1\text{H-NMR}$ (d_6 -DMSO, 400 MHz, ppm): 11.70 (bs, 1H, NH), 9.82 (bs, 1H, OH), 8.38 (s, 1H, CH), 8.31 (d, 1H, $J = 8.7$ Hz, quinoline), 8.16 (d, 1H, $J = 4.8$ Hz, pyridine), 8.02 (d, 1H, $J = 8.7$ Hz, quinoline), 7.58 (m, 1H, pyridine), 7.45 (t, 1H, $J = 7.6$ Hz, quinoline), 7.39 (d, 1H, $J = 7.9$ Hz, quinoline), 7.13 (d, 1H, $J = 7.3$ Hz, quinoline), 6.86 (d, 1H, $J = 8.6$ Hz, pyridine), 6.68 (m, 1H, pyridine), 4.11 (m, 4H, piperazine), 3.70 (m, 4H, piperazine). $^{13}\text{C-NMR}$ (d_6 -DMSO, 100 MHz, ppm): 181.3, 159.0, 153.8, 152.3, 148.0, 144.2, 138.6, 138.1, 137.0, 129.1, 128.6, 118.3, 118.0, 113.6, 112.6, 107.5, 50.2, 44.7. MP: 176-177°C. HRMS-ESI-TOF: 393.1490 [$\text{M} + \text{H}$] $^+$ ($\text{C}_{20}\text{H}_{21}\text{N}_6\text{O}\text{S}$; Exact Mass: 393.1498). $\text{Log}P_{\text{calc}}$: 2.885.

(E)-N'-((8-Hydroxyquinolin-2-yl)methylene)-4-(pyrazin-2-yl)piperazine-1-carbothiohydrazide (3e)



Yield: 86%. Purity: 99.8%. $^1\text{H-NMR}$ (d_6 -DMSO, 400 MHz, ppm): 11.72 (bs, 1H, NH), 9.82 (bs, 1H, OH), 8.38 (s, 1H, CH), 8.36 (m, 1H, pyrazine), 8.31 (d, 1H, $J=8.7$ Hz, quinoline), 8.13 (m, 1H, pyrazine), 8.02 (d, 1H, $J=8.7$ Hz, quinoline), 7.89 (m, 1H, pyrazine), 7.45 (t, 1H, $J=7.6$ Hz, quinoline), 7.39 (d, 1H, $J=7.5$ Hz, quinoline), 7.13 (d, 1H, $J=6.7$ Hz, quinoline), 4.13 (m, 4H, piperazine), 3.78 (m, 4H, piperazine). $^{13}\text{C-NMR}$ (d_6 -DMSO, 100 MHz, ppm): 181.4, 154.7, 153.8, 152.2, 144.3, 141.9, 138.6, 137.0, 133.1, 131.7, 129.2, 128.6, 118.3, 118.0, 112.6, 49.9, 44.0. MP: 200-201°C. HRMS-ESI-TOF: 394.1448 $[\text{M} + \text{H}]^+$ ($\text{C}_{19}\text{H}_{20}\text{N}_7\text{OS}$; Exact Mass: 394.1450). $\text{Log}P_{\text{calc}}$: 2.121.

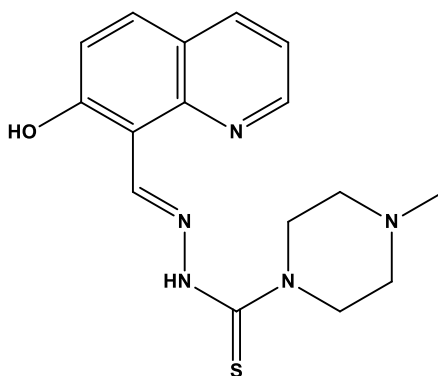
(E)-N-Cyclohexyl-2-((8-hydroxyquinolin-2-yl)methylene)-N-methylhydrazinecarbo-thioamide (3f)



Yield: 65%. Purity: 98.01%. $^1\text{H-NMR}$ (d_6 -DMSO, 400 MHz, ppm): 11.33 (bs, 1H, NH), 9.77 (bs, 1H, OH), 8.39 (s, 1H, CH), 8.30 (d, 1H, $J=8.8$ Hz, quinoline), 7.99 (d, 1H, $J=8.8$ Hz, quinoline), 7.44 (t, 1H, $J=7.6$ Hz, quinoline), 7.38 (dd, 1H, $J_1=8.0$ Hz; $J_2=1.2$ Hz, quinoline), 7.11 (dd, 1H, $J_1=7.2$ Hz; 1.2 Hz, quinoline), 4.74 (bs, 1H, C_1 -cyclohexyl), 3.14 (s, 3H, CH_3), 1.80 (m, 4H, cyclohexyl), 1.58 (m, 3H, cyclohexyl),

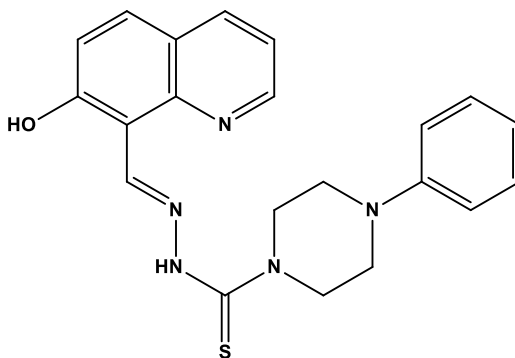
1.32 (m, 2H, cyclohexyl), 1.16 (t, 1H, $J = 11.4$ Hz, cyclohexyl). $^{13}\text{C-NMR}$ (d_6 -DMSO, 100 MHz, ppm): 181.2, 153.8, 152.5, 144.1, 138.6, 136.9, 129.1, 128.4, 118.3, 117.90, 112.6, 61.2, 39.8, 35.0, 29.7, 25.7, 25.4. MP: 164-165°C. HRMS-EI: 342.1513 ($\text{C}_{18}\text{H}_{22}\text{N}_4\text{OS}$; Exact Mass: 342.1514). $\text{Log}P_{\text{calc}}$: 4.193.

(*E*)-4-Ethyl-*N'*-((7-hydroxyquinolin-8-yl)methylene)piperazine-1-carbothiohydrazide (4a)



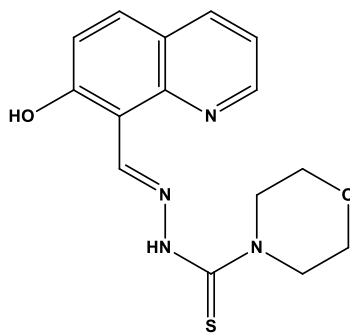
Yield: 76.5%. Purity: 95.35%. $^1\text{H-NMR}$ (d_6 -DMSO, 400 MHz, ppm): 13.23 (bs, 1H, NH), 11.59 (bs, 1H, OH), 9.76 (s, 1H, CH), 8.84 (d, 1H; $J = 2.8$ Hz, quinoline), 8.30 (d, 1H; $J = 8.1$ Hz, quinoline), 7.92 (d, 1H, $J = 9.0$ Hz, quinoline), 7.42 (dd, 1H, $J_1 = 8.1$ Hz, $J_2 = 4.3$ Hz, quinoline), 7.28 (d, 1H, $J = 9.0$ Hz, quinoline), 3.97 (m, 4H, piperazine), 2.51 (m, 6H, piperazine, CH_2), 1.05 (t, $J = 7.2$ Hz, 3H, CH_3). $^{13}\text{C-NMR}$ (d_6 -DMSO, 100 MHz, ppm): 179.2, 160.4, 150.6, 147.0, 144.9, 136.9, 131.6, 122.2, 120.8, 119.7, 111.0, 52.3, 51.7, 48.2, 12.1. MP: 145-146°C. HRMS-EI: 343.1464 ($\text{C}_{17}\text{H}_{21}\text{N}_5\text{OS}$; Exact Mass: 343.1467). $\text{Log}P_{\text{calc}}$: 2.931.

(*E*)-*N'*-((7-Hydroxyquinolin-8-yl)methylene)-4-phenylpiperazine-1-carbothiohydrazide (4b)



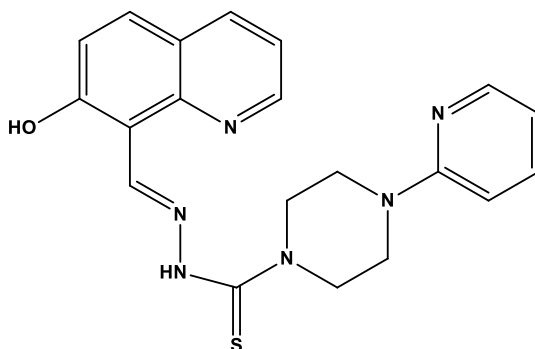
Yield: 67%. Purity: 96.12%. $^1\text{H-NMR}$ (d_6 -DMSO, 400 MHz, ppm): 13.14 (bs, 1H, NH), 11.83 (bs, 1H, OH), 9.83 (s, 1H, CH), 8.87 (m, 1H, quinoline), 8.32 (d, 1H, $J = 8.0$ Hz, quinoline), 7.95 (d, 1H, $J = 9.0$ Hz, quinoline), 7.45 (dd, 1H, $J_1 = 8.0$ Hz, $J_2 = 4.2$ Hz, quinoline), 7.31 (d, 1H, $J = 8.9$ Hz, quinoline), 7.25 (t, 2H, $J = 7.7$ Hz, phenyl), 7.00 (d, 2H, $J = 8.2$ Hz, phenyl), 6.82 (t, 1H, $J = 7.1$ Hz, phenyl), 4.13 (m, 4H, piperazine), 3.29 (m, 4H, piperazine). $^{13}\text{C-NMR}$ (d_6 -DMSO, 100 MHz, ppm): 179.2, 159.8, 150.9, 150.7, 146.9, 145.2, 137.0, 131.6, 129.5, 122.4, 120.4, 119.9, 119.6, 115.9, 111.2, 48.3, 48.2. MP: 212-213°C. HRMS-EI: 391.1470 ($\text{C}_{21}\text{H}_{21}\text{N}_5\text{OS}$; Exact Mass: 391.1467). $\text{Log}P_{\text{calc}}$: 3.833.

(E)-N'-((7-Hydroxyquinolin-8-yl)methylene)morpholine-4-carbothiohydrazide (4c)



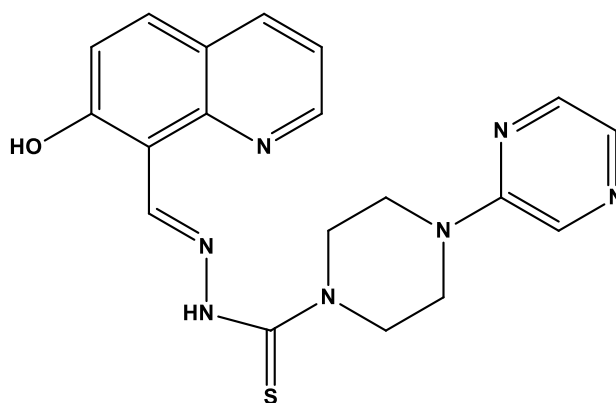
Yield: 76%. Purity: 96.22%. $^1\text{H-NMR}$ (d_6 -DMSO, 400 MHz, ppm): 13.10 (bs, 1H, NH), 11.75 (bs, 1H, OH), 9.81 (s, 1H, CH), 8.87 (m, 1H, quinoline), 8.33 (d, 1H, $J = 7.8$ Hz, quinoline), 7.95 (d, 1H, $J = 9.0$ Hz, quinoline), 7.45 (dd, 1H, $J_1 = 8.0$ Hz, $J_2 = 4.3$ Hz, quinoline), 7.31 (d, 1H, $J = 8.9$ Hz, quinoline), 3.97 (m, 4H, piperazine), 3.69 (m, 4H, piperazine). $^{13}\text{C-NMR}$ (d_6 -DMSO, 100 MHz, ppm): 179.5, 159.7, 150.7, 146.8, 145.3, 137.1, 131.6, 122.4, 120.4, 119.9, 111.2, 66.2, 49.1. MP: 198-199°C. HRMS-EI: 316.0982 ($\text{C}_{15}\text{H}_{16}\text{N}_4\text{O}_2\text{S}$; Exact Mass: 316.0994). $\text{Log}P_{\text{calc}}$: 1.841.

(E)-N'-((7-Hydroxyquinolin-8-yl)methylene)-4-(pyridin-2-yl)piperazine-1-carbothiohydrazide (4d)



Yield: 72%. Purity: 95.29%. ¹H-NMR (*d*₆-DMSO, 400 MHz, ppm): 13.14 (bs, 1H, NH), 11.80 (s, 1H, OH), 9.83 (s, 1H, CH), 8.86 (dd, 1H, *J*₁ = 4.2, *J*₂ = 1.6 Hz, quinoline), 8.32 (dd, 1H, *J*₁ = 8.2, *J*₂ = 1.7 Hz, quinoline), 8.15 (dd, 1H, *J*₁ = 4.9, *J*₂ = 1.6 Hz, pyridine), 7.95 (d, 1H, *J* = 9.0 Hz, quinoline), 7.58 (ddd, 1H, *J*₁ = 8.8, *J*₂ = 7.2, *J*₃ = 1.9 Hz, pyridine), 7.45 (dd, 1H, *J*₁ = 8.2 Hz, *J*₂ = 4.3 Hz, quinoline), 7.32 (d, 1H, *J* = 8.6 Hz, quinoline), 6.87 (d, 1H, *J* = 8.6 Hz, pyridine), 6.68 (dd, 1H, *J*₁ = 7.0, *J*₂ = 5.0 Hz, pyridine), 4.11 (m, 4H, piperazine), 3.66 (m, 4H, piperazine). ¹³C-NMR (*d*₆-DMSO, 100 MHz, ppm): 179.2, 159.3, 158.9, 150.6, 148.0, 146.9, 145.2, 138.1, 137.0, 131.6, 122.3, 120.4, 119.8, 113.7, 111.9, 107.5, 56.5, 48.1. MP: 186-187°C. HRMS-ESI-TOF: 393.1493 [M + H]⁺ (C₂₀H₂₁N₆OS; Exact Mass: 393.1498). Log*P*_{calc}: 2.885.

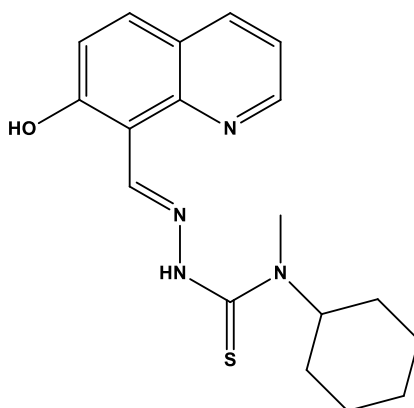
(E)-N'-((7-Hydroxyquinolin-8-yl)methylene)-4-(pyrazin-2-yl)piperazine-1-carbothiohydrazide (4e)



Yield: 76%. Purity: 98.37%. ¹H-NMR (*d*₆-DMSO, 400 MHz, ppm): 13.13 (bs, 1H, NH), 11.82 (bs, 1H, OH), 9.84 (s, 1H, CH), 8.87 (d, 1H, *J* = 2.5 Hz, quinoline), 8.37 (s, 1H, pyrazine), 8.33 (d, 1H, *J* = 7.9 Hz, quinoline), 8.13 (s, 1H, pyrazine), 7.95 (d, 1H, *J* = 9.0 Hz, quinoline), 7.89 (d, 1H, *J* = 2.3 Hz, pyrazine), 7.45 (dd, 1H, *J*₁ = 8.0,

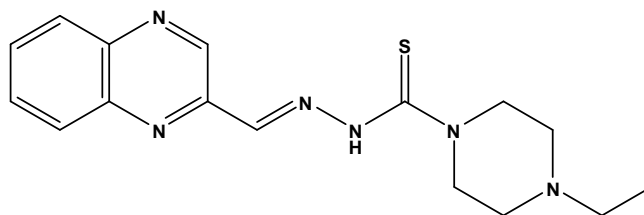
$J_2 = 4.2$ Hz, quinoline), 7.32 (d, 1H, $J = 8.4$ Hz, quinoline), 4.13 (m, 4H, piperazine), 3.74 (m, 4H, piperazine). $^{13}\text{C-NMR}$ (d_6 -DMSO, 100 MHz, ppm): 179.3, 159.8, 154.7, 150.7, 146.9, 145.3, 141.9, 137.0, 133.1, 131.8, 131.6, 122.4, 120.4, 119.9, 111.2, 56.5, 47.8. MP: 209-210°C. HRMS-ESI-TOF: 394.1446 $[\text{M} + \text{H}]^+$ ($\text{C}_{19}\text{H}_{20}\text{N}_7\text{OS}$; Exact Mass: 394.1450). $\text{Log}P_{\text{calc}}$: 2.121.

(E)-N-Cyclohexyl-2-((7-hydroxyquinolin-8-yl)methylene)-N-methylhydrazine carbothioamide (4f)



Yield: 76%. Purity: 95.46%. $^1\text{H-NMR}$ (d_6 -DMSO, 400 MHz, ppm): 13.26 (bs, 1H, NH), 11.20 (bs, 1H, OH), 9.82 (s, 1H, CH), 8.85 (dd, 1H, $J_1 = 4.0$ Hz; $J_2 = 1.6$ Hz, quinoline), 8.30 (dd, $J_1 = 8.0$ Hz, $J_2 = 1.9$ Hz, quinoline), 7.92 (d, 1H, $J = 9.0$ Hz, quinoline), 7.43 (dd, 1H, $J_1 = 8.1$ Hz, $J_2 = 4.3$ Hz, quinoline), 7.29 (d, 1H, $J = 9.0$ Hz, quinoline), 5.00 (bs, 1H, C₁-cyclohexyl), 3.10 (s, 3H, CH₃), 1.79 (m, 4H, cyclohexyl), 1.50 (m, 3H, cyclohexyl), 1.35 (m, 2H, cyclohexyl), 1.06 (t, 1H, $J = 6.8$ Hz, cyclohexyl). $^{13}\text{C-NMR}$ (d_6 -DMSO, 100 MHz, ppm): 179.0, 160.1, 150.5, 147.0, 144.8, 136.9, 131.4, 122.3, 120.6, 119.7, 111.2, 59.5, 32.7, 29.6, 25.7, 25.4, 24.2. MP: 184-185°C. HRMS-EI: 342.1512 ($\text{C}_{18}\text{H}_{22}\text{N}_4\text{OS}$; Exact Mass: 342.1514). $\text{Log}P_{\text{calc}}$: 4.1935.

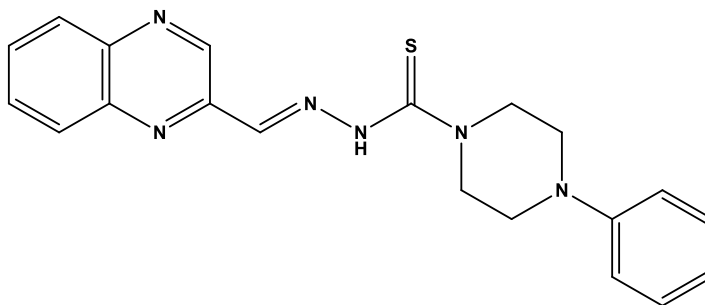
(E)-4-Ethyl-N'-(quinoxalin-2-ylmethylene)piperazine-1-carbothiohydrazide (5a)



Yield: 86%. Purity: 96.00%. $^1\text{H-NMR}$ (d_6 -DMSO, 500 MHz, ppm): 11.69 (bs, 1H, NH), 9.34 (s, 1H, quinoxaline), 8.32 (s, 1H, quinoxaline), 8.09 (t, 2H, $J = 9.1$ Hz,

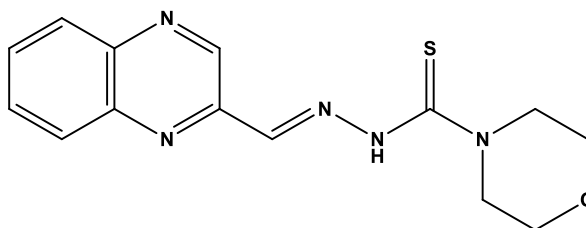
quinoxaline), 7.91 – 7.80 (m, 2H, quinoxaline), 3.98 (m, 4H, piperazine), 3.34 (m, 4H, piperazine), 2.39 (q, 2H, $J = 7.1$ Hz, CH₂), 1.04 (t, 3H, $J = 7.2$ Hz, CH₃). ¹³C-NMR (*d*₆-DMSO, 125 MHz, ppm): 181.0, 149.1, 148.9, 143.2, 141.8, 141.8, 131.2, 130.9, 129.4, 129.4, 52.7, 51.8, 50.7, 12.4. MP: 150-151°C. HRMS-ESI-TOF: 329.1544 [M + H]⁺ (C₁₆H₂₁N₆S; Exact Mass: 329.1548). Log*P*_{calc}: 2.136.

(*E*)-4-Phenyl-*N'*-(quinoxalin-2-ylmethylene)piperazine-1-carbothiohydrazide (5b)



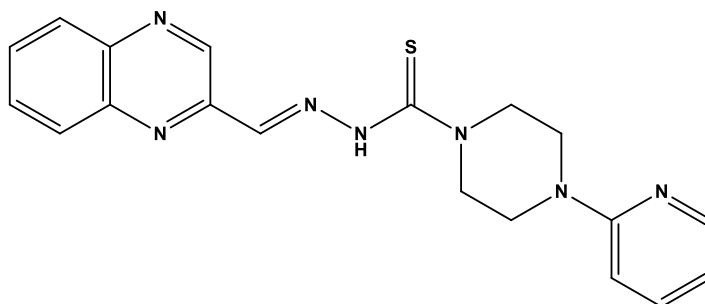
Yield: 69%. Purity: 99.10%. ¹H-NMR (*d*₆-DMSO, 400 MHz, ppm): 11.82 (bs, 1H, NH), 9.39 (s, 1H, quinoxaline), 8.36 (s, 1H; CH), 8.10 (t, 2H, $J = 7.2$ Hz, quinoxaline), 7.87 (m, 2H, quinoxaline), 7.26 (t, 2H, $J = 8.0$ Hz, phenyl), 7.00 (d, 2H, $J = 8.1$ Hz, phenyl), 6.82 (t, 1H, $J = 7.2$ Hz, phenyl), 4.15 (m, 4H, piperazine), 3.33 (m, 4H, piperazine). ¹³C-NMR (*d*₆-DMSO, 100 MHz, ppm): 181.1; 150.9; 149.1; 143.3; 142.0; 141.9; 141.8; 131.2; 130.9; 129.5; 129.5; 119.6; 115.9; 50.4; 48.5. MP: 168-169°C. HRMS-ESI-TOF: 377.1546 [M + H]⁺ (C₂₀H₂₁N₆S; Exact Mass: 377.1548). Log*P*_{calc}: 3.038.

(*E*)-*N'*-(Quinoxalin-2-ylmethylene)morpholine-4-carbothiohydrazide (5c)



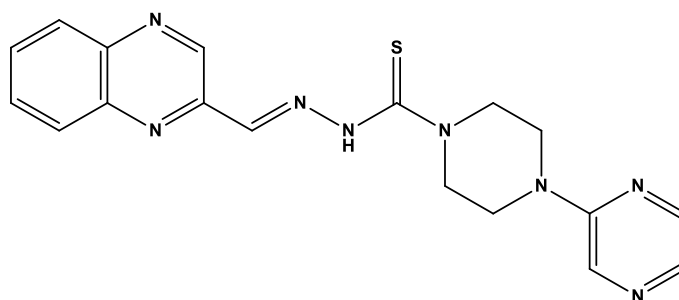
Yield: 83%. Purity: 99.00%. ¹H-NMR (*d*₆-DMSO, 400 MHz, ppm): 11.56 (bs, 1H, NH), 9.34 (s, 1H, quinoxaline), 8.33 (s, 1H, CH), 8.09 (m, 2H, quinoxaline), 7.85 (m, 2H, quinoxaline), 4.00 (m, 4H, piperazine), 3.73 (s, 4H, piperazine). ¹³C-NMR (*d*₆-DMSO, 100 MHz, ppm): 181.3, 149.0, 143.3, 142.0, 141.8, 141.7, 131.2, 130.9, 129.4, 66.5, 51.3. MP: 176-177°C. HRMS-ESI-TOF: 324.0892 [M + Na]⁺ (C₁₄H₁₅N₅OSNa; Exact Mass: 324.0895). Log*P*_{calc}: 1.046.

(E)-4-(Pyridin-2-yl)-N'-(quinoxalin-2-ylmethylene)piperazine-1-carbothiohydrazide (5d)



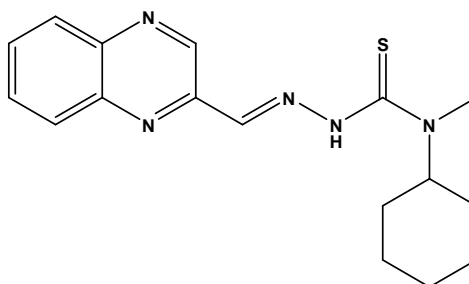
Yield: 69%. Purity: 98.45%. $^1\text{H-NMR}$ (d_6 -DMSO, 400 MHz, ppm): 11.79 (s, 1H, NH), 9.39 (s, 1H, quinoxaline), 8.36 (s, 1H, CH), 8.15 (d, 1H, $J= 3.2$ Hz, pyridine), 8.10 (m, 2H, quinoxaline), 7.87 (m, 2H, quinoxaline), 7.58 (t, 1H, $J= 7.2$ Hz, pyridine), 6.85 (d, 1H, $J= 8.0$ Hz, pyridine), 6.68 (t, 1H, $J= 5.6$ Hz, pyridine), 4.12 (m, 4H, piperazine), 3.70 (m, 4H, piperazine). $^{13}\text{C-NMR}$ (d_6 -DMSO, 100 MHz, ppm): 181.2, 159.0, 149.1, 148.1, 143.3, 141.9, 141.9, 141.8, 138.1, 131.2, 130.9, 129.5, 113.7, 107.5, 50.3, 44.7. MP: 190-191°C. HRMS-EI: 377.1405($\text{C}_{19}\text{H}_{19}\text{N}_7\text{S}$; Exact Mass: 377.1423). $\text{Log}P_{\text{calc}}$: 2.09.

(E)-4-(Pyrazin-2-yl)-N'-(quinoxalin-2-ylmethylene)piperazine-1-carbothiohydrazide (5e)



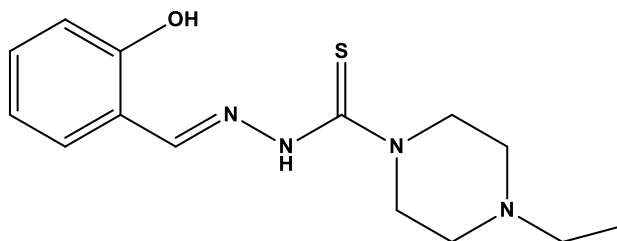
Yield: 79 %. Purity: 95.37%. $^1\text{H-NMR}$ (d_6 -DMSO, 400 MHz, ppm): 11.81 (bs, 1H, NH), 9.40 (s, 1H, quinoxaline), 8.36 (m, 2H, CH, pyrazine), 8.13-8.08 (m, 3H, quinoxaline, pyrazine), 7.89-7.84 (m, 3H, quinoxaline, pyrazine), 4.15 (m, 4H, piperazine), 3.79 (m, 4H, piperazine). $^{13}\text{C-NMR}$ (d_6 -DMSO, 100 MHz, ppm): 181.2, 154.7, 149.1, 143.3, 142.0, 141.9, 141.9, 141.8, 133.1, 131.7, 131.2, 130.9, 129.4, 129.3, 50.01, 44.0. MP: 186-187°C. HRMS-ESI-TOF: 401.1270 [$\text{M} + \text{Na}$] $^+$ ($\text{C}_{18}\text{H}_{18}\text{N}_8\text{SNa}$; Exact Mass: 401.1273). $\text{Log}P_{\text{calc}}$: 1.325.

(E)-N-Cyclohexyl-N-methyl-2-(quinoxalin-2-ylmethylene)hydrazinecarbothioamide (5f)



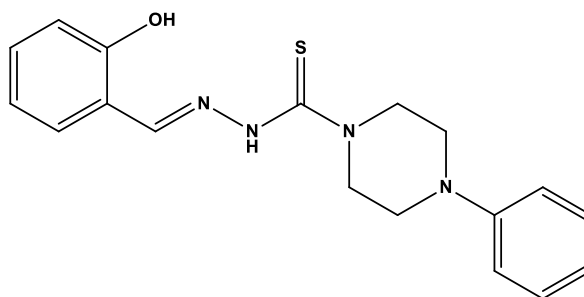
Yield: 78%. Purity: 98.70%. $^1\text{H-NMR}$ (d_6 -DMSO, 400 MHz, ppm): 11.44 (bs, 1H, NH), 9.36 (s, 1H, quinoxaline), 8.38 (s, 1H, CH), 8.12-8.07 (m, 2H, quinoxaline), 7.88-7.85 (m, 2H, quinoxaline), 4.74 (bs, 1H, C₁-cyclohexyl), 3.16 (s, 3H, CH₃), 1.80 (m, 4H, cyclohexyl), 1.58 (m, 3H, cyclohexyl), 1.32 (m, 2H, cyclohexyl), 1.16 (t, 1H, $J = 12.8$ Hz, cyclohexyl). $^{13}\text{C-NMR}$ (d_6 -DMSO, 100 MHz, ppm): 181.0, 149.3, 143.2, 141.9, 141.8, 131.2, 130.8, 129.4, 129.4, 61.3, 35.1, 29.7, 25.7, 25.4. MP: 154-155°C. HRMS-EI: 327.1513 (C₁₇H₂₁N₅S; Exact Mass: 327.1518). Log P_{calc} : 3.398.

(E)-4-Ethyl-N'-(2-hydroxybenzylidene)piperazine-1-carbothiohydrazide (6a)



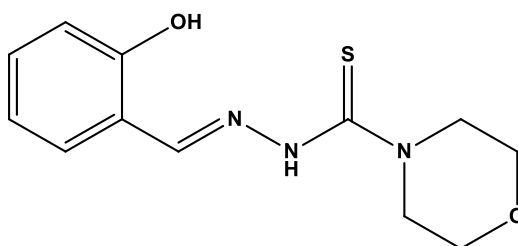
Yield: 86%. Purity: 95.2%. $^1\text{H-NMR}$ (d_6 -DMSO, 400 MHz, ppm): 11.60 (bs, 1H, NH), 8.46 (s, 1H, CH), 7.41 (dd, 1H, $J_1 = 7.9$ Hz, $J_2 = 1.6$ Hz, phenyl), 7.27 (td, 1H, $J_1 = 7.8$ Hz, $J_2 = 7.4$ Hz, $J_3 = 1.7$ Hz, phenyl), 6.92-6.88 (m, 2H, phenyl), 3.92 (m, 4H, piperazine), 2.45 (m, 4H, piperazine), 2.35 (m, 2H, CH₂), 1.03 (t, 3H, $J = 7.2$ Hz, CH₃). $^{13}\text{C-NMR}$ (d_6 -DMSO, 100 MHz, ppm): 183.0, 159.0, 148.0, 138.0, 128.5, 121.2, 118.6, 117.5, 57.2, 44.4, 12.5. MP: 160-161°C. HRMS-ESI-TOF: 293.1434 [$\text{M} + \text{H}$]⁺ (C₁₄H₂₁N₄OS; Exact Mass: 293.1436). Log P_{calc} : 2.832.

(E)-N'-(2-Hydroxybenzylidene)-4-phenylpiperazine-1-carbothiohydrazide (6b)



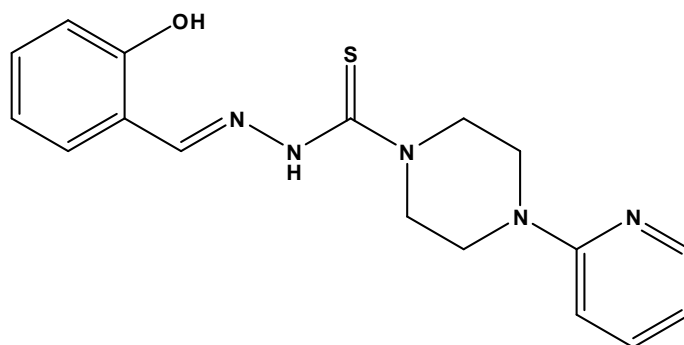
Yield: 89%. Purity: 96.12%. MP: 206-207°C [207-209°C; [4]].

(E)-N'-(2-Hydroxybenzylidene)morpholine-4-carbothiohydrazide (6c)



Yield: 91%. Purity: 95.96%. MP: 196-197°C [195°C; [4]].

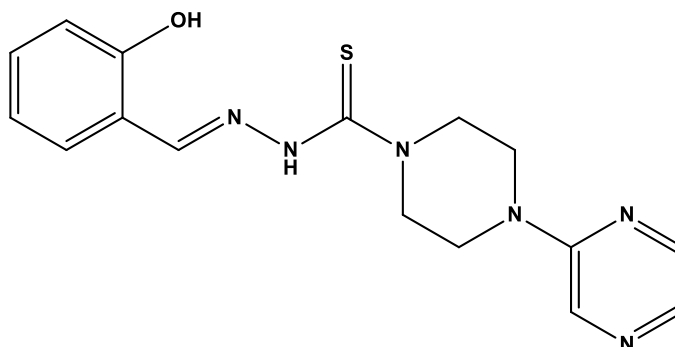
(E)-N'-(2-Hydroxybenzylidene)-4-(pyridin-2-yl)piperazine-1-carbothiohydrazide (6d)



Yield: 88%. Purity: 99.3%. ¹H-NMR (*d*₆-DMSO, 400 MHz, ppm): 11.56 (bs, 1H, NH), 11.54 (bs, 1H, OH), 8.50 (s, 1H, CH), 8.15 (dd, 1H, *J*₁ = 4.7 Hz, *J*₂ = 1.4 Hz, pyridine), 7.58 (ddd, *J*₁ = 8.9 Hz, *J*₂ = 7.2 Hz, *J*₃ = 1.9 Hz, pyridine), 7.45–7.40 (m, 1H, phenyl), 7.32–7.24 (m, 2H, phenyl), 6.91 (dd, 1H, *J*₁ = 7.7, *J*₂ = 4.5 Hz, phenyl), 6.86 (d, 1H, *J* = 8.6 Hz, pyridine), 6.68 (dd, 1H, *J*₁ = 6.9 Hz, *J*₂ = 5.0 Hz), 4.14–3.98 (m, 4H, piperazine), 3.67–3.59 (m, 4H, piperazine). ¹³C-NMR (*d*₆-DMSO, 100 MHz, ppm): 179.8, 158.9, 157.6, 148.0, 146.8, 138.1, 131.3, 130.4, 119.5, 119.0, 117.0, 113.7,

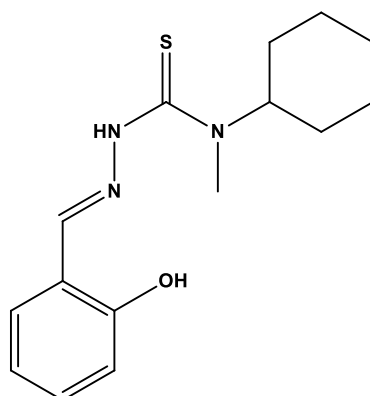
107.5, 48.4, 44.4. MP: 191-192°C. HRMS-ESI-TOF: 342.1385 [M+H]⁺ (C₁₇H₂₀N₅OS; Exact Mass: 342.1389). Log*P*_{calc}: 2.283.

(E)-N'-(2-Hydroxybenzylidene)-4-(pyrazin-2-yl)piperazine-1-carbothiohydrazide (6e)



Yield: 89%. Purity: 98.9%. ¹H-NMR (*d*₆-DMSO, 400 MHz, ppm): 11.56 (bs, 1H, NH), 11.54 (bs, 1H, OH), 8.51 (s, 1H, CH), 8.35 (d, 1H, *J* = 1.6 Hz, pyrazine), 8.12 (s, 1H, pyrazine), 7.88 (d, 1H, *J* = 2.6 Hz, pyrazine), 7.43 (dd, 1H, *J*₁ = 7.8 Hz, *J*₂ = 1.7 Hz, phenyl), 7.28 (t, 1H, *J* = 8.0 Hz, phenyl), 6.97–6.82 (m, 2H, phenyl), 4.09 (m, 4H, piperazine), 3.73 (m, 4H, piperazine). ¹³C-NMR (*d*₆-DMSO, 100 MHz, ppm): 179.8, 157.6, 154.7, 141.9, 133.1, 131.8, 131.4, 130.4, 119.6, 119.0, 117.0, 48.1, 43.7. MP: 189-190°C. HRMS-ESI-TOF: 343.1343 (C₁₆H₁₉N₆OS; Exact Mass: 343.1341). Log*P*_{calc}: 1.518.

(E)-N-Cyclohexyl-2-(2-hydroxybenzylidene)-N-methylhydrazinecarbothioamide (6f)



Yield: 74%. Purity: 95.89%. ¹H-NMR (*d*₆-DMSO, 400 MHz, ppm): 11.73 (bs, 1H, NH), 11.13 (bs, 1H, OH), 8.52 (s, 1H, CH), 7.38 (dd, 1H, *J*₁ = 7.8, *J*₂ = 1.4 Hz, 1H, phenyl), 7.27 (t, 1H, *J* = 7.6 Hz, phenyl), 6.94–6.85 (m, 2H, phenyl), 4.98 (bs, 1H, C₁-

cyclohexyl), 3.07 (s, 3H, CH₃), 1.79 (m, 4H, cyclohexyl), 1.50 (m, 3H, cyclohexyl), 1.29 (m, 2H, cyclohexyl), 1.14 (t, 1H, *J* = 15.4 Hz, cyclohexyl). ¹³C-NMR (*d*₆-DMSO, 100 MHz, ppm): 179.4, 157.6, 146.8, 131.2, 130.6, 119.5, 118.9, 117.0, 59.8, 32.9, 29.5, 25.7, 25.4. MP: 145-146°C. HRMS-EI: 291.1401 (C₁₅H₂₁N₃OS; Exact Mass: 291.1405). Log*P*_{calc}: 3.591.

S1.2 X-ray data for selected thiosemicarbazones and thiosemicarbazides

X-ray crystal data were collected on an Oxford Diffraction Gemini A Ultra diffractometer using graphite monochromated Mo K α radiation at a temperature of 295.0(2) K with ω scan mode. Polarization, Lorentz and empirical absorption corrections were applied using spherical harmonics implemented in the SCALE3 ABSPACK scaling algorithm (CrysAlis RED, Oxford Diffraction Ltd., Version 1.171.29.2). The structures were solved by direct methods and subsequently completed from Fourier difference recycling. All the non-hydrogen atoms were refined anisotropically using full-matrix, least-squares analysis. All hydrogen atoms were located from the difference maps after four cycles of anisotropic refinement, and refined using a riding model. The OLEX2 [7], SHELXS97 and SHELXL97 [8] programs were used for all calculations. All data were deposited with the Cambridge Crystallographic Data Center (CCDC 918418 & 919683).

Figure S1. The crystal structure of 4-ethylpiperazine-1-carbothiohydrazide (**a**).

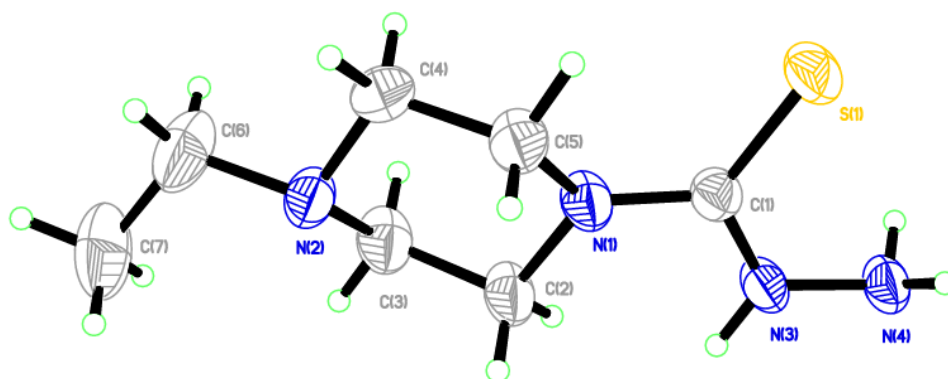


Figure S2. The crystal structure of *Z*-*N'*-(di(pyridin-2-yl)methylene)-4-(pyridin-2-yl)piperazine-1-carbothiohydrazide (**1d**).

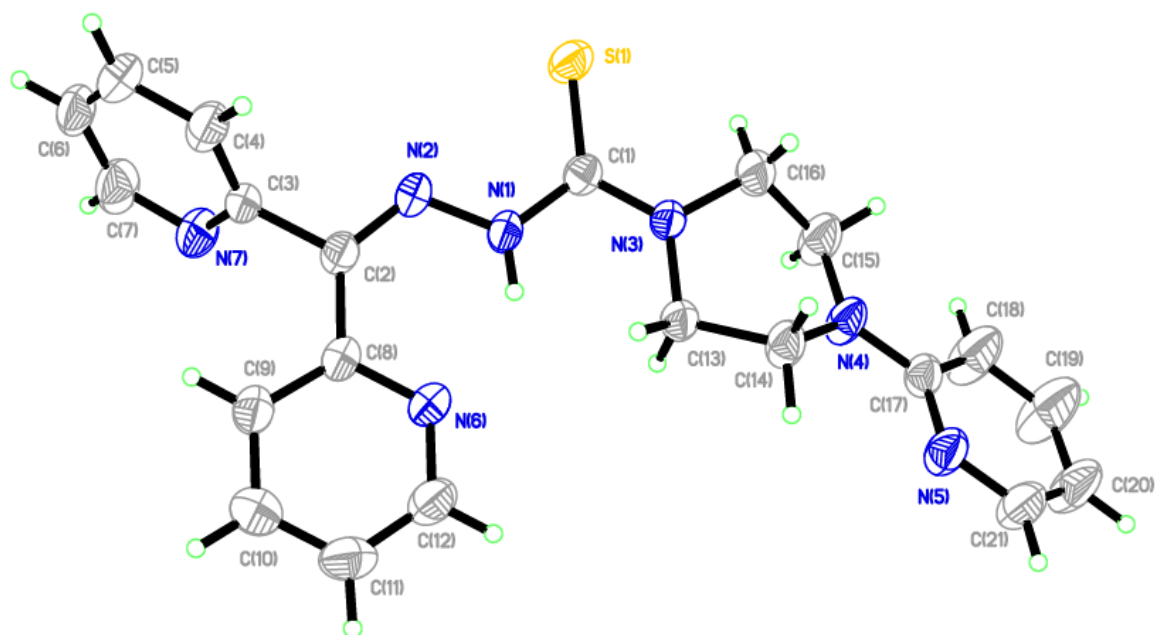


Table S1. Crystal data of **a** and **1d**.

	4-Ethylpiperazine-1-carbothiohydrazide (a)	Z-N'-(Di(pyridin-2-yl)methylene)-4-(pyridin-2-yl)piperazine-1-carbothiohydrazide (1d)
Formula	C ₇ H ₁₆ N ₄ S	C ₂₁ H ₂₁ N ₇ S
Formula weight	188.3	403.51
Crystal system	Monoclinic	Triclinic
Space group	<i>C2/c</i>	<i>P</i> $\bar{1}$
Color	White	Yellow
a (Å)	12.3069(7)	9.2850(6)
b (Å)	8.0115(4)	9.5201(8)
c (Å)	21.0221(12)	11.6512(7)
α (°)	90	76.265(6)
β (°)	101.825(6)	88.780(5)
γ (°)	90	79.734(6)
V (Å³)	2028.72(19)	984.19(12)
T (K)	295	295
D_{Calc} (mg/m³)	1.233	1.362
Z	8	2
R₁ (obsd data)	0.0350(1490)	0.0444(2603)
wR₂ (all data)	0.0934(1789)	0.1174(3480)
CCDC no.	918418	919683

S1.3 HPLC purity data

Table S2. HPLC purity data for all chelators of series 1-6.

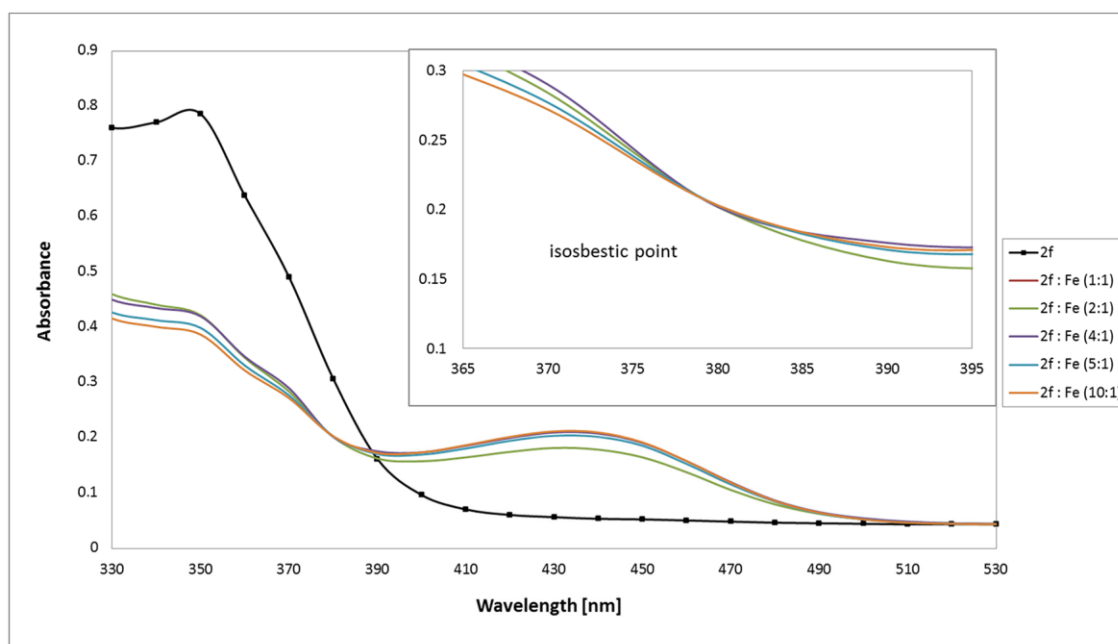
Compound	t_R (min)	Purity (%)
1a	2.34	97.32
1b	2.07	98.65
1c	2.15	96.32
1d	2.15	95.62
1e	2.25	95.45
2a	1.98	96.67
2b	1.96	98.00
2c	2.0	97.42
2d	2.05	97.87
2e	2.02	98.98
2f	1.98	99.12
3a	2.4	95.03
3b	2.5	96.59
3c	2.52	95.77
3d	2.39	99.25
3e	2.53	99.8
3f	2.56	98.01
4a	2.0	95.35
4b	2.01	96.12
4c	2.07	96.22
4d	1.98	98.00
4e	2.1	98.37
4f	2.01	95.46
5a	1.99	96.00
5b	1.98	99.10
5c	2.0	99.00
5d	2.05	98.45
5e	2.11	95.37
5f	1.98	98.70

6a	2.54	95.2
6b	1.96	96.12
6c	2.00	95.96
6d	2.02	99.3
6e	2.06	98.9
6f	1.97	95.89

S1.4 Isosbestic curves

The ligand and complexes were prepared by dissolving the ligand (0.1 mM) in DMSO and various concentrations of FeCl₃ were added to obtain the following ligand:Fe³⁺ ratios: 1:1, 2:1, 4:1, 5:1, and 10:1. The collected spectra were overlaid to observe isosbestic points.

Figure S3. The absorbance spectrum of **2f** and its Fe³⁺ complexes prepared *in situ* to obtain 1:1, 2:1, 4:1, 5:1, and 10:1 ligand:Fe ratios.



S2. References

1. Ghose AK, Crippen GM (1987) Atomic physicochemical parameters for three-dimensional-structure-directed quantitative structure–activity relationships. 2. Modeling dispersive and hydrophobic interactions. *J Chem Inf Comput Sci* 27: 21-35.
2. Viswanadhan VN, Ghose AK, Revankar GR, Robins RK (1987) Atomic physicochemical parameters for 3-dimensional-structure directed quantitative structure–activity relationships 4. Additional parameters for hydrophobic and dispersive interactions and their application for an automated superposition of certain naturally-occurring nucleoside antibiotics. *J Chem Inf Comput Sci* 29: 163–172.
3. Broto P, Moreau G, Vandycke C (1984) Molecular structures: Perception, autocorrelation descriptor and SAR studies. System of atomic contributions for the calculation of the n-octanol/water partition coefficients. *Eur J Med Chem Chim Theor* 19: 71-78.
4. Spalinska K, Foks H, Kedzia A, Wierzbowska M, Kwapisz E, et al. (2006) Synthesis and antibacterial activity of substituted thiosemicarbazides and of 1,3,4-thiadiazole or 1,2,4-triazole derivatives. *Phospho Sulfur* 181: 609-625.
5. Milczarska B, Foks H, Zwolska Z (2005) Studies on pyrazine derivatives, XLII: Synthesis and tuberculostatic activity of 6-(1,4-dioxo-8-azaspiro-[4, 5]-decano)- and 6-(1-ethoxycarbonylpiperazino)-pyrazinocarboxylic acid derivatives. *Phospho Sulfur* 180: 1977-1992.
6. Lovejoy DB, Sharp DM, Seebacher N, Obeidy P, Prichard T, et al. (2012) Novel second-generation di-2-pyridylketone thiosemicarbazones show synergism with standard chemotherapeutics and demonstrate potent activity against lung cancer xenografts after oral and intravenous administration in vivo. *J Med Chem* 55: 7230-7244.
7. Dolomanov OV, Bourhis LJ, Gildea RJ, Howard JAK, Puschmann H (2009) OLEX2: A complete structure solution, refinement and analysis program. *J Appl Cryst* 42: 339-341.

8. Sheldrick GM (2008) A short history of SHELX. *Acta Cryst A*64: 112-122.

Příloha V

Potůčková E, Roh J, Macháček M, Stariat J, Šesták V, Jansová H, Hašková P, Jirkovská A, Vávrová K, Kovaříková P, Richardson DR, Šimůnek T. *In vitro* characterization of pharmacological properties of the anticancer iron chelator Bp4eT and its phase I metabolites.

***In vitro* characterization of pharmacological properties of the anticancer iron chelator Bp4eT and its phase I metabolites.**

**Eliška Potůčková¹, Jaroslav Roh², Miloslav Macháček¹, Ján Stariat³, Vít Šesták³,
Hana Jansová¹, Pavlína Hašková¹, Anna Jirkovská¹, Kateřina Vávrová², Petra
Kovaříková³, Des R. Richardson⁴, Tomáš Šimůnek^{1,*}**

¹Department of Biochemical Sciences, Charles University in Prague, Faculty of Pharmacy in Hradec Králové, Czech Republic.

²Department of Inorganic and Organic Chemistry, Charles University in Prague, Faculty of Pharmacy in Hradec Králové, Czech Republic.

³Department of Pharmaceutical Chemistry and Drug Control, Charles University in Prague, Faculty of Pharmacy in Hradec Králové, Czech Republic.

⁴Molecular Pharmacology and Pathology Program, Bosch Institute and Department of Pathology, University of Sydney, Sydney, Australia.

***Author for correspondence:**

Dr. Tomáš Šimůnek

Charles University in Prague, Faculty of Pharmacy

Department of Biochemical Sciences

Heyrovského 1203

500 05 Hradec Králové

Czech Republic

Tel.: +420-495-067-422; Fax: +420-495-067-168

E-mail: Tomas.Simunek@faf.cuni.cz

Abstract

2-benzoylpyridine 4-ethyl-3-thiosemicarbazone (Bp4eT) is novel antineoplastic and antiretroviral thiosemicarbazone iron chelator. Recently, the metabolites of Bp4eT were identified after its incubation with human and rat liver microsomal fractions as well as in plasma, urine and feces after i.v. administration of Bp4eT to rats. Bp4eT undergoes oxidation to N^3 -ethyl- N^1 -[phenyl(pyridin-2-yl)methylene] formamidrazone and to 2-benzoylpyridine 4-ethyl-3-semicarbazone. The aim of this study was to characterize the cytotoxic activities of Bp4eT and its metabolites on both cancer cells (HL-60 human promyelocytic leukemia, MCF-7 human breast adenocarcinoma, HCT116 human colon carcinoma and A549 human lung adenocarcinoma) and normal cell lines (H9c2 neonatal rat-derived cardiomyoblasts and 3T3 mouse embryo fibroblasts) and to assess their abilities to mobilize iron from cells and to form redox active complexes with iron. The abilities to bind intracellular labile iron pool, the ^{59}Fe mobilization from cells and the prevention of iron uptake from ^{59}Fe -labeled human transferrin were examined on MCF-7 cells. The same cell line was also used for cell cycle analysis and the assessments of the mode(s) of cell death. Bp4eT was confirmed as a highly potent and selective antineoplastic agent that induces S phase cell cycle arrest, mitochondrial depolarization and apoptosis. Both studied metabolites showed at least 300 times lower cytotoxic activities towards all studied cell lines as compared to their parent substance. Both metabolites also lost the abilities to promote redox cycling of iron ions, to bind iron from labile cellular pool, ^{59}Fe mobilizing activity and at the same time they almost did not prevent the ^{59}Fe uptake from ^{59}Fe -labeled transferrin. Hence, this study demonstrates that highly active iron chelator Bp4eT is metabolized to non-toxic and pharmacologically inactive substances, which is important for further development of this drug candidate.

Keywords:

Iron chelator; Thiosemicarbazone; Bp4eT; Antineoplastic agent; Metabolism.

Abbreviations:

Bp4eA; N^3 -ethyl- N^1 -[phenyl(pyridine-2yl)methylene]formamidrazne; Bp4eS, 2-benzoylpyridine 4-ethylsemicarbazone; Bp4eT, 2-benzoylpyridine 4-ethyl-3-thiosemicarbazone; DFO, deferoxamine; EDTA, ethylenediaminetetraacetic acid; IC_{50} , half-maximal inhibitory concentration; IBE, iron binding equivalents; LIP, labile iron pool; MDC, monodansyl cadaverine; ROS, reactive oxygen species.

1 Introduction

Iron chelation therapy was originally designed to alleviate the toxic effects of excess iron evident in iron-overload diseases. However, some iron chelator-metal complexes have also gained interest due to their high redox activity and cytotoxic properties that have potential for cancer chemotherapy (Buss, Torti et al. 2003; Saletta, Rahmanto et al. 2011). The subgroup of thiosemicarbazone iron chelators showed high antineoplastic efficiency in both *in vitro* and *in vivo* studies and some substances also in phase I clinical trials (Lane, Mills et al. 2014). 2-Benzoylpyridine 4-ethyl-3-thiosemicarbazone (Bp4eT) is one of the thiosemicarbazones with favorable properties for potential use in anticancer treatment (Kalinowski, Yu et al. 2007; Merlot, Pantarat et al. 2010; Debebe, Nekhai et al. 2012).

Bp4eT was firstly synthesized and described by West *et al.* (West, Ives et al. 1995). Later, it was shown to be an iron chelator with low $Fe^{3+/2+}$ redox potential (Kalinowski, Yu et al. 2007) which results in toxic reactive oxygen species (ROS) formation in solution (Kalinowski, Yu et al. 2007) and also in SK-N-MC human neuroepithelioma cells (Stefani, Punnia-Moorthy et al. 2011). Bp4eT has shown high cytotoxic activity towards SK-N-MC human neuroblastoma cells and low toxicity to human fibroblasts MRC-5 (Stefani, Punnia-Moorthy et al. 2011). During the 28-day administration of Bp4eT to mice, no alterations of body or organ weights, hematological indices or organ histology were observed and the mice remained healthy for up to 7 weeks (Yu, Suryo Rahmanto et al. 2012), even though, the study of Quach et al. (Quach, Gutierrez et al. 2012) showed an ability of Bp4eT to potentiate methemoglobin formation in red blood cells and their lysates. However, the methemoglobin formation of Bp4eT was weaker than that caused by other well-known thiosemicarbazones, Dp44mT or triapine (Quach, Gutierrez et al. 2012).

Apart from anticancer activity, the inhibition potential of Bp4eT towards HIV-1 transcription was studied (Debebe, Ammosova et al. 2011). Bp4eT showed high inhibition activity towards HIV-1 transcription with low toxicity to CEM cells (Debebe, Ammosova et al. 2011). The IC_{50} (half-maximal inhibitory concentration) of Bp4eT on HIV-1 transcription using 293T cells was comparable to clinically used antiretrovirotic agent, roscovitin (Debebe, Ammosova et al. 2011).

To choose a right route for administration to live organism the investigation of transport across enterocytes and cell membranes is very important. Debebe et al studied

the transport across enterocytes on confluent monolayers of Caco-2 cells (Debebe, Nekhai et al. 2012), that are established model for enterocytes (Delie and Rubas 1997). Their results show that Bp4eT can permeate through Caco-2 monolayers with permeability values similar to orally administered drugs (Debebe, Nekhai et al. 2012). The other study processed by Merlot et al. observed the cellular uptake of Bp4eT by cancer cells using ^{14}C -labeled Bp4eT (Merlot, Pantarat et al. 2010; Merlot, Pantarat et al. 2013). These studies found out that Bp4eT crossed the cellular membrane of SK-N-MC neuroepithelioma cells by passive diffusion (Merlot, Pantarat et al. 2010) and that the Bp4eT-iron complexes accumulated in the cells in higher amount than free Bp4eT (Merlot, Pantarat et al. 2013). The body distribution and the excretion ways of ^{14}C -labeled Bp4eT were studied on mice (Merlot, Pantarat et al. 2013). Bp4eT was rapidly excreted by urine when the highest amount of Bp4eT was excreted after 1 h post injection. The excretion by feces was slowed down by passing through gastrointestinal tract and it reached the maximal excreted dose after 24 h after injection. The main deposition of Bp4eT in a mouse body was observed in excretion tissues (Merlot, Pantarat et al. 2013).

Using the LC/MS methods, Bp4eT was identified to exist in two isomer forms *E* and *Z*. The solid Bp4eT is presented only in its *Z* form and it is converted to *E* isomer in water environment (Stariat, Kovarikova et al. 2010). In recent study, three phase I metabolites of Bp4eT following its incubation with rat or human liver subcellular fractions and *in vivo* experiments were identified (Stariat, Sestak et al. 2012). The Bp4eT was oxidized to its semicarbazone analog 2-benzoylpyridine-4-ethyl-3-semicarbazone (Bp4eS) and to N^3 -ethyl- N^1 -[phenyl(pyridin-2-yl)methylene]formamidrazone (Bp4eA) metabolite which was further hydroxylated. Unfortunately the specific localization of that hydroxyl group on the phenyl ring was not possible to identify (Stariat, Sestak et al. 2012). The Bp4eS metabolite was identified in two isomers *E* and *Z* that were, in contrast to the mother substance Bp4eT, both stable in solid form. The analysis revealed that *E*-Bp4eT was converted to *E*-Bp4eS and *Z*-Bp4eT to *Z*-Bp4eS (Stariat, Suprunova et al. 2013). In the initial pharmacokinetic study, basic pharmacokinetic parameters for Bp4eT and Bp4eA were calculated. Whereas the exposition of Bp4eS was below 1.5 % of the Bp4eT (100 %), the Bp4eA metabolite appeared to be more important because its exposition was calculated to 20 % of the parent substance (Stariat, Suprunova et al. 2013).

Metabolites may represent an important part in pharmacological properties of some drugs as the observed effects can be aggregates of effects exerted by various intermediates formed within the body (Chiu, Thompson et al. 1995; Lin and Lu 1997). Hence, in this study, we aimed to characterize *in vitro* cytotoxic activities of Bp4eT and its two well defined metabolites, Bp4eA and Bp4eS (Fig. 1) on four human cancer cell lines and two non-cancerous cell lines. We examined the capability of the substances to bind iron from labile iron pool (LIP) in cancer cells, and also to mobilize ^{59}Fe from cells and to prevent the uptake of ^{59}Fe from $^{59}\text{Fe}_2\text{transferrin}$ to cells. The ability of iron complexes of Bp4eT and its metabolites to promote ROS formation was investigated using ascorbate oxidation assay. Furthermore, the cell cycle progression and a mode of cell death after their exposure to Bp4eT and its metabolites were determined.

2 Materials and methods

2.1 Chemicals

Bp4eT was synthesized according to Kalinowski et al. (Kalinowski, Yu et al. 2007) and its metabolites were synthesized as described by Stariat et al. (Stariat, Sestak et al. 2012; Stariat, Suprunova et al. 2013). Constituents for various buffers and other chemicals (*e.g.*, various iron salts) were purchased from Sigma-Aldrich (St. Luis, MO, USA) or Penta (Prague, Czech Republic) and were of the highest pharmaceutical or analytical grade available.

2.2 Cell cultures

The MCF-7 human breast adenocarcinoma cell line was purchased from the European Collection of Cell Cultures (ECACC; Salisbury, UK). The HL-60 human promyelocytic leukemia cells, HCT116 human colorectal carcinoma cells, A549 human lung adenocarcinoma cells, H9c2 cell line, derived from embryonic rat heart tissue, and 3T3 mouse embryo fibroblasts were obtained from the American Type Culture Collection (ATCC; Manassas, VA, USA). MCF-7, HCT116, A549, 3T3 and H9c2 cells were cultured in Dulbecco's modified Eagle's medium (DMEM; Lonza, Basel, Switzerland) with or, in case of MCF-7 cells, without phenol red, supplemented with 10% (v/v) heat-inactivated fetal bovine serum (FBS; Lonza), 1% penicillin/streptomycin solution (Lonza) and 10 mM HEPES buffer (pH 7.0 - 7.6; Sigma-Aldrich). HL-60 cells were maintained in RPMI medium (Sigma-Aldrich) supplemented with 10% heat-inactivated FBS and 1% penicillin/streptomycin solution. All the cell lines were cultured in 75 cm² tissue culture flasks (TPP, Trasadingen, Switzerland) at 37°C in a humidified atmosphere of 5% CO₂. Sub-confluent cells or, in case of HL-60 cells, a thick suspension, were sub-cultured every 3-4 days.

2.3 Cytotoxicity studies

For cytotoxicity experiments on cancer cells, cells were seeded in 96-well plates (TPP) at a density of 5,000 cells per well (MCF-7), 10,000 cells per well (HL-60) or 2,000 cells per well (HCT116 and A549). Cells were seeded in the plates 24 h prior an addition of studied substances. For cytotoxicity studies on non-cancerous cells, the 3T3

and H9c2 cells were seeded in 96-well plates at a density of 10,000 cells per well and 24 h after the seeding and 24 h prior to the experiments, the medium was changed to serum- and pyruvate-free DMEM (Sigma-Aldrich). Cytotoxicity effects of Bp4eT and its metabolites were studied at different concentrations after 72 h incubations. In order to dissolve lipophilic agents, 0.1% dimethyl sulfoxide (v/v) (DMSO; Sigma-Aldrich) was present in the culture medium of all groups. At this concentration DMSO had no effect on cellular proliferation or viability. Viabilities of cells were determined using MTT assay, based on the ability of active mitochondria to change yellow 3-(4,5-dimethylthiazol-2-yl)-2,5-diphenyltetrazolium bromide tetrazole (MTT; Sigma-Aldrich) to purple formazan. The MTT assay was performed according to manufacturer's instructions. The optical density of soluble MTT was measured at $\lambda = 570$ nm, subtracting the $\lambda = 690$ nm background using Tecan Infinite 200M plate reader (Tecan Group, Männedorf, Switzerland). The viability or proliferation of experimental groups was expressed as percentage of untreated controls (100 %).

2.4 Calcein-AM assay for assessment of rate of cell membrane permeation and access to the labile iron pool

The experiments were performed according to Glickstein et al. (Glickstein, El et al. 2006) with slight modifications. MCF-7 cells were seeded in 96-well plates (10,000 cells per well) and let to adhere for 24 h. Cells were loaded with iron using the iron donor, 530 $\mu\text{g}/\text{mL}$ ferric ammonium citrate (Richardson and Baker 1992), 24 h prior to the experiment, and the cells were then washed. To prevent potential interference (especially with regard to various trace elements), the medium was replaced with the ADS buffer (prepared using Millipore water supplemented with 116 mM NaCl, 5.3 mM KCl, 1 mM CaCl₂, 1.2 mM MgSO₄, 1.13 mM NaH₂PO₄, 5 mM D-glucose, and 20 mM HEPES, pH 7.4). Cells were then loaded with a 2 μM concentration of the cell-permeable calcein green acetoxymethyl ester (calcein-AM; Molecular Probes, Oregon, USA) for 30 min/37 °C and washed. Cellular esterases cleave acetoxymethyl groups to form the cell membrane-impermeable compound, calcein green, whose fluorescence is quenched by ferric ammonium citrate. Intracellular fluorescence ($\lambda_{\text{ex}} = 488$ nm; $\lambda_{\text{em}} = 530$ nm) was then followed as a function of time (10 min after the addition of 10 μM Bp4eT or its metabolites) at 37 °C using the Tecan Infinite 200M plate reader. The iron

chelation efficiency in cells was expressed as a percentage of efficiency of the parent chelator Bp4eT (100 %).

2.5 Preparation of ^{59}Fe - transferrin

Human transferrin (Sigma) was labeled with ^{56}Fe or ^{59}Fe (PerkinElmer, Massachusetts, USA) to produce $^{56}\text{Fe}_2\text{transferrin}$ or $^{59}\text{Fe}_2\text{transferrin}$, respectively, of the final specific activity 500 pCi/pmol Fe as previously described (Richardson, Tran et al. 1995; Richardson and Milnes 1997). Unbound ^{59}Fe was removed by exhaustive vacuum dialysis against a large excess of 0.15 M NaCl buffered to pH 7.4 with 1.4 % NaHCO_3 by standard methods (Richardson, Tran et al. 1995; Richardson and Milnes 1997).

2.5.1 The effect of chelators on mobilizing cellular ^{59}Fe

To examine the ability of studied substances to mobilize ^{59}Fe from MCF-7 cells, iron efflux experiments were performed using established techniques (Baker, Richardson et al. 1992; Richardson, Tran et al. 1995). In brief, after pre-labeling of confluent MCF-7 cells on 6-well plates with $0.75\ \mu\text{M}$ ^{59}Fe -Tf for 3 h/ 37°C , the cells were washed four times with ice-cold PBS and then subsequently incubated with $25\ \mu\text{M}$ concentration of each chelator for 3 h/ 37°C . The overlying media containing released ^{59}Fe was then separated from the cells. Radioactivity was measured in both the cells and supernatant using a γ -scintillation counter (Wallac Wizard 3, Turku, Finland).

2.5.2 Effect of the chelators at preventing cellular ^{59}Fe uptake from ^{59}Fe -transferrin.

The ability of the chelators to prevent cellular ^{59}Fe uptake from ^{59}Fe -transferrin was examined using standard techniques (Becker and Richardson 1999; Richardson, Sharpe et al. 2006). In brief, confluent MCF-7 cells on 6-well plates were incubated with $0.75\ \mu\text{M}$ ^{59}Fe -Tf for 3 h/ 37°C in the presence of the $25\ \mu\text{M}$ chelators. The cells were then washed four times with ice-cold PBS and internalized ^{59}Fe was determined by incubating the cell monolayer for 30 min/ 4°C with the 1 mg/mL general protease, Pronase (Sigma-Aldrich). The cells were then removed from the monolayer with a plastic spatula and centrifuged for 1 min/ $12,000\text{g}$. The supernatant represents

membrane-bound, Pronase-sensitive ^{59}Fe that was released by the protease, while the Pronase-insensitive fraction represents internalized ^{59}Fe (Richardson, Tran et al. 1995; Becker and Richardson 1999; Richardson, Sharpe et al. 2006). The amount of internalized iron was expressed as a percentage of iron internalized by control (untreated) cells (100 %).

2.6 Ascorbate oxidation assay for analysis of redox activity of iron complexes

The ascorbate oxidation assay was used to assess the redox activities of the iron complexes of chelators in buffered solution using an established protocol (Richardson, Sharpe et al. 2006; Mladenka, Kalinowski et al. 2009). In brief, 100 μM ascorbic acid was prepared immediately prior to the experiment and incubated either alone or in the presence of 10 μM Fe^{3+} , added as ferric chloride in a 50-fold molar excess (500 μM) of citrate and chelators. Chelators were assayed at iron binding equivalents (IBE) of 0.1 (excess of iron), 1 (fully charged iron – chelator complexes) and 3 (excess of free chelator). Chelators ethylenediaminetetraacetic acid (EDTA) and deferoxamine (DFO) were used as positive and negative controls, respectively, as their redox activity has been well characterized (Chaston, Watts et al. 2004). The decrease in absorbance at 265 nm, which is proportional to ascorbate oxidation, was measured after 10 and 40 min incubation at room temperature using the Tecan Infinite 200M plate reader. The decrease of absorbance between the two time points was calculated and expressed as a percentage of control group without chelator (100 %).

2.7 Cell cycle analysis

For cell cycle analysis, the MCF-7 cells were seeded in 60 mm petri dishes at a density of 240,000 cells per dish and incubated with tested chelators for 72 h. The cells were then harvested by trypsinization, centrifuged at 300xg, washed in PBS with 5% of FBS (PBS+FBS) and suspended in small amount of PBS+FBS. Then ice-cold 70% ethanol was added drop-wise and the cells were fixed overnight at -20°C . After fixation, ethanol was removed by centrifugation, cells were washed in PBS+FBS and resuspended in 4 mM sodium citrate in PBS. Finally, the cells were incubated with 200 $\mu\text{g}/\text{mL}$ RNase A (Sigma-Aldrich) and 30 $\mu\text{g}/\text{mL}$ propidium iodide (Molecular Probes,

Eugene, OR, USA) for 30 min/37°C. Cells were analyzed using Accuri C6 flow cytometer (Becton Dickinson and Company, San Jose, CA USA). Propidium iodide was excited at 488 nm and fluorescence analyzed at 585 nm (FL-2). 10,000 events were collected per analysis.

2.8 Fluorescence microscopy assessments

The autophagy/apoptosis/necrosis staining of MCF-7 cells and changes of lysosomal and mitochondrial morphology were observed using an Eclipse Ti inverted epifluorescence microscope (Nikon, Tokyo, Japan), that was equipped with a cooled digital camera Zyla 5.5 sCMOS (Andor Technology, Belfast, UK), and NIS-Elements C 4.1 software (Laboratory Imaging, Prague, Czech Republic). The MCF-7 cells were seeded in 6-well plates with a cover slips on the bottom at a density of 150,000 cells/well and incubated as described above with or without 10 or 100 nM Bp4eT.

To determine the way of cellular death after Bp4eT administration the triple staining with monodansyl cadaverine (50 μ M; λ_{ex} = 390 nm; λ_{em} = 455 nm; MDC; Sigma-Aldrich), annexin V-FITC (5 μ l/mL; λ_{ex} = 495 nm; λ_{em} = 519 nm; Invitrogen, Carlsbad, CA, USA), and propidium iodide (5 μ g/mL; λ_{ex} = 560 nm; λ_{em} = 630 nm) was used. MDC is a specific marker of autophagosomes and lysosomes with blue fluorescence. The autophagosomes can be distinguished from lysosomes (blue dots) as they are shaped to big and bright granula. As a positive control for autophagy, MCF-7 cells incubated with 1 nM rapamycin (Sigma-Aldrich) for 30 min/37°C, as rapamycin is an established inductor of autophagy (Kralova, Benesova et al. 2012). The anticoagulant protein Annexin V has high affinity to phosphatidylserine, which is translocated to the surface of both early- and late-stage apoptotic cells (van Engeland, Nieland et al. 1998). Thus, Annexin V-FITC served as a marker of apoptosis when the apoptotic cells had green fluorescent cytoplasmic membranes. Propidium iodide intercalates to nuclear DNA and stains it with red fluorescence. Propidium iodide is a necrotic marker or a marker of late stage apoptosis as it does not permeate to cells with intact cytoplasmic membrane. The cells were incubated with the probes for 10min/37°C, then the cells were washed with fresh cultivation medium and images were captured using the microscope set-up outlined above.

To determine the influence of Bp4eT to lysosomal and mitochondrial morphology the cells were incubated with organelle specific probes LysoTracker® Blue DND-22 (2.5 μ M; λ_{ex} = 373 nm; λ_{em} = 422 nm; Molecular Probes) for lysosomes, and MitoTracker® Green FM (0.25 μ M; λ_{ex} = 490 nm; λ_{em} = 516 nm; Molecular Probes) for mitochondria for 10 min/37°C. The cells were then washed with fresh cultivation medium and images were captured using the microscope set-up outlined above.

2.9 Caspase activity assessments

For caspase activity assessment the MCF-7 cells were incubated with 100nM Bp4eT or its metabolites for 3, 24 or 72 h/37°C at 96-well plates, as described above. Then the cells were lysed by adding 100 μ l of cold lysis buffer (100 mM HEPES, 10 mM CHAPS, 10 mM DL-dithiothreitol, pH 7.4) to 100 μ l medium in each well. Lysates were immediately frozen at -80°C. Melted lysates were used for caspase activity assessments by luminescent kits for caspases 3/7, 8 and 9 (Promega, Madison, WI, USA). The luminescence was measured using Tecan Infinite 200M plate reader. Caspase activities of experimental groups were corrected for a cellular viability of each group and were expressed as a percentage of activities of untreated control (100 %).

2.10 Data analysis and statistics

SigmaStat for Windows 3.5 (Systat Software, San Jose, CA, USA) statistical software was used in this study. The data are expressed as the mean \pm SD of a given number of experiments. Statistical significance was determined using a one-way ANOVA with a Bonferroni *post-hoc* test (comparisons of multiple groups against the corresponding control). The results were considered to be statistically significant when $p < 0.05$. The IC₅₀ values were calculated using CalcuSyn 2.0 software (Biosoft, Cambridge, UK). The cell cycle analysis was evaluated using MultiCycle AV Software (Phoenix Flow Systems, San Diego, CA, USA).

3 Results and Discussion

Bp4eT is a promising antineoplastic (Kalinowski, Yu et al. 2007) and antiretroviral (Debebe, Ammosova et al. 2011) thiosemicarbazone iron chelator. However, its metabolism (Stariat, Sestak et al. 2012) and preliminary pharmacokinetics (Stariat, Suprunova et al. 2013) have been only recently described. Hence, the aim of our recent study was to investigate the *in vitro* effects of the chelator Bp4eT and its metabolites (Bp4eA and Bp4eS) and to compare the activities of Bp4eT metabolites to their parent substance.

3.1 Bp4eT is metabolized into substances with at least 300 times lower cytotoxic effects to both cancer and non-cancerous cells

The cytotoxic effects of Bp4eT and its metabolites Bp4eA (mixture of *E* and *Z* isomers) and Bp4eS (in two isomeric forms *E* and *Z*) towards cancer cells were studied using HL-60 human promyelocytic leukemia, MCF-7 human breast adenocarcinoma, HCT116 human colorectal carcinoma and A549 human lung adenocarcinoma cell lines, as well as towards two non-cancerous cells, namely H9c2 rat cardiomyoblasts, and 3T3 mouse fibroblasts. Following the 72 h incubations, the parent substance Bp4eT showed very high cytotoxic efficiency on HL-60, MCF-7 and HCT116 cells, where the IC₅₀ values ranged from 3 to 15 nM concentrations (Table 1 and Fig. 2A). The IC₅₀ value on A549 cells was still rather low (IC₅₀ = 0.593 ± 0.148 μM), nevertheless, it was comparable to the toxic effects of Bp4eT on H9c2 cells representing cardiac tissue (IC₅₀ = 0.524 ± 0.157 μM). This result can suggest possible cardiotoxicity of Bp4eT if used at concentrations for lung cancer treatment. This is consistent with the study where a methemoglobin formation activity was observed, however, this activity was lower than that of other promising thiosemicarbazones (Quach, Gutierrez et al. 2012). The IC₅₀ value for 3T3 fibroblast cells was two times higher than that for H9c2 cells. Calculated selectivity ratios of Bp4eT towards cancer cells were high for HL-60, MCF-7 and HCT116 cell lines (Table 2), which is consistent with previous studies marking Bp4eT as a potent and selective antineoplastic agent (Kalinowski, Yu et al. 2007; Miao, Xu et al. 2010). The cytotoxicity of Bp4eT towards A549 lung carcinoma was similar to the cytotoxicity towards H9c2 cells. Hence, the lung cancers seem not to be appropriate targets for Bp4eT as the effective concentration of Bp4eT for antineoplastic activity to

H1299 lung carcinoma cells (Miao, Xu et al. 2010) was similar to A549 cells in this study.

The Bp4eT metabolites showed markedly decreased cytotoxicity to both cancer and non-cancerous cell lines (Table 1 and Fig. 2) as their IC₅₀ values were at least 300 times higher than those of the parent agent. Bp4eA that was identified as the preferred metabolite of Bp4eT (Stariat, Suprunova et al. 2013) was more cytotoxic towards cancer cells from the two studied metabolites. Its IC₅₀ values on cancer cells ranged from 52 µM in HL-60 cells to 207 µM in A549 cells (Table 1). The cytotoxicity of Bp4eA towards non-cancerous cells was lower (IC₅₀ H9c2 = 416.1 ± 122.1 µM and IC₅₀ 3T3 = 1027.4 ± 203.9 µM), which is also obvious from the calculated selectivity ratios in Table 2. Importantly, the toxic concentrations of metabolites to non-proliferating cells were not reached in plasma during the pharmacokinetic study of Stariat *et al.*, where the highest concentration of Bp4eA reached after 300 minutes post *i.v.* administration of Bp4eT was under 1 µM (Stariat, Suprunova et al. 2013). This clearly suggests that Bp4eA appears in plasma in non-toxic concentrations.

Both *E* and *Z* isomers of Bp4eS metabolite were identified in plasma only at very low concentrations under the low limit of quantification (Stariat, Suprunova et al. 2013). Our results showed that this metabolite was even less antiproliferatively active than the Bp4eA (Table 1 and Fig. 2). The IC₅₀ values of Bp4eS on cancer cells ranged from 46 to 536 µM, whereas in the case of non-cancerous H9c2 and 3T3 cells they were 343 µM and >1 mM, respectively. Surprisingly, each cell line showed different sensitivity to the isomers. Whereas the HL-60 and H9c2 cells were more sensitive to *Z*-Bp4eS, MCF-7 cells were equally sensitive to both isomers, and HCT116 and A549 cells were more sensitive to *E*-Bp4eS. The selectivity of the Bp4eS cytotoxic action is not much determined, especially when the selectivity ratios are calculated for H9c2 cells. However, the cytotoxic effects appeared at so high concentrations that we can say Bp4eS has no cytotoxic effect in a body.

3.2 The effect of Bp4eT metabolites to chelate iron from labile iron pool, to mobilize cellular ^{59}Fe and to prevent cellular ^{59}Fe uptake from $^{59}\text{Fe}_2$ transferrin is negligible compared to the effect of Bp4eT

Iron chelation and withdrawing are believed to be the basis of the mechanism of action of thiosemicarbazone chelators (Kalinowski, Yu et al. 2007; Merlot, Kalinowski et al. 2013). That is why the ability of Bp4eT and its metabolites to chelate iron from LIP was investigated in this study using the calcein-AM assay. The addition of 10 μM Bp4eT caused time dependent increase of fluorescence up to 221 fluorescence units (Fig. 3A). The addition of Bp4eT metabolites had almost no effect (Fig. 3A). When we expressed the fluorescence in $t = 600$ sec as a percentage of Bp4eT fluorescence (Fig. 3B), the Bp4eA had only 5.9 % of its activity and Bp4eS even less (*E*-Bp4eS 0.0 % and *Z*-Bp4eS 1.0 %).

For investigation of the ability to promote iron mobilization from cells the MCF-7 cells were loaded by ^{59}Fe and then incubated for 3h/37°C with studied substances. Bp4eT was able to release 46.4 % of loaded ^{59}Fe from cells (Fig. 4A). Both Bp4eT metabolites did not release significantly more iron than untreated control (about 3.5 % of accumulated iron).

We also examined the ability of Bp4eT and its metabolites to prevent uptake of ^{59}Fe to MCF-7 cells from $^{59}\text{Fe}_2$ transferrin. The MCF-7 cells were co-incubated with Bp4eT or its metabolites and $^{59}\text{Fe}_2$ transferrin for 3h/37°C. When the cells were incubated with Bp4eT they absorbed only 11.5 % of the ^{59}Fe internalized by untreated control (Fig. 4B). Both Bp4eA and Bp4eS did not prevent the ^{59}Fe uptake.

From the results of all these chelation experiments we can conclude that the metabolites of Bp4eT lost their chelation abilities. Only the parent Bp4eT contains a thioamide moiety that readily tautomerizes to imidothiol moiety, allowing the sulfur atom to firmly bind the iron (Supplementary fig. 1). The iron is additionally coordinated with the pyridine and hydrazone nitrogens. The metabolite Bp4eA with a formamidrazone moiety in place of the original thiosemicarbazone does not contain sulfur, which therefore seems to be crucial chelating atom of Bp4eT. In addition, the imide double bond of such formamidrazone will most likely be conjugated with the hydrazone double bond and the resulting structure is not able to bind the iron properly.

Even if we consider the second possible localization of the formamidrazone double bond, the iron could only be chelated by three weak coordination bonds (Supplementary Fig. 1). The reason for the low chelation abilities of the semicarbazone Bp4eS is probably different. In the semicarbazone, the amide highly prevails over the imidol tautomer, thus the carbonyl oxygen of Bp4eS binds the iron less strongly compared to the sulfur atom in the parent thiosemicabazone Bp4eT (Supplementary Fig. 1).

3.3 Bp4eT metabolites do not form redox active iron complexes

Since the chelator Bp4eT was identified to form redox active complexes with iron (Kalinowski, Yu et al. 2007; Stefani, Punnia-Moorthy et al. 2011) the redox activity of Bp4eT and its metabolites was studied using the ascorbate oxidation assay. The effect of Bp4eT and its metabolites to oxidation of ascorbate in presence of iron was assayed in three IBEs (0.1; 1 and 3). IBE 1 is reached when chelator and iron create fully charged complex, in means 1 molecule of hexadentate chelator for 1 atom of iron (e.g. DFO or EDTA) or two molecules of tridentate chelators for 1 atom of iron (e.g. Bp4eT). The IBE 0.1 means the excess of iron (ten times more than chelator) and IBE 3 means three times exceed chelator to iron. The resulting change of ascorbate absorbance was expressed as percentage of control group (ascorbate with free iron, 100 %).

To see typical antioxidant and prooxidative profiles of chelators the antioxidant chelator DFO and prooxidative EDTA were assayed. DFO showed less oxidized ascorbate in IBE 3 (DFO excess) than in IBE 0.1 (iron excess) (Fig. 5). EDTA showed completely adverse profile, when in IBE 3 the amount of oxidized ascorbate was higher than in IBE 0.1. The parent substance Bp4eT showed significant ($p < 0.001$) prooxidative properties similar to that of EDTA (Fig. 5). None of the Bp4eT metabolites showed significant effect different from control values. Hence, these findings support the notion that the metabolites lost their chelation activity and that is why they also no more affect the redox behavior of iron.

3.4 Bp4eT causes cell cycle arrest in S-phase

Iron deprivation is known to cause G₁/S cell cycle arrest to rapidly proliferating cancer cells (Lederman, Cohen et al. 1984; Le and Richardson 2002). Therefore, we performed a cell cycle analysis of MCF-7 cells incubated with 100 nM Bp4eT and its

metabolites for 72 h. This concentration of Bp4eT lead to decrease of MCF-7 proliferation to 27 % of control group (Fig. 2A). Interestingly, the G₁ phase of cell cycle did not significantly ($p < 0.05$) differ from control after treatment by any of the tested substances (Fig. 6). However, following the Bp4eT treatment, the S phase was significantly ($p < 0.001$) increased to 35% compared to 15% of control group and the G₂/M phase of Bp4eT-treated cells was significantly ($p < 0.001$) decreased to 12% compared to 33% of control group. This effect show the arrest of MCF-7 cells in S phase of cell cycle, which is consistent with previous studies with other iron chelators on the MCF-7 cells (Mackova, Hruskova et al. 2012) and this seems to be typical for this cell line. Both Bp4eT metabolites did not shown any significant effect on S phase and only minimal changes in G₂/M phase (Fig. 6).

3.5 Bp4eT treatment leads to apoptosis in MCF-7 cells

The fluorescence microscopy of MCF-7 cells was used for estimation of the predominant mechanism(s) of cell death. We considered autophagy, apoptosis and necrosis. The triple staining employed the autophagy probe MDC (blue fluorescence), the monoclonal antibody for signaling molecule phosphatidylserin, annexin V-FITC conjugate (green fluorescence), and the chromatin dye of necrotic cells propidium iodide (red fluorescence). Epifluorescence microscopy revealed blue lysosomes in control (untreated) cells (Fig. 7i), whereas after the 30 min incubation with 1 nM rapamycin, a positive control substance, known to induce autophagy (Kralova, Benesova et al. 2012), there were distinctively larger blue-fluorescent autophagosomes (Fig. 7ii). After the 72 h treatment of cells by 10 and 100 nM Bp4eT, no autophagosomes were apparent (Fig. 7iii and iv), suggesting that Bp4eT does not induce an autophagy in MCF-7 cells. On the other hand, dose-dependent increase in number of AnnexinV-stained apoptotic cells or bodies with green-fluorescent plasma membrane, and late-stage apoptotic or necrotic cells with green fluorescent cellular membrane and propidium iodide-stained red nucleus was conspicuous after Bp4eT treatment (Fig. 7iii and iv).

To further distinguish the apoptotic and necrotic cell death induced by Bp4eT the double staining of lysosomes (blue fluorescence) and mitochondria (green fluorescence) was used. Lysosomes are usually enlarged and then disrupted by necrotic

cell death (Ono, Kim et al. 2003) whereas mitochondria are predominately depolarized and disrupted during apoptotic cell death, particularly following the intrinsic apoptotic pathway activation (Fulda and Debatin 2006). In Fig. 8, no difference in a number or appearance of lysosomes is apparent comparing control and Bp4eT-treated (10 and 100 nM) cells (Fig. 8). In contrast, a pronounced difference of control mitochondria and mitochondria of Bp4eT-treated cells was observed. The mitochondria of control cells were green rod-shaped particles (Fig. 8i) whereas Bp4eT treatment caused a mitochondrial swelling in both studied doses and the transition of the mitochondrial shape to granular appearance (Fig. 8ii and iii). Hence, these results further suggested the contribution of apoptosis on the Bp4eT-induced MCF-7 cell death.

To further investigate the Bp4eT and its metabolites with respect to apoptosis activation, we determined the activities of caspases - the key enzymes of apoptotic signaling. The activities of an effector caspase 7, an extrinsic apoptotic pathway caspase 8 and an intrinsic apoptotic pathway caspase 9 were measured after 3 h, 24 h and 72 h incubations of MCF-7 cells with Bp4eT or its metabolites, all in 100 nM concentration. The caspase 3 activity was not considered as MCF-7 cells are known to lack caspase 3 expression and a bypassed apoptotic cascade (Liang, Yan et al. 2001). The two Bp4eT metabolites did not activate any of tested caspases, indicating that they were unable to induce apoptosis in the applied concentration (Fig. 9). The parent chelator Bp4eT did not activate caspases after 3 h incubation (Fig. 9A), however, at 24 and 72 h time periods, the increase of caspase activity occurred (Fig. 9 B and C). Initiator caspases were increased to 125% (both caspases 8 and 9) of control after 24 h and to 189% (caspase 8) and 249% (caspase 9) of control after 72 h, suggesting rather unspecific early activation of both intrinsic and extrinsic apoptotic pathways and later the dominance of intrinsic activation consistent with observed mitochondrial swelling (Fig. 8). The effector caspase 7 was the most active enzyme from the tested caspases as its activity was significantly increased to 203% of control after 24 h and to 318% of control after 72 h incubation with 100 nM Bp4eT (Fig. 9 B and C).

3.6 Conclusions

The results of this study show that Bp4eT is a highly potent and specific antineoplastic iron chelator causing S-phase cell cycle arrest, mitochondrial

depolarization and apoptotic cell death. The metabolic conversion of thiosemicarbazone group of Bp4eT to amidrazone or semicarbazone moiety leads to diminished iron chelation and mobilization activity, loss of redox activity of iron complexes and two orders of magnitude reduction of antiproliferative activity and toxicity. Hence, the examined metabolites of Bp4eT apparently do not make contribution to its pharmacological actions. These results are important and will be used for further development of this drug candidate.

Acknowledgements

This study was supported by the Charles University (grants GAUK 299511, SVV 260065 and 260062) and the Czech Science Foundation (grant 13-15008S).

Conflict of Interest Disclosure

The authors declare no competing financial interests.

References

- Baker, E., D. Richardson, et al. (1992). "Evaluation of the iron chelation potential of hydrazones of pyridoxal, salicylaldehyde and 2-hydroxy-1-naphthylaldehyde using the hepatocyte in culture." Hepatology **15**(3): 492-501.
- Becker, E. and D. R. Richardson (1999). "Development of novel aroylhydrazone ligands for iron chelation therapy: 2-pyridylcarboxaldehyde isonicotinoyl hydrazone analogs." J Lab Clin Med **134**(5): 510-521.
- Buss, J. L., F. M. Torti, et al. (2003). "The role of iron chelation in cancer therapy." Current Medicinal Chemistry **10**(12): 1021-1034.
- Debebe, Z., T. Ammosova, et al. (2011). "Iron chelators of the di-2-pyridylketone thiosemicarbazone and 2-benzoylpyridine thiosemicarbazone series inhibit HIV-1 transcription: identification of novel cellular targets--iron, cyclin-dependent kinase (CDK) 2, and CDK9." Mol Pharmacol **79**(1): 185-196.
- Debebe, Z., S. Nekhai, et al. (2012). "Development of a sensitive HPLC method to measure in vitro permeability of E- and Z-isomeric forms of thiosemicarbazones in Caco-2 monolayers." J Chromatogr B Analyt Technol Biomed Life Sci **906**: 25-32.
- Delie, F. and W. Rubas (1997). "A human colonic cell line sharing similarities with enterocytes as a model to examine oral absorption: advantages and limitations of the Caco-2 model." Crit Rev Ther Drug Carrier Syst **14**(3): 221-286.
- Fulda, S. and K. M. Debatin (2006). "Extrinsic versus intrinsic apoptosis pathways in anticancer chemotherapy." Oncogene **25**(34): 4798-4811.
- Glickstein, H., R. B. El, et al. (2006). "Action of chelators in iron-loaded cardiac cells: Accessibility to intracellular labile iron and functional consequences." Blood **108**(9): 3195-3203.
- Chaston, T. B., R. N. Watts, et al. (2004). "Potent antitumor activity of novel iron chelators derived from di-2-pyridylketone isonicotinoyl hydrazone involves fenton-derived free radical generation." Clin Cancer Res **10**(21): 7365-7374.

- Chiu, S. H., K. A. Thompson, et al. (1995). "The role of drug metabolism in drug discovery: a case study in the selection of an oxytocin receptor antagonist for development." Toxicol Pathol **23**(2): 124-130.
- Kalinowski, D. S., Y. Yu, et al. (2007). "Design, synthesis, and characterization of novel iron chelators: structure-activity relationships of the 2-benzoylpyridine thiosemicarbazone series and their 3-nitrobenzoyl analogues as potent antitumor agents." J Med Chem **50**(15): 3716-3729.
- Kralova, V., S. Benesova, et al. (2012). "Selenite-induced apoptosis and autophagy in colon cancer cells." Toxicol In Vitro **26**(2): 258-268.
- Lane, D. J., T. M. Mills, et al. (2014). "Expanding horizons in iron chelation and the treatment of cancer: Role of iron in the regulation of ER stress and the epithelial-mesenchymal transition." Biochim Biophys Acta **1845**(2): 166-181.
- Le, N. T. and D. R. Richardson (2002). "The role of iron in cell cycle progression and the proliferation of neoplastic cells." Biochim Biophys Acta **1603**(1): 31-46.
- Lederman, H. M., A. Cohen, et al. (1984). "Deferoxamine: a reversible S-phase inhibitor of human lymphocyte proliferation." Blood **64**(3): 748-753.
- Liang, Y., C. Yan, et al. (2001). "Apoptosis in the absence of caspase 3." Oncogene **20**(45): 6570-6578.
- Lin, J. H. and A. Y. Lu (1997). "Role of pharmacokinetics and metabolism in drug discovery and development." Pharmacol Rev **49**(4): 403-449.
- Mackova, E., K. Hruskova, et al. (2012). "Methyl and ethyl ketone analogs of salicylaldehyde isonicotinoyl hydrazone: novel iron chelators with selective antiproliferative action." Chem Biol Interact **197**(2-3): 69-79.
- Merlot, A. M., D. S. Kalinowski, et al. (2013). "Novel chelators for cancer treatment: where are we now?" Antioxid Redox Signal **18**(8): 973-1006.

- Merlot, A. M., N. Pantarat, et al. (2010). "Membrane transport and intracellular sequestration of novel thiosemicarbazone chelators for the treatment of cancer." Mol Pharmacol **78**(4): 675-684.
- Merlot, A. M., N. Pantarat, et al. (2013). "Cellular uptake of the antitumor agent Dp44mT occurs via a carrier/receptor-mediated mechanism." Mol Pharmacol **84**(6): 911-924.
- Miao, Q., D. Xu, et al. (2010). "Amphiphilic hyper-branched co-polymer nanoparticles for the controlled delivery of anti-tumor agents." Biomaterials **31**(28): 7364-7375.
- Mladenka, P., D. S. Kalinowski, et al. (2009). "The novel iron chelator, 2-pyridylcarboxaldehyde 2-thiophenecarboxyl hydrazone, reduces catecholamine-mediated myocardial toxicity." Chem Res Toxicol **22**(1): 208-217.
- Ono, K., S. O. Kim, et al. (2003). "Susceptibility of lysosomes to rupture is a determinant for plasma membrane disruption in tumor necrosis factor alpha-induced cell death." Mol Cell Biol **23**(2): 665-676.
- Quach, P., E. Gutierrez, et al. (2012). "Methemoglobin formation by triapine, di-2-pyridylketone-4,4-dimethyl-3-thiosemicarbazone (Dp44mT), and other anticancer thiosemicarbazones: identification of novel thiosemicarbazones and therapeutics that prevent this effect." Mol Pharmacol **82**(1): 105-114.
- Richardson, D. and E. Baker (1992). "Two mechanisms of iron uptake from transferrin by melanoma cells. The effect of desferrioxamine and ferric ammonium citrate." J Biol Chem **267**(20): 13972-13979.
- Richardson, D. R. and K. Milnes (1997). "The potential of iron chelators of the pyridoxal isonicotinoyl hydrazone class as effective antiproliferative agents II: the mechanism of action of ligands derived from salicylaldehyde benzoyl hydrazone and 2-hydroxy-1-naphthylaldehyde benzoyl hydrazone." Blood **89**(8): 3025-3038.

- Richardson, D. R., P. C. Sharpe, et al. (2006). "Dipyridyl thiosemicarbazone chelators with potent and selective antitumor activity form iron complexes with redox activity." J Med Chem **49**(22): 6510-6521.
- Richardson, D. R., E. H. Tran, et al. (1995). "The potential of iron chelators of the pyridoxal isonicotinoyl hydrazone class as effective antiproliferative agents." Blood **86**(11): 4295-4306.
- Saletta, F., Y. S. Rahmanto, et al. (2011). "Cellular Iron Depletion and the Mechanisms Involved in the Iron-dependent Regulation of the Growth Arrest and DNA Damage Family of Genes." Journal of Biological Chemistry **286**(41): 35396-35406.
- Stariat, J., P. Kovarikova, et al. (2010). "Development of an LC-MS/MS method for analysis of interconvertible Z/E isomers of the novel anticancer agent, Bp4eT." Anal Bioanal Chem **397**(1): 161-171.
- Stariat, J., V. Sestak, et al. (2012). "LC-MS/MS identification of the principal in vitro and in vivo phase I metabolites of the novel thiosemicarbazone anti-cancer drug, Bp4eT." Anal Bioanal Chem **403**(1): 309-321.
- Stariat, J., V. Suprunova, et al. (2013). "Simultaneous determination of the novel thiosemicarbazone anti-cancer agent, Bp4eT, and its main phase I metabolites in plasma: Application to a pilot pharmacokinetic study in rats." Biomed Chromatogr.
- Stefani, C., G. Punnia-Moorthy, et al. (2011). "Halogenated 2'-benzoylpyridine thiosemicarbazone (XBpT) chelators with potent and selective anti-neoplastic activity: relationship to intracellular redox activity." J Med Chem **54**(19): 6936-6948.
- van Engeland, M., L. J. Nieland, et al. (1998). "Annexin V-affinity assay: a review on an apoptosis detection system based on phosphatidylserine exposure." Cytometry **31**(1): 1-9.

West, D. X., J. S. Ives, et al. (1995). "Copper(II) Complexes of 2-Benzoylpyridine N-4-Substituted Thiosemicarbazones." Polyhedron **14**(15-16): 2189-2200.

Yu, Y., Y. Suryo Rahmanto, et al. (2012). "Bp44mT: an orally active iron chelator of the thiosemicarbazone class with potent anti-tumour efficacy." Br J Pharmacol **165**(1): 148-166.

Tables

Table 1. Cytotoxic effects of Bp4eT and its metabolites towards both neoplastic and non-cancerous cell lines. Bp4eT and its metabolites have been incubated with HL-60, MCF-7, HCT116 and A549 cancer cells or H9c2 and 3T3 non-cancerous cells for 72 h/37°C. Cellular viability was determined using the MTT test and the IC₅₀ values (half-maximal inhibitory concentrations) were calculated using CalcuSyn 2.0 software. Mean ± SD; *n* ≥ 4 experiments.

	IC ₅₀ (μM)					
	HL-60	MCF-7	HCT116	A549	H9c2	3T3
Bp4eT	0.003 ± 0.001	0.015 ± 0.002	0.008 ± 0.001	0.593 ± 0.148	0.524 ± 0.157	1.309 ± 0.337
Bp4eA	52.1 ± 3.3	59.4 ± 8.9	111.5 ± 20.9	206.8 ± 46.1	416.1 ± 122.1	1027.4 ± 203.9
<i>E</i> -Bp4eS	150.6 ± 9.1	208.5 ± 43.9	95.4 ± 10.4	247.9 ± 28.4	883.8 ± 278.6	>1000
<i>Z</i> -Bp4eS	46.2 ± 1.5	197.6 ± 20.9	337.0 ± 48.5	535.9 ± 147.2	343.2 ± 95.1	>1000

Table 2. Selectivity ratios of cytotoxic effects of Bp4eT and its metabolites towards neoplastic and non-cancerous cells. The selectivity ratios were calculated as ratios of IC₅₀ concentrations from cancerous and non-cancerous cells. The higher the selectivity ratio is, the more selective is the anticancer action and the safety of the substance.

	IC ₅₀ neoplastic cells / IC ₅₀ non-cancerous cells							
	H9c2/ HL-60	3T3/ HL-60	H9c2/ MCF-7	3T3/ MCF-7	H9c2/ HCT116	3T3/ HCT116	H9c2/ A549	3T3/ A549
Bp4eT	174.7	436.3	34.9	87.3	65.5	163.6	0.9	2.2
Bp4eA	8.0	19.7	7.0	17.3	3.7	9.2	2.0	5.0
<i>E</i> -Bp4eS	5.9	>6.6	4.2	>4.8	9.3	>10.5	3.6	>4.0
<i>Z</i> -Bp4eS	7.4	>21.6	1.7	>5.1	1.0	>3.0	0.6	>1.9

Figure legends

Figure 1. Chemical structures of Bp4eT and its metabolites and indication of *E/Z* isomerism. Bp4eT, 2-benzoylpyridine 4-ethyl-3-thiosemicarbazone; Bp4eA; *N*³-ethyl-*N*¹-[phenyl(pyridine-2yl)methylene]formamidrazne; Bp4eS, 2-benzoylpyridine 4-ethylsemicarbazone.

Figure 2. Cytotoxic effects of the chelator Bp4eT (A) and its metabolites Bp4eA (B) and both *E* (C) and *Z* (D) isomers of Bp4eS. For determination of cytotoxic activities on cancer cells, HL-60, MCF-7, HCT116 and A549 cell lines were incubated with studied substances for 72 h. Cytotoxicity studies on non-cancerous cells were performed using 72 h incubation of studied substances with H9c2 and 3T3 cell lines. Mean \pm SD; $n \geq 4$ experiments.

Figure 3. The capability of Bp4eA and Bp4eS to bind iron from labile iron pool (LIP) of MCF-7 cells was negligible compared to parent chelator Bp4eT. The abilities of studied substances to chelate free iron from LIP in MCF-7 cells were measured using calcein-AM assay. The fluorescence of free calcein after the addition of 10 μ M Bp4eT or its metabolites were observed for 10 min (A). The intensity of fluorescence in $t = 10$ min of measurement of metabolites was expressed as a percentage of the fluorescence produced by Bp4eT (B). Mean \pm SD; $n = 6$ experiments. Statistical significance (ANOVA): * $p < 0.05$, ** $p < 0.01$, *** $p < 0.001$ as compared to chelator Bp4eT.

Figure 4. The metabolites of Bp4eT lost the ability to mobilize ⁵⁹Fe from prelabeled MCF-7 cells (A) and to prevent the uptake of ⁵⁹Fe from ⁵⁹Fe₂transferrin by MCF-7 cells (B). The promotion of ⁵⁹Fe release from prelabeled MCF-7 cells (A) and the inhibition of internalized ⁵⁹Fe uptake from ⁵⁹Fe₂transferrin by MCF-7 cells (B) were determined after 3 h/37°C incubations with 25 μ M concentrations of studied substances. Mean \pm SD; $n \geq 3$ experiments. Statistical significance (ANOVA): * $p < 0.05$, ** $p < 0.01$, *** $p < 0.001$ as compared to the control (untreated) group.

Figure 5. In contrast to Bp4eT, its metabolites Bp4eA and Bp4eS were not able to form redox active complexes with iron. For this assessment the ascorbate oxidation

assay was used. Bp4eT and its metabolites were assayed at iron binding equivalents (IBE) of 0.1 (excess of iron), 1 (fully charged iron – chelator complex) and 3 (excess of free chelator). Chelators DFO and EDTA were used as antioxidative or prooxidative controls, respectively. Results are expressed as a percentage of control group without chelator in the same IBE (100 %). Mean \pm SD; $n \geq 3$ experiments. Statistical significance (ANOVA): * $p < 0.05$, ** $p < 0.01$, *** $p < 0.001$ as compared to the control group (iron with ascorbate) in the same IBE.

Figure 6. Bp4eT caused increase of S phase and decrease of G₂/M phase of cell cycle whereas its metabolites did not. MCF-7 cells were incubated for 72 h with 100 nM Bp4eT or its metabolites, Bp4eA and Bp4eS, in the same concentration. The cell cycle analysis was processed by flow cytometry using propidium iodide. Phase quantification was evaluated using MultiCycle AV Software. Mean \pm SD; $n \geq 3$ experiments. Statistical significance (ANOVA): * $p < 0.05$, ** $p < 0.01$, *** $p < 0.001$ as compared to the control (untreated) group.

Figure 7. Epifluorescence microscopy estimation of autophagy, apoptosis or necrosis after Bp4eT treatment. MCF-7 cells were incubated for 72 h with 10 or 100 nM Bp4eT. 1nM rapamycin was incubated with MCF-7 cells for 30 min to serve as a positive control for autophagy to distinguish autophagosomes (large, blue-fluorescent granules) from intact lysosomes (blue-fluorescent dots) labelled with the MDC probe. The green fluorescence of plasma membrane labeled with annexin V-FITC is a sign of apoptotic cells or bodies. The red-fluorescent nuclei stained with propidium iodide (or yellow when overlaid with green fluorescence of cellular membrane) are nuclei of necrotic or late-stage apoptotic cells with altered cell membrane integrity. Scale bars represent 50 μ m.

Figure 8. Bp4eT treatment does not affect lysosomes, but causes a mitochondrial swelling. MCF-7 cells were incubated for 72 h with 10 or 100 nM Bp4eT then stained 10 min with lysosomal probe LysoTracker® (blue) and mitochondrial probe MitoTracker® (green). Scale bars represent 50 μ m.

Figure 9. Bp4eT causes an increase of caspase activities whereas its metabolites do not. MCF-7 cells were incubated for 3 h (A), 24 h (B) and 72 h (C) with 100 nM Bp4eT or its metabolites, Bp4eA and Bp4eS, in the same concentration. The caspase activities were then assayed in cellular lysates. The activities were related to cell viabilities and the results were expressed as a percentage of control. Mean \pm SD; $n = 4$ experiments. Statistical significance (ANOVA): * $p < 0.05$, ** $p < 0.01$, *** $p < 0.001$ as compared to the control (untreated) group.

Figures

Figure 1.

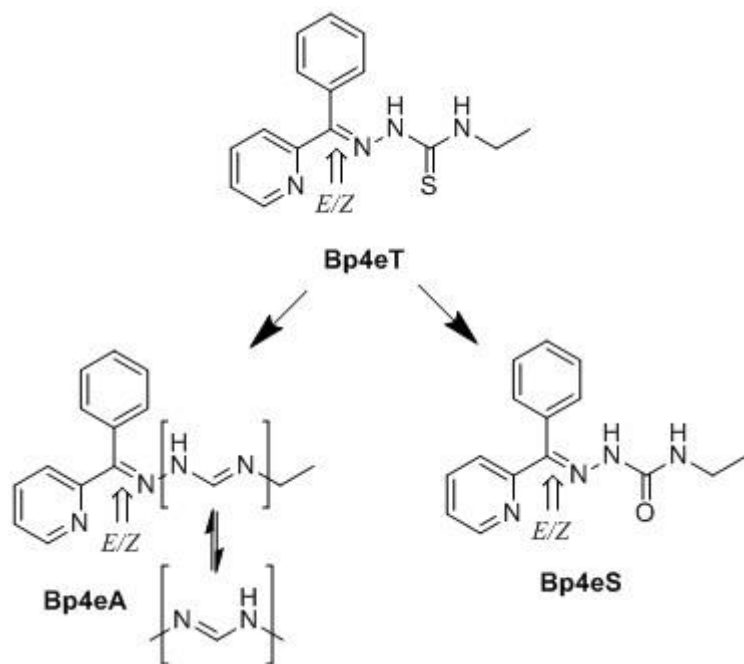


Figure 2.

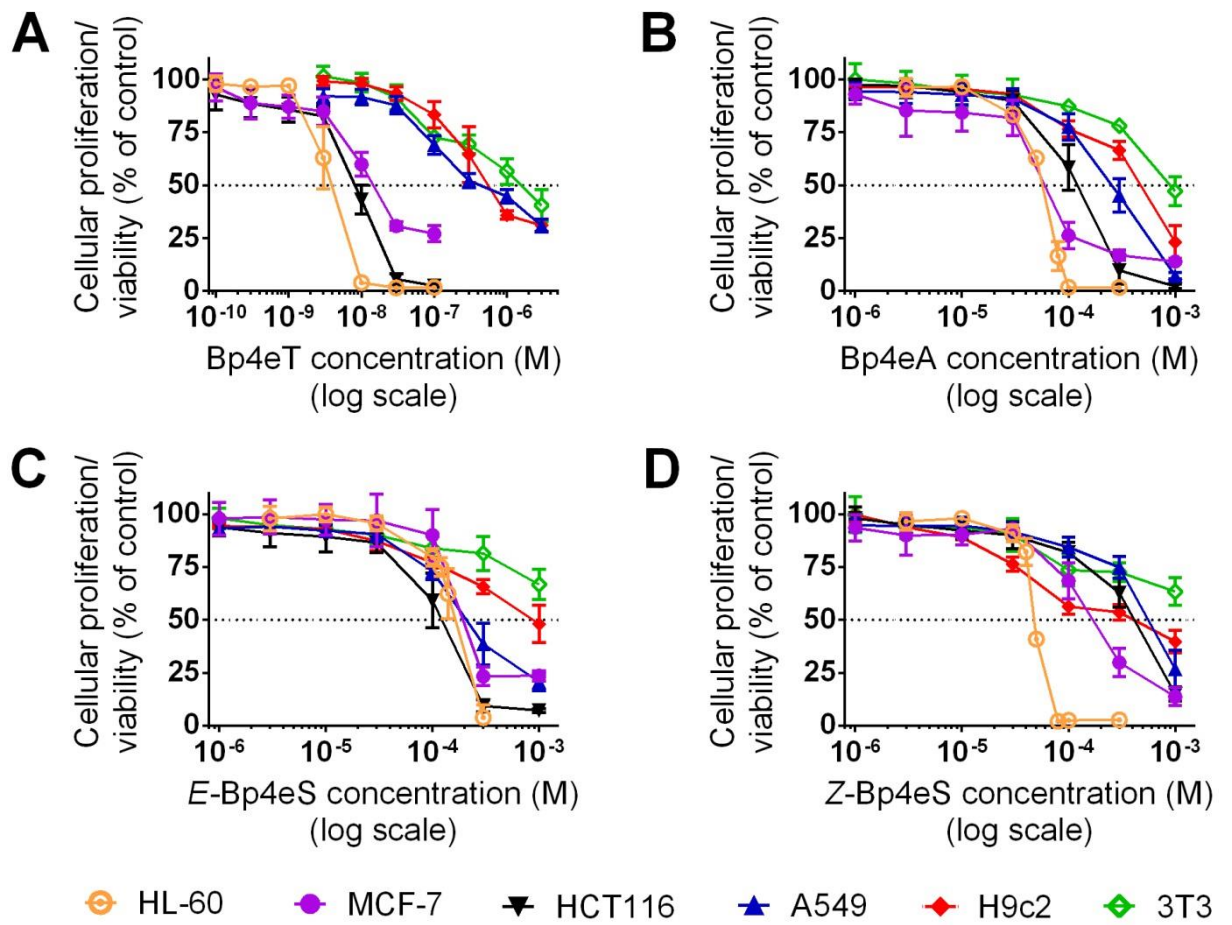


Figure 3.

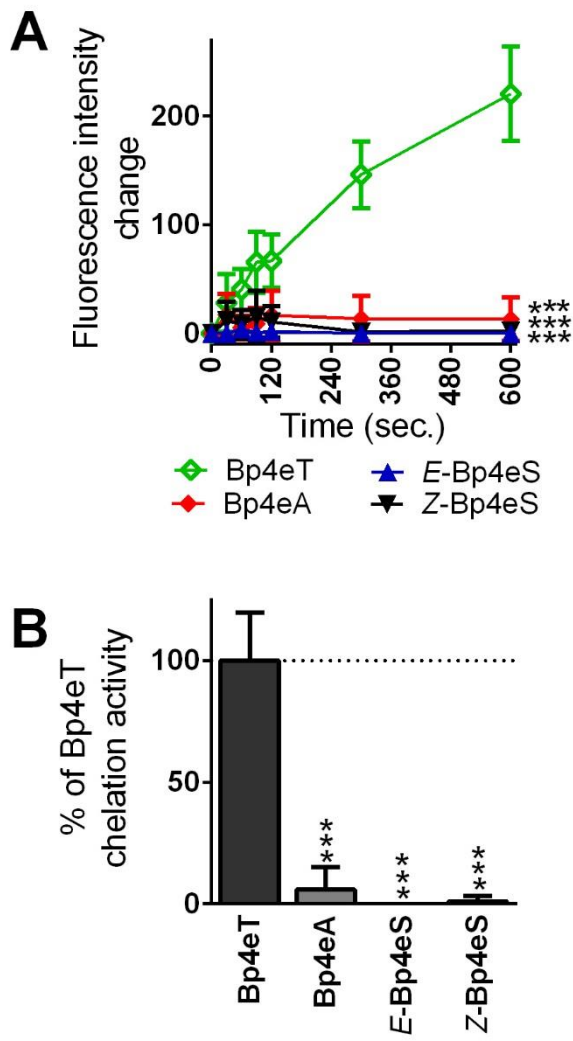


Figure 4.

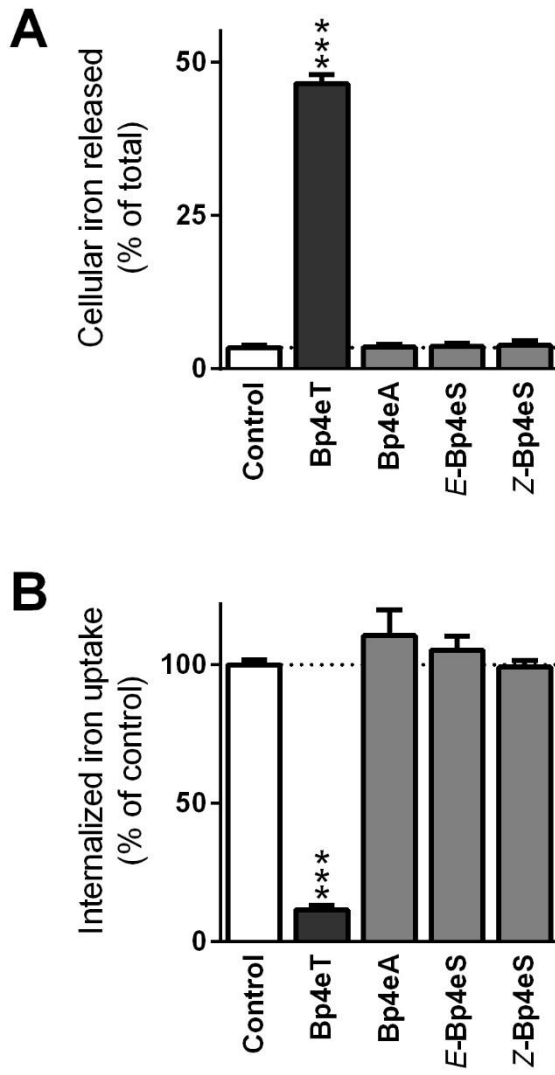


Figure 5.

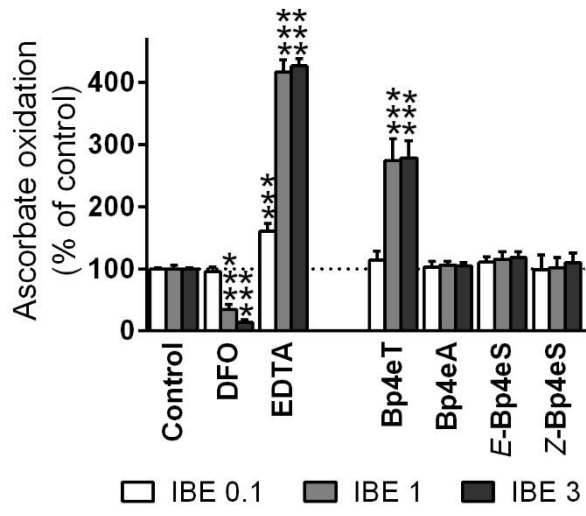


Figure 6.

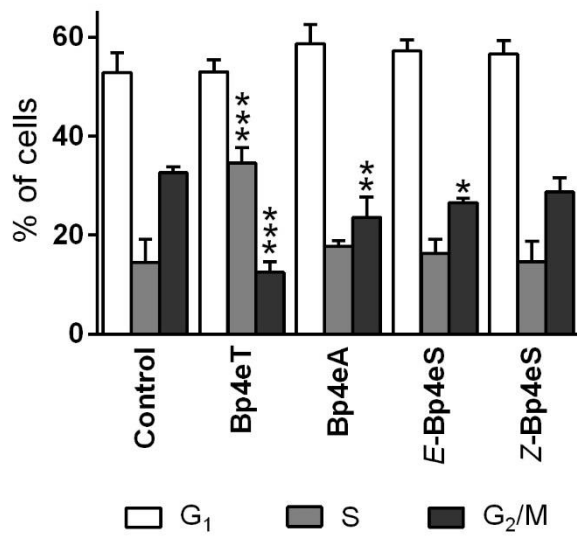


Figure 7.

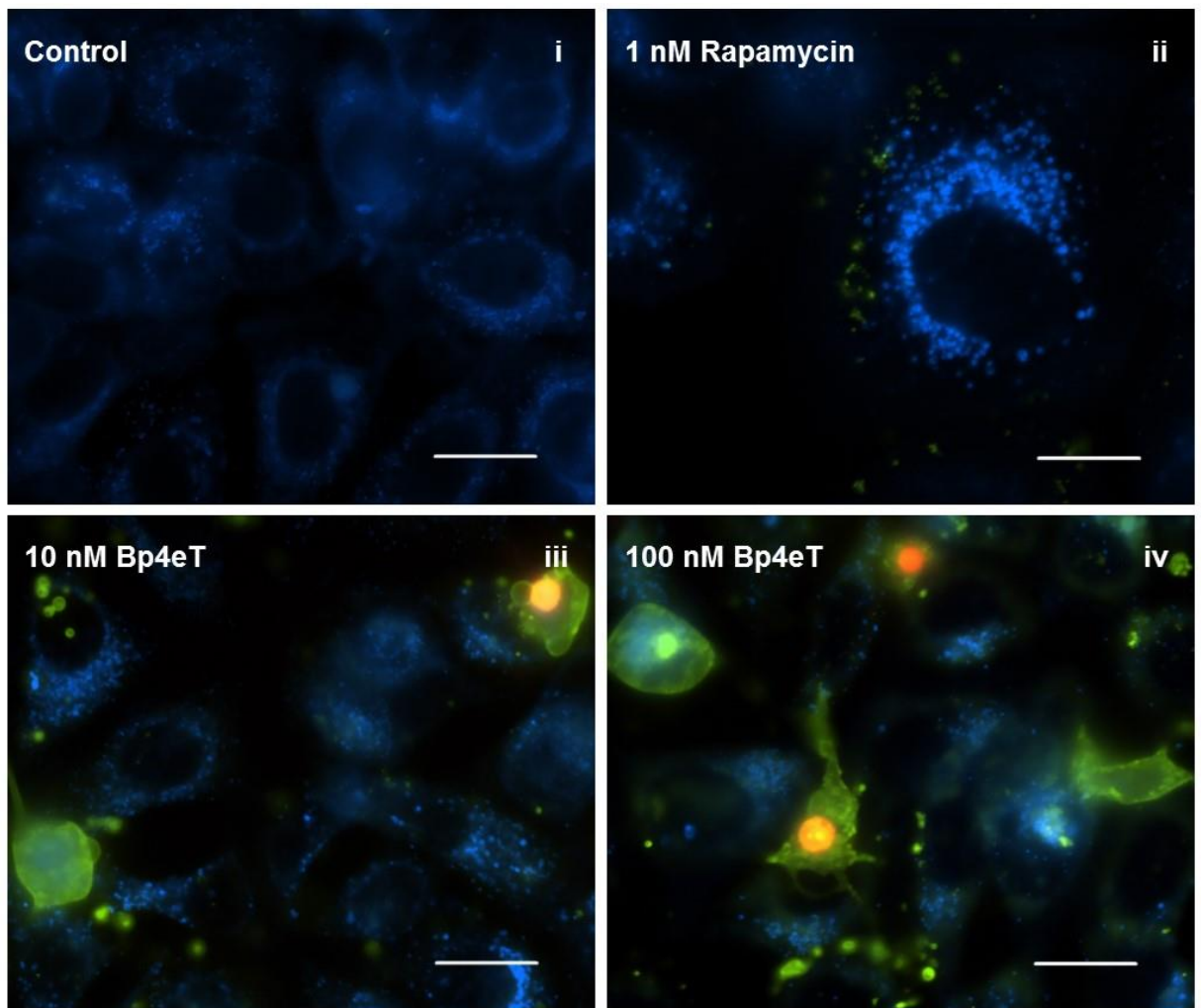


Figure 8.

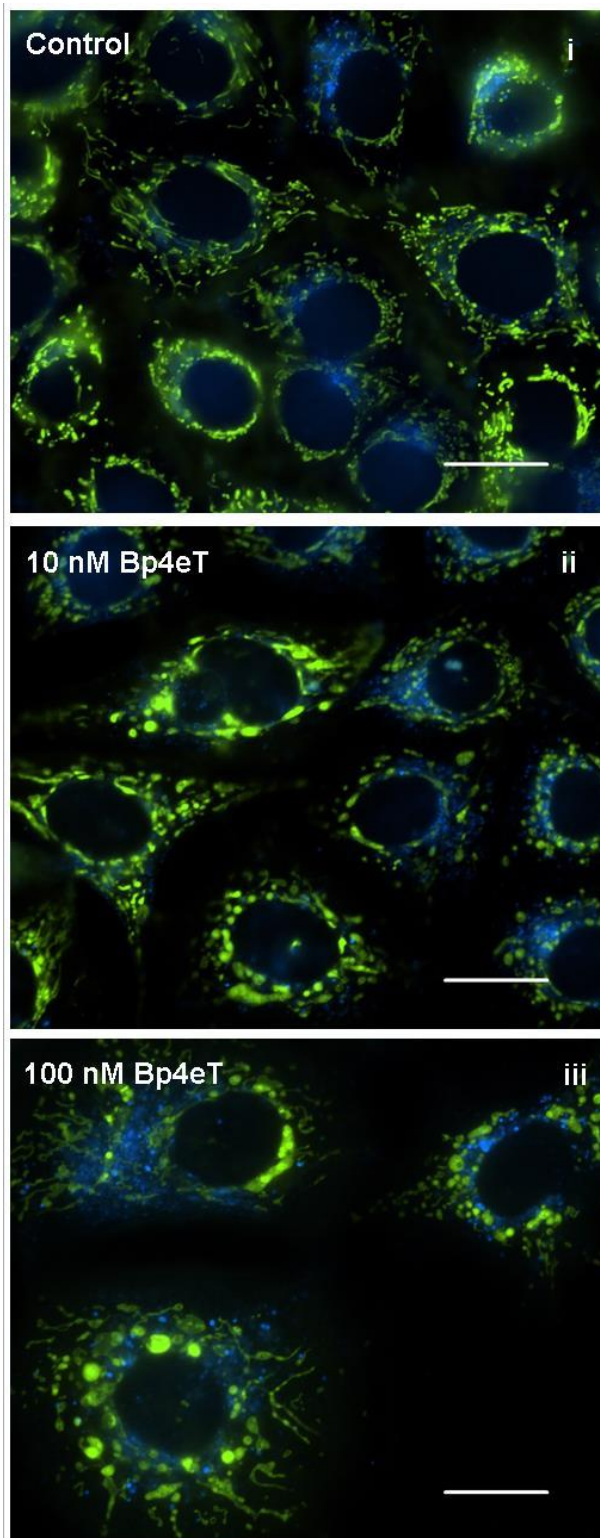
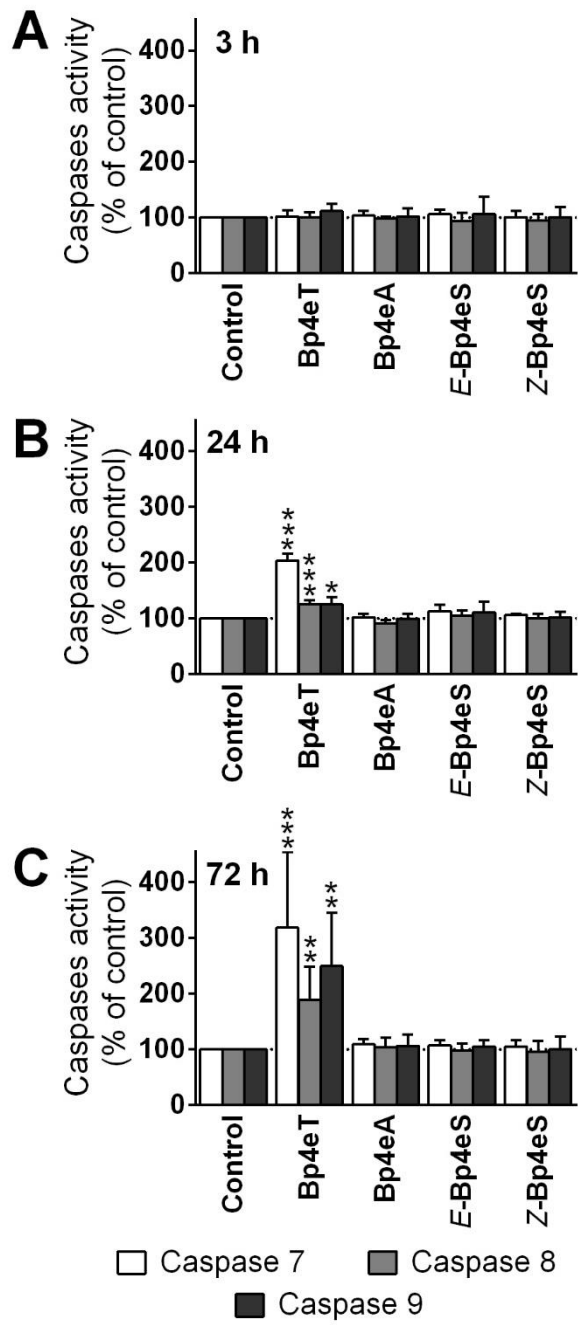


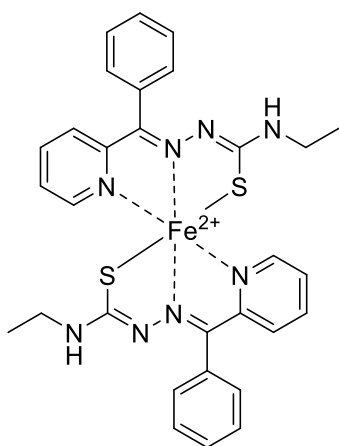
Figure 9.



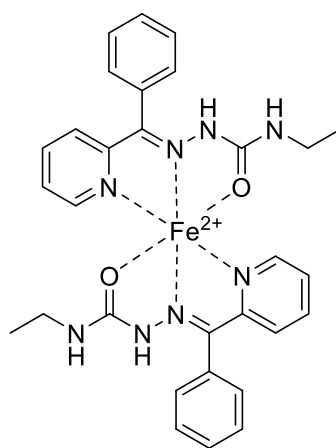
Supplementary Figure Legend

Supplementary Figure 1. Expected iron complexes of Bp4eT and its metabolites.

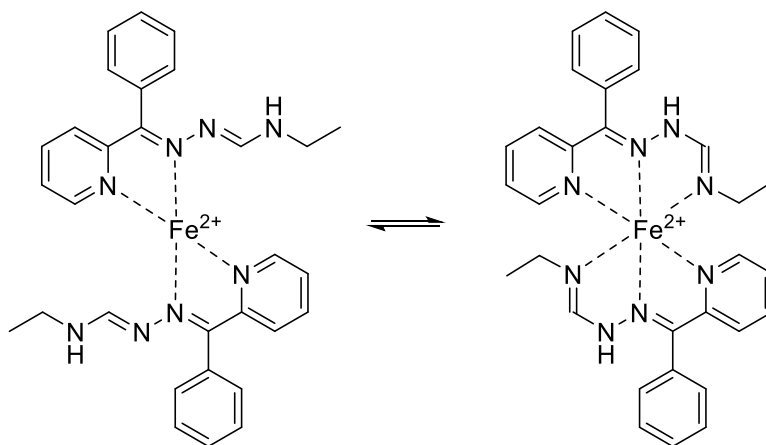
Supplementary Figure 1.



Bp4eT



Bp4eS



Bp4eA

Příloha VI

Bendová P, Macková E, Hašková P, Vávrová A, Jirkovský E, Štěřba M, Popelová O, Kalinowski DS, Kovaříková P, Vávrová K, Richardson DR, Šimůnek T. Comparison of clinically used and experimental iron chelators for protection against oxidative stress-induced cellular injury. *Chem Res Toxicol*. 2010; **23**(6):1105-14.

IF₂₀₁₀ = 4,148

Příloha VII

Vávrová A, Jansová H, Macková E, Macháček M, Hašková P, Tichotová L, Štěrba M, Šimůnek T. Catalytic inhibitors of topoisomerase II differently modulate the toxicity of anthracyclines in cardiac and cancer cells. *PLoS One*. 2013; **8**(10):e76676.

IF₂₀₁₂ = 3,730